

Clemson University

TigerPrints

All Dissertations

Dissertations

May 2020

Investigating Metal-Mediated DNA Damage Prevention by Antioxidants and Examining the Role of Metals in Fluconazole-Mediated DNA Damage

Andrea A. E. Gaertner

Clemson University, agaertn@g.clemson.edu

Follow this and additional works at: https://tigerprints.clemson.edu/all_dissertations

Recommended Citation

Gaertner, Andrea A. E., "Investigating Metal-Mediated DNA Damage Prevention by Antioxidants and Examining the Role of Metals in Fluconazole-Mediated DNA Damage" (2020). *All Dissertations*. 2577. https://tigerprints.clemson.edu/all_dissertations/2577

This Dissertation is brought to you for free and open access by the Dissertations at TigerPrints. It has been accepted for inclusion in All Dissertations by an authorized administrator of TigerPrints. For more information, please contact kokeefe@clemson.edu.

INVESTIGATING METAL-MEDIATED DNA DAMAGE PREVENTION BY
ANTIOXIDANTS AND EXAMINING THE ROLE OF METALS IN FLUCONAZOLE-
MEDIATED DNA DAMAGE

A Dissertation
Presented to
the Graduate School of
Clemson University

In Partial Fulfillment
of the Requirements for the Degree
Doctor of Philosophy
Chemistry

by
Andrea Augusta Elisabeth Gaertner
May 2020

Accepted by:
Dr. Julia L. Brumaghim, Committee Chair
Dr. William T. Pennington
Dr. Lukasz Kozubowski
Dr. Daniel C. Whitehead

ABSTRACT

Reactive oxygen species (ROS) play an important role in the development of many diseases. Common assays to test the ability of hydrophobic compounds to prevent oxidative stress are radical scavenging assays and cell studies. However, these radical assays often do not accurately reflect biological outcomes, and the use of different cell lines limits the ability to directly compare compound efficacy (Chapter 1). Results from DNA damage prevention assays can directly compare antioxidant efficacy, but these assays have been limited to water-soluble compounds. Chapter 2 discusses the first assay that quantifiably evaluates the ability of hydrophobic compounds to prevent metal-mediated DNA damage inhibition via gel electrophoresis. This assay allows biologically relevant evaluation of compounds for their effectiveness under consistent conditions. The glutathione peroxidase mimic ebselen and its derivatives prevent copper-mediated DNA damage (IC_{50} values 280-450 μ M), but do not significantly inhibit iron-mediated DNA damage. In combination with radical scavenging assays, these biologically relevant assays enable identification of structure-function relationships for hydrophobic antioxidant compounds and drugs.

Studies presented in Chapter 3 investigate the effect of metal binding on drug properties. Fluconazole (FLC) binds both iron and copper, and stabilizes Cu^+ and Fe^{2+} over Cu^{2+} and Fe^{3+} , respectively, as measured by cyclic voltammetry. Using gel electrophoresis assays, the effects of FLC on copper- and iron-mediated DNA damage were determined. FLC does not cause DNA damage by itself, but addition of FLC lowers the concentration of Fe^{2+} or Cu^+ needed to cause 50% DNA damage (EC_{50}) by 50 and 40 %, respectively, increasing reactive oxygen species production.

The studies described in Chapter 4 investigate the antioxidant capabilities of a series of plant-derived, procyanidin-rich condensed tannins (CTs) with different structural features for their ability to inhibit copper (IC_{50} $162.5 \pm 0.3 \mu\text{M}$ to 27% DNA damage inhibition at the highest concentration) and iron-mediated (IC_{50} 0.75 ± 0.01 to $4.96 \pm 0.01 \mu\text{M}$) DNA damage. The activity of CTs are compared to six commercially available polyphenolic compounds. This is the first study to investigate structure-activity relationships for CTs and their abilities to prevent metal-mediated DNA damage.

DEDICATION

I dedicate this dissertation to my grandparents Erna (1926-2017) and Wilhelm (1925-2017) Gärtner and Elfriede (1936-2017) and Hans (1933-2007) Jackwert that sadly passed away during this journey. In addition, I would like to dedicate this to my great-uncle Dr. John Richard Aspland (1936-2019), Emeritus Professor at Clemson University.

“If you have never wept bitter tears because a wonderful story has come to an end and you must take your leave of the characters with whom you have shared so many adventures, whom you have loved and admired, for whom you have hoped and feared, and without whose company life seems empty and meaningless. If such things have not been part of your own experience, you probably won't understand what Bastian did next.”

—Michael Ende, *The Neverending Story*

“At certain junctures in the course of existence, unique moments occur when everyone and everything, even the most distant stars, combine to bring about something that could not have happened before and will never happen again. Few people know how to take advantage of these critical moments, unfortunately, and they often pass unnoticed. When someone does recognize them, however, great things happen in the world.”

—Michael Ende, “Momo”

ACKNOWLEDGMENTS

I would like to thank my advisor, Julia L. Brumaghim, for allowing me to be part of her group and mentoring me through the past years to become a better scientist.

Thank you to my family, my aunt, and group members that have become friends for their support, the coffee breaks and the help. I would like to thank Barbara Lewis for always having an open door and, over the years, becoming a very close friend. I would also like to thank Will and Robin and the rest of the staff for helping me numerous times. Thank you to my undergrads Michelle Tam, Connor LeRoy, Jenn Haines, James Rider, and Mogan Duffy for their help during the years.

TABLE OF CONTENTS

	Page
TITLE PAGE	i
ABSTRACT.....	ii
DEDICATION	iv
ACKNOWLEDGMENTS	v
LIST OF TABLES	viii
LIST OF FIGURES	xiv
CHAPTER	
I. SHOULD AND CAN THE ORAC ANTIOXIDANT ASSAY BE REPLACED?	1
1.1. Introduction.....	1
1.2. Assays Measuring Antioxidant Radical Scavenging	9
1.3. Assays Measuring the Metal Reducing Power of Antioxidants	13
1.4. Are cellular assays better than in vitro assays?.....	16
1.5. Conclusions.....	18
1.6. Dissertation Overview	18
1.7. References.....	21
II. DEVELOPMENT OF A NEW ASSAY TO EVALUATE ANTIOXIDANT ACTIVITY OF HYDROPHOBIC COMPOUNDS UNDER BIOLOGICAL RELEVANT CONDITIONS	32
2.1. Introduction.....	32
2.2. Results and Discussion	36
2.3. Conclusions.....	56
2.4. Experimental Methods.....	58
2.5.Supporting Information.....	62
2.6.References.....	108

Table of Contents (Continued)

	Page
III. FLUCONAZOLE PRODUCES REACTIVE OXYGEN SPECIES IN THE PRESENCE OF COPPER AND IRON TO CAUSE DNA DAMAGE	121
3.1. Introduction.....	121
3.2. Results and Discussion	125
3.3. Conclusions.....	131
3.4. Experimental Methods.....	132
3.5. Supporting Information.....	135
3.6. References.....	151
IV. INVESTIGATION OF PROCYANIDIN-RICH CONDENSED TANNINS FOR PREVENTION OF COPPER- AND IRON-MEDIATED DNA DAMAGE	156
4.1. Introduction.....	156
4.2. Results and Discussion	159
4.3. Conclusions.....	170
4.4. Experimental Methods.....	171
4.5. Supporting Information.....	176
4.6. References.....	182
APPENDICES	188
A: Copyright Permission for Work Presented in Chapter 3	188

LIST OF TABLES

Table	Page
2.1. IC ₅₀ values for polyphenol prevention of iron-mediated DNA damage under high (1.7 M) and low (10 mM) ethanol conditions and polyphenol scavenging of DPPH.....	45
2.2. IC ₅₀ values for metal-mediated DNA damage prevention and DPPH scavenging of selones and ebselen and ebsulfur derivatives (NP = IC ₅₀ value not obtained due to solubility issues).....	48
2.3. Gel electrophoresis results for EC DNA damage assays with Fe ²⁺ and H ₂ O ₂	74
2.4. Gel electrophoresis results for GA DNA damage assays with Fe ²⁺ and H ₂ O ₂	74
2.5. Gel electrophoresis results for PCA DNA damage assays with Fe ²⁺ and H ₂ O ₂	75
2.6. Gel electrophoresis results for TA DNA damage assays with Fe ²⁺ and H ₂ O ₂	75
2.7. Gel electrophoresis results for EGC DNA damage assays with Fe ²⁺ and H ₂ O ₂	76
2.8. Gel electrophoresis results for EGCG DNA damage assays with Fe ²⁺ and H ₂ O ₂	76
2.9. Gel electrophoresis results for sepy ^{Me} DNA damage assays with Fe ²⁺ and H ₂ O ₂	77
2.10. Gel electrophoresis results for pyridine DNA damage assays with Fe ²⁺ and H ₂ O ₂	77
2.11. Gel electrophoresis results for bipy DNA damage assays with Fe ²⁺ and H ₂ O ₂	78
2.12. Gel electrophoresis results for bipy DNA damage assays with Cu ⁺ and H ₂ O ₂	78

List of Tables (Continued)

Table	Page
2.13. Gel electrophoresis results for dmise DNA damage assays with Fe ²⁺ and H ₂ O ₂	79
2.14. Gel electrophoresis results for dmise DNA damage assays with Cu ⁺ and H ₂ O ₂	79
2.15. Gel electrophoresis results for ebis DNA damage assays with Fe ²⁺ and H ₂ O ₂	80
2.16. Gel electrophoresis results for ebis DNA damage assays with Cu ⁺ and H ₂ O ₂	80
2.17. Gel electrophoresis results for Trolox DNA damage assays with Fe ²⁺ and H ₂ O ₂ and 1.7 M ethanol.	81
2.18. Gel electrophoresis results for Trolox DNA damage assays with Fe ²⁺ , H ₂ O ₂ , and 10 mM ethanol.	81
2.19. Gel electrophoresis results for Trolox DNA damage assays with Cu ⁺ , H ₂ O ₂ , and 1.7M ethanol.	82
2.20. Gel electrophoresis results for Trolox DNA damage assays with Cu ⁺ , H ₂ O ₂ , and 10 mM ethanol.	82
2.21. Gel electrophoresis results for Edaravone DNA damage assays with Fe ²⁺ and H ₂ O ₂	83
2.22. Gel electrophoresis results for Edaravone DNA damage assays with Cu ⁺ and H ₂ O ₂	83
2.23. Gel electrophoresis results for Ebselen DNA damage assays with Fe ²⁺ and H ₂ O ₂	84
2.24. Gel electrophoresis results for Ebselen DNA damage assays with Cu ⁺ and H ₂ O ₂	84
2.25. Gel electrophoresis results for ebselen- <i>N</i> -acetic acid DNA damage assays with Fe ²⁺ and H ₂ O ₂	85

List of Tables (Continued)

Table	Page
2.26. Gel electrophoresis results for ebselen- <i>N</i> -acetic acid DNA damage assays with Cu ⁺ and H ₂ O ₂	85
2.27. Gel electrophoresis results for ebselen-7-carboxylic acid DNA damage assays with Fe ²⁺ and H ₂ O ₂	86
2.28. Gel electrophoresis results for ebselen-7-carboxylic acid methyl ester DNA damage assays with Fe ²⁺ and H ₂ O ₂	87
2.29. Gel electrophoresis results for ebsulfur-7-carboxylic acid DNA damage assays with Cu ⁺ and H ₂ O ₂	88
2.30. Gel electrophoresis results for ebsulfur-7-carboxylic acid DNA damage assays with Cu ⁺ and H ₂ O ₂	89
2.31. Gel electrophoresis results for ebsulfur-7-carboxylic acid methyl ester DNA damage assays with Cu ⁺ , and 50 μM H ₂ O ₂	90
2.32. DPPH scavenging assay results for EC.	91
2.33. DPPH scavenging assay results for GA.....	92
2.34. DPPH scavenging assay results for PCA.....	93
2.35. DPPH scavenging assay results for TA.	94
2.36. DPPH scavenging assay results for EGCG.....	95
2.37. DPPH scavenging assay results for sepy ^{Me}	96
2.38. DPPH scavenging assay results for pyridine.	97
2.39. DPPH scavenging assay results for bipy.	98
2.40. DPPH scavenging assay results for dmise.	99
2.41. DPPH scavenging assay results for ebis.	100
2.42. DPPH scavenging assay results for Trolox.....	101

List of Tables (Continued)

Table	Page
2.43. DPPH scavenging assay results for Edaravone.	102
2.44. DPPH scavenging assay results for Ebselen.	103
3.1. EC ₅₀ table of iron or copper with and without FLC and the effect of ascorbate (AA).	129
3.2. MALDI mass spectrometry data for FLC with Fe ²⁺ and Cu ²⁺ prepared in H ₂ O.	135
3.3. CV data for FLC with Fe ²⁺ and Cu ²⁺	136
3.4. Gel electrophoresis results for FLC DNA damage assays with Cu ²⁺ and H ₂ O ₂	143
3.5. Gel electrophoresis results for FLC DNA damage assays with Cu ²⁺ ascorbate (AA) and H ₂ O ₂	143
3.6. Gel electrophoresis results for FLC DNA damage assays with Cu ²⁺ and ascorbate (AA).	144
3.7. Gel electrophoresis results for FLC DNA damage assays with Cu ²⁺	144
3.8. Gel electrophoresis results for CuSO ₄ DNA damage assays with ascorbate (AA).	145
3.9. Gel electrophoresis results for DNA damage assays with Cu ²⁺ , ascorbate (AA), and H ₂ O ₂	145
3.10. Gel electrophoresis results for FLC DNA damage assays with Fe ²⁺ and H ₂ O ₂	146
3.11. Gel electrophoresis results for Fe ²⁺ DNA damage assays with H ₂ O ₂	146
3.12. Gel electrophoresis results for FLC DNA damage assays with Fe ²⁺	147
3.13. Gel electrophoresis results for Fe ²⁺ DNA damage assays.	147
3.14. Gel electrophoresis results for Fe ²⁺ DNA damage assays with ascorbate (AA).	148

List of Tables (Continued)

Table	Page
3.15. Gel electrophoresis results for Fe ²⁺ DNA damage assays with ascorbate (AA), FLC and H ₂ O ₂	148
3.16. Gel electrophoresis results for Fe ²⁺ DNA damage assays with ascorbate (AA) and FLC.....	149
3.17. Gel electrophoresis results for Fe ²⁺ DNA damage assays with ascorbate (AA) and H ₂ O ₂	149
3.18. Gel electrophoresis results for Fe ²⁺ DNA damage assays with H ₂ O ₂ , and DFO.	150
3.19. Statistical analysis of Fe ²⁺ and Fe ²⁺ FLC DNA damage through one-tailed t-test analysis.....	150
4.1. Classification of condensed tannin flavan-3-ol subunits and interflavan-3-ol linkages (ND = not detected).....	160
4.2. IC ₅₀ values for metal-mediated DNA damage prevention by CTs of the indicated foods	164
4.3. Gel electrophoresis results for Cu ⁺ DNA damage prevention assays with <i>Vaccinium macrocarpon</i> condensed tannins	178
4.4. Gel electrophoresis results for Fe ²⁺ DNA damage prevention assays with <i>Vaccinium macrocarpon</i> condensed tannins.	178
4.5. Gel electrophoresis results for Cu ⁺ DNA damage prevention assays with <i>Vitis vinifera</i> seed condensed tannins	179
4.6. Gel electrophoresis results for Fe ²⁺ DNA damage prevention assays with <i>Vitis vinifera</i> seed condensed tannins	179
4.7. Gel electrophoresis results for Cu ⁺ DNA damage prevention assays with <i>Humulus lupulus</i> condensed tannins.....	180
4.8. Gel electrophoresis results for Fe ²⁺ DNA damage prevention assays with <i>Humulus lupulus</i> condensed tannins.....	180

List of Tables (Continued)

Table	Page
4.9. Gel electrophoresis results for Cu ⁺ DNA damage prevention assays with <i>Tilia inflorrescentia</i> condensed tannins	181
4.10. Gel electrophoresis results for Fe ²⁺ DNA damage prevention assays with <i>Tilia inflorrescentia</i> condensed tannins	181

LIST OF FIGURES

Figure	Page
1.1. Classification of assays to evaluate antioxidant activity in vivo and in cells by assay type.	4
1.2. <i>In vitro</i> antioxidant assays classified by mechanism.	4
1.3. Antioxidants can prevent metal-mediated DNA damage through different mechanisms.	8
2.1. Structures of A) the radicals DPPH and ABTS commonly used in antioxidant assays, B) Trolox and Edaravone, known radical scavengers, C) various selones and pyridine derivatives, and D) ebselen and ebsulfur derivatives.	34
2.2. Dose-response curves for iron-mediated DNA damage with 10 mM (diamonds) and 1.7 M ethanol (circles) with increasing Fe ²⁺ concentrations.	39
2.3. EPR spectra of A) Fe ²⁺ , H ₂ O ₂ , and DMPO in MES buffer (10 mM, pH 6) without ethanol after a) 5 min and b) 45 min, with 1.7 M ethanol after c) 5 min and d) 30 min, and with 425 mM ethanol after e) 5 min and f) 45 min. B) Cu ²⁺ ascorbate, H ₂ O ₂ , and DMPO in 10 mM MOPS buffer (10 mM, pH 7) without ethanol after a) 5 min and b) 45 min, and with 1.7 M ethanol after c) 5 min and d) 45 min.	41
2.4. Structures of selected polyphenols examined in this chapter.	42
2.5. Gel electrophoresis images showing tannic acid (TA) prevention of iron-mediated DNA damage. MW: 1 kb molecular weight marker; lane 1: plasmid DNA (p); lane 2: p + H ₂ O ₂ ; lane 3: p + 20 μM TA + H ₂ O ₂ + 1.7 M ethanol; lane 4: p + Fe ²⁺ (2 μM) + H ₂ O ₂ + ethanol (10 mM); lane 5: p + Fe ²⁺ (15 μM) + H ₂ O ₂ + ethanol (1.7 M); lanes 6-12: Fe ²⁺ (15 μM) + H ₂ O ₂ + ethanol (1.7 M) + TA (0.1, 1, 2.5, 5, 7.5, 10, and 20 μM, respectively).	43
2.6. IC ₅₀ plots for prevention of iron-mediated DNA damage in the presence of 10 mM and 1.7 M ethanol for A) sepyMe and B) tannic acid.	44

List of Figures (Continued)

Figure	Page
2.7. Correlation of polyphenol IC ₅₀ values for prevention of DNA damage under high and low ethanol concentrations. Error bars are within symbols.	45
2.8. Gel electrophoresis images showing ebselen prevention of copper- and iron-mediated DNA damage. MW: 1 kb molecular weight marker; lane 1: plasmid DNA (p); lane 2: p + H ₂ O ₂ and A) lane 3: p + 400 μM ebselen + H ₂ O ₂ + 1.7 M ethanol; lane 4: p + Cu ²⁺ (6 μM) + ascorbate (7.5 μM) + H ₂ O ₂ + ethanol (10 mM); lane 5: p + Cu ²⁺ (6 μM) + ascorbate (7.5 μM) + H ₂ O ₂ + ethanol (1.7 M); lanes 6-13: Cu ²⁺ (6 μM) + ascorbate (7.5 μM) + H ₂ O ₂ + ethanol (1.7 M) + ebselen (1, 10, 50, 100, 200, 300, and 400 μM , respectively); B) lane 3: p + 400 μM ebselen + H ₂ O ₂ + 1.7 M ethanol; lane 4: p + Fe ²⁺ (2 μM) + H ₂ O ₂ + ethanol (10 mM); lane 5: p + Fe ²⁺ (15 μM) + H ₂ O ₂ + ethanol (1.7 M); lanes 6-12: Fe ²⁺ (15 μM) + H ₂ O ₂ + ethanol (1.7 M) + ebselen (1, 10, 50, 100, 200, 300, and 400 μM, respectively).	53
2.9. Dose-response curve for ebselen prevention of copper-mediated DNA damage under high-ethanol conditions.	54

List of Figures (Continued)

Figure	Page
<p>2.10. Gel image of iron-mediated DNA damage prevention by EC, GA, PCA, EGC, and EGCG. For all gel images MW: 1 kb molecular weight marker; lane 1: plasmid DNA (p); lane 2: p + H₂O₂. (50 μM); A) lane 3: p + H₂O₂+ EC (2000 μM); lane 4: p + Fe²⁺ (2 μM) + H₂O₂ + ethanol (10 mM); lane 5: p + Fe²⁺ (15 μM) + H₂O₂+ ethanol (1.7 M); lanes 6-14: p + H₂O₂ + FeSO₄ (15 μM) + EC (1, 10, 50, 100, 250, 500, 750, 1000, and 2000 μM, respectively); B) lane 3: p + H₂O₂ + GA (1000 μM); lane 4: p + Fe²⁺ (2 μM) + H₂O₂+ ethanol (10 mM); lane 5: p + Fe²⁺ (15 μM) + H₂O₂ + ethanol (1.7 M); lanes 6-14: p + H₂O₂+ FeSO₄ (15 μM) + GA (1, 10, 50, 75, 100, 250, 500, 750, and 1000 μM, respectively); C) lane 3: p + H₂O₂ + PCA (2000 μM) lane 4: p + Fe²⁺ (2 μM) + H₂O₂ + ethanol (10 mM); lane 5: p + Fe²⁺ (15 μM) + H₂O₂ + ethanol (1.7 M); lanes 6-14: p + H₂O₂ + FeSO₄ (15 μM) + PCA (1, 10, 50, 100, 250, 500, 750, 1000, and 2000 μM, respectively); D) lane 3: p + H₂O₂+ EGC (2000 μM); lane 4: p + Fe²⁺ (2 μM) + H₂O₂+ ethanol (10 mM); lane 5: p + Fe²⁺ (15 μM) + H₂O₂+ ethanol (1.7 M); lanes 6-14: p + H₂O₂ + FeSO₄ (15 μM) + EGC (1, 10, 50, 100, 250, 500, 750, 1000, and 2000 μM, respectively); E) lane 3: p + H₂O₂+ EGCC (500 μM); lane 4: p + Fe²⁺ (2 μM) + H₂O₂ + ethanol (10 mM); lane 5: p + Fe²⁺ (15 μM) + H₂O₂+ ethanol (1.7 M); lanes 6-14: p + H₂O₂+FeSO₄ (15 μM) + EGCG (0.1, 1, 5, 10, 25, 50, 100, 250, and 500 μM, respectively).</p>	62
<p>2.11. Gel image of copper- and iron-mediated DNA damage prevention by Trolox. For all gel images MW: 1 kb molecular weight marker; lane 1: plasmid DNA (p); lane 2: p + H₂O₂. (50 μM); A) lane 3: p + H₂O₂+ Trolox (2000 μM); lane 4: p + Cu²⁺ (6 μM) + ascorbate (7.5 μM) + H₂O₂ + ethanol (10 mM); lanes 5-13: p + H₂O₂+ Cu²⁺ (6 μM) + ascorbate (7.5 μM) +Trolox (0.1, 1, 5, 10, 50, 100, 500, 1000, 2000 μM, respectively); B) lane 3: p + H₂O₂ + Trolox (1000 μM); lane 4: p + Cu²⁺ (6 μM) + ascorbate (7.5 μM) + H₂O₂ + ethanol (10 mM); lane 5: p + Cu²⁺ (6 μM) + ascorbate (7.5 μM) + H₂O₂ + ethanol (1.7 M); lanes 6-13: p + H₂O₂ + Cu²⁺ (6 μM) + ascorbate (7.5 μM) +Trolox (0.1, 1, 5, 10, 50, 100, 500, and 1000 μM, respectively); C) lane 3: p + H₂O₂ + Trolox (2000 μM); lane 4: p +Fe²⁺ (2 μM) + H₂O₂ + ethanol (10 mM); lane 5: p + Fe²⁺ (15 μM) + H₂O₂ + ethanol (1.7 M); lanes 6-10: p + H₂O₂ + Fe²⁺ (15 μM) +Trolox (10, 50, 100, 500, and 1000 μM, respectively); D) lane 3: p + H₂O₂ + Trolox (2000 μM); lane 4: p + Fe²⁺ (2 μM) + H₂O₂ + ethanol (10 mM); lanes 5-13: p + H₂O₂ + FeSO₄ (2 μM) +Trolox (0.1, 1, 5, 10, 50, 100, 500, 1000, and 2000 μM, respectively).</p>	63

List of Figures (Continued)

Figure	Page
<p>2.12. Gel image of iron-mediated DNA damage prevention by dmise, ebis, bipy, pyridine, sepy^{Me}, and Edaravone. For all gel images MW: 1 kb molecular weight marker; lane 1: plasmid DNA (p); lane 2: p + H₂O₂ (50 μM); A) lane 3: p + H₂O₂ + dmise (4000 μM); lane 4: p + Fe²⁺ (2 μM) + H₂O₂ + ethanol (10 mM); lane 5: p + H₂O₂ + Fe²⁺ (15 μM) + ethanol (1.7 M); lanes 6-15: p + H₂O₂ + Fe²⁺ (15 μM) + dmise (0.5, 1, 10, 50, 100, 400, 1000, 2000, and 4000 μM, respectively); B) lane 3: p + H₂O₂ + ebis (400 μM); lane 4: p + Fe²⁺ (2 μM) + H₂O₂ + ethanol (10 mM); lane 5: p + H₂O₂ + Fe²⁺ (15 μM) + ethanol (1.7 M); lanes 6-14: p + H₂O₂ + Fe²⁺ (15 μM) + ebis (0.1, 0.5, 1, 5, 10, 50, 100, 200, and 400 μM, respectively); C) lane 3: p + H₂O₂ + bipy (1000 μM); lane 4: p + Fe²⁺ (2 μM) + H₂O₂ + ethanol (10 mM); lane 5: p + H₂O₂ + Fe²⁺ (15 μM) + ethanol (1.7 M); lanes 6-12: p + H₂O₂ + Fe²⁺ (15 μM) + bipy (0.5, 1, 10, 50, 100, 400, and 1000 μM, respectively); D) lane 3: p + H₂O₂ + pyridine (2000 μM); lane 4: p + Fe²⁺ (2 μM) + H₂O₂ + ethanol (10 mM); lane 5: p + H₂O₂ + Fe²⁺ (15 μM) + ethanol (1.7 M); lanes 6-14: p + H₂O₂ + Fe²⁺ (15 μM) + pyridine (1, 10, 50, 100, 250, 500, 750, 1000, and 2000 μM, respectively); E) lane 3: p + H₂O₂ + sepy^{Me} (2000 μM); lane 4: p + Fe²⁺ (2 μM) + H₂O₂ + ethanol (10 mM); lane 5: p + H₂O₂ + Fe²⁺ (15 μM) + ethanol (1.7 M); lanes 6-14: p + H₂O₂ + Fe²⁺ (15 μM) + sepy^{Me} (1, 10, 50, 100, 250, 500, 750, 1000 and 2000 μM, respectively); F) lane 3: p + H₂O₂ + Edaravone (1000 μM); lane 4: p + Fe²⁺ (2 μM) + H₂O₂ + ethanol (10 mM); lane 5: p + H₂O₂ + Fe²⁺ (15 μM) + ethanol (1.7 M); lanes 6-14: p + H₂O₂ + Fe²⁺ (15 μM) + Edaravone (0.1, 1, 5, 10, 50, 100, 500, and 1000 μM, respectively).....</p>	64

List of Figures (Continued)

Figure	Page
2.13. Gel image of copper-mediated DNA damage prevention by dmise, ebis, bipy, and edaravone. For all gel images MW: 1 kb molecular weight marker; lane 1: plasmid DNA (p); lane 2: p + H ₂ O ₂ . (50 μM); A) lane 3: p + H ₂ O ₂ + dmise (4000 μM); lane 4: p + Cu ²⁺ (6 μM) + ascorbate (7.5 μM) + H ₂ O ₂ + ethanol (10 mM); lane 5: p + H ₂ O ₂ + Cu ²⁺ (6 μM) + ascorbate (7.5 μM) + ethanol (1.7 M); lanes 6-14: p + H ₂ O ₂ + Cu ²⁺ (6 μM) + ascorbate (7.5 μM) + dmise (1, 10, 50, 100, 400, 750, 1000, 2000, and 4000 μM, respectively); B) lane 3: p + H ₂ O ₂ + ebis (100 μM); lane 4: p + Cu ²⁺ (6 μM) + ascorbate (7.5 μM) + H ₂ O ₂ + ethanol (10 mM); lane 5: p + H ₂ O ₂ + Cu ²⁺ (6 μM) + ascorbate (7.5 μM) + ethanol (1.7 M); lanes 6-11: p + H ₂ O ₂ + Cu ²⁺ (6 μM) + ascorbate (7.5 μM) + ebis (0.5, 1, 5, 10, 50, and 100 μM, respectively); C) lane 3: p + H ₂ O ₂ + bipy (1000 μM); lane 4: p + Cu ²⁺ (6 μM) + ascorbate (7.5 μM) + H ₂ O ₂ + ethanol (10 mM); lane 5: p + H ₂ O ₂ + Cu ²⁺ (6 μM) + ascorbate (7.5 μM) + ethanol (1.7 M); lanes 6-14: p + H ₂ O ₂ + Cu ²⁺ (6 μM) + ascorbate (7.5 μM) + bipy (0.5, 1, 5, 10, 50, 100, 500, and 1000 μM, respectively); D) lane 3: p + H ₂ O ₂ + edaravone (1000 μM); lane 4: p + Cu ²⁺ (6 μM) + ascorbate (7.5 μM) + H ₂ O ₂ + ethanol (10 mM); lane 5: p + H ₂ O ₂ + Cu ²⁺ (6 μM) + ascorbate (7.5 μM) + ethanol (1.7 M); lanes 6-13: p + H ₂ O ₂ + Cu ²⁺ (6 μM) + ascorbate (7.5 μM) + Edaravone (0.1, 1, 5, 10, 50, 100, 500, and 1000 μM, respectively).	65

List of Figures (Continued)

Figure	Page
<p>2.14. Gel image of iron-mediated DNA damage prevention by ebselen-<i>N</i>-acetic acid, ebselen-7-carboxylic acid, ebsulfur-<i>N</i>-acetic acid, and ebsulfur-7-carboxylic acid methyl ester. For all gel images MW: 1 kb molecular weight marker; lane 1: plasmid DNA (p); lane 2: p + H₂O₂ (50 μM); A) lane 3: p + H₂O₂ + ebselen-<i>N</i>-acetic acid (700 μM); lane 4: p + Fe²⁺ (2 μM) + H₂O₂ + ethanol (10 mM); lane 5: p + H₂O₂ + Fe²⁺ (15 μM) + ethanol (1.7 M); lanes 6-15: p + H₂O₂ + Fe²⁺ (15 μM) + ebselen-<i>N</i>-acetic acid (1, 10, 50, 100, 200, 300, 400, 500, 600, and 700 μM, respectively); B) lane 3: p + H₂O₂ + ebselen-7-carboxylic acid (700 μM); lane 4: p + Fe²⁺ (2 μM) + H₂O₂ + ethanol (10 mM); lane 5: p + H₂O₂ + Fe²⁺ (15 μM) + ethanol (1.7 M); lanes 6-14: p + H₂O₂ + Fe²⁺ (15 μM) + ebselen-7-carboxylic acid (1, 10, 50, 100, 200, 300, 400, 500, 600 and 700 μM, respectively); C) lane 3: p + H₂O₂ + ebsulfur-<i>N</i>-acetic acid (400 μM); lane 4: p + Fe²⁺ (2 μM) + H₂O₂ + ethanol (10 mM); lane 5: p + H₂O₂ + Fe²⁺ (15 μM) + ethanol (1.7 M); lanes 6-12: p + H₂O₂ + Fe²⁺ (15 μM) + ebsulfur-<i>N</i>-acetic acid (1, 50, 100, 200, 300 and 400 μM, respectively); D) lane 3: p + H₂O₂ + ebsulfur-7-carboxylic acid methyl ester (400 μM); lane 4: p + Fe²⁺ (2 μM) + H₂O₂ + ethanol (10 mM); lane 5: p + H₂O₂ + Fe²⁺ (15 μM) + ethanol (1.7 M); lanes 6-14: p + H₂O₂ + Fe²⁺ (15 μM) + ebsulfur-7-carboxylic acid methyl ester (1, 50, 100, 200, 300, and 400 μM).....</p>	66

List of Figures (Continued)

Figure	Page
<p>2.15. Gel image of copper-mediated DNA damage prevention ebselen-<i>N</i>-acetic acid, ebselen-7-carboxylic acid, ebsulfur-7-carboxylic acid methyl ester, ebsulfur-<i>N</i>-acetic acid, ebsulfur-7-carboxylic acid methyl ester. For all gel images MW: 1 kb molecular weight marker; lane 1: plasmid DNA (p); lane 2: p + H₂O₂. (50 μM); A) lane 3: p + H₂O₂ + ebselen-<i>N</i>-acetic acid (700 μM); lane 4: p + Cu²⁺ (6 μM) + ascorbate (7.5 μM) + H₂O₂ + ethanol (10 mM); lane 5: p + H₂O₂ + Cu²⁺ (6 μM) + ascorbate (7.5 μM) + ethanol (1.7 M); lanes 6-14: p + H₂O₂ + Cu²⁺ (6 μM) + ascorbate (7.5 μM) + ebselen-<i>N</i>-acetic acid (1, 10, 50, 100, 200, 300, 400, 500, 600, and 700 μM, respectively); B) lane 3: p + H₂O₂ + ebselen-7-carboxylic acid (700 μM); lane 4: p + Cu²⁺ (6 μM) + ascorbate (7.5 μM) + H₂O₂ + ethanol (10 mM); lane 5: p + H₂O₂ + Cu²⁺ (6 μM) + ascorbate (7.5 μM) + ethanol (1.7 M); lanes 6-11: p + H₂O₂ + Cu²⁺ (6 μM) + ascorbate (7.5 μM) + ebselen-7-carboxylic acid (1, 10, 50, 100, 200, 300, 400, 500, 600, and 700 μM, respectively); C) lane 3: p + H₂O₂ + ebsulfur-7-carboxylic acid methyl ester (700 μM); lane 4: p + Cu²⁺ (6 μM) + ascorbate (7.5 μM) + H₂O₂ + ethanol (10 mM); lane 5: p + H₂O₂ + Cu²⁺ (6 μM) + ascorbate (7.5 μM) + ethanol (1.7 M); lanes 6-14: p + H₂O₂ + Cu²⁺ (6 μM) + ascorbate (7.5 μM) + ebsulfur-7-carboxylic acid methyl ester (1, 10, 50, 100, 200, 300, 400, 500, 600 and 700 μM, respectively); D) lane 3: p + H₂O₂ + ebsulfur-<i>N</i>-acetic acid (400 μM); lane 4: p + Cu²⁺ (6 μM) + ascorbate (7.5 μM) + H₂O₂ + ethanol (10 mM); lane 5: p + H₂O₂ + Cu²⁺ (6 μM) + ascorbate (7.5 μM) + ethanol (1.7 M); lanes 6-13: p + H₂O₂ + Cu²⁺ (6 μM) + ascorbate (7.5 μM) + ebsulfur-<i>N</i>-acetic acid (1, 50, 100, 200, 300 and 400 μM, respectively). E) lane 3: p + H₂O₂ + ebsulfur-7-carboxylic acid methyl ester (400 μM); lane 4: p + Cu²⁺ (6 μM) + ascorbate (7.5 μM) + H₂O₂ + ethanol (10 mM); lane 5: p + H₂O₂ + Cu²⁺ (6 μM) + ascorbate (7.5 μM) + ethanol (1.7 M); lanes 6-13: p + H₂O₂ + Cu²⁺ (6 μM) + ascorbate (7.5 μM) + ebsulfur-7-carboxylic acid methyl ester (1, 50, 100, 200, 300 and 400 μM, respectively).....</p>	67
<p>2.16. Dose-response curves for iron-mediated DNA damage prevention under high-ethanol (1.7 M) conditions for A) tannic acid, B) protocatechuic acid, C) gallic acid, D) epicatechin, E) epigallocatechin gallate, and F) epigallocatechin.....</p>	68

List of Figures (Continued)

Figure	Page
2.17. Dose-response curves for A) copper-mediated DNA damage prevention by Trolox under high-ethanol conditions (1.7 M), B) iron-mediated DNA damage prevention by Trolox and 1.7 M ethanol, C) copper-mediated DNA damage with Trolox and 10 mM ethanol, and D) iron-mediated DNA damage with Trolox and 10 mM ethanol.	69
2.18. Dose-response curves for iron-mediated DNA damage prevention under ethanol (1.7 M) conditions for A) dmise, B) ebis, C) bipy, D) Edaravone, E) pyridine, and F) sepy ^{Me}	70
2.19. Dose-response curves for copper-mediated DNA damage prevention under high-ethanol (1.7 M) conditions for A) dmise, B) ebis, C) bipy, and D) Edaravone.	71
2.20. Dose-response curves for iron-mediated DNA damage prevention under high-ethanol (1.7 M) conditions for A) ebselen, B) ebselen- <i>N</i> -acetic acid, C) ebsulfur-7-carboxylic acid, and D) ebulfur-7-carboxylic acid methyl ester.	72
2.21. Dose-response curves for copper-mediated DNA damage prevention under high-ethanol conditions (1.7 M) for A) ebselen, B) ebselen- <i>N</i> -acetic acid, C) ebsulfur- <i>N</i> -acetic acid, D) ebsulfur-7-carboxylic acid, E) ebulfur-7-carboxylic acid methyl ester, and F) ebselen-7-carboxylic acid methyl ester.	73
2.22. Dose-response plot for EC in the DPPH-scavenging assay. Error bars are smaller than the data point symbols.	91
2.23. Dose-response plot for GA in the DPPH-scavenging assay. Error bars are smaller than the data point symbols.	92
2.24. Dose-response plot for PCA in the DPPH-scavenging assay. Error bars are smaller than the data point symbols.	93
2.25. Dose-response plot for TA in the DPPH-scavenging assay. Error bars are smaller than the data point symbols.	94
2.26. Dose-response plot for EGCG in the DPPH-scavenging assay. Error bars are smaller than the data point symbols.	95

List of Figures (Continued)

Figure	Page
2.27. Dose-response plot for sepy ^{Me} in the DPPH-scavenging assay. Error bars are smaller than the data point symbols.....	96
2.28. Dose-response plot for pyridine in the DPPH-scavenging assay. Error bars are smaller than the data point symbols.....	97
2.29. Dose-response plot for bipy in the DPPH-scavenging assay. Error bars are smaller than the data point symbols.....	98
2.30. Dose-response plot for dmise in the DPPH-scavenging assay. Error bars are smaller than the data point symbols.....	99
2.31. Dose-response plot for ebis in the DPPH-scavenging assay. Error bars are smaller than the data point symbols.....	100
2.32. Dose-response plot for Trolox in the DPPH-scavenging assay. Error bars are smaller than the data point symbols.....	101
2.33. Dose-response plot for Edaravone in the DPPH-scavenging assay. Error bars are smaller than the data point symbols.....	102
2.34. Dose-response plot for ebselen in the DPPH-scavenging assay. Error bars are smaller than the data point symbols.....	103
2.35. EPR spectra of Cu ²⁺ (300 μM), ascorbic acid (375 μM), H ₂ O ₂ (2.5 mM) and DMPO (30 mM) at the indicated time points.....	104
2.36. EPR spectra of Cu ²⁺ (300 μM), ascorbic acid (375 μM), H ₂ O ₂ (2.5 mM), DMPO (30 mM), and ethanol (1.7 M) at the indicated time points.....	105
2.37. EPR spectra of Fe ²⁺ (300 μM), H ₂ O ₂ (2.5 mM), and DMPO (30 mM) at the indicated time points.	106
2.38. EPR spectra of Fe ²⁺ (300 μM), H ₂ O ₂ (2.5 mM), DMPO (30 mM), and ethanol (1.7 M) at the indicated time points.	106
2.39. EPR spectra of Fe ²⁺ (300 μM), H ₂ O ₂ (2.5 mM), DMPO (30 mM), and ethanol (875 mM) at the indicated time points.	107

List of Figures (Continued)

Figure	Page
2.40. EPR spectra of Fe ²⁺ (300 μM), H ₂ O ₂ (2.5 mM), DMPO (30 mM), and ethanol (425 mM) at the indicated time points.	107
3.1. Structures of fluconazole (FLC) and deferoxamine (DFO).....	122
3.2. Gel electrophoresis images showing FLC-metal-mediated DNA damage for MW: 1 kb molecular weight marker; lane 1: plasmid DNA (p); lane 2: p + H ₂ O ₂ ; A) lane 3: p + FLC (50 μM) + H ₂ O ₂ ; lane 4: p + FLC (50 μM); lane 5: p + FeSO ₄ (2 μM) + H ₂ O ₂ ; lanes 6-13: p + H ₂ O ₂ + FLC (0.01, 0.1, 0.5, 1, 2, 4, 10, 50 μM, respectively) and FeSO ₄ (0.005, 0.05, 0.25, 0.5, 1, 2, 5, and 25 μM, respectively); B) lane 3: p + H ₂ O ₂ + FLC (25 μM); lane 4: p + FLC (25 μM); lane 5: p + H ₂ O ₂ + CuSO ₄ (6 μM) + ascorbate (7.5 μM); lane 6: p + H ₂ O ₂ + CuSO ₄ (12.5 μM); lanes 7-12: p + H ₂ O ₂ + FLC (0.1, 1, 5, 10, 18, 25 μM, respectively) + CuSO ₄ (0.05, 0.5, 2.5, 5, 9, and 12.5 μM, respectively).	127
3.3. Dose-response curves of DNA damage by A) Fe ²⁺ , H ₂ O ₂ with and without FLC and B) Cu ²⁺ , H ₂ O ₂ , and ascorbate (AA) with and without FLC (1.25 equiv. ascorbate was added to reduce Cu ²⁺ to Cu ⁺).....	128
3.4. Percent DNA damage comparing Fe ²⁺ (2 μM) + H ₂ O ₂ , Fe ²⁺ (9 μM) + DFO (9 μM) + H ₂ O ₂ with the addition of indicated FLC concentrations (3 μM, 9 μM, 27 μM, and 81 μM, respectively).	131
3.5. MALDI-TOF spectra of the identified A) [Cu(FLC) ₂ (OH)] ⁺ and B) [Fe(FLC) ₂] ⁺ complexes	135
3.6. Cyclic voltammograms for A) CuSO ₄ (100 μM), B) 1:2 Cu ²⁺ :FLC (100 μM:200 μM) in MOPS buffer (10 mM, pH 7.0), C) FeSO ₄ (300 μM), and D) 1:2 Fe ²⁺ :FLC (300 μM:600 μM) in MES buffer (10 mM, pH 6.0). All contain KNO ₃ (10 mM) as a supporting electrolyte. All samples were cycled at a scan rate of 100 mV/s.....	136
3.7. Cyclic voltammograms for FLC (300 μM) in MES buffer (10 mM, pH 6.0) with KNO ₃ (10 mM) as a supporting electrolyte. The solution was cycled at a scan rate of 100 mV/s.	137

List of Figures (Continued)

Figure Page

3.8. Gel image of DNA damage by iron with and without H₂O₂ and FLC. For all gel images, MW: 1 kb molecular weight marker; lane 1: plasmid DNA (p); lane 2: p + H₂O₂. (50 μM); A) lane 3: p + FeSO₄ (2 μM) + H₂O₂; lanes 4-12: p + FeSO₄ (0.05, 0.5, 5, 25, 37.5, 50, 75, 100, and 150 μM, respectively); B) lanes 3-10: p + H₂O₂ + FeSO₄, (0.005, 0.5, 0.25, 0.5, 1, 2, 5, and 12.5 μM, respectively); C) lane 3: p + FLC (200 μM), lane 4: p + FeSO₄ (2 μM) + H₂O₂; lanes 5-10: p + FLC (0.1, 1, 10, 50, 100, and 200 μM respectively) + FeSO₄ (0.05, 0.5, 5, 25, 50, and 100 μM, respectively).... 137

3.9. Gel image of DNA damage by iron with and without H₂O₂ and FLC and ascorbate. For all gel images MW: 1 kb molecular weight marker; lane 1: plasmid DNA (p); lane 2: p + H₂O₂. (50 μM); A) lane 3: p + ascorbate (375 μM); lane 4: p + FeSO₄ (2 μM) + H₂O₂; lane 5-11: p + FeSO₄ (2, 10, 25, 50, 100, 150, and 500 μM, respectively) + ascorbate (2.5, 12.5, 31.25, 62.5, 125, 187.5, and 375 μM, respectively); B) lane 3: p + FLC (600 μM), lane 4: p + H₂O₂ + FeSO₄ (2 μM); lanes 5-11: p + FeSO₄ (2, 10, 25, 50, 100, 150, and 300 μM, respectively) + AA (3.5, 12.5, 31.25, 62.5, 125, 187.5, 375 μM, respectively) + FLC (4, 20, 50, 100, 200, 300, and 600 μM, respectively); C) lane 3: p + H₂O₂ + FeSO₄ (2 μM); lanes 4-12: p + FeSO₄ (0.005, 0.5, 0.25, 0.5, 0.75, 1, 1.5, 2 and 5 μM, respectively) + ascorbate (0.00625, 0.0625, 0.3125, 0.625, 0.9375, 1.25, 1.875, 2.5, and 6.25 μM, respectively); D) lane 3: p + H₂O₂ + FLC (20 μM) + AA (12.5 μM); lane 4: p + H₂O₂ + FeSO₄ (2 μM); lanes 5-13: p + H₂O₂ + FeSO₄ (0.005, 0.5, 0.25, 0.5, 0.75, 1, 1.5, 2, and 5 μM, respectively) + FLC (0.01, 0.1, 0.5, 1, 1.5, 2, 3, 4, and 10 μM, respectively) + AA (0.00625, 0.0625, 0.3125, 0.625, 0.9375, 1.25, 1.875, 2.5, and 6.25 μM, respectively). 138

List of Figures (Continued)

Figure	Page
<p>3.10. Gel image of DNA damage by copper FLC, H₂O₂ and, where indicated, ascorbate. For all gel images MW: 1 kb molecular weight marker; lane 1: plasmid DNA (p); lane 2: p + H₂O₂. (50 μM); A) lanes 3-15: p + H₂O₂ + CuSO₄ (0.05, 0.5, 2, 3, 4, 5, 6, 7, 8, and 12.5 μM, respectively) + AA (0.0625, 0.625, 2.5, 3.75, 5, 6.25, 7.5, 8.75, 10, and 15.625 μM, respectively); B) lane 3: p + FLC (600 μM); lane 4: p + H₂O₂ + CuSO₄ (6 μM) + ascorbate (7.5 μM); lane 5: p + CuSO₄ (300 μM); lanes 6-11: p + FLC (0.1, 1, 10, 100, 300, and 600 μM, respectively) + CuSO₄ (0.05, 0.5, 5, 50, 150, and 300 μM, respectively); C) lane 3: p + FLC (600 μM); lane 4: p + H₂O₂ + CuSO₄ (6 μM) + ascorbate (7.5 μM); lanes 5-12: p + CuSO₄ (0.05, 0.5, 5, 12.5, 25, 50, 150, and 300 μM, respectively) + ascorbate (0.0625, 0.625, 6.25, 15.625, 31.25, 62.5, 187.5, and 375 μM, respectively) + FLC (0.1, 1, 10, 25, 50, 100, 300, and 600 μM, respectively); D) lane 3: p + H₂O₂ + FLC (25 μM); lane 4: p + FLC (25 μM); lane 5: p + H₂O₂ + CuSO₄ (6 μM) + ascorbate (7.5 μM); lane 6: p + H₂O₂ + CuSO₄ (12.5 μM); lanes 7-12: p + H₂O₂ + FLC (0.1, 1, 5, 10, 18, and 25 μM, respectively) + CuSO₄ (0.05, 0.5, 2.5, 5, 9, and 12.5 μM, respectively); E) lane 3: p + H₂O₂ + FLC (600 μM); lane 4: p + FLC (600 μM); lane 5: p + H₂O₂+ FLC (600 μM) + ascorbate (375 μM); lane 6: p + FLC (600 μM) + ascorbate (375 μM); lane 7: p + H₂O₂ + CuSO₄ (6 μM) + ascorbate (7.5 μM); lanes 8-15: p + H₂O₂+ CuSO₄ (0.05, 0.5, 5, 12.5, 25, 50, 150, 300 μM, respectively) + ascorbate (0.0625, 0.625, 6.25, 15.625, 31.25, 62.5, 87.5, 375 μM, respectively) + FLC (0.1, 1, 10, 25, 50, 100, 300, and 600 μM, respectively).</p>	139
<p>3.11. Gel image of DNA damage by copper or iron FLC, H₂O₂ and DFO. For all gel images MW: 1 kb molecular weight marker; lane 1: plasmid DNA (p); lane 2: p + H₂O₂ (50 μM); A) lane 3: p + H₂O₂+ DFO (50 μM); lane 4: p + DFO (50 μM); lane 5: p + FeSO₄ (50 μM) + DFO (50 μM); lane 6: p + H₂O₂ + FeSO₄ (2 μM); lanes 7-8: p + H₂O₂ + FeSO₄ (0.1, 1, 2, 5, 7.5, 10, 25, and 50 μM, respectively) + DFO (0.1, 1, 2, 5, 7.5, 10, 25, and 50 μM, respectively, respectively); B) lane 3: p + FeSO₄ (9 μM); lane 4: p + H₂O₂ + FLC (9 μM); lane 5: p + H₂O₂ + FeSO₄ (9 μM) + DFO (9 μM); lane 6: p + FeSO₄ (9 μM) + DFO (9 μM); lane 7: p + H₂O₂ + FeSO₄ (2 μM); lane 8-10: p + H₂O₂ + FeSO₄ (9 μM) + DFO (9 μM) + FLC (3 μM); lanes 11-13: p + H₂O₂ + FeSO₄ (9 μM) + DFO (9 μM) + FLC (9 μM); lanes 14-16: p + H₂O₂ + FeSO₄ (9 μM) + DFO (9 μM) + FLC (27 μM); lanes 17-19: p + H₂O₂ + FeSO₄ (9 μM),+ DFO (9 μM) + FLC (81 μM). .</p>	140

List of Figures (Continued)

Figure	Page
3.12. Dose-response curves for DNA damage by A) Cu ²⁺ and FLC, B) Cu ²⁺ , FLC, and H ₂ O ₂ , and C) Cu ²⁺ and ascorbate with and without FLC.	141
3.13. Dose-response curves for DNA damage by A) Fe ²⁺ ; B) Fe ²⁺ and FLC; C) Fe ²⁺ and ascorbate (AA) with and without FLC; D) Fe ²⁺ , ascorbate, and H ₂ O ₂ with and without FLC; and E) Fe ²⁺ , DFO, and H ₂ O ₂	142
4.1. In box: Structures of catechol and gallol groups and their metal coordination modes. Outside box: an example condensed tannin structure showing A-type and B-type linkages, selected polyphenol structures, and the structure of 2,2-diphenyl-1-picrylhydrazyl (DPPH)....	157
4.2. Agarose gel electrophoresis images of DNA treated with various concentrations of <i>V. macrocarpon</i> CTs with A) Cu ²⁺ (6 μM) and ascorbate (7.5 μM) or B) Fe ²⁺ (2 μM) and H ₂ O ₂ . Damaged (nicked) plasmid DNA (p) is the top band and undamaged (supercoiled) DNA is in the bottom band. Lanes are MW: 1 kb DNA ladder; 1: p; 2: p + H ₂ O ₂ (50 μM); A) 3: p + H ₂ O ₂ + <i>V. macrocarpon</i> CTs (200 mg/L); 4: p + H ₂ O ₂ + Cu ²⁺ (6 μM) + ascorbate (7.5 μM); 5-14: p + H ₂ O ₂ + Cu ²⁺ (6 μM) + ascorbate + <i>V. macrocarpon</i> CTs (0.1, 1, 5, 15, 25, 50, 100, and 200 mg/L respectively). B) 3: p + H ₂ O ₂ + <i>V. macrocarpon</i> CTs (5 mg/L); 4: p + H ₂ O ₂ + Fe ²⁺ (2 μM); 5-13: p + H ₂ O ₂ + Fe ²⁺ (2 μM) + <i>V. macrocarpon</i> CTs (0.001, 0.01, 0.1, 0.5, 1, 2.5, and 5 mg/L respectively).	162
4.3. Dose-response curves for copper- and iron-mediated DNA damage prevention by A) <i>V. macrocarpon</i> CTs, B) <i>V. vinifera</i> seed CTs, C) <i>H. lupulus</i> CTs (the data point at 0.01 mg/L was excluded from the iron-mediated DNA damage fit due to its negative value), and D) <i>T. inflorescentia</i> CTs (the data points at 0.1 and 0.5 mg/L were excluded from the iron-mediated DNA damage due to their negative values).	163

List of Figures (Continued)

Figure	Page
<p>4.4. Agarose gel electrophoresis images of copper-mediated DNA damage prevention with <i>Vitis vinifera</i> seed, <i>Humulus lupulus</i>, or <i>Tilia inflorrescentia</i> condensed tannins. Lanes are: MW: 1 kb molecular weight marker; lane 1: plasmid DNA (p); lane 2: p + H₂O₂ (50 μM); A) lane 3: p + 200 mg/L <i>V. vinifera</i> seed + H₂O₂, lane 4: p + Cu²⁺ (6 μM) + ascorbate (7.5 μM) + H₂O₂; lanes 5-13: p + Cu²⁺ + ascorbate + H₂O₂ + 0.1, 1, 5, 10, 15, 25, 50, 100, and 200 mg/L <i>V. vinifera</i> seed, respectively; B) lane 3: p + 200 mg/L <i>H. lupulus</i> + H₂O₂, lane 4: p + Cu²⁺ (6 μM) + ascorbate (7.5 μM) + H₂O₂; lanes 5-13: p + Cu²⁺ + ascorbate + H₂O₂ + 0.1, 1, 5, 10, 15, 25, 50, 100, and 200 mg/L <i>H. lupulus</i>, respectively; C) lane 3: p + 200 mg/L <i>T. inflorrescentia</i> + H₂O₂, lane 4: p + Cu²⁺ (6 μM) + ascorbate (7.5 μM) + H₂O₂; lanes 5-13: p + Cu²⁺ + ascorbate + H₂O₂ + 0.1, 1, 5, 10, 15, 25, 50, 100, and 200 mg/L <i>T. inflorrescentia</i>, respectively.....</p>	176
<p>4.5. Agarose gel electrophoresis images of iron-mediated DNA damage prevention with <i>Vitis vinifera</i> seed, <i>Humulus lupulus</i>, or <i>Tilia inflorrescentia</i> condensed tannins. Lanes are: MW: 1kb molecular weight marker; lane 1: plasmid DNA (p); lane 2: p + H₂O₂ (50 μM); A) lane 3: p + 200 mg/L <i>V. vinifera</i> seed + H₂O₂, lane 4: p + Fe²⁺ (2 μM) + H₂O₂; lane 5-14: p + Fe²⁺ + H₂O₂ + 0.001, 0.01, 0.1, 0.5, 1, 2.5, 5, 10, 25, and 50 mg/L <i>V. vinifera</i> seed, respectively; B) lane 3: p + 200 mg/L <i>H. lupulus</i> + H₂O₂, lane 4: p + Fe²⁺ (2 μM) + H₂O₂; lane 5-14: p + Fe²⁺ + H₂O₂ + 0.001, 0.01, 0.1, 0.5, 1, 2.5, 5, 10, 25, and 50 mg/L <i>H. lupulus</i>, respectively; C) lane 3: p + 200 mg/L <i>T. inflorrescentia</i> + H₂O₂, lane 4: p + Fe²⁺ (2 μM) + H₂O₂; lane 5-14: p + Fe²⁺ + H₂O₂ + 0.001, 0.01, 0.1, 0.5, 1, 2.5, 5, 10, 25, and 50 mg/L <i>T. inflorrescentia</i>, respectively.</p>	177

LIST OF SCHEMES

Scheme	Page
1.1. Thermal decomposition to obtain the AAPH radical used in the ORAC assay.....	3

CHAPTER ONE

SHOULD AND CAN THE ORAC ANTIOXIDANT ASSAY BE REPLACED?

1.1 Introduction

Why Do We Care About Antioxidants? Reactive oxygen species (ROS), such as superoxide (O_2^{2-}) and hydroxyl radical ($\cdot OH$), and reactive nitrogen species (RNS), such as $ONOO^-$ and $NO\cdot$,¹⁻⁶ control a variety of physiological responses such as changes in gene expression, apoptosis, and proliferation.⁷ ROS and RNS play an important role in the development of many diseases,^{6,8,9} including atherosclerosis,¹⁰ neurodegenerative diseases,^{6,11-15} inflammation,^{6,15,16} cancer,¹⁷⁻¹⁹ and aging.^{1,3,20-23} A diverse array of antioxidants, including polyphenols, vitamins C and E, and carotenoids, can prevent damage caused by ROS.²⁴⁻²⁸ Therefore, researchers have attempted to quantify and compare the ability of antioxidants to prevent ROS damage and to understand the mechanisms by which they prevent this damage.

Currently, there is no accepted “total antioxidant parameter” as a nutritional index available for the labeling of food and biological fluids due to the lack of standardized quantitation methods,²⁹ and many reviews have been published about various issues and opinions about antioxidant measurement.³⁰⁻³⁸ Frankel and Meyer³⁸ point out the difficulties with using one-dimensional methods to evaluate multifunctional food and biological antioxidants. The authors suggest a suitable protocol should fulfill several factors; (a) have a biologically relevant substrate, (b) be tested under various oxidation conditions, (c) measure initial and secondary oxidation products, (d) compare antioxidants at the same

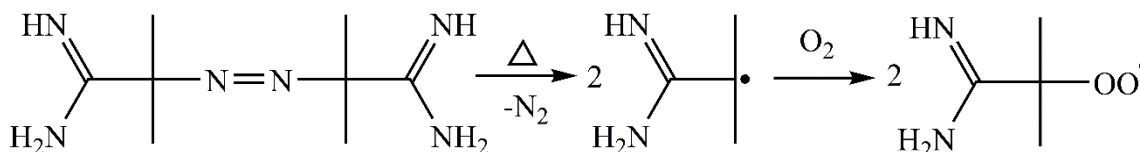
molar concentrations of active components, and (e) quantify antioxidants on the basis of induction period, percent inhibition, rates of hydroperoxide formation or decomposition, or IC₅₀ (concentration to inhibit 50% damage) values. The many assays for measuring antioxidant efficacy are different in terms of substrates, probes, reaction conditions, quantitation methods, solvents, and radical sources. Thus, it is extremely challenging to compare results from different assays.³⁸ In addition, new assays claiming to measure antioxidant capacity are continually being introduced.^{39,40}

This Chapter does not discuss all antioxidant assays in their complexity and variations. Instead, the intent of this review is to illustrate the diversity and complexity of the topic and to highlight aspects that are often neglected, such as biological relevance and difficulty in comparison between different assays. Where possible, review articles are referenced for further reading about common antioxidant assays and their limitations.

The History of The Oxygen Radical Absorbance Capacity Assay. The oxygen radical absorbance capacity (ORAC) assay has found broad application for measuring the antioxidant capacity of botanical⁴¹ and biological³⁶ samples. In 2007, the United States Department of Agriculture (USDA) released the first database of antioxidant activity for 277 selected foods followed by 326 additional entries in 2010. The USDA published these tables to compare various foods and food additives using a standardized method so that nutraceutical companies could use them to educate consumers about the comparative antioxidant benefits of products.^{42, 46} In 2012, the USDA withdrew all of their ORAC tables for two reasons: 1) the routine misuse by food and dietary supplement companies to promote products, and 2) the *in vitro* ORAC data for antioxidant capacity of foods did not

predict *in vivo* effects, coupled with mixed results in clinical trials to test the benefits of dietary antioxidants.⁴³

The ORAC method does not use a biologically relevant radical, and does not measure prevention of ROS or RNS generation.⁴² However, the number of publications using ORAC as method for antioxidant measurement is steadily increasing every year (2003: 16; 2012: 182; 2019: 249 new publications).⁴⁴ This assay uses a peroxy radical generator, 2,2'-azobis(2-amidinopropane) dihydrochloride (AAPH; Figure 1.1) and measures the decrease in fluorescence due to oxidative degradation at 510 and 700 nm. Radical scavengers protect the fluorescent molecule from reacting with the peroxy radical.



Scheme 1.1. Thermal decomposition to obtain the AAPH radical used in the ORAC assay.

Özyürek et al.²⁹ discuss the importance of terminology when comparing antioxidants, since some assays measure antioxidant activity and others antioxidant capacity. Antioxidant activity typically describes the kinetics of quenching reactive species and is usually expressed as reaction rates or scavenging percentages per unit time, whereas antioxidant capacity is the thermodynamic conversion efficiency of reactive species by antioxidants, such as the number of moles of reactive species scavenged by one mole of antioxidant during a fixed time period. Both are important factors in measuring antioxidant efficacy. Antioxidant assays can be classified with respect to their approaches: type of ROS response measured *in vivo* or *in vitro* or mechanism of action (Figures 1.1 and 1.2).²⁹

Indirect Enzymatic Assays	Nonenzymatic Assays	Cellular Assays	Direct Enzymatic Assays
<ul style="list-style-type: none"> • Reduced Glutathione (GSH) Estimation • Lipid Peroxidation (LPO) Assay • LDL Oxidation 	<ul style="list-style-type: none"> • Enhanced Chemiluminescence (ECL) • FRAP • TBARS • ABTS • Folin-Ciocalteu Method • DPPH • CUPRAC • TEAC • ORAC 	<ul style="list-style-type: none"> • Polyphenol Content Analysis • Total Antioxidant Capacity • Protein Oxidation • Cellular Antioxidant Activity (CAA) Assay • Dye-substrate Oxidation Method 	<ul style="list-style-type: none"> • Superoxide Dismutase (SOD) Method • Catalase (CAT) • Glutathione Peroxidase (GSHPx) Estimation • Glutathione Reductase (GR) • Glutathione-S-transferase (GSt) Assay

Figure 1.1. Classification of assays to evaluate antioxidant activity *in vivo* and in cells by assay type.

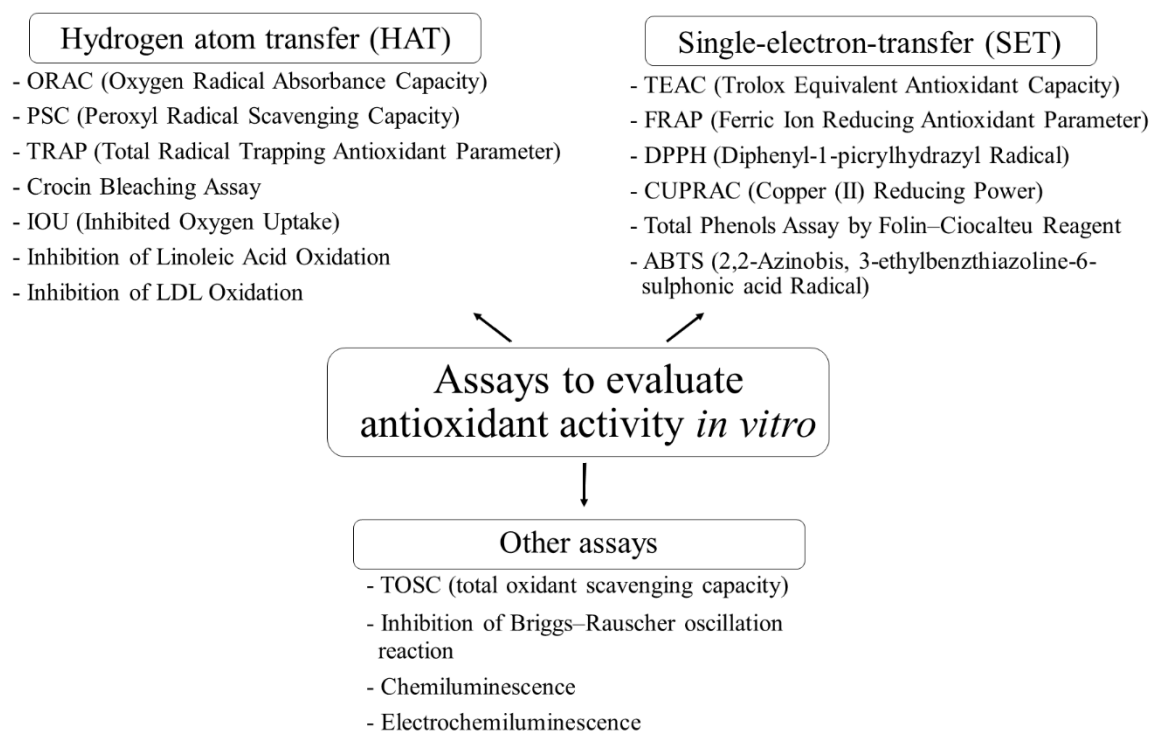


Figure 1.2. *In vitro* antioxidant assays classified by mechanism.

Antioxidant assays are often grouped by their general mechanism (Figure 1.2), such as hydrogen atom transfer (HAT; Reaction 1) and single electron-transfer (SET; Reaction 2), where AH represents the antioxidant in these reactions and M represents an electron donor, for example a metal. HAT assays are usually competitive and measure antioxidant activity, whereas SET assays are usually noncompetitive, evaluate total antioxidant capacity, and involve a redox reaction with the probe.^{30,45}

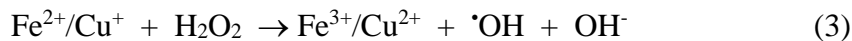


In the competitive HAT assays, the oxidant reacts with a target species, leading to changes in its spectroscopic properties that are measured by changes in absorbance, fluorescence, or luminescence. Antioxidants typically compete against another molecule, such as fluorescein, for the oxidant. Thus, less fluorescein is oxidized by the ROS in the presence of an antioxidant, and quantitation is derived from the kinetic curves obtained.⁴⁵ HAT assays can involve photochemically unstable radicals or incomplete trapping of radicals by the antioxidant, resulting in an underestimation of antioxidant activity.

SET-based assays measure the capacity of an antioxidant to reduce an oxidant resulting in a color or fluorescence change.^{30,32} SET assays are quantified by the degree of the color change, which is proportional to antioxidant concentration.³⁰ These assays assume a correlation of antioxidant capacity with reducing capacity.³⁰ This mechanistic picture is complicated by the fact that antioxidants can react through multiple mechanisms rather than through only one predominant mechanism.⁴⁶ Therefore, the division of antioxidant

activity into two major mechanistic classes of assays may result in neglecting to consider multiple possible antioxidant mechanisms that may also be dose-dependent.

Metals Are Important But Neglected. Hydroxyl radical ($\cdot\text{OH}$) is generated by the oxidation of primarily iron and copper *in vivo* and *in vitro* (Reaction 3).⁴⁷ Iron-mediated formation of $\cdot\text{OH}$ from hydrogen peroxide (H_2O_2) is the primary cause of DNA damage and cell death under oxidative stress conditions in prokaryotes⁴⁸ and eukaryotes, including humans.⁴⁹⁻⁵¹ The reduced metal ions can be regenerated by cellular reductants, making hydroxyl radical generation catalytic in cells.^{51,52} Oxidative DNA damage occurs in two ways: damage to the phosphate backbone resulting in strand breaks and oxidation of the nucleotide bases. Both types of DNA damage can be quantified.⁵³⁻⁵⁸



Copper and iron play important roles in various diseases, including Alzheimer's and Parkinson's diseases, among others.^{6,11-15,59} The hydroxyl radical is likely the final facilitator of most radical induced tissue damage.^{60,61} Almost all ROS give rise to hydroxyl radical formation, and the hydroxyl radical is extremely short-lived, reacting with almost every type of molecule found in living cells including sugars, amino acids, lipids, and nucleotides.⁶⁰ Although hydroxyl radical formation can occur in several ways, the most important mechanism *in vivo* is through transition-metal-catalyzed decomposition of superoxide and hydrogen peroxide.⁵⁹

Iron-mediated DNA damage is the most investigated, since it is the underlying cause of many diseases.^{16,18,23-25,29-35,47} Non-protein-bound Fe^{2+} concentrations are around 10 μM in *E. coli* and humans.⁶³ Under oxidative stress conditions, these concentrations can

increase to 80–320 μM in *E. coli*,^{47,52,62,63} and Linn *et al.*^{48,64,65} have shown that iron-mediated DNA damage is the underlying cause of cell death of *E. coli* under oxidative stress. Iron coordinates to DNA *in vivo* resulting in the production of the hydroxyl radical in close proximity.⁴⁸

Copper concentrations in human serum can range from 10 to 25 mM ^{47,66,67} but increase to 0.1 mM under several metabolic processes.^{47,68} DNA damage can be detected through backbone breakage, base oxidation, inter- and intra-strand crosslinking, and DNA–protein crosslinking.⁴⁷ Cu^{2+} and has been shown to coordinate to the DNA double helix and promote double-strand breakage through the Fenton-like reaction (Reaction 3).^{69–71} Halliwell *et al.*^{72,73} emphasized that oxidative DNA damage is an important biomarker for ROS damage. DNA is one of the most important biomolecules and target of ROS and there are numerous mechanisms to counteract DNA damage.^{72,74}

Duthie *et al.*⁷⁵ have described the ability of antioxidants to prevent oxidation through different mechanisms: 1) transition metal coordination to prevent radical formation, 2) reducing high concentrations of $\text{O}_2^{\cdot-}$, and 3) scavenging radicals (Figure 1.3). Since antioxidants can prevent metal-DNA damage through several mechanisms, it is important to measure direct DNA damage instead of individual mechanisms to gain a complete picture of antioxidant activity.

The Issue with Trolox. A common standard to measure antioxidant activity is 6-hydroxy-2, 5, 7, 8-tetranethylchroman-2-carboxylic acid (Trolox), a water soluble Vitamin E derivative.⁷⁶ It was first reported by Cort in 1975^{77,78} and was quickly adopted as a positive control for *in vitro*^{79,80} and *in vivo*⁸¹ assays, with tested antioxidants compared to

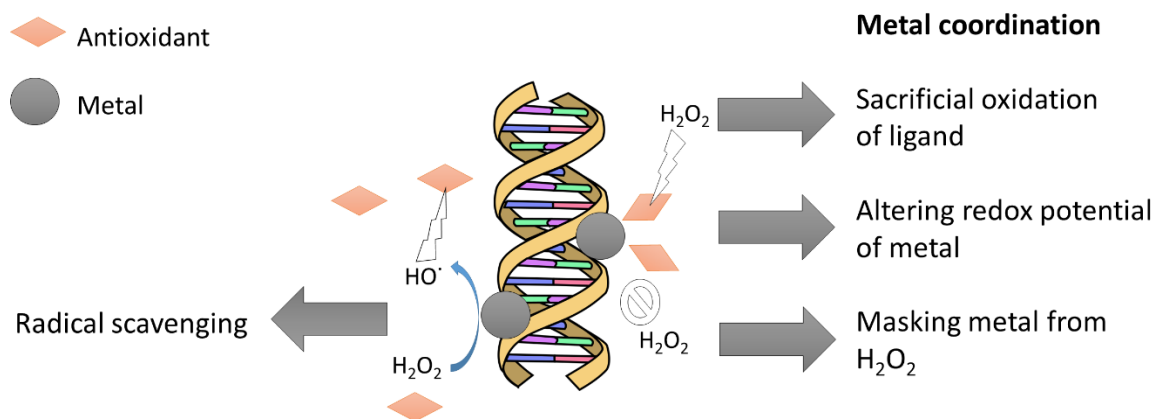


Figure 1.3. Antioxidants can prevent metal-mediated DNA damage through different mechanisms.

it using the Trolox equivalent (TE) metric. Trolox is a known radical scavenger, but the exact mechanism of its activity is not fully understood.⁸²

One of the primary issues with using Trolox as a standard, which is not commonly discussed, is that comparing antioxidants to a compound that can only scavenge radicals results in the neglect of other mechanisms by which antioxidants may prevent damage. For example, glutathione (GSH), a naturally occurring antioxidant with intracellular concentrations of up to 10 mM,⁸³ plays an important role in metal homeostasis and can prevent oxidative DNA damage by metal coordination.⁸⁴ Perron *et al.*²⁴ correlated the pK_a of the most acidic phenolic hydrogen for polyphenols versus their iron-mediated DNA damage prevention ability. These results established iron binding as the mechanism of the observed antioxidant activity. In addition, Vacek *et al.*⁸⁵ highlighted the importance of copper-chelation for the DNA damaging ability of the semi-synthetic flav-onolignan 7-O-galloylsilybin using electrochemistry and density-functional theory (DFT) calculations.

1.2 Assays Measuring Antioxidant Radical Scavenging

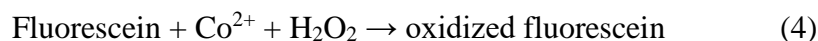
Oxygen Radical Absorbance Capacity Assay. The oxygen radical absorbance capacity (ORAC) assay combines two different factors, inhibition time and degree of inhibition. Initially, the intensity of the fluorescent molecule β -phycoerythrin is measured. Peroxyl radicals, generated through thermal decomposition, react with β -phycoerythrin, resulting in a decrease in fluorescence. Trolox (1.0 $\mu\text{M/L}$) is used as a standard for this assay, and antioxidant activity is expressed in Trolox equivalents (TE)/g. In theory, antioxidants react with the peroxyl radical, preventing the expected fluorescence decrease (Scheme 1.1).⁷⁶

Use of β -phycoerythrin has some shortcomings, including variability in its reactivity with peroxyl radicals, photobleaching, and interactions with polyphenols by non-specific binding. These issues resulted in the testing of alternatives such as 3',6'-dihydroxyspiro[isobenzofuran-1[3H],9'[9H]-xanthen]-3-one and dichlorofluorescein.⁷⁶ The most established fluorescent molecule is fluorescein since it is cheap and can be used with little interference from tested antioxidants.⁴²

The ORAC assay was first introduced by Cao *et al.*⁸⁶ in 1993 and quickly became very popular due to its ease of use after Cao and Prior's modifications.^{30,87,88} In 2003, the USDA rewarded the collaborating Brunswick and Prior a Small Business Innovation Research (SBIR) grant to develop ORAC assays for singlet oxygen, hydroperoxide, and superoxide anion.⁴² This panel of ORAC tests was hoped to provide a comprehensive antioxidant profile with applications across nutritional and human health markets. Due to the extended development of ORAC assays, standardized protocols for various solvent

systems and sample origins exist. Advantages of these ORAC assays are therefore flexibility in solvent choice, either aqueous or organic as well as ease of measurement.^{89,90} Disadvantages of ORAC assay, including the use of non-biological relevant radical, the lack of measuring ROS or RNS generation, and misuse by food and dietary supplement companies, have been discussed previously in the *History of The Oxygen Radical Absorbance Capacity Assay* section.

Hydroxyl Radical Averting Capacity (HORAC) Assay. The hydroxyl radical averting capacity (HORAC) assay is based on oxidation of fluorescein by hydroxyl radical *via* HAT. Hydroxyl radical is generated by treating H₂O₂ with Co²⁺ (Reaction 4), as first reported by Ou *et al.*⁸⁹ In this assay, samples such as food items, extracts, or individual compounds, are dissolved in methanol and diluted with phosphate buffer (pH 7.4), and the antioxidant binds Co²⁺ to prevent hydroxyl radical formation. Antioxidant effectiveness is based on the inhibition of fluorescein oxidation by hydroxyl radical through a HAT mechanism. Although the quantification is similar to the ORAC assay, there is no correlation between the results of the two assays.⁸⁹



2,2-Diphenyl-1-picrylhydrazyl radical assay. The 2,2-diphenyl-1-picrylhydrazyl radical (DPPH) assay was developed by Blois⁹¹ in 1958, and it is one of the most common antioxidant assays. Sanchez-Moreno *et al.*⁹² suggested that the DPPH assay was an easy and accurate method for measuring the antioxidant capacity of fruit and vegetable juices or extracts. DPPH radical is a very stable, nitrogen-based radical, and it is commercially available. DPPH is reduced by receiving a hydrogen atom from an antioxidant to form the

corresponding hydrazine.⁹³ This assay measures decolorization through radical quenching of the violet DPPH at 515 nm. DPPH assays are commonly carried out in methanol or a methanol/water mixture,^{94,95} and results are measured after a defined time period, typically 30 minutes.⁹⁴

DPPH is sensitive to oxygen, some Lewis bases, and solvents.⁹⁶ In addition, DPPH has very limited aqueous solubility, and the interference of antioxidant absorbances with DPPH absorbances can present a problem for quantitative analysis.³⁴ An advantage of the DPPH assay is that the reaction time can be adjusted based on the reactivity and size of the antioxidant.⁹⁷ Several reviews further discuss the pitfalls of this assay, including reproducibility among different laboratories; limited stability if the solution is not prepared relatively fresh, resulting in issues with long-duration experiments; its low solubility in aqueous solutions; and interference caused by amino acids, peptides, or proteins due to the ability of DPPH to deprotonate them.^{79,80,98}

2,2'-Azinobis(3-ethyl-benzothiazoline-6-sulfonic acid assay. The 2,2'-azinobis(3-ethyl-benzothiazoline-6-sulfonic acid (ABTS) assay, also sometimes called the Trolox equivalent antioxidant capacity (TEAC) assay, is a discoloration assay used for lipophilic and hydrophilic antioxidants first introduced by Re *et al.*⁹⁹ The pre-formed radical cation of 2,2'-azinobis-(3-ethylbenzothiazoline-6-sulfonic acid, ABTS^{•+}) is generated by ABTS oxidation with potassium persulfate, and it is reduced in the presence of hydrogen-donating antioxidants in ethanol or phosphate buffer.⁹⁹ Antioxidant activity is measured by the depletion of the colored ABTS^{•+}, measured at 734 nm.⁹⁹ Antioxidant activity is expressed as the concentration of antioxidants giving the same percentage change in absorbance as

1mM Trolox resulting in the unit Trolox-equivalent antioxidant capacity (TEAC/mg).³⁷ ABTS assay results correlate better with the ORAC assay results than DPPH assay results.¹⁰⁰ In addition, the ABTS radical has multiple wavelengths that allow analysis with less interference than DPPH. The ABTS radical (unlike DPPH) is soluble in water, allowing for the testing of both hydrophobic and hydrophilic compounds. The ABTS radical is only stable for several minutes at room temperature, significantly impacting reproducibility of results.¹⁰¹

Thiobarbituric-Acid-Reactive-Substance Assay. The thiobarbituric-acid-reactive-substance assay (TBARS) has been used for the estimation of lipid peroxidation since the early 1950s. It is considered an index of lipid peroxidation.¹⁰² Malondialdehyde (MDA) is produced as a side product by autooxidation or reaction with ROS and enzymatic degradation of polyunsaturated fatty acids in cells. The reactive aldehyde, MDA causes toxic stress in cells as it reacts with proteins and DNA. In the TBARS assay, MDA reacts with two equivalents of thiobarbituric acid (TBA) by an acid-catalyzed, nucleophilic-addition reaction, resulting in a pink color that can be measured at 532 nm.^{102–104} This method is sensitive to low levels of MDA in cells, but it may overestimate the amount of cellular MDA,^{102,105} since cellular carbohydrates and phenylpropanoid-type pigments can interfere with TBARS results. This interference can become a significant issue, since different plants and cells have different carbohydrate concentrations and their concentrations can vary depending on previously induced stress.^{102,104,106–108} The advantages of the TBARS assay is its simplicity, its inexpensiveness, and its ability to be used in high throughput assays and processed with minimal sample manipulation.

Enhanced Chemiluminescence Assay. The enhanced chemiluminescence (ECL) assay, first introduced by Hirayama *et al.*,¹⁰⁹ is based on the measurement of enhanced luminescence of the luminol radical compared to luminol, so the reaction is dependent on the constant production of luminol-based radicals. In the original assay, the hydroxyl radical was generated by the Fenton reaction (Reaction 3, using H₂O₂, Fe²⁺, and luminol in a borate buffer (pH 7.4)).¹⁰⁹ More common currently is the use of horse radish peroxidase (HRP)-catalyzed oxidation of the chemiluminescent luminol by hydrogen peroxide.¹¹⁰ Antioxidants scavenge the luminol radical, resulting in a temporary loss of emission at 425 nm.^{110,111} Emission resumes after the antioxidant is consumed, and antioxidant effectiveness is obtained from comparison to standard calibration curves and measures time of depressed light emission versus the concentration of the antioxidant in μmol/L.^{111,112} Once again, Trolox is commonly used as a standard.¹¹¹ Advantages of the ECL assay include the ability to use it for high-throughput screening due to its rapid measurement time, typically 40 to 45 minutes.^{112,113} The assay can be performed using organic or aqueous solvents, but direct comparisons between different assays performed in different solvent systems is difficult.

1.3. Assays Measuring the Metal Reducing Power of Antioxidants

The Ferric Reduction Antioxidant Power Assay. The ferric reduction antioxidant power (FRAP) assay was first introduced by Benzie and Strain¹¹⁴ in 1996 for the evaluation of the antioxidant capacity of human plasma and was later extended for other uses.⁷⁶ A variety of samples can be analyzed using this method, including fruits, juices,

tissue samples, plasma, blood, and nutritional supplements. Antioxidant activity is evaluated from reduction of the $\text{Fe}^{\text{III}}(\text{TPTZ})_2\text{Cl}_3$ (TPTZ = 2,4,6-tri(2-pyridyl)-s-triazine) complex to the Fe^{2+} complex in acetate buffer (pH 3.6). The increasing blue color of the Fe^{2+} complex can be measured at 593 nm with an extinction factor of $22,230 \text{ M}^{-1}\text{cm}^{-1}$. FRAP values can be obtained by the comparison of the absorbance change in the test mixture with those obtained from a calibration curve derived from increasing concentrations of Fe^{2+} . The reference for antioxidant activity in this assay is most commonly Trolox and sometimes ascorbic acid or uric acid, with units typically expressed as Trolox equivalents (mg/100 g).

The reduction potential of the Fe^{3+} salt to Fe^{2+} (~0.70 V) is comparable to ABTS^{•-} in the Trolox equivalent antioxidant capacity (TEAC) assay (0.68 V). The difference between the FRAP and TEAC assays is the pH of the reaction; the TEAC assay is performed at a neutral pH, whereas FRAP is performed at a pH of 3.6. This is one of the biggest disadvantages of FRAP, since it is not performed at a physiologically relevant pH. The reaction is also non-specific, there can be possible iron chelation interference, and it is not suitable for slowly reactive polyphenol compounds. In addition, it cannot evaluate the antioxidant activity of species that act by hydrogen transfer, such as many natural occurring thiols (including glutathione or proteins).⁷⁶

The advantages of the FRAP and TEAC assays are their simplicity, since no special or expensive equipment is necessary, reagents are simple to prepare, and it is reproducible and fast (30 min or less) with a straightforward procedure that can be automated, semi-automated or performed manually.¹¹⁴

The Cupric Reducing Antioxidant Capacity Assay. The cupric reducing antioxidant capacity (CUPRAC) assay is similar to the FRAP assay, since it is based on measuring an antioxidant's ability to reduce copper(II)-neocuproine (Cu(II)-Nc) or copper(II)-bathocuproine in ammonium acetate buffer (pH 7).²⁹ This assay was first introduced in 2004 by Apak *et al.*¹¹⁵ and is an electron transfer assay. Cu²⁺ reduction is quantified by decreasing absorbances at 490 and 450 nm, respectively,^{29,76} with the degree of color directly correlated to the antioxidant concentration.²⁹ The reaction is complete after 30 min and therefore fairly fast, similar to the FRAP and TEAC assays. Antioxidant capacity is reported in Trolox equivalents, defined as the reducing potency of a 1 mM Trolox solution.²⁹ Unlike FRAP, CUPRAC can measure thiols such as glutathione.

The Folin-Ciocateu Total Phenolic Assay. The Folin-Ciocateu (FC) method was originally developed for protein determination by taking advantage of the Folin reagent's reactivity with the tyrosine residues in proteins.¹¹⁶ Singleton *et al.*^{30,117} adapted this assay to determine the polyphenol content in wine. This assay oxidizes phenol compounds through a semioquinone radicals into quinones¹¹⁷ in alkaline solution (pH 10) using the Folin reagent, molybdotungstophosphate heteropolyanion (3H₂O-P₂O₅-13WO₃-5MoO₃-10H₂O). The resulting reduced Folin reagent has a yellow color with an absorbance maximum of 765 nm.¹¹⁸ Advantages of the FC assay are its simplicity, since it does not require specialized equipment, and its long wavelength for measuring activity that minimizes antioxidant interference.¹¹⁸ Reducing agents, such as ascorbic acid or certain amino acids, interfere with FC analyses and can result in an overestimation of phenolic content in the sample.¹¹⁸

1.4 Are cellular assays better than *in vitro* assays?

The results of *in vitro* antioxidant assays, as described previously, often do not correlate with biological relevance due to solvent, radical source, or other issues. An alternative would be to assess antioxidant activity in cells, but this approach comes with an alternate set of concerns. For example, different cell types differ in oxidative stress responses, repair mechanisms, and other features that affect antioxidant behavior, making comparisons between cell lines extremely unreliable.^{119–123} Even if one cell line were to be selected as an exemplar, it is not clear what selection criteria would be most relevant.¹²⁴ Additionally, cells are complex systems, and even cells of the same type can differ in levels of glutathione, superoxide dismutase, glutathione peroxidase, and/or DNA repair enzymes depending on culturing conditions and the nature of the assays, differences that would alter the experimental results.^{120,121,123,125} Another challenge is establishing antioxidants cell permeability and therefore intracellular concentrations. Because cells take time to culture and assay, typically significantly more time than is required for *in vitro* assays, this hinders high-throughput screening. In addition, the cell culturing process can increase oxidative stress, resulting in the alteration of results.¹²⁴ And lastly, the question of how to assess the damage caused by cellular oxidative stress is critical.^{72,74,126} Commonly used cellular assays of oxidative stress typically measure one mechanism for antioxidant activity and unrelated cellular conditions can alter the results. For example, the TBARS assay measures lipid peroxidation and, as previously discussed, the results of this assay can be influenced by cellular carbohydrate levels. Thus, measuring only antioxidant prevention of cell death using this assay are sometimes unreliable and could neglect oxidative stress that results in

DNA mutations rather than lipid peroxidation. An advantage of cellular assays is that they account for absorption, intracellular distribution, metabolism, and excretion.¹²⁷ The assessment of each contributor can be time intensive and difficult for high throughput screening, making cellular assays typically not the first choice in antioxidant evaluation.

This Chapter provides an overview of the vast number of antioxidant assays. The ORAC assay was viewed as one of the most promising of a wide variety of antioxidant assays prior to the USDA withdrawing ORAC assay results in 2012. Since then, no assay has been identified as a suitable replacement for the ORAC assay due to the variety of different parameters each assay encompasses, such as radical source, solvent, measurement technique, and mechanisms assessed, as described in this Chapter. In addition, each assay has different sensitivities to antioxidant interference, oxygen, light, and other issues that need to be accounted for when comparing assay results. All of these variances result in different advantages, disadvantages, and limitations of each assay. There are several reviews¹²⁷⁻¹³¹ about antioxidants in clinical trials^{128,129,132} discussing these challenges. Since there are still knowledge gaps on the mechanisms of bioavailability, biotransformation, and action of antioxidant supplements, it is a current challenge to choose the most appropriate assay to obtain meaningful and comparable results.¹³¹ In addition, the number of antioxidants tested to date, the use of pharmacological and not dietary doses may produce harmful effects, and insufficient duration of the clinical trials also has made large scale studies a challenge.¹³⁰

1.5 Conclusions

The assessment and ranking of antioxidant activity is truly complex. Most assays focus on one possible mechanism (e.g., SET or HAT) or use organic solvents and radicals that are not biologically relevant. These issues resulted in the USDA's withdrawal of the prominent ORAC assay in 2012, an assay that has not been replaced. All these issues highlight that it is an utopic thought one assay could assess all the different aspects of antioxidant activity. The best approach for testing and comparing antioxidants is to selectively test the antioxidants for targeted purposes and carefully consider the limitations of each method.

1.6 Dissertation overview

In addition to the work presented in this dissertation, I have contributed to several other manuscripts and publications.¹³²⁻¹³⁷ I conducted EPR spectroscopy experiments to verify the proposed reaction mechanism of Cu^{2+} with methimazole (MMI). I was the first to provide proof of thiyl radical formation upon MMI reduction of Cu^{2+} to Cu^+ .¹³³ I also conducted DNA damage assays with a $[\text{Ru}(\text{MMI})_6]\text{Cl}_3$ that showed the improved antioxidant properties of the complex compared to MMI in preventing iron-mediated DNA damage.¹³⁴ Additionally, I performed copper- and iron-DNA damage assays for penicillamine to correlate the resulting IC_{50} values to the corresponding stability constants of selected thiol- and selenone-containing amino acids,¹³⁵ and I have also performed similar DNA damage assays to evaluate the ability of tinidazole complexes to induce DNA damage.¹³⁶ In collaboration with Dr. Craig Goodman, I developed a protocol using H9c2,

RASC, and RAOSMC cell lines to evaluate polyphenol toxicity and ability to prevent cell death under regular and high iron-conditions.¹³⁷ Furthermore, I expanded our understanding of thione- and selenone-containing imidazoles by highlighting the importance of aromaticity, denticity, and the effects of various electron-donating and -withdrawing substituents.¹³⁸

In this dissertation, Chapter 1 reviews the issues arising from *in vitro* antioxidant evaluation techniques. Although a significant number of reviews explain and compare the various methods for evaluating antioxidant ability, this Chapter focuses on discussing these techniques in light of replacing the ORAC standard for antioxidant activity after the USDA withdrew it in 2012. Chapter 1 also provides an overview of the issues surrounding antioxidant evaluation including the biological relevance of these assays.

Chapter 2 discusses development of the first antioxidant assay that enables the evaluation of hydrophobic compounds to prevent metal-mediated DNA damage. Most current antioxidant assays only focus on a specific antioxidant mechanism, such as radical scavenging or the ability to reduce copper and iron. Both classes of assays commonly use non-biologically relevant radicals and organic solvents. This new hydrophobic gel electrophoresis assay allows the evaluation of copper- and iron-mediated DNA damage of hydrophobic compounds under biologically relevant conditions.

In this work, we demonstrate that copper and iron produce different damaging species upon reaction with H₂O₂ that are therefore differently affected by increasing ethanol concentrations. EPR spectra show that high-ethanol concentrations completely scavenge iron-generated hydroxyl radical, whereas the damaging species produced by copper and H₂O₂ is longer-lived and not readily scavenged. A variety of iron-binding

polyphenol antioxidants were tested for their ability to prevent iron-mediated DNA damage under high-ethanol conditions, and their IC₅₀ values correlate well with those obtained under low-ethanol conditions, indicating the significance of metal coordination in preventing iron-mediated DNA damage under these conditions.

This new assay enabled evaluation of hydrophobic ebselen analogs and provides insight into their antioxidant mechanisms. This is the first assay that enables the quantifiable evaluation of metal-mediated DNA damage prevention of hydrophobic compounds under biologically relevant conditions and allows for the direct comparison of a variety of antioxidants to enable development of structure-function relationships.

The work presented in Chapter 3 investigates the role of fluconazole (FLC) in the production of ROS by copper and iron.¹³⁹ Electrochemical studies demonstrate that FLC-metal binding favors Cu⁺ and Fe²⁺ over Cu²⁺ and Fe³⁺, respectively, and mass spectrometry studies reveal FLC-metal coordination ratios of only 2:1 with copper and iron. Plasmid DNA damage studies show that FLC causes no DNA damage by itself or in combination with H₂O₂ or ascorbate, but, in the presence of hydrogen peroxide, FLC significantly enhances the ability of copper and iron to cause DNA damage. Research to date has primarily focused on ergosterol depletion by FLC that results in the disruption of the cell membrane of *C. neoformans* and causes growth inhibition. However, the results in this Chapter indicate that the biological mechanism of action for FLC is more complex and likely involves metal ions. Since the FLC resistance of *C. neoformans* is increasing, exploring FLC-metal interactions may provide a pathway to enhance DNA damage to the pathogen and reduce the development of resistant strains.

In Chapter 4, four different condensed tannins (CTs) from *V. macrocarpon*, *H. lupulus*, *V. vinifera* seed, and *T. inflorescentia* were tested for their ability to prevent metal-mediated DNA damage. *V. macrocarpon* CTs are the most effective at inhibiting both copper- and iron-mediated DNA damage. Although *H. lupulus*, *V. vinifera* seed, and *T. inflorescentia* CTs prevent little-to-no copper-mediated DNA damage, they prevent significantly more iron-mediated DNA damage at low micromolar concentrations. Only *H. lupulus* and *T. inflorescentia* CTs promote iron-mediated DNA damage at very low (0.1 and 1 mg/L) concentrations in addition to antioxidant activity at higher concentrations, the first report of this dual activity with iron. CTs with A-type linkages, such as in *V. macrocarpon* may more effectively inhibit copper- and iron-mediated DNA damage than CTs with B-type linkages. In addition, higher percentages of catechin compared to epicatechin subunits and higher percentages of galloylation may also reduce CT antioxidant activity. This is the first study to investigate the ability of CTs with several different structural characteristics for prevention metal-mediated DNA damage. Although further study is required to firmly establish structure-activity trends among a variety of CTs, these results demonstrate the significant effects of CT structural features on antioxidant efficacy.

1.7. References

- (1) Azzi, A. *Biochem. Biophys. Res. Commun.* **2007**, *362*, 230–232.
- (2) Imlay, J. A.; Linn, S. *Science* **1988**, *240*, 1302–1309.

- (3) Battin, E. E.; Zimmerman, M. T.; Ramoutar, R. R.; Quarles, C. E.; Brumaghim, J. L. *Metallomics* **2011**, *3*, 503–512.
- (4) Garcia, C. R.; Angele-Martinez, C.; Wilkes, J. A.; Wang, H. C.; Battin, E. E.; Brumaghim, J. L. *Dalton Trans* **2012**, *41*, 6458–6467.
- (5) Patel, R. P.; McAndrew, J.; Sellak, H.; White, C.R.; Jo, H.; Freeman, B. A.; Darley-Usmar, V. M. *Biochim. Biophys. Acta* **1999**, *1411*, 385–400.
- (6) Martínez, M. C.; Andriantsitohaina, R. *Antiox. Redox Signal.* **2009**, *11*, 669–702.
- (7) Begonja, A. J.; Teichmann, L.; Geiger, J.; Gambaryan, S.; Walter, U. *Blood Cells Mol. Dis.* **2006**, *36*, 166–170.
- (8) Halliwell, B.; Gutteridge, J. M.C. *Mol. Asp. Med.* **1985**, *8*, 89–193.
- (9) Cross, C. E.; Halliwell, B.; Borish, E. T.; Pryor, W. A.; Ames, B. N.; Saul, R. L.; McCord, J. M.; Harman, D. *Ann. Intern. Med.* **1987**, *107*, 526–545.
- (10) Aust, S. D.; Morehouse, L. A.; Thomas, C. E. *J. Free Radic. Biol. Med.* **1985**, *1*, 3–25.
- (11) Oswald, M. C. W.; Garnham, N.; Sweeney, S. T.; Landgraf, M. *FEBS Lett.* **2018**, *592*, 679–691.
- (12) Akhtar, M. J.; Ahamed, M.; Alhadlaq, H. A.; Alshamsan, A. *Biochim. Biophys. Acta* **2017**, *1861*, 802–813.
- (13) Dixon, S. J.; Stockwell, B. R. *Nature Chem. Biol.* **2014**, *10*, 9–17.
- (14) Saeidnia, S.; Abdollahi, M. *Toxicol. Appl. Pharmacol.* **2013**, *273*, 442–455.
- (15) Heneka, M. T.; O'Banion, M. K. *J. Neuroimmunol.* **2007**, *184*, 69–91.

- (16) Fetoni, A. R.; Paciello, F.; Rolesi, R.; Paludetti, G.; Troiani, D. *Free Radic. Biol. Med.* **2019**, *135*, 46–59.
- (17) Moody, C. S.; Hassan, H. M. *Proc. Natl. Acad. Sci. USA* **1982**, *79*, 2855–2859.
- (18) Weitzman, S. A.; Weitberg, A. B.; Clark, E. P.; Stossel, T. P. *Science* **1985**, *227*, 1231–1233.
- (19) Brawn, M. K.; Fridovich, I. *J. Biol. Chem.* **1985**, *260*, 922–925.
- (20) Bhabak, K. P.; Mughesh, G. *Chem. Eur. J.* **2010**, *16*, 1175–1185.
- (21) Lee, S. H.; Blair, I. A. *Trends Cardiovasc. Med.* **2001**, *11*, 148–155.
- (22) Jeremy, J. Y.; Yim, A. P.; Wan, S.; Angelini, G. D. *J. Card. Surg.* **2002**, *17*, 324–327.
- (23) Hureau, C.; Faller, P. *Biochimie* **2009**, *91*, 1212–1217.
- (24) Perron, N. R.; Brumaghim, J. L. *Cell Biochem. Biophys.* **2009**, *53*, 75–100.
- (25) Guaiquil, V. H.; Vera, J. C.; Golde, D. W. *J. Biol Chem.* **2001**, *276*, 40955–40961.
- (26) Reczek, C. R.; Chandel, N. S. *Science* **2015**, *350*, 1317–1318.
- (27) Ni, Y.; Eng, C. *Clin. Cancer Res.* **2012**, *18*, 4954–4961.
- (28) Fiedor, J.; Burda, K. *Nutrients* **2014**, *6*, 466–488.
- (29) Özyürek, M.; Güçlü, K.; Tütem, E.; Başkan, K. S.; Erçağ, E.; Esin Çelik, S.; Baki, S.; Yıldız, L.; Karaman, Ş.; Apak, R. *Anal. Methods* **2011**, *3*, 2439.
- (30) Huang, D.; Ou, B.; Prior, R. L. *J. Agric. Food Chem.* **2005**, *53*, 1841–1856.
- (31) Apak, R.; Çapanoğlu, E.; Shahidi, F. *Measurement of antioxidant activity and capacity: Recent trends and applications*. Wiley: Hoboken, NJ, USA, 2018.

- (32) Apak, R.; Özyürek, M.; Güçlü, K.; Çapanoğlu, E. *J. Agric. Food Chem.* **2016**, *64*, 997–1027.
- (33) Alam, M. N.; Bristi, N. J.; Rafiquzzaman, M. *Saudi Pharm. J.* **2013**, *21*, 143–152.
- (34) Arnao, M. B. *Trends Food Sci. Technol.* **2000**, *11*, 419–421.
- (35) Bartosz, G. *Free Radic. Res.* **2010**, *44*, 711–720.
- (36) Cao, G.; Prior, R. L. *Clin. Chem.* **1998**, *44*, 1309–1315.
- (37) Caroch, M.; Ferreira, I. C. F. R. *Food Chem. Toxicol.* **2013**, *51*, 15–25.
- (38) Frankel, E. N.; Meyer, A. S. *J. Sci. Food Agric.* **2000**, *80*, 1925–1941.
- (39) Buratti, S.; Pellegrini, N.; Brenna, O. V.; Mannino, S. *J. Agric. Food Chem.* **2001**, *49*, 5136–5141.
- (40) Cervellati, R.; Höner, K.; Furrow, S. D.; Neddens, C.; Costa, S. *HCA* **2001**, *84*, 3533–3547.
- (41) Prior, R. L.; Cao, G. *J. AOAC Int.* **2000**, *83*, 950–956.
- (42) Bank, G.; Schauss, A. *Nutraceuticals World* **2004**, 68–71.
- (43) Cunningham, E. *J. Acad. Nutr. Diet.* **2013**, *113*, 740.
- (44) SciFinder; Chemical Abstracts Service: Columbus, OH; <https://scifinder.cas.org> (accessed December 15, 2019).
- (45) Apak, R.; Özyürek, M.; Güçlü, K.; Çapanoğlu, E. *J. Agric. Food Chem.* **2016**, *64*, 1028–1045.
- (46) Francenia Santos-Sánchez, N.; Salas-Coronado, R.; Villanueva-Cañongo, C.; Hernández-Carlos, B. *Antioxidants Physiology Volume 5*; IntechOpen: London, 2019.

- (47) Angelé-Martínez, C.; Goodman, C.; Brumaghim, J. *Metallomics* **2014**, *6*, 1358–1381.
- (48) Imlay, J. A.; Linn, S. *Science* **1988**, *240*, 1302–1309.
- (49) Hoffmann, M.E.; Mello-Filho, A. C.; Meneghini, R. *Biochim. Biophys Acta* **1984**, *781*, 234–238.
- (50) Mello-Filho, A. C.; Meneghini, R. *Mut. Res.* **1991**, *251*, 109–113.
- (51) Battin, E. E.; Perron, N. R.; Brumaghim, J. L. *Inorg. Chem.* **2006**, *45*, 499–501.
- (52) Woodmansee, A. N.; Imlay, J. A. *J. Biol. Chem.* **2002**, *277*, 34055–34066.
- (53) Nakagawa, O.; Ono, S.; Tsujimoto, A.; Li, Z.; Sasaki, S. *Nucleosides Nucleotides Nucleic Acids* **2007**, *26*, 645–649.
- (54) Weimann, A.; Belling, D.; Poulsen, H. E. *Nucleic Acids Res.* **2002**, *30*, E7.
- (55) Shigenaga, M. K.; Aboujaoude, E. N.; Chen, Q.; Ames, B. N. In *Oxygen radicals in biological systems*. Academic: San Diego, London, 1994; pp 16–33.
- (56) Helbock, H. J.; Beckman, K. B.; Ames, B. N. In *Oxidants and antioxidants*. Academic: San Diego, Calif., London, 1999; pp 156–166.
- (57) Loft, S.; Poulsen, H. E. *Oxidants and antioxidants*. Academic: San Diego, Calif., London, 1999; pp 166–184.
- (58) Zheng, L.-F.; Dai, F.; Zhou, B.; Yang, L.; Liu, Z.-L. *Food Chem. Tox.* **2008**, *46*, 149–156.
- (59) Stohs, S. *Free Radic. Biol. Med.* **1995**, *18*, 321–336.
- (60) Young, I. S.; Woodside, J. V. *J. Clin. Path.* **2001**, *54*, 176–186.

- (61) Lloyd, R. V.; Hanna, P. M.; Mason, R. P. *Free Radic. Biol. Med.* **1997**, *22*, 885–888.
- (62) Keyer, K.; Imlay, J. A. *Proc. Natl. Acad. Sci. USA* **1996**, *93*, 13635–13640.
- (63) Woodmansee, A. N.; Imlay, J. A. In *Superoxide dismutase*. Academic Press: San Diego, London, 2002; pp 3–9.
- (64) Imlay, J. A.; Linn, S. *J. Bacteriol.* **1987**, *169*, 2967–2976.
- (65) Imlay, J. A.; Chin, S. M.; Linn, S. *Science* **1988**, *240*, 640–642.
- (66) Stöckel, J.; Safar, J.; Wallace, A. C.; Cohen, F. E.; Prusiner, S. B. *Biochemistry* **1998**, *37*, 7185–7193.
- (67) Gaggelli, E.; Kozłowski, H.; Valensin, D.; Valensin, G. *Chem. Rev.* **2006**, *106*, 1995–2044.
- (68) Hopt, A.; Korte, S.; Fink, H.; Panne, U.; Niessner, R.; Jahn, R.; Kretschmar, H.; Herms, J. *J. Neurosci. Meth.* **2003**, *128*, 159–172.
- (69) Liu, C. *J. Inorg. Biochem.* **1999**, *75*, 233–240.
- (70) Chikira, M.; Ng, C. H.; Palaniandavar, M. *Int. J. Mol. Sci.* **2015**, *16*, 22754–22780.
- (71) Galindo-Murillo, R.; García-Ramos, J. C.; Ruiz-Azuara, L.; Cheatham, T. E.; Cortés-Guzmán, F. *Nucleic Acids Res.* **2015**, *43*, 5364–5376.
- (72) Halliwell, B. *Am. J. Clin. Nutr.* **2000**, *72*, 1082–1087.
- (73) Halliwell, B.; Aruoma, O. I. *FEBS Lett.* **1991**, *281*, 9–19.
- (74) Halliwell, B. *Free Radic. Biol. Med.* **2002**, *32*, 968–974.
- (75) Duthie, G. G. *Proc. Nutr. Soc.* **1999**, *58*, 1015–1024.
- (76) Shivakumar, A.; Yogendra Kumar, M. S. *Crit. Rev. Anal. Chem.* **2018**, *48*, 214–236.

- (77) Cort, W. M. *Food Technol.* **1975**, *29*, 46–48.
- (78) Cort, W. M.; Scott, J. W.; Araujo, M.; Mergens, W. J.; Cannalunga, M. A.; Osadca, M.; Harley, H.; Parrish, D. R.; Pool, W. R. *J. Am. Oil Chem. Soc.* **1975**, *52*, 174–178.
- (79) Schaich, K. M.; Tian, X.; Xie, J. J. *Funct. Foods* **2015**, *18*, 782–796.
- (80) Stasko, A.; Brezová, V.; Biskupic, S.; Misík, V. *Free Radic. Res.* **2007**, *41*, 379–390.
- (81) Hamad, I.; Arda, N.; Pekmez, M.; Karaer, S.; Temizkan, G. *J. Nat. Sci. Biol. Med.* **2010**, *1*, 16–21.
- (82) Cordes, T.; Vogelsang, J.; Tinnefeld, P. *J. Am. Chem. Soc.* **2009**, *131*, 5018–5019.
- (83) Forman, H. J.; Zhang, H.; Rinna, A. *Mol. Asp. Med.* **2008**, *30*, 1–12.
- (84) Jozefczak, M.; Remans, T.; Vangronsveld, J.; Cuypers, A. *Int. J. Mmol. Sci.* **2012**, *13*, 3145–3175.
- (85) Vacek, J.; Zatloukalová, M.; Desmier, T.; Nezhodová, V.; Hrbáč, J.; Kubala, M.; Křen, V.; Ulrichová, J.; Trouillas, P. *Chem.-Biol. Interact.* **2013**, *205*, 173–180.
- (86) Cao, G.; Alessio, H. M.; Cutler, R. G. *Free Radic. Biol. Med.* **1993**, *14*, 303–311.
- (87) Huang, D.; Ou, B.; Hampsch-Woodill, M.; Flanagan, J. A.; Deemer, E. K. *J. Agric. Food Chem.* **2002**, *50*, 1815–1821.
- (88) Ou, B.; Hampsch-Woodill, M.; Prior, R. L. *J. Agric. Food Chem.* **2001**, *49*, 4619–4626.
- (89) Ou, B.; Hampsch-Woodill, M.; Flanagan, J.; Deemer, E. K.; Prior, R. L.; Huang, D. *J. Agric. Food Chem.* **2002**, *50*, 2772–2777.

- (90) Cao, G.; Verdon, C. P.; Wu, A. H.; Wang, H.; Prior, R. L. *Clin. Chem.* **1995**, *41*, 1738–1744.
- (91) Blois, M. S. *Nature* **1958**, *181*, 1199–1200.
- (92) Sanchez-Moreno, C. *Food Sci. Technol. Int.* **2002**, *8*, 121–137.
- (93) Contreras-Guzman, E. S.; Strong, F. C. *J. Assoc. Off. Anal. Chem.* **1982**, 1215–1222.
- (94) Kedare, S. B.; Singh, R. P. *J. Food Sci. Technol.* **2011**, *48*, 412–422.
- (95) Prior, R. L.; Wu, X.; Schaich, K. *J. Agric. Food Chem.* **2005**, *53*, 4290–4302.
- (96) Ancerewicz, J.; Migliavacca, E.; Carrupt, P. A.; Testa, B.; Brée, F.; Zini, R.; Tillement, J. P.; Labidalle, S.; Guyot, D.; Chauvet-Monges, A. M. *Free Radic. Biol. Med.* **1998**, *25*, 113–120.
- (97) Prakash, B.; Shukla, R.; Singh, P.; Kumar, A.; Mishra, P. K.; Dubey, N. K. *Int. J. Food Microbiol.* **2010**, *142*, 114–119.
- (98) Zheng, L.; Lin, L.; Su, G.; Zhao, Q.; Zhao, M. *Food Res. Int.* **2015**, *76*, 359–365.
- (99) Re, R.; Pellegrini, N.; Proteggente, A.; Pannala, A.; Yang, M.; Rice-Evans, C. *Free Radic. Biol. Med.* **1999**, *26*, 1231–1237.
- (100) Floegel, A.; Kim, D.-O.; Chung, S.-J.; Koo, S. I.; Chun, O. K. *J. Food Compos. Anal.* **2011**, *24*, 1043–1048.
- (101) Romay, C.; Pascual, C.; Lissi, E. A. *Braz. J. Med. Biol. Res.* **1996**, *29*, 175–183.
- (102) Hodges, D. M.; DeLong, J. M.; Forney, C. F.; Prange, R. K. *Planta* **1999**, *207*, 604–611.

- (103) Kappus, H. *Lipid Peroxidation: Mechanism, Analysis, Enzymology and Biological Relevance* Academic Press, London, UK, 1985.
- (104) Janero, D. R. *Free Radic. Biol. Med.* **1990**, *9*, 515–540.
- (105) Landry, L. G.; Chapple, C. C.; Last, R. L. *Plant Phys.* **1995**, *109*, 1159–1166.
- (106) Valenzuela, A. *Life Sci.* **1991**, *48*, 301–309.
- (107) Du, Z.; Bramlage, W. J. *J. Agric. Food Chem.* **1992**, *40*, 1566–1570.
- (108) Heath, R. L.; Packer, L. *Arch. Biochem. Biophys.* **1968**, *125*, 189–198.
- (109) Hirayama, O.; Yida, M. *Anal. Biochem.* **1997**, *251*, 297–299.
- (110) Khan, P.; Idrees, D.; Moxley, M. A.; Corbett, J. A.; Ahmad, F.; Figura von, G.; Sly, W. S.; Waheed, A.; Hassan, M. I. *Appl. Biochem. Biotechnol.* **2014**, *173*, 333–355.
- (111) Chapple, I. L.; Mason, G. I.; Garner, I.; Matthews, J. B.; Thorpe, G. H.; Maxwell, S. R.; Whitehead, T. P. *Ann. Clin. Biochem.* **1997**, *34*, 412–421.
- (112) Whitehead, T. P.; Thorpe, G.H.G.; Maxwell, S.R.J. *Anal. Chim. Acta* **1992**, *266*, 265–277.
- (113) Said, T. M.; Kattal, N.; Sharma, R. K.; Sikka, S. C.; Thomas, A. J.; Mascha, E.; Agarwal, A. *J. Androl.* **2003**, *24*, 676–680.
- (114) Benzie, I. F.; Strain, J. J. *Anal. Biochem.* **1996**, *239*, 70–76.
- (115) Apak, R.; Güçlü, K.; Ozyürek, M.; Karademir, S. E. *J. Agric. Food Chem.* **2004**, *52*, 7970–7981.
- (116) Folin, O.; Ciocalteu, V. *J. Biol. Chem.* **1927**, 627–650.
- (117) Singleton, V. L.; Orthofer, R.; Lamuela-Raventós, R. M. In *Oxidants and Antioxidants Part A*. Elsevier, 1999; pp 152–178.

- (118) Berker, K. I.; Ozdemir Olgun, F. A.; Ozyurt, D.; Demirata, B.; Apak, R. *J. Agric. Food Chem.* **2013**, *61*, 4783–4791.
- (119) Rahmat, A.; Kumar, V.; Fong, L. M.; Endrini, S.; Sani, H. A. *Asia Pac. J. Clin. Nutr.* **2004**, *13*, 308–311.
- (120) Rodic, S.; Vincent, M. D. *Int. J. Cancer* **2018**, *142*, 440–448.
- (121) Carmichael, J.; Mitchell, J. B.; Friedman, N.; Gazdar, A. F.; Russo, A. *Br. J. Cancer* **1988**, *58*, 437–440.
- (122) Efferth, T.; Oesch, F. *Biochem. Pharmacol.* **2004**, *68*, 3–10.
- (123) Wataha, J. C.; Hanks, C. T.; Sun, Z. *Dent. Mater.* **1994**, *10*, 156–161.
- (124) Halliwell, B. *FEBS Lett.* **2003**, *540*, 3–6.
- (125) Liu, C.; Liu, H.; Li, Y.; Wu, Z.; Zhu, Y.; Wang, T.; Gao, A. C.; Chen, J.; Zhou, Q. *Mol. Carcinog.* **2012**, *51*, 303–314.
- (126) Halliwell, B.; Whiteman, M. *Br. J. Pharmacol.* **2004**, *142*, 231–255.
- (127) Hermans, N.; Cos, P.; Maes, L.; Bruyne, T. de; Vanden Berghe, D.; Vlietinck, A. J.; Pieters, L. *Curr. Med. Chem.* **2007**, *14*, 417–430.
- (128) Steinhubl, S. R. *Am. J. Cardiol.* **2008**, *101*, 14D-19D.
- (129) Goodman, M.; Bostick, R. M.; Kucuk, O.; Jones, D. P. *Free Radic. Biol. Med.* **2011**, *51*, 1068–1084.
- (130) Bjelakovic, G.; Gluud, C. *J. Nat. Cancer Inst.* **2007**, *99*, 742–743.
- (131) Myung, S.-K.; Kim, Y.; Ju, W.; Choi, H. J.; Bae, W. K. *Ann. Oncol.* **2010**, *21*, 166–179.

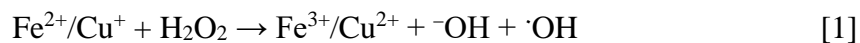
- (132) Palacio, C.; Mooradian, A. D. In *Oxidative stress and antioxidant protection*. Wiley New Jersey, 2016; pp 493–506.
- (133) Murphy, J. M.; Gaertner, A. A. E.; Owen, A.; Studer, S.; McMillen, C. D.; Wetzler, M.; Brumaghim, J. L. *Inorg. Chim. Acta*, *submitted*.
- (134) Abbas, M.; Gaertner, A. A. E.; McMillen, C. D.; Brumaghim, J. L., *submitted*.
- (135) Murphy, J. M.; Gaertner, A. A. E.; Williams, T.; McMillen, C. D.; Powell, B. A.; Brumaghim, J. L. *J. Inorg. Biochem.* **2019**, *195*, 20–30.
- (136) Castro-Ramírez, R.; Ortiz-Pastrana, N.; Caballero, A. B.; Zimmerman, M. T.; Stadelman, B. S.; Gaertner, A. A. E.; Brumaghim, J. L.; Korrodi-Gregório, L.; Pérez-Tomás, R.; Gamez, P. *Dalton Trans.* **2018**, *47*, 7551–7560.
- (137) Goodman, C.; Gaertner, A. A. E.; Brumaghim, J. L., *in preparation*.
- (138) Zimmerman, M. T.; Gaertner, A. A. E.; DiMarco, K.; Duffy, M.; Tam, M.; LeRoy, C.; Haines, J.; Rider, J.; Rabon, A.D., Brumaghim, J.L., *in preparation*.
- (139) Peng, C. A.; Gaertner, A. A. E.; Henriquez, S. A.; Fang, D.; Colon-Reyes, R. J.; Brumaghim, J. L.; Kozubowski, L. *PLoS One* **2018**, *13*, 318-337.

CHAPTER TWO
DEVELOPMENT OF A NEW ASSAY TO EVALUATE ANTIOXIDANT ACTIVITY
OF HYDROPHOBIC COMPOUNDS UNDER BIOLOGICALLY RELEVANT
CONDITIONS

2.1 Introduction

The term “oxidative stress” is commonly used to describe the increased production that can be caused, for example, by inflammation or the decreased elimination of reactive oxygen species (ROS), such as superoxide ($O_2^{\cdot-}$) and hydroxyl radical ($\cdot OH$).¹⁻⁴ ROS control various vital physiological responses such as changes in gene expression, apoptosis, and cell proliferation.⁵ ROS also play an important role in the development of many diseases,^{6,7} such as atherosclerosis,⁸ neural degenerative diseases,⁹⁻¹³ inflammation,^{13,14} cancer,¹⁵⁻¹⁷ and aging.^{1,3,18-21}

Molecular oxygen in the cell is converted to $O_2^{\cdot-}$ and H_2O_2 by direct oxidation of flavoproteins, and Halliwell *et al.*²²⁻²⁵ have demonstrated that transition metals play an essential role in ROS production.²⁶⁻²⁸ Iron reacts with hydrogen peroxide to produce the hydroxyl radical²⁹ (Reaction 1) that attacks the DNA at a deoxyribose sugar moiety,³⁰ abstracting a hydrogen atom at the 4' position. Hydroxyl radical also oxidizes lipids, small molecules, and proteins. The oxidized Fe^{3+} or Cu^{2+} can be regenerated by ascorbic acid reduction²³ or reaction with the reduced form of nicotinamide adenine dinucleotide (NADH).^{2,31} H_2O_2 can be produced catalytically as well as nonenzymatically through the proportionation of superoxide,³² and from natural cellular respiration.³³



Duthie *et al.*³³ have described the ability of antioxidants to prevent oxidation using three different mechanisms: 1) coordination to transition metals catalysts to prevent initiating radical formation, 2) decreasing localized $\text{O}_2^{\cdot-}$ concentrations to reduce oxidation reactions, and 3) preventing the initiation reactions by scavenging free radicals that can abstract H from molecules. Common *in vitro* assays testing antioxidant activity primarily focus on their radical scavenging ability. Some of the most common radicals used in these assays include 2,2'-diphenyl-1-picryl-hydrazyl (DPPH)³⁴⁻³⁶ or 2,2'-azino-bis(3-ethylbenzothiazoline-6-sulfonic acid (ABTS; Figure 2.1).^{36,37} Both DPPH and ABTS form stable organic radicals, very different from most ROS, especially hydroxyl radical. In addition, these radical scavenging assays are typically performed in organic solvents.³⁷⁻³⁹ Thus, the primary measures of antioxidant ability to scavenge radicals are not very biologically relevant and often do not accurately reflect antioxidant prevention of DNA damage.^{37,40}

Other assays evaluate the ability of antioxidants to reduce Fe^{3+} or Cu^{2+} , including the ferric reduction antioxidant power (FRAP) assay⁴¹ or the cupric reducing antioxidant capacity (CUPRAC) assay.⁴² These assays only assess one possible mechanism by which antioxidants can prevent damage. In addition, FRAP assays are conducted at a pH of 3.6, a non-biological pH, whereas CUPRAC assays are conducted at biological pH 7. Since typical radical scavenging and metal reduction assays are not wholly biologically relevant and only examine one potential mechanism of action, cell survival assays are also used to

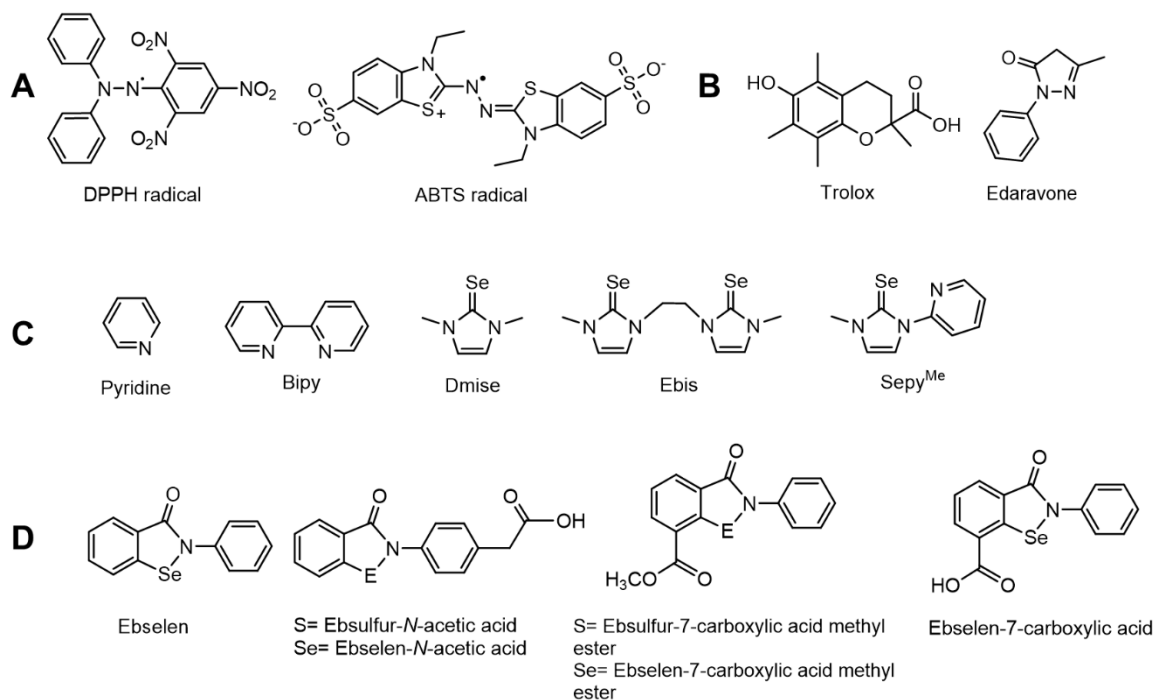


Figure 2.1. Structures of A) the radicals DPPH and ABTS commonly used in antioxidant assays, B) Trolox and Edaravone, known radical scavengers, C) various selones and pyridine derivatives, and D) ebselen and ebsulfur derivatives.

establish and compare antioxidant ability.^{43–45} However, the use of different cell lines for these assays limits the ability to compare results, and antioxidant efficacy and toxicity issues limit the ability to screen many compounds.^{46–48} In addition, all these assays generate different distinct values as they are based on different underlying mechanisms and processes for antioxidant activity

After the development of the ORAC assay for singlet oxygen, peroxyxynitrite, hydroxyl radical, and superoxide radical anion in 1993⁴⁹ and subsequent modifications for use in different solvent systems.^{50–53} Development of standard protocols for these ORAC assays, making them straightforward, adaptable to many different sample types, and able to be run in both aqueous and organic solvent systems.^{54,55} In 2007, the first ORAC assay

database of 277 selected foods or food additives was released by the United States Department of Agriculture (USDA), followed by 326 additional entries in 2010. The USDA published these tables to compare various foods and food additives using a standardized method so that nutraceutical companies could use them to educate consumers about the comparative antioxidant benefits of products.^{53,46} In 2012, the USDA withdrew all their ORAC tables for two reasons: 1) the routine misuse by food and dietary supplement companies to promote products, and 2) the fact that *in vitro* ORAC data for antioxidant capacity of foods did not predict *in vivo* effects, coupled with mixed results in clinical trials testing the benefits of dietary antioxidants.^{56,43,49}

Due to the lack of correlations between ORAC results and observed biological effects, in 2012, the USDA discontinued the use of this assay and even entirely deleted the ORAC database from their website.^{36,57,58} They stated the lack of understanding surrounding antioxidant metabolic pathways and mechanisms of action in addition to the lack of correlation between the measured antioxidant activities and biological effects as a reason for this decision.^{36,57} Due to these challenges, no other standard assay or method of evaluating and comparing antioxidant activity has been put into place since 2012.

In cells, apoptosis occurs when cellular damage exceeds cellular capabilities to repair it. Mitochondrial dysfunction, respiratory chain inhibition, loss of inner mitochondrial membrane potential, and increased mitochondrial membrane permeability are all types of ROS damage that result in apoptosis.⁵⁹ DNA fragmentation is also associated with late stage apoptosis.^{59,60} Oxidative-stress-induced apoptosis may represent an antimutagenic and carcinogenic defense mechanism to eradicate cells with unreparable

DNA damage.⁶⁰ Therefore, investigating DNA damage prevention through antioxidants is an important aspect to be studied.⁶¹ Often, antioxidants are studied with radical scavenging assays, such as DPPH or ABTS assays, and their results are directly converted to the ability of the compound to prevent DNA damage without direct measurements using DNA.⁶²

Results from DNA damage prevention assays can directly compare antioxidant efficacy, but these assays are limited to testing water-soluble compounds.^{63–68} Sies *et al.*⁶⁹ tried to evaluate peroxynitrite-induced DNA damage prevention of the hydrophobic antioxidant ebselen, but quantification of the results was problematic because the scavenging of methanol was not sufficiently accounted for, only one concentration of Ebselen was tested, and adequate control lanes of the compound itself are missing. The assay presented in this work mimics the cellular environment by measuring metal-mediated DNA damage caused by the hydroxyl radical, the same mechanisms that cause DNA damage and cell death.^{70–75} In addition, DNA damage prevention is quantifiable and the limitation of water-solubility is reduced. This new assay enables the testing and comparison of water-insoluble compounds such as ebselen and Edaravone, among others, as described in this work.

2.2 Results and Discussion

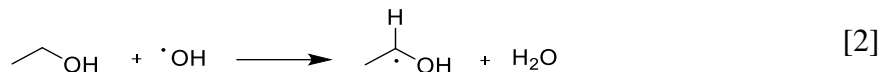
These more hydrophobic DNA gel electrophoresis assays determine the ability of compounds to prevent copper- or iron-mediated DNA damage by hydroxyl radical (Reaction 1) under biologically relevant conditions.^{76–79} The pH and NaCl concentrations are adjusted to biological relevant conditions⁸⁰ and ethanol is used to mimic organic radical

scavengers in the cell. Copper concentrations in human serum can range from 10 to 25 mM⁸¹⁻⁸³ but increase to 0.1 mM under several metabolic processes.^{82,84} DNA damage such as backbone breakage, base oxidation, inter- and intra-strand crosslinking, and DNA–protein crosslinking, can be detected.⁸² In this assay, Cu⁺ coordinates DNA and promotes single-strand breakage by the Fenton-like reaction (Reaction 1),⁸⁵⁻⁸⁷ and damaged and undamaged DNA is separated by gel electrophoresis. Halliwell *et al.*^{23,61} emphasized that oxidative DNA damage is an important biomarker for cellular ROS damage, and DNA is one of the most important biomolecules and target of ROS damage.^{61,88}

In these assays, iron or copper and hydrogen peroxide are used in concentrations similar to those found in cells. *E. coli* grown in standard media have concentrations of labile iron iron that it is not bound in proteins and can participate in radical generation between 15-30 μM, depending on growth conditions.^{30,89} The supercoiled (undamaged) and nicked (damaged) plasmid DNA is separated using gel electrophoresis, allowing a quantitative analysis of antioxidant activity.

Effects of increased ethanol concentrations. Linn *et al.*^{70,90-93} studied the effect of ethanol on DNA damage caused by the Fenton reaction (Reaction 1). In the presence of hydrogen peroxide, they determined three modes of DNA damage by iron-generated hydroxyl radical: Mode I damage is caused by loosely DNA-bound Fe²⁺ and is moderately reduced by ethanol scavenging (Reaction 2); Mode II damage results from tightly DNA-base-coordinated Fe²⁺ and is very resistant to ethanol scavenging; and Mode III damage results from labile Fe²⁺ in solution, which is readily scavenged by ethanol. The ethanyl,

like other alkyl radicals, can lead directly or indirectly to the production of DNA-derived radicals and form DNA-8-allylguanine adducts.⁹⁴⁻⁹⁷



Therefore, in DNA gel electrophoresis assays similar to the one introduced in this Chapter, Perron *et al.*,⁹⁸ who themselves refined the gel electrophoresis assay developed by Henle *et al.*,⁹² used ethanol (10 mM) to mimic naturally occurring organic compounds in cells that can act as radical scavengers. Ethanol is not a common additive in plasmid DNA gel-electrophoresis studies: less than 10 reports of ethanol or methanol addition in these types of assays exist,^{69,92,99-101} and none examine antioxidant prevention of DNA damage. Sies *et al.*⁶⁹ used methanol only to dissolve hydrophobic compounds, and did not thoroughly investigate the effect of methanol's radical scavenging ability on DNA damage.

To make DNA damage prevention studies with more hydrophobic compounds possible in these new DNA damage assays, the ethanol concentration is increased from 10 mM to 1.7 M. The hydrophobic antioxidant compounds are dissolved in 100% ethanol and 1 μL of this stock solution is added to a total volume of 10 μL , resulting in the ethanol concentration of 1.7 M. This 1700-fold increase in ethanol has no significant effect on copper-mediated DNA damage by Cu^+ (6 μM with 50 μM H_2O_2 ; pH 7), with $94 \pm 4\%$ and $93 \pm 4\%$ DNA damage at 1.7 M and 10 mM ethanol, respectively.

In contrast, iron-mediated DNA damage prevention by Fe^{2+} dependent upon ethanol concentration. Under low-ethanol (10 mM) conditions, 2 μM Fe^{2+} in the presence of hydrogen peroxide results in $92 \pm 3\%$ DNA damage, but under high-ethanol (1.7 M) conditions (both at pH 6 to prevent iron precipitation¹⁰²), no DNA damage is observed at

this Fe^{2+} concentration. At constant H_2O_2 concentration, increasing DNA damage with increasing Fe^{2+} concentration is observed at 10 mM and 1.7 M ethanol, respectively (Figure 2.2), but in all cases, more Fe^{2+} is required to damage the same percentage of DNA under low- and high-ethanol conditions. For these hydrophobic gel assays under high-ethanol conditions, a concentration of 15 μM Fe^{2+} was chosen because of its high percentage of DNA damage (~90%), similar to the DNA damage percentage under low-ethanol conditions with 2 μM Fe^{2+} . This direct correlation between increased Fe^{2+} concentrations and increased DNA damage (Figure 2.2) at different ethanol concentrations has not been previously examined. This difference between the effects of ethanol on copper- and iron-mediated DNA damage is likely due to the metals producing different damaging species. Fe^{2+} reacts with H_2O_2 to produce hydroxyl radical,^{103,104} as has been thoroughly established *in vitro*^{103,105} and in cells.^{106–110} The DNA-damaging species produced by Cu^+ has been extensively studied, and many suggest generation of hydroxyl radical from the reaction of

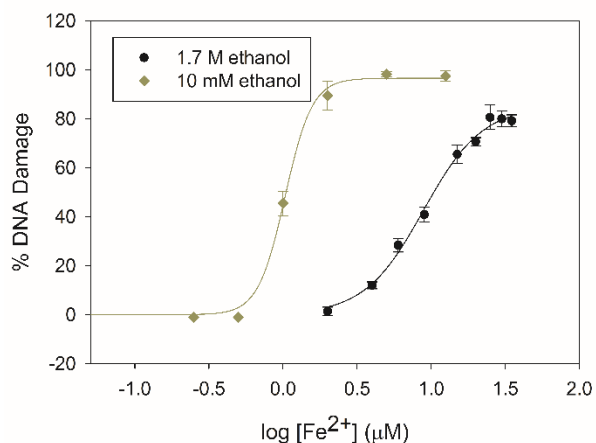


Figure 2.2: Dose-response curves for iron-mediated DNA damage with 10 mM (diamonds) and 1.7 M ethanol (circles) with increasing Fe^{2+} concentrations.

Cu^+ and H_2O_2 .^{24,111–116} Ingraham *et al.*¹¹⁷ was one of the first to suggest that hydroxyl radical is not the primary radical formed, followed by many studies supporting his hypothesis,^{8,67,117–122} although the exact identity of the oxidizing species has not been determined. It is clear, however, that compared to Fe^{2+} in the presence of hydrogen peroxide, Cu^+ forms a more stable oxidant that is much less susceptible to radical scavengers such as ethanol.^{123,124}

Electron paramagnetic spectroscopy. EPR experiments were conducted to further explore the influence of ethanol on copper- and iron-generated radical species. These studies were carried out at room temperature in the presence of the spin trap 5,5-dimethyl-1-pyrroline-*N*-oxide (DMPO) to observe the radicals produced. High ethanol concentrations (1.7 M) completely prevent formation of the DMPO-OH adduct with Fe^{2+} (300 μM) and H_2O_2 . When the concentration of ethanol is reduced to 425 mM, the DMPO-OH signal starts to appear (Figure 2.7A), indicating that ethanol directly prevents hydroxyl radical generation.

With Cu^+ under similar conditions, the DMPO-OH adduct is observed without ethanol addition. With ethanol, both DMPO-OH and DMPO-ethanyl adducts are observed (Figure 2.3), consistent with immediate hydroxyl radical formation and subsequent ethanol scavenging of this radical.^{125–129} These results highlight that Cu^+ and H_2O_2 form an oxidizing agent less readily scavenged by ethanol than the oxidizing agent formed by Fe^{2+} and H_2O_2 .¹²⁴ This is the first study of DMPO-OH radical generation by copper and iron with varying ethanol concentrations (Figure 2.35-2.40).

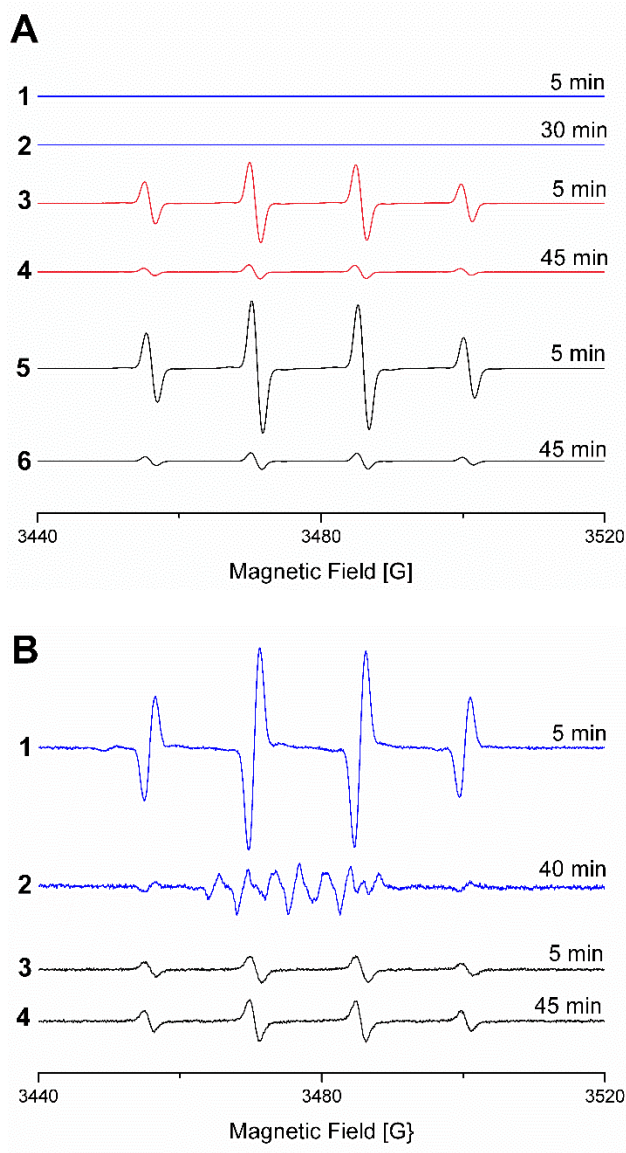


Figure 2.3. EPR spectra of A) Fe²⁺, H₂O₂, and DMPO in MES buffer (10 mM, pH 6) with 1.7 M ethanol after 1) 5 min and 2) 30 min, with 425 mM ethanol after 3) 5 min and 4) 45 min, and without ethanol after 5) 5 min and 6) 45 min (due to signal overload spectra without ethanol were collected with lower receiver gain of 10³ versus 10⁵ for all other spectra), and B) Cu²⁺ ascorbate, H₂O₂, and DMPO in MOPS buffer (10 mM, pH 7) with 1.7 M ethanol after 1) 5 min and 2) 40 min and without ethanol after 3) 5 min and 4) 45 min.

Correlating antioxidant behavior in high- and low-ethanol DNA damage prevention assays. To evaluate the impact high-ethanol concentrations have on antioxidant prevention of iron-mediated DNA damage, a set of six polyphenols (Figure 2.4) were tested

for their ability to prevent DNA damage under high- and low-ethanol conditions. Polyphenol antioxidant activity has been extensively studied, and polyphenol compounds are well-known iron chelators^{76,98,130} and radical scavengers,^{131–134} making them ideal for a comparison study.

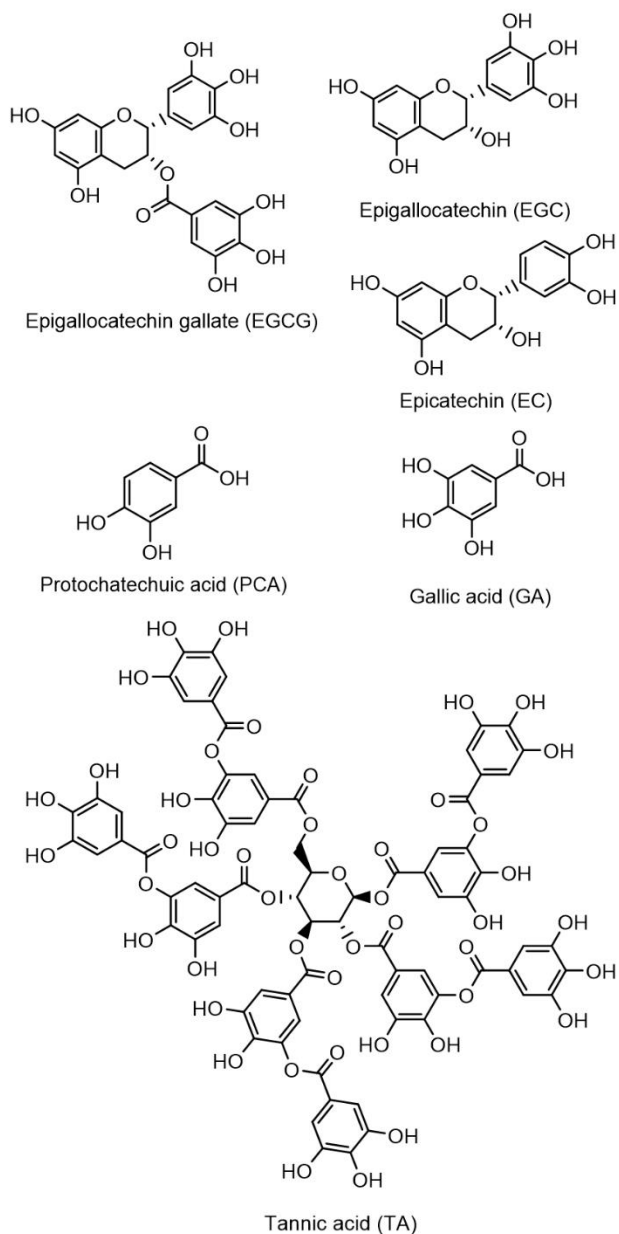


Figure 2.4. Structures of selected polyphenols examined in this chapter.

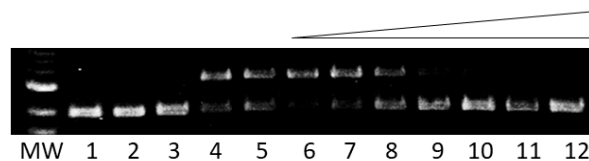


Figure 2.5. Gel electrophoresis images showing tannic acid (TA) prevention of iron-mediated DNA damage. MW: 1 kb molecular weight marker; lane 1: plasmid DNA (p); lane 2: p + H₂O₂; lane 3: p + 20 μM TA + H₂O₂ + 1.7 M ethanol; lane 4: p + Fe²⁺ (2 μM) + H₂O₂ + ethanol (10 mM); lane 5: p + Fe²⁺ (15 μM) + H₂O₂ + ethanol (1.7 M); lanes 6-12: Fe²⁺ (15 μM) + H₂O₂ + ethanol (1.7 M) + TA (0.1, 1, 2.5, 5, 7.5, 10, and 20 μM, respectively).

These gel assays were conducted under low- and high-ethanol conditions with either Fe²⁺ (2 and 15 μM for low-ethanol and high-ethanol conditions, respectively) with hydrogen peroxide (50 μM). Addition of polyphenol compounds prevent iron-mediated DNA damage as shown in the gel images for tannic acid in Figure 2.5. The DNA bands in Lane 3 indicate that TA does not cause DNA damage in the presence of H₂O₂, but Fe²⁺ and H₂O₂ cause over 90% damage (Figure 2.5, lane 4). The same amount of DNA damage occurs with Fe²⁺ (15 μM) and H₂O₂ with 1.7 M ethanol (Figure 2.5, lane 5). Increasing TA concentrations up to 20 μM (Figure 2.5, lanes 6-12) prevent this iron-mediated DNA damage. The plasmid DNA band intensities from these studies were quantified, and the resulting data were fit with a dose-response curve to determine the tannic acid concentration required to inhibit 50% DNA damage (IC₅₀ value; Figure 2.6A); the IC₅₀ value for TA prevention of iron-mediated DNA damage with 1.7 M ethanol is 2.27 ± 0.01 μM (Table 2.1). Due to the susceptibility of iron-generated hydroxyl radical to ethanol scavenging, iron concentrations are 7.5 times higher in the high-ethanol (15 μM Fe²⁺) than in the low-ethanol (2 μM Fe²⁺) assay conditions. It is therefore consistent that the polyphenol IC₅₀ values for prevention of iron-mediated DNA damage under high-ethanol

conditions (2.27-1432 μM) are higher than those determined under low-ethanol conditions (0.3 to 58.9 μM ; Table 2.1).

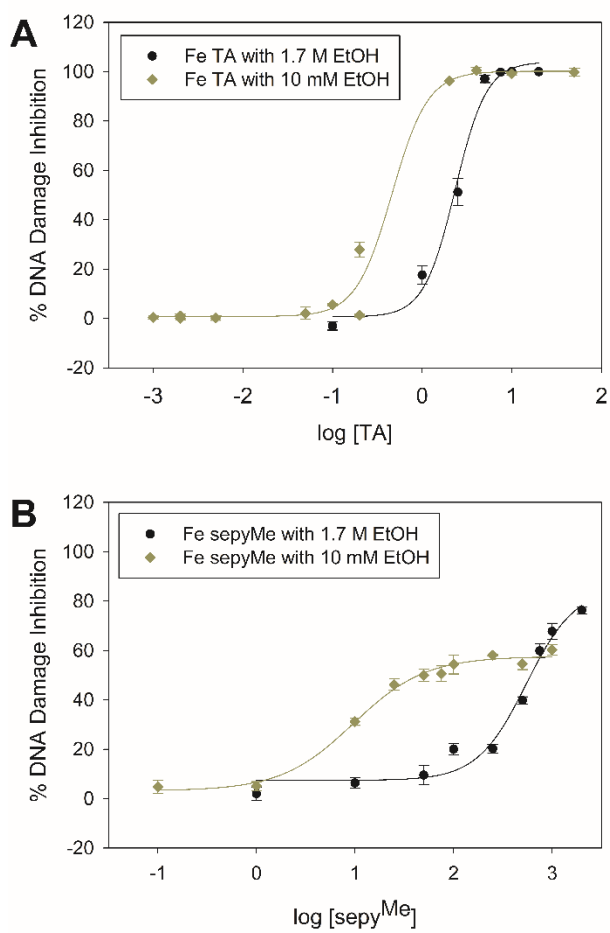


Figure 2.6. IC₅₀ plots for prevention of iron-mediated DNA damage in the presence of 10 mM and 1.7 M ethanol for A) sepy^{Me} and B) tannic acid.

Table 2.1. IC₅₀ values for polyphenol prevention of iron-mediated DNA damage under high (1.7 M) and low (10 mM) ethanol conditions and polyphenol scavenging of DPPH.

Compound	Fe ²⁺ IC ₅₀ [μM] high ethanol	Fe ²⁺ IC ₅₀ [μM] low ethanol	DPPH IC ₅₀ [μM]
TA	2.27 ± 0.01	0.3 ± 0.1 ^a	1.00 ± 0.01
GA	82.0 ± 0.2	15.2 ± 0.1 ^b	10.44 ± 0.02
PCA	281 ± 1	34.7 ± 0.3 ^b	124.2 ± 0.1
EGC	723 ± 2	11.6 ± 0.2 ^b	3.38 ± 0.01
EGCG	14.0 ± 0.1	1.10 ± 0.01 ^b	3.40 ± 0.01
EC	1432 ± 3	58.9 ± 0.5 ^b	28.97 ± 0.02

^aIC₅₀ values from reference ¹³⁵. ^bIC₅₀ values from reference ⁹⁸.

To determine whether a correlation exists between the polyphenol IC₅₀ values from the low- and high-ethanol DNA assays, the log IC₅₀ values were plotted together (Figure 2.7), resulting in a linear fit with a high R² value of 0.872. The catechol or gallol groups of these polyphenol compounds coordinate iron, and Perron *et al.*^{76,98} established that, under low-ethanol conditions, the polyphenol IC₅₀ values can be predicted by their first phenolic pK_a, highlighting the importance of iron binding for their antioxidant activity. Since polyphenols exhibit a range of antioxidant and prooxidant behavior in DNA damage assays with copper under low-ethanol conditions,⁷⁶ similar DNA damage prevention correlations under high- and low-ethanol conditions were not explored for copper.

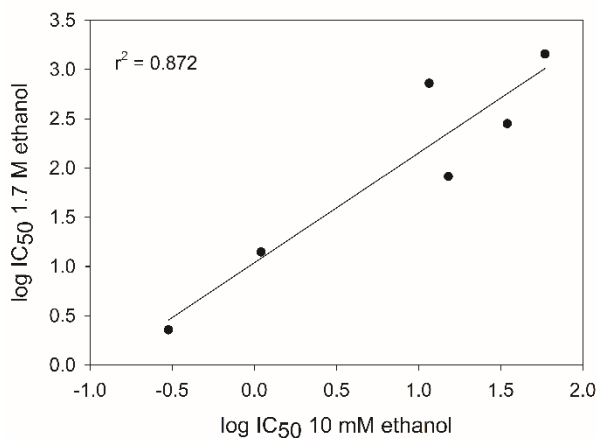


Figure 2.7 Correlation of polyphenol IC₅₀ values for prevention of DNA damage under high and low ethanol concentrations. Error bars are within symbols.

Metal-binding to prevent DNA damage. DNA is one of the most important biomolecules and a target of damage by ROS, and there are numerous mechanisms to counteract DNA damage.^{61,88} Halliwell *et al.*^{23,61} emphasized that oxidative DNA damage is an important biomarker for ROS damage. As a result, antioxidant behavior often is studied using radical scavenging assays (such as DPPH or ABTS assays), and these results are then sometimes translated to the ability of the antioxidants to prevent DNA damage without performing direct DNA damage measurements.⁶² Linn *et al.*^{70,71,136} demonstrated that iron-mediated DNA damage is the underlying cause of cell death of *E. coli* under oxidative stress, and others have shown similar behavior in eukaryotic cells, including human cells.^{70,71,136} This damage arises because Fe²⁺ coordinates to DNA *in vivo* resulting in hydroxyl radical production in close proximity to the DNA and subsequent oxidative damage.⁷¹ Antioxidant-metal coordination plays an important role in preventing metal-mediated DNA damage,^{63,76,135,137} since the antioxidant can bind the metal ion where hydroxyl radical is generated and prevent its release. Thus, directly measuring antioxidant prevention of DNA damage is an important and distinct aspect of understanding antioxidant behavior.⁶¹

To study and compare the effect of metal chelation on DNA damage under high- and low-ethanol conditions, four compounds that systematically differ in their metal-coordination properties were tested under 10 mM and 1.7 M ethanol conditions. *N,N'*-dimethylimidazole selenone (dmise) is an imidazole selenone well-studied for its ability to coordinate copper and iron through selenium,¹³⁸⁻¹⁴⁰ and 2,2'-bipyridine (bipy) is also an extremely well-studied nitrogen chelating ligand for iron and copper (Figure 2.1C).^{141,142}

These two metal-binding motifs are combined in (2-mercapto-1-methylimidazolyl)-pyridine selone (sepy^{Me}), a bidentate ligand that can coordinate through the selone Se and the pyridine nitrogen atoms.¹⁴³ Ethyl-bis(imidazole) selone (ebis) is also a bidentate ligand, binding metals through both selenium atoms.¹³⁸ Bidentate ligands coordinate more strongly to metal ions than monodentate ligands with similar coordination sites.

Since the polyphenols showed the importance of metal interaction for the observed DNA damage prevention, we used these five compounds to compare different antioxidant characteristics such as denticity and different metal coordination sites to explore this role. Pyridine and bipy and borderline bases and are expected to coordinate more strongly to borderline Fe²⁺ than to soft Cu⁺. Selones, on the other hand, are soft bases and therefore coordinate better to Cu⁺ than Fe²⁺. In addition, bidentate ligands, such as bipy and ebis, should coordinate more strongly to metals than their monodentate analogs. If metal coordination plays a significant role in this DNA damage prevention assay, these trends should be reflected in the IC₅₀ values obtained.

Increasing ethanol concentrations increases the copper-mediated DNA damage IC₅₀ value of dmise from ~240 to 312.8 ± 0.7 μM (Table 2.2). With iron-mediated DNA damage, the dmise IC₅₀ value increases from 3.68 ± 0.01 to 658 ± 2 μM, respectively, a 179-fold difference (Table 2.2). For ebis, IC₅₀ values for copper-mediated DNA damage decrease somewhat with increasing ethanol concentration: 8.20 ± 0.02 and 13.09 ± 0.03 μM, respectively, for high- and low-ethanol conditions. Similar to dmise, the ebis IC₅₀ value for iron-mediated DNA damage prevention increases more dramatically with increasing ethanol concentrations (IC₅₀ values of 3.2 ± 0.9 and 140.5 ± 0.3 μM,

Table 2.2. IC₅₀ values for metal-mediated DNA damage prevention and DPPH scavenging of selones and ebselen and ebsulfur derivatives (NP = IC₅₀ value not obtained due to solubility issues, NA = IC₅₀ value not tested).

Compound	Cu ⁺ IC ₅₀ [μM] high ethanol	Cu ⁺ IC ₅₀ [μM] low ethanol	Fe ²⁺ IC ₅₀ [μM] high ethanol	Fe ²⁺ IC ₅₀ [μM] low ethanol	DPPH IC ₅₀ [μM]
Dmise	312.8 ± 0.7	~240 ^{a,b}	658 ± 2	3.68 ± 0.01 ^b	199.7 ± 0.1
Ebis	8.20 ± 0.02	13.09 ± 0.03 ^b	140.5 ± 0.3	3.2 ± 0.9 ^b	1.12 ± 0.01
Sepy ^{Me}	-	11.85 ± 0.01 ^b	603 ± 1	44.7 ± 0.1 ^b	107.4 ± 0.1
Bipy	2.56 ± 0.01	NP	22.18 ± 0.04	NP	no scavenging 0.1 – 1000 μM
Pyridine	NA	NA	no inhibition 1-2000 μM	NA	No scavenging 0.1 – 1000 μM
Ebselen	280.7 ± 0.8	NP	no inhibition 1-400 μM	NP	no scavenging 0.1 – 500 μM
Ebselen- <i>N</i> -acetic acid	581 ± 4	NP	no inhibition 1-700 μM	NP	NA
Ebselen-7-carboxylic acid	213.3 ± 0.6	NP	235.3 ± 0.6	NP	NA
Ebselen-7-carboxylic acid methyl ester	51.2 ± 0.1	NP	no inhibition 1-700 μM	NP	NA
Ebsulfur-acetic acid	no inhibition 1-700 μM	NP	no inhibition 1-700 μM	NP	NA
Ebsulfur-7-carboxylic acid methyl ester	no inhibition 1-400 μM	NP	no inhibition 1-400 μM	NP	NA
Edaravone	no inhibition 1-1000 μM	NP	no inhibition 1-1000 μM	NP	~3.08 ^a
Trolox	no inhibition 1-1000 μM	no inhibition 1-1000 μM	no inhibition 1-1000 μM	728.5 ± 2.4	6.82 ± 0.01

Estimated IC₅₀; no fit could be obtained due to concentration limitations. ^{b)} IC₅₀ values from reference ¹⁴³.

respectively). This increase in IC₅₀ values for iron- compared to copper-mediated DNA damage prevention is consistent with the expected trend that favors selenium-copper over selenium-iron coordination. In addition, IC₅₀ values for the bidentate ebis compared to the monodentate dmise are 38- and 18-fold higher for prevention of copper-mediated DNA damage under high and low ethanol concentrations, respectively, and 5-fold higher for prevention of iron-mediated DNA damage under high ethanol concentrations.

The same denticity trends hold true for monodentate and bidentate nitrogen donor ligands: pyridine does not exhibit any iron-mediated DNA damage prevention (1 – 2000 μM), but bipy has IC₅₀ values of 2.56 ± 0.01 and of 22.18 ± 0.04 μM for copper- and iron-mediated DNA damage prevention at high-ethanol concentrations (no low-ethanol IC₅₀ values can be obtained due to the poor water solubility of bipy). For the mixed-donor, bidentate selone sepy^{Me}, IC₅₀ values are 44.7 ± 0.1 and 603 ± 1 μM for iron-mediated DNA damage prevention under low- and high-ethanol conditions, respectively. The IC₅₀ value for sepy^{Me} is smaller than that determined for dmise, indicating that addition of the pyridine substituent increases iron-mediated DNA-damage prevention, consistent with metal-binding being a mechanistic factor in these high-ethanol DNA damage assays.

Since bipy, sepy^{Me}, dmise, and ebis are established metal chelators,^{138,144,145} a well-known radical scavenger Edaravone, a substituted 2-pyrazolin-5-one (Figure 2.1B), was tested to establish the importance of metal coordination in this assay. Edaravone was approved by the Federal Drug Administration (FDA) in 2017 as the first drug for the treatment of amyotrophic lateral sclerosis (ALS),¹⁴⁶⁻¹⁴⁹ a fatal degenerative disease that affects the motor neurons connecting the brain and spinal cord, leading to paralysis and

death.¹⁵⁰ ALS results from mutations in the gene encoding the ubiquitous antioxidant enzyme Cu,Zn-superoxide dismutase (SOD1). This enzyme scavenges superoxide radical, decomposing it into oxygen and hydrogen peroxide, to maintain cellular redox balance.^{151,152} SOD1 is also a major copper-binding protein that regulates cellular copper homeostasis,^{152,153} and SOD1 mutations may cause disruption of copper homeostasis and increased copper levels in the spinal cord.¹⁵³ In addition, Homma *et al.*¹⁴⁸ observed that Edaravone effectively prevents ferroptosis in Hepa 1–6 cells, a process triggered by iron-generated hydroxyl radical (Reaction 1) that results in lipid peroxidation and cell death.¹⁴⁸

The exact mechanism of action of Edaravone in the treatment of ALS is unknown, but it is thought to be a radical scavenger *in vivo*,¹⁵⁰ and Edaravone is soluble in acetic acid, methanol, or ethanol, but poorly soluble in water.¹⁵⁰ In contrast, Trolox (Figure 2.1B), is a fairly water-soluble vitamin E derivative that is also a well-studied radical scavenger.^{154–157} It is commonly used as a standard against which antioxidant activity is compared in ROS scavenging assays, expressed as Trolox equivalents (TE).⁵¹ Because of the established radical scavenging abilities of Trolox and Edaravone, we wanted to compare results of our high-ethanol DNA gel electrophoresis assays to those of the DPPH radical scavenging assay for these compounds. Antioxidants such as Edaravone and Trolox that do not coordinate metals but act as radical scavengers should not prevent metal-mediated DNA damage under high-ethanol conditions.

In these assays, Edaravone does not prevent copper- or iron-mediated DNA damage but scavenges DPPH with an IC₅₀ value of 3.08 μM (Table 2.2), consistent with other studies.^{158–160} Trolox also does not prevent copper- or iron-mediated DNA damage under

high-ethanol conditions, but it does have a very high IC₅₀ value of 728 μM for iron-mediated DNA damage under low-ethanol conditions. These results highlight a shortcoming with the use of Trolox as a gold standard for antioxidant assays: comparing every antioxidant to a compound that can only scavenge radicals likely results in the neglect of other potential antioxidant mechanisms. As highlighted by the use of known metal chelators, metal chelation plays an important role in antioxidant prevention of metal-mediated DNA damage under high-ethanol conditions.

Examining DNA damage prevention abilities for hydrophobic compounds.

Hydrophobic antioxidants have a lot of potential, especially in the area of neuropharmaceuticals, where biodistribution of drugs is limited by the blood-brain barrier (BBB) that prevents transit of >98% of small molecules.¹⁶¹ Water-soluble drugs can be structurally modified to become lipid-soluble drugs that can cross the BBB, but issues arise with *in vitro* screening since current models vary greatly in cost, technical demands, and intended applications.^{161,162}

The hydrophobic antioxidant drug ebselen is another example of how an assay to evaluate hydrophobic compounds for their abilities to prevent biologically relevant DNA damage could greatly benefit development of more potent antioxidant drugs. Ebselen (Figure 2.1D) was developed in the early 1980s by Helmut Sies *et al.*¹⁶³ as a glutathione peroxidase (GPx) mimic to prevent oxidative damage by hydrogen peroxide, measurements performed in organic solvents due to ebselen's insolubility in water.¹⁶⁴⁻¹⁶⁷ Ebselen also prevents oxidative stress in cultured cells as well as in Se-deficient mice, an effect independent of endogenous GPx expression.¹⁶⁸ In the 1980s and 1990s, ebselen was

examined in clinical trials for treatment of brain ischemia during stroke, and approved in Japan for this purpose,¹⁶⁹ but in the U.S., it failed in clinical trials for treatment of asthma, atherosclerosis, cerebral infarction, myocardial ischemia, peptic ulcer, and rheumatic disorder due to insufficient efficacy compared to placebo and concerns regarding its toxicity.^{14,111} Ebselen is currently in Phase II clinical trials for hearing loss and tinnitus and in phase I/II trials for Meniere's disease, tobramycin-induced ototoxicity, chemotherapy-induced hearing loss, and as a treatment for bipolar disorder.^{166,170,171}

Despite its setbacks in clinical trials, ebselen continues to be the standard for measuring small-molecule GPx-like activity, and it is a well-established ROS scavenger,¹⁷²⁻¹⁷⁵ although its biological mechanisms are not firmly established. One major issue preventing more biologically relevant studies of the antioxidant activity of ebselen and ebselen derivatives is its very limited water solubility (13.6 μ g/mL or 50 μ M). Our high-ethanol DNA damage prevention assay is capable of testing DNA damage even for hydrophobic compounds such as ebselen with water-solubilities of as little as 25 μ M.

Sies *et al.*⁶⁹ tested the ability of ebselen to inhibit peroxynitrite-induced DNA damage in a 1% methanol system (0.2 M). Since methanol scavenges radicals similarly to ethanol,^{69,176} the DNA damage control lane exhibited only 25% damage in this study. Although it was reported that 50 μ M ebselen inhibits 43% of DNA damage caused by peroxynitrite (100 μ M),⁶⁹ this translates to prevention of only 14% DNA damage. Due to this small difference in DNA damage inhibition, and since the experiment was only performed once, not in triplicate, it is not clear that the observed inhibition is significantly different from the control.

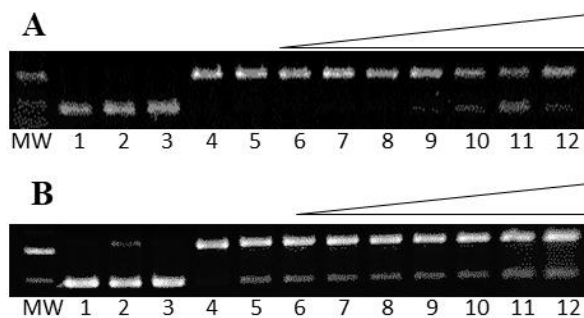


Figure 2.8. Gel electrophoresis images showing ebselen prevention of copper- and iron-mediated DNA damage. MW: 1 kb molecular weight marker; lane 1: plasmid DNA (p); lane 2: p + H₂O₂ and A) lane 3: p + 400 μM ebselen + H₂O₂ + 1.7 M ethanol; lane 4: p + Cu²⁺ (6 μM) + ascorbate (7.5 μM) + H₂O₂ + ethanol (10 mM); lane 5: p + Cu²⁺ (6 μM) + ascorbate (7.5 μM) + H₂O₂ + ethanol (1.7 M); lanes 6-13: Cu²⁺ (6 μM) + ascorbate (7.5 μM) + H₂O₂ + ethanol (1.7 M) + ebselen (1, 10, 50, 100, 200, 300, and 400 μM, respectively). B) lane 3: p + 400 μM ebselen + H₂O₂ + 1.7 M ethanol; lane 4: p + Fe²⁺ (2 μM) + H₂O₂ + ethanol (10 mM); lane 5: p + Fe²⁺ (15 μM) + H₂O₂ + ethanol (1.7 M); lanes 6-12: Fe²⁺ (15 μM) + H₂O₂ + ethanol (1.7 M) + ebselen (1, 10, 50, 100, 200, 300, and 400 μM, respectively).

In contrast, we tested ebselen for prevention of copper-mediated DNA damage in our high-ethanol assay. As shown in Figure 2.8A, Cu⁺/H₂O₂ causes over 86 ± 4% DNA damage (Figure 2.8A, lane 5; 1.25 equiv ascorbate is added to reduce Cu²⁺ to the DNA-damaging Cu⁺²³), comparable to DNA damage prevention observed under low-ethanol conditions 85 ± 2%, lane 4). A similar amount of DNA damage occurs under high- (on average 90 ± 5%) and low- (on average 89 ± 3%) ethanol conditions in the presence of Fe²⁺ and H₂O₂ (Figure 2.8B, lanes 4 and 5).

Ebselen alone does not cause DNA damage in the presence of H₂O₂ (lane 3), but increasing ebselen concentrations up to 400 μM (Figures 2.8A and B, lanes 6-13) prevents copper-mediated DNA damage. Even under these more hydrophobic conditions, the upper concentration range is limited by ebselen's solubility in aqueous 1.7 M ethanol solution. At the same concentrations, ebselen prevents no iron-mediated DNA damage.

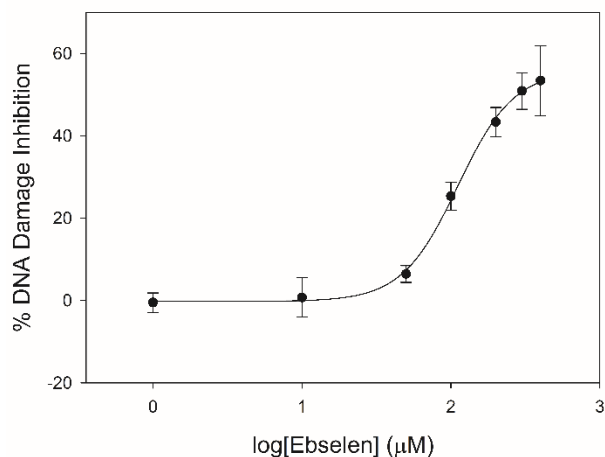


Figure 2.9. Dose-response curve for ebselen prevention of copper-mediated DNA damage under high-ethanol conditions.

These gel data were fit with a dose-response curve (Figure 2.9), and the IC_{50} value for ebselen prevention of copper-mediated DNA damage is $280.7 \pm 0.8 \mu\text{M}$. Due to ebselen's limited water solubility, our method is the first to determine an IC_{50} value for its ability to prevent DNA damage, a biologically relevant endpoint. Although it is an excellent radical scavenger (Table 2.2), ebselen shows only modest ability to prevent metal-mediated DNA damage, a primary cause of cell death under oxidative stress conditions.^{70,71,90,92,93,177}

The ability to test hydrophobic compounds such as ebselen for their ability to prevent metal-mediated DNA damage opens up a new area of antioxidant investigations, including development of more effective ebselen derivatives to prevent this DNA damage. Ebselen derivatives¹⁷⁸ were selected for testing using our high-ethanol DNA damage prevention studies based on the presence of structural features that might enhance metal coordination. Similar to ebselen itself, these ebselen derivatives were examined for their

ability to prevent metal-mediated DNA damage under high-ethanol conditions, the first study to examine the ability of ebselen derivatives to prevent DNA damage.

Similar to ebselen, all the tested ebselen derivatives more effectively prevent copper-mediated DNA damage than iron-mediated damage, with only ebselen-7-carboxylic acid (Figure 2.1) able to prevent iron-mediated DNA damage (IC_{50} of $235.3 \pm 0.6 \mu\text{M}$; Table 2.2). In addition, the selenium-containing ebselen derivatives are more effective than their sulfur analogs, highlighting the importance of selenium for antioxidant activity of these compounds. This is unsurprising, since ebsulfur is a less-effective GPx mimic compared to ebselen.¹⁰¹

Carboxylic acid moieties are known metal coordination sites,^{179,180} and addition of a carboxylate group to ebselen to form ebselen-7-carboxylic acid lowers the IC_{50} value for copper-mediated DNA damage prevention from 280.7 ± 0.8 to $213.3 \pm 0.6 \mu\text{M}$. The methyl ester of this compound is the most effective at preventing copper-mediated DNA damage, with an over-four-fold increase in activity compared to ebselen-7-carboxylic acid. Moving the carboxylate group to the *para*-position of the phenyl ring in ebselen-*N*-acetic acid decreases its ability to prevent copper-mediated DNA damage relative to ebselen.

Ebselen-7-carboxylic acid is also the only ebselen derivative that prevents iron-mediated DNA damage, likely due to the potential chelating site of the carboxylate oxygen and the selenium. Blocking this carboxylate oxygen with a methyl group in ebselen-7-carboxylic acid methyl ester, prevents all activity, further suggesting that antioxidant activity ebselen-7-carboxylic acid results from iron binding at this site. Ebselen and its derivatives more effectively prevent copper- over iron-mediated DNA damage, a results

that likely arises because of the soft selenium more strongly interacting with the soft Cu^+ than the borderline Fe^{2+} , although adding a hard oxygen donor near the selenium site with the potential for bidentate binding makes ebselen-7-carboxylic acid nearly equivalent in its ability to prevent copper- and iron-mediated DNA damage.

We have demonstrated that this DNA damage prevention assay permits assessment of hydrophobic compounds that cannot otherwise be investigated using DNA damage methods, including Edaravone, ebselen, and ebselen derivatives. Since we are examining DNA damage prevention directly, this assay is more biologically relevant than typical radical scavenging assays, and avoids the need to dubiously extend radical scavenging results to the more complex system of DNA damage prevention. This more hydrophobic DNA damage prevention assay is a significant step forward that will allow development of more effective hydrophobic antioxidants for the treatment and prevention of diseases caused by oxidative stress.

2.3 Conclusions

Most antioxidant assays only focus on specific antioxidant mechanism, such as radical scavenging or the reduction potential of copper and iron. Both classes of assays commonly use long-lived radicals, organic solvents, or other non-biologically relevant conditions. This resulted in the USDA distancing itself from ORAC results in 2012. In addition, DNA damage assays have been limited to hydrophobic compounds, and DPPH and ABTS assays, among others, have been translated into DNA damage prevention results without actually testing the compounds directly with DNA. We present the first gel

electrophoresis assay that allows the evaluation of copper- and iron-mediated DNA damage of hydrophobic compounds under biologically relevant conditions.

Iron-mediated DNA damage is more susceptible to increased ethanol concentrations than copper. This is reflected in the decade-long discussion of the actual oxidizing species produced by the Fenton- and Fenton-like reactions. This study demonstrates the differential susceptibility of the Fenton and Fenton-like reaction to ethanol through EPR spectroscopy experiments. Metal interactions play a major role in this assay, highlighted by the trends observed for polyphenol prevention of iron-mediated DNA damage, since iron binding is an established antioxidant mechanism for these compounds. In addition, the importance of metal coordination was also demonstrated by examining the IC₅₀ value trends of a group of ligands with nitrogen- and seleno moieties for prevention of copper- and iron-mediated DNA damage. Edaravone and Trolox, radical scavengers that do not coordinate to metals, show no activity in this assay. Although Edaravone is used to treat ALS that has been associated with elevated copper concentrations, our results suggest that Edaravone's mechanism of action likely does not involve significant copper interaction.

For the first time, this assay allowed biologically relevant DNA damage prevention testing for seleno and seleno derivatives. Seleno prevents only copper-mediated DNA damage, but addition of a carboxylate group to form a potential metal chelating site allows seleno-7-carboxylic acid to prevent both copper- and iron-mediated DNA damage. By testing a variety of potential antioxidants using this hydrophobic DNA damage assay, we showed that this new assay can be used to evaluate and compare new classes of compounds,

such as drugs that might cross the BBB, and can give insight into mechanisms for antioxidant behavior. This assay could potentially be used for the screening of new drugs to slow the process of Alzheimer's, Parkinson's and other diseases caused by oxidative stress.

2.4 Experimental Methods

Materials. Water was deionized (diH_2O) using a Nano Pure DIamond Ultrapure H_2O system (Barnstead International). 3-(*N*-morpholino)propanesulfonic acid (MOPS; Sigma), 2-(*N*-morpholino)ethanesulfonic acid (MES; BDH), NaCl (99.999% Alfa Aesar), CuSO_4 (Fisher), FeSO_4 (Acros), H_2O_2 (Fisher), DMPO (Cayman Chemicals), ascorbic acid (Alfa Aesar), DPPH (Alfa Aesar), Edaravone (Acros), Trolox (Acros), methanol (Sigma-Aldrich), pyridine (Alfa Aesar), bipy (Chem-Implex), GA (Acros), EC (Sigma), TA (Sigma Aldrich), PCA (Frontier Scientific), EGC (TCI), EGCG (Enzo), agarose (Sigma), Chelex (Sigma), and ebselen (Acros) were used as received. The ebselen derivatives (Figure 1D) were provided by Dr. Daniel Whitehead and Dr. Heeren Gordhan in the Department of Chemistry at Clemson University.

EPR spectroscopy. To prepare EPR samples, $\text{Cu}(\text{SO}_4)_2 \cdot 3\text{H}_2\text{O}$ (300 μM), ascorbic acid (375 μM), and H_2O_2 (2.5 mM), and indicated ethanol concentrations was added to an aqueous solution of MOPS (pH 7, 10 mM). DMPO (30 mM) was added to all the samples as a spin trap. Iron-containing samples were prepared with FeSO_4 (300 μM), H_2O_2 (2.5 mM) and DMPO (30 mM) with indicated ethanol concentrations in MES (pH 6, 10 mM). Deionized water was added to a final volume of 500 μL . EPR spectra were measured on a

Bruker EMX spectrometer at room temperature in a quartz flat cell. Spectra centered at 3431.24 G were acquired with a sweep width of 100 G. The modulation amplitude was 2.00 G with time and conversion constants of 81.92 s, and microwave power and frequency were 1.99 mW and 9.756 GHz, respectively.

DPPH assay. DPPH solutions (1.2 mg in 30 mL methanol, 100 μ M) were prepared fresh before each experiment: 0.5 mL of sample with indicated concentrations in methanol were combined with 1 mL of DPPH solution (100 μ M) with a final concentration of 67 μ M DPPH in methanol. The samples were incubated for 30 min in the dark, and spectra were taken at 515 nm on a Thermo Electron Corporation BioMate3 UV-visible spectrometer. Percentages of DPPH scavenging were calculated using the equation %DPPH scavenged = $((A-A_0)/(A_T-A_0))*100$, where A is the absorbance of the incubated sample and DPPH, A_0 is the absorbance of DPPH in methanol, and A_T is the absorbance of DPPH incubated with 50 μ M Trolox.

Plasmid DNA transfection, amplification, and purification. Plasmid DNA (pBSSK) was purified from DH1 *E. coli* competent cells using a ZyppyTM Plasmid Miniprep Kit (400 count, Zymo Research). Tris-EDTA buffer (pH 8.01) was used to elute the plasmid DNA from the spin columns. Plasmid was dialyzed against 130 mM NaCl for 24 h at 4°C to ensure all Tris-EDTA buffer and metal contaminants were removed, and plasmid concentration was determined by UV-vis spectroscopy at a wavelength of 260 nm. Absorbance ratios of $A_{250}/A_{260} \geq 0.95$ and $A_{260}/A_{280} \geq 1.8$ were determined for DNA used in all experiments. Plasmid purity was determined through digestion of plasmid (0.1 pmol) with Sac I and KpnI in a mixture of NEB buffer and bovine serum albumin at 37°C for

90 min. Digested plasmids were compared to an undigested plasmid sample and a 1 kb molecular weight marker using gel electrophoresis.

DNA damage gel electrophoresis experiments. Samples were prepped at room temperature by adding MOPS (10 mM, pH 7.0) or MES (10 mM, pH 6), NaCl (130 mM) and enough Deionized water to have a final volume of 10 μ L at the end. In a cold room at 4 °C, the compounds were dissolved in ethanol (100% proof), added to the indicated lanes and mixed. This step was performed below room temperature to minimize ethanol evaporation and reduce deviation between experiments. After the mixture warmed up to room temperature, the indicated concentrations of $\text{CuSO}_4 \cdot 5\text{H}_2\text{O}$, ascorbate (7.5 μ M, to reduce Cu^{2+} to Cu^+), and indicated compound were combined in an acid-washed (1 M HCl for ~ 1 h) microcentrifuge tubes and allowed to stand for 5 min at room temperature. Plasmid (pBSSK, 0.1 pmol in 130 mmol NaCl) was then added to the reaction mixtures and they were allowed to stand for 5 min at room temperature. H_2O_2 (50 μ M) was added and allowed to react at room temperature for 30 min. EDTA (50 μ M) was added after 30 min to quench the reactions. For the Fe^{2+} DNA damage experiments, the indicated concentrations of $\text{FeSO}_4 \cdot 7\text{H}_2\text{O}$ and MES (10 mM, pH 6.0) were used, and no ascorbate was added. All concentrations are final concentrations in a 10 μ M volume.

Samples were loaded into a 1% agarose gel in a TAE running buffer (50 \times); damaged and undamaged plasmid was separated by electrophoresis (140 V for 60 min). Gels were stained using ethidium bromide and imaged using UV light. The amounts of nicked (damaged) and circular (undamaged) were analyzed using UViProMW (Jencons Scientific Inc., 2007). Intensity of circular plasmid was multiplied by 1.24, due to the lower binding

affinity of ethidium bromide to supercoiled plasmid.^{63,181} Intensities of the nicked and supercoiled bands were normalized for each lane so that % nicked + % supercoiled = 100%. All percentages were corrected for residual nicked DNA prior to calculation. Results were obtained in triplicate for all experiments, and standard deviations are represented as error bars. The plots of percent DNA damage versus log concentration of copper or iron were fit to a variable-slope sigmoidal dose-response curve using SigmaPlot (v. 11.0, Systat Software, Inc.).

IC₅₀ Determination. Plots of percent inhibition of DNA damage versus log concentration of the indicated compound were fit to a variable slope sigmoidal dose-response curve using SigmaPlot, version 11 (Systat Software, Inc.). IC₅₀ value errors were calculated from error propagation of the gel electrophoresis measurements. Statistical significance was determined by calculating p values at 95% confidence (p < 0.05 indicates significance) as described by Perkowski et al.¹⁸² Data from DNA damage assays are provided in Tables 2.3-2.10.

2.5. Supporting Information

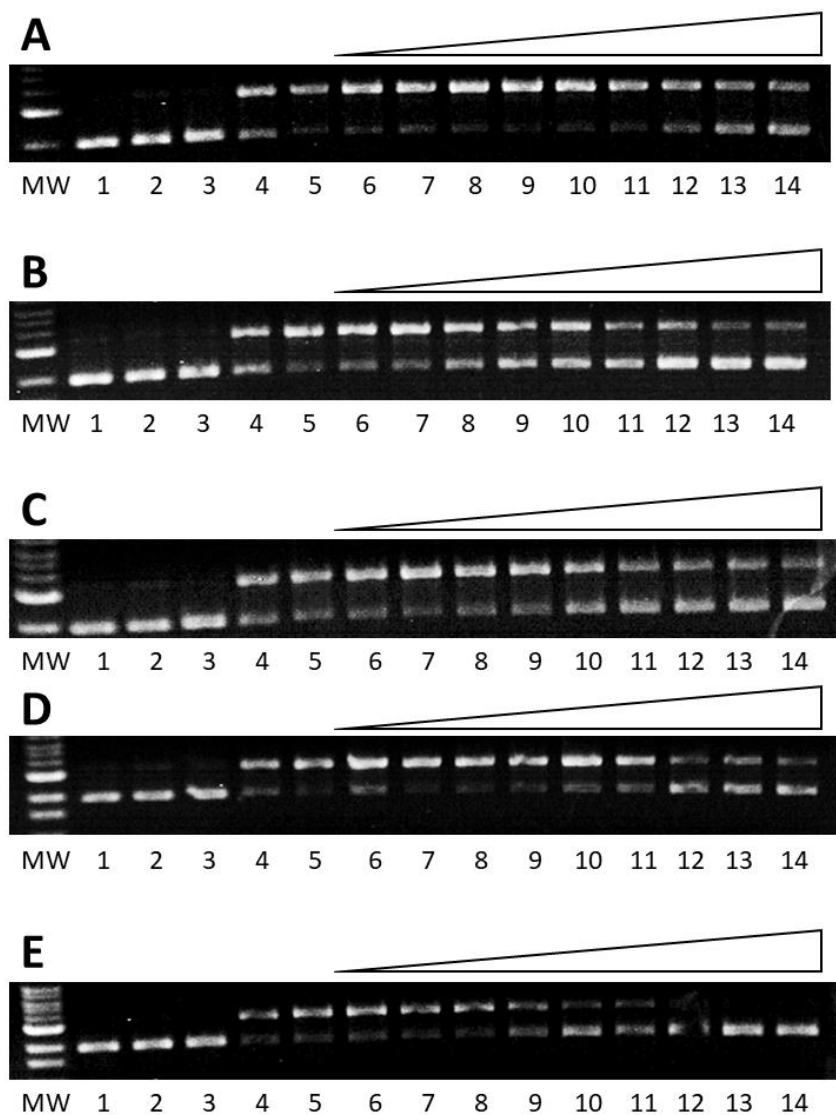


Figure 2.10. Gel image of iron-mediated DNA damage prevention by EC, GA, PCA, EGC, and EGCG. For all gel images MW: 1 kb molecular weight marker; lane 1: plasmid DNA (p); lane 2: p + H₂O₂ (50 μM); A) lane 3: p + H₂O₂ + EC (2000 μM); lane 4: p + Fe²⁺ (2 μM) + H₂O₂ + ethanol (10 mM); lane 5: p + Fe²⁺ (15 μM) + H₂O₂ + ethanol (1.7 M); lanes 6-14: p + H₂O₂ + FeSO₄ (15 μM) + EC (1, 10, 50, 100, 250, 500, 750, 1000, and 2000 μM, respectively); B) lane 3: p + H₂O₂ + GA (1000 μM); lane 4: p + Fe²⁺ (2 μM) + H₂O₂ + ethanol (10 mM); lane 5: p + Fe²⁺ (15 μM) + H₂O₂ + ethanol (1.7 M); lanes 6-14: p + H₂O₂ + FeSO₄ (15 μM) + GA (1, 10, 50, 75, 100, 250, 500, 750, and 1000 μM, respectively); C) lane 3: p + H₂O₂ + PCA (2000 μM); lane 4: p + Fe²⁺ (2 μM) + H₂O₂ + ethanol (10 mM); lane 5: p + Fe²⁺ (15 μM) + H₂O₂ + ethanol (1.7 M); lanes 6-14: p + H₂O₂ + FeSO₄ (15 μM) + PCA (1, 10, 50, 100, 250, 500, 750, 1000, and 2000 μM, respectively); D) lane 3: p + H₂O₂ + EGC (2000 μM); lane 4: p + Fe²⁺ (2 μM) + H₂O₂ + ethanol (10 mM); lane 5: p + Fe²⁺ (15 μM) + H₂O₂ + ethanol (1.7 M); lanes 6-14: p + H₂O₂ + FeSO₄ (15 μM) + EGC (1, 10, 50, 100, 250, 500, 750, 1000, and 2000 μM, respectively); E) lane 3: p + H₂O₂ + EGCG (500 μM); lane 4: p + Fe²⁺ (2 μM) + H₂O₂ + ethanol (10 mM); lane 5: p + Fe²⁺ (15 μM) + H₂O₂ + ethanol (1.7 M); lanes 6-14: p + H₂O₂ + FeSO₄ (15 μM) + EGCG (0.1, 1, 5, 10, 25, 50, 100, 250, and 500 μM, respectively).

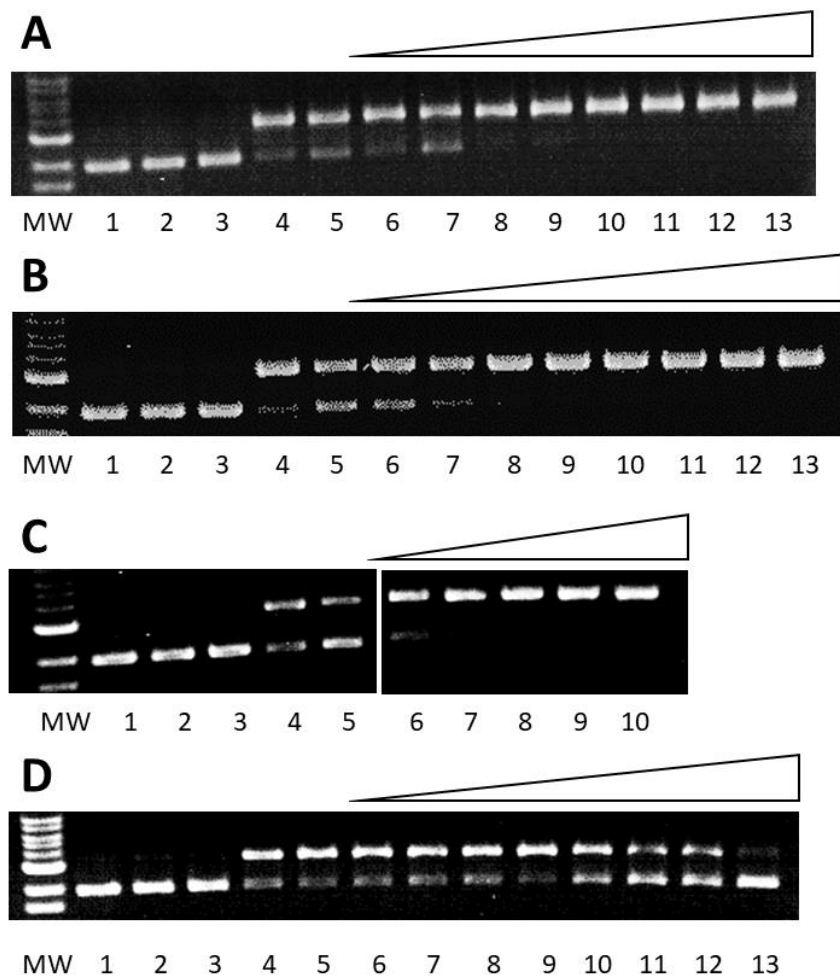


Figure 2.11. Gel image of copper- and iron-mediated DNA damage prevention by Trolox. For all gel images MW: 1 kb molecular weight marker; lane 1: plasmid DNA (p); lane 2: p + H₂O₂ (50 μM); A) lane 3: p + H₂O₂ + Trolox (2000 μM); lane 4: p + Cu²⁺ (6 μM) + ascorbate (7.5 μM) + H₂O₂ + ethanol (10 mM); lanes 5-13: p + H₂O₂ + Cu²⁺ (6 μM) + ascorbate (7.5 μM) + Trolox (0.1, 1, 5, 10, 50, 100, 500, 1000, and 2000 μM, respectively); B) lane 3: p + H₂O₂ + Trolox (1000 μM); lane 4: p + Cu²⁺ (6 μM) + ascorbate (7.5 μM) + H₂O₂ + ethanol (10 mM); lane 5: p + Cu²⁺ (6 μM) + ascorbate (7.5 μM) + H₂O₂ + ethanol (1.7 M); lanes 6-13: p + H₂O₂ + Cu²⁺ (6 μM) + ascorbate (7.5 μM) + Trolox (0.1, 1, 5, 10, 50, 100, 500, and 1000 μM, respectively); C) lane 3: p + H₂O₂ + Trolox (2000 μM); lane 4: p + Fe²⁺ (2 μM) + H₂O₂ + ethanol (10 mM); lane 5: p + Fe²⁺ (15 μM) + H₂O₂ + ethanol (1.7 M); lanes 6-10: p + H₂O₂ + Fe²⁺ (15 μM) + Trolox (10, 50, 100, 500, and 1000 μM, respectively); D) lane 3: p + H₂O₂ + Trolox (2000 μM); lane 4: p + Fe²⁺ (2 μM) + H₂O₂ + ethanol (10 mM); lanes 5-13: p + H₂O₂ + FeSO₄ (2 μM) + Trolox (0.1, 1, 5, 10, 50, 100, 500, 1000, and 2000 μM, respectively).

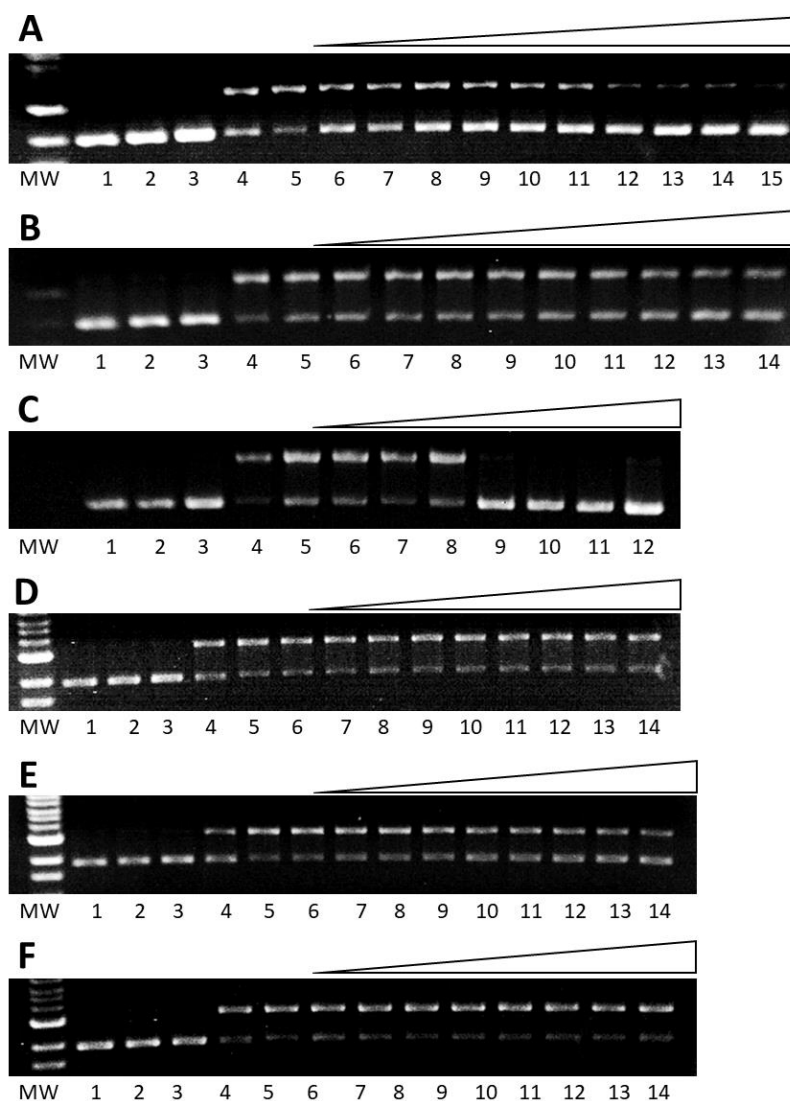


Figure 2.12. Gel image of iron-mediated DNA damage prevention by dmise, ebis, bipy, pyridine, sepy^{Me}, and Edaravone. For all gel images MW: 1 kb molecular weight marker; lane 1: plasmid DNA (p); lane 2: p + H₂O₂. (50 μM); A) lane 3: p + H₂O₂ + dmise (4000 μM); lane 4: p + Fe²⁺ (2 μM) + H₂O₂ + ethanol (10 mM); lane 5: p + H₂O₂ + Fe²⁺ (15 μM) + ethanol (1.7 M); lanes 6-15: p + H₂O₂ + Fe²⁺ (15 μM) + dmise (0.5, 1, 10, 50, 100, 400, 1000, 2000, and 4000 μM, respectively); B) lane 3: p + H₂O₂ + ebis (400 μM); lane 4: p + Fe²⁺ (2 μM) + H₂O₂ + ethanol (10 mM); lane 5: p + H₂O₂ + Fe²⁺ (15 μM) + ethanol (1.7 M); lanes 6-14: p + H₂O₂ + Fe²⁺ (15 μM) + ebis (0.1, 0.5, 1, 5, 10, 50, 100, 200 and 400 μM, respectively); C) lane 3: p + H₂O₂ + bipy (1000 μM); lane 4: p + Fe²⁺ (2 μM) + H₂O₂ + ethanol (10 mM); lane 5: p + H₂O₂ + Fe²⁺ (15 μM) + ethanol (1.7 M); lanes 6-12: p + H₂O₂ + Fe²⁺ (15 μM) + bipy (0.5, 1, 10, 50, 100, 400, and 1000 μM, respectively); D) lane 3: p + H₂O₂ + pyridine (2000 μM); lane 4: p + Fe²⁺ (2 μM) + H₂O₂ + ethanol (10 mM); lane 5: p + H₂O₂ + Fe²⁺ (15 μM) + ethanol (1.7 M); lanes 6-14: p + H₂O₂ + Fe²⁺ (15 μM) + pyridine (1, 10, 50, 100, 250, 500, 750, 1000, and 2000 μM, respectively); E) lane 3: p + H₂O₂ + sepy^{Me} (2000 μM); lane 4: p + Fe²⁺ (2 μM) + H₂O₂ + ethanol (10 mM); lane 5: p + H₂O₂ + Fe²⁺ (15 μM) + ethanol (1.7 M); lanes 6-14: p + H₂O₂ + Fe²⁺ (15 μM) + sepy^{Me} (1, 10, 50, 100, 250, 500, 750, 1000 and 2000 μM, respectively); F) lane 3: p + H₂O₂ + Edaravone (1000 μM); lane 4: p + Fe²⁺ (2 μM) + H₂O₂ + ethanol (10 mM); lane 5: p + H₂O₂ + Fe²⁺ (15 μM) + ethanol (1.7 M); lanes 6-14: p + H₂O₂ + Fe²⁺ (15 μM) + Edaravone (0.1, 1, 5, 10, 50, 100, 500, and 1000 μM, respectively).

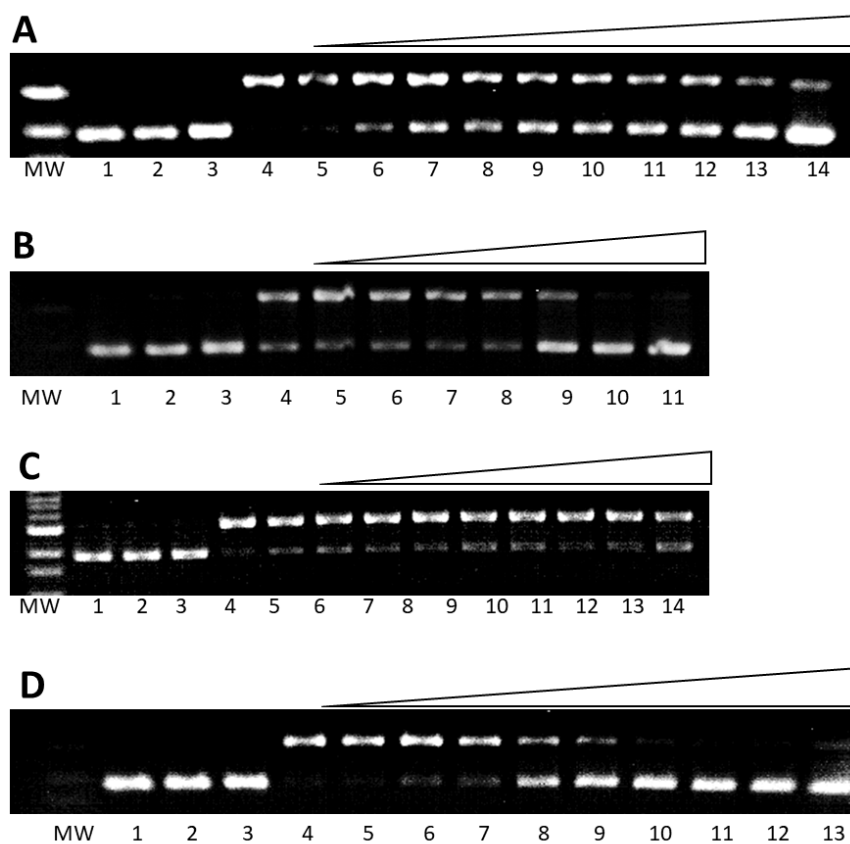


Figure 2.13. Gel image of copper-mediated DNA damage prevention by dmise, ebis, bipy, and Edaravone. For all gel images MW: 1 kb molecular weight marker; lane 1: plasmid DNA (p); lane 2: p + H₂O₂. (50 μM); A) lane 3: p + H₂O₂ + dmise (4000 μM); lane 4: p + Cu²⁺ (6 μM) + ascorbate (7.5 μM) + H₂O₂ + ethanol (10 mM); lane 5: p + H₂O₂ + Cu²⁺ (6 μM) + ascorbate (7.5 μM) + ethanol (1.7 M); lanes 6-14: p + H₂O₂ + Cu²⁺ (6 μM) + ascorbate (7.5 μM) +dmise (1, 10, 50, 100, 400, 750, 1000, 2000, and 4000 μM, respectively); B) lane 3: p + H₂O₂ + ebis (100 μM); lane 4: p + Cu²⁺ (6 μM) + ascorbate (7.5 μM) + H₂O₂ + ethanol (10 mM); lane 5: p + H₂O₂ + Cu²⁺ (6 μM) + ascorbate (7.5 μM) + ethanol (1.7 M); lanes 6-11: p + H₂O₂ + Cu²⁺ (6 μM) + ascorbate (7.5 μM) +ebis (0.5, 1, 5, 10, 50, and 100 μM, respectively); C) lane 3: p + H₂O₂ + bipy (1000 μM); lane 4: p + Cu²⁺ (6 μM) + ascorbate (7.5 μM) + H₂O₂ + ethanol (10 mM); lane 5: p + H₂O₂ + Cu²⁺ (6 μM) + ascorbate (7.5 μM) + ethanol (1.7 M); lanes 6-14: p + H₂O₂ + Cu²⁺ (6 μM) + ascorbate (7.5 μM) +bipy (0.5, 1, 5, 10, 50, 100, 500, and 1000 μM, respectively); D) lane 3: p + H₂O₂ + Edaravone (1000 μM); lane 4: p + Cu²⁺ (6 μM) + ascorbate (7.5 μM) + H₂O₂ + ethanol (10 mM); lane 5: p + H₂O₂ + Cu²⁺ (6 μM) + ascorbate (7.5 μM) + ethanol (1.7 M); lanes 6-13: p + H₂O₂ + Cu²⁺ (6 μM) + ascorbate (7.5 μM) + Edaravone (0.1, 1, 5, 10, 50, 100, 500, and 1000 μM, respectively).

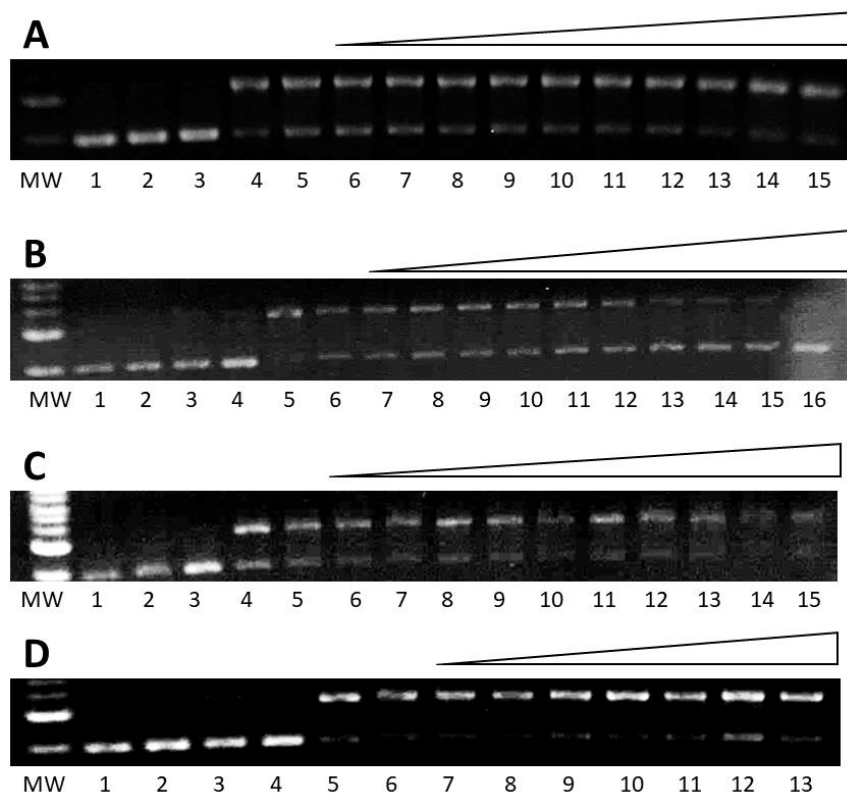


Figure 2.14. Gel image of iron-mediated DNA damage prevention by ebselen-*N*-acetic acid, ebselen-7-carboxylic acid, ebsulfur-*N*-acetic acid, and ebsulfur-7-carboxylic acid methyl ester. For all gel images MW: 1 kb molecular weight marker; lane 1: plasmid DNA (p); lane 2: p + H₂O₂. (50 μM); A) lane 3: p + H₂O₂ + ebselen-*N*-acetic acid (700 μM); lane 4: p + Fe²⁺ (2 μM) + H₂O₂ + ethanol (10 mM); lane 5: p + H₂O₂ + Fe²⁺ (15 μM) + ethanol (1.7 M); lanes 6-15: p + H₂O₂ + Fe²⁺ (15 μM) + ebselen-*N*-acetic acid (1, 10, 50, 100, 200, 300, 400, 500, 600, and 700 μM, respectively); B) lane 3: p + H₂O₂ + ebselen-7-carboxylic acid (700 μM); lane 4: p + Fe²⁺ (2 μM) + H₂O₂ + ethanol (10 mM); lane 5: p + H₂O₂ + Fe²⁺ (15 μM) + ethanol (1.7 M); lanes 6-14: p + H₂O₂ + Fe²⁺ (15 μM) + ebselen-7-carboxylic acid (1, 10, 50, 100, 200, 300, 400, 500, 600, and 700 μM, respectively); C) lane 3: p + H₂O₂ + ebsulfur-*N*-acetic acid (400 μM); lane 4: p + Fe²⁺ (2 μM) + H₂O₂ + ethanol (10 mM); lane 5: p + H₂O₂ + Fe²⁺ (15 μM) + ethanol (1.7 M); lanes 6-12: p + H₂O₂ + Fe²⁺ (15 μM) + ebsulfur-*N*-acetic acid (1, 50, 100, 200, 300, and 400 μM, respectively); D) lane 3: p + H₂O₂ + ebsulfur-7-carboxylic acid methyl ester (400 μM); lane 4: p + Fe²⁺ (2 μM) + H₂O₂ + ethanol (10 mM); lane 5: p + H₂O₂ + Fe²⁺ (15 μM) + ethanol (1.7 M); lanes 6-13: p + H₂O₂ + Fe²⁺ (15 μM) + ebsulfur-7-carboxylic acid methyl ester (1, 50, 100, 200, 300 and 400 μM).

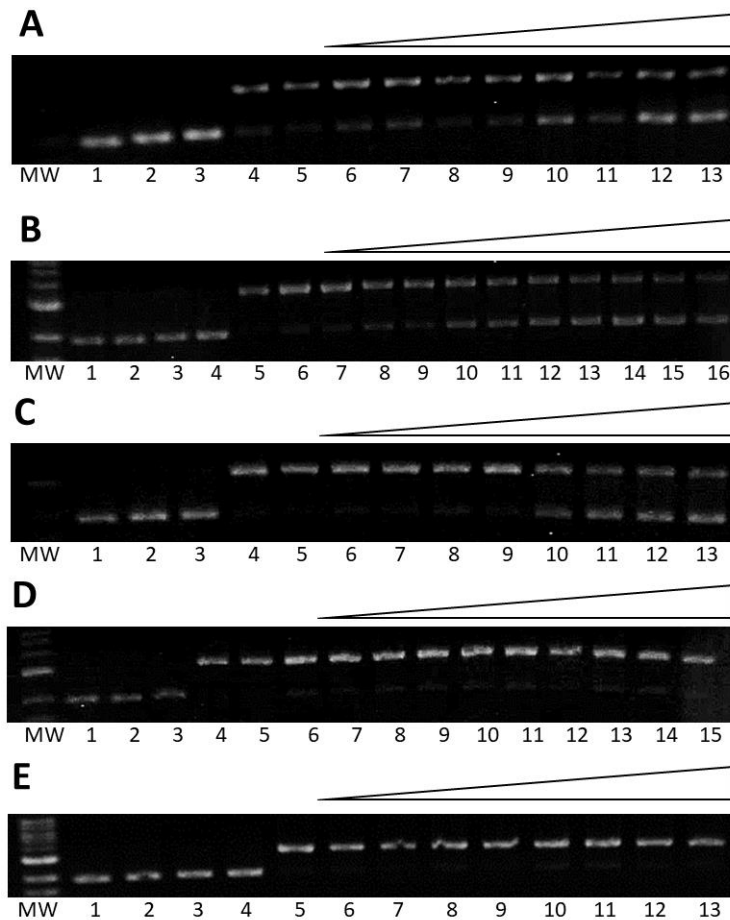


Figure 2.15. Gel image of copper-mediated DNA damage prevention ebselen-*N*-acetic acid, ebselen-7-carboxylic acid, ebsulfur-7-carboxylic acid methyl ester, ebsulfur-*N*-acetic acid, ebsulfur-7-carboxylic acid methyl ester. For all gel images MW: 1 kb molecular weight marker; lane 1: plasmid DNA (p); lane 2: p + H₂O₂. (50 μM); A) lane 3: p + H₂O₂ + ebselen-*N*-acetic acid (700 μM); lane 4: p + Cu²⁺ (6 μM) + ascorbate (7.5 μM) + H₂O₂ + ethanol (10 mM); lane 5: p + H₂O₂ + Cu²⁺ (6 μM) + ascorbate (7.5 μM) + ethanol (1.7 M); lanes 7-13: p + H₂O₂ + Cu²⁺ (6 μM) + ascorbate (7.5 μM) + ebselen-*N*-acetic acid (1, 10, 50, 100, 200, 300, 400, 500, 600, and 700 μM, respectively); B) lane 3: p + H₂O₂ + ebselen-7-carboxylic acid (700 μM); lane 4: p + Cu²⁺ (6 μM) + ascorbate (7.5 μM) + H₂O₂ + ethanol (10 mM); lane 5: p + H₂O₂ + Cu²⁺ (6 μM) + ascorbate (7.5 μM) + ethanol (1.7 M); lanes 7-16: p + H₂O₂ + Cu²⁺ (6 μM) + ascorbate (7.5 μM) ebselen-7-carboxylic acid (1, 10, 50, 100, 200, 300, 400, 500, 600 and 700 μM, respectively); C) lane 3: p + H₂O₂ + ebsulfur-7-carboxylic acid methyl ester (700 μM); lane 4: p + Cu²⁺ (6 μM) + ascorbate (7.5 μM) + H₂O₂ + ethanol (10 mM); lane 5: p + H₂O₂ + Cu²⁺ (6 μM) + ascorbate (7.5 μM) + ethanol (1.7 M); lanes 7-15: p + H₂O₂ + Cu²⁺ (6 μM) + ascorbate (7.5 μM) + ebsulfur-7-carboxylic acid methyl ester (1, 10, 50, 100, 200, 300, 400, 500, 600 and 700 μM, respectively); D) lane 3: p + H₂O₂ + ebsulfur-*N*-acetic acid (400 μM); lane 4: p + Cu²⁺ (6 μM) + ascorbate (7.5 μM) + H₂O₂ + ethanol (10 mM); lane 5: p + H₂O₂ + Cu²⁺ (6 μM) + ascorbate (7.5 μM) + ethanol (1.7 M); lanes 7-13: p + H₂O₂ + Cu²⁺ (6 μM) + ascorbate (7.5 μM) + ebsulfur-*N*-acetic acid (1, 50, 100, 200, 300 and 400 μM, respectively); E) lane 3: p + H₂O₂ + ebsulfur-7-carboxylic acid methyl ester (400 μM); lane 4: p + Cu²⁺ (6 μM) + ascorbate (7.5 μM) + H₂O₂ + ethanol (10 mM); lane 5: p + H₂O₂ + Cu²⁺ (6 μM) + ascorbate (7.5 μM) + ethanol (1.7 M); lanes 7-13: p + H₂O₂ + Cu²⁺ (6 μM) + ascorbate (7.5 μM) + ebsulfur-7-carboxylic acid methyl ester (1, 50, 100, 200, 300 and 400 μM, respectively).

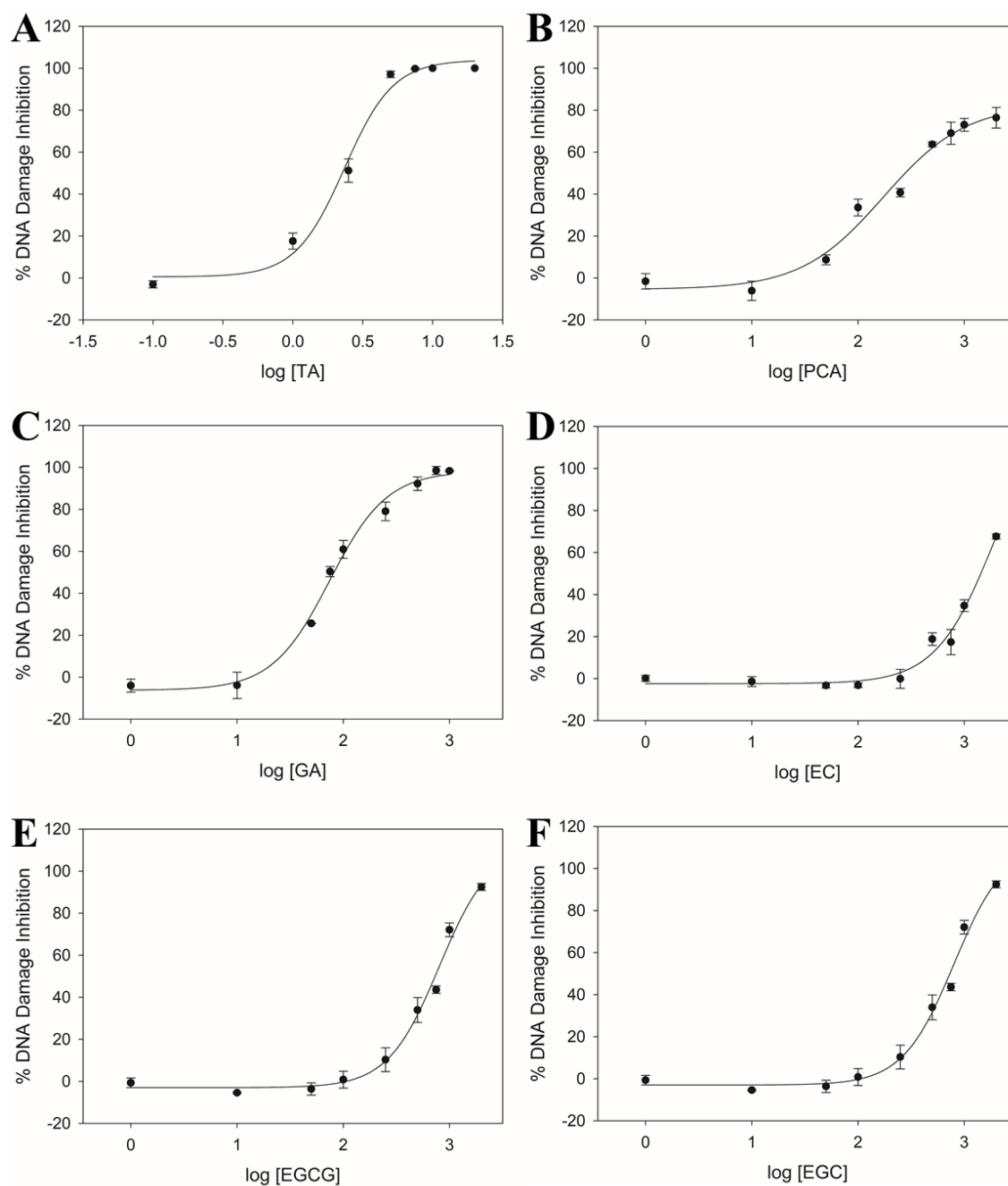


Figure 2.16. Dose-response curves for iron-mediated DNA damage prevention under high-ethanol (1.7 M) conditions for A) tannic acid, B) protocatechuic acid, C) gallic acid, D) epicatechin, E) epigallocatechin gallate, and F) epigallocatechin.

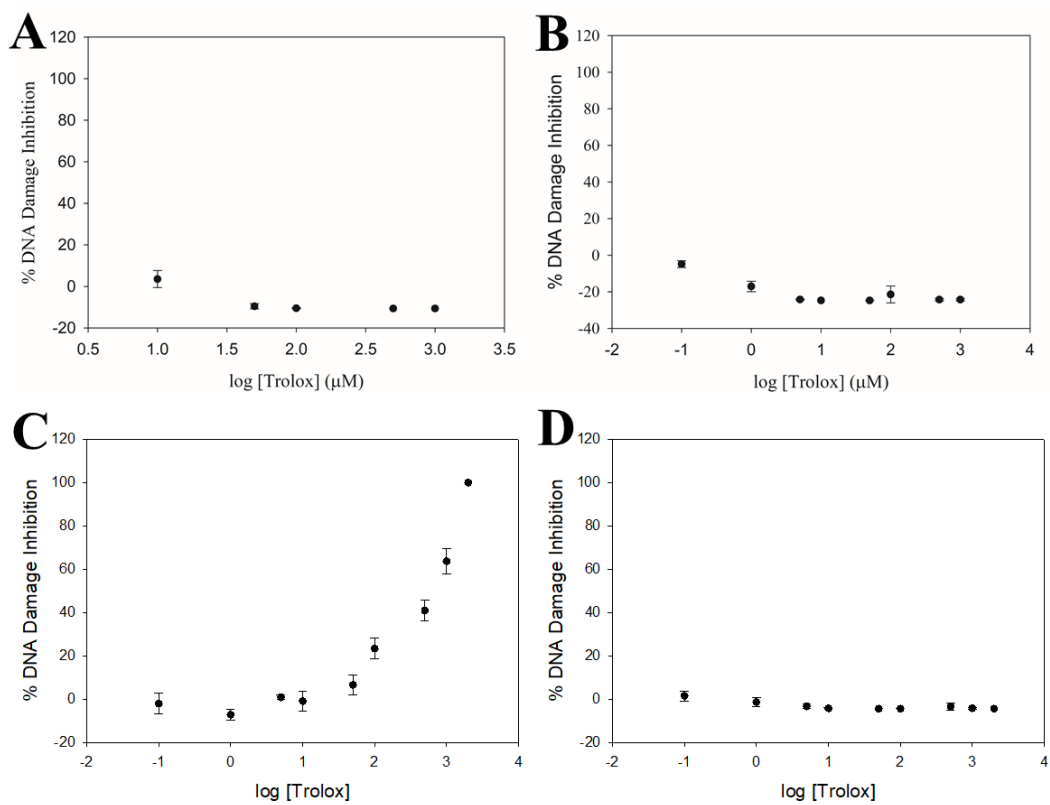


Figure 2.17. Dose-response curves for A) copper-mediated DNA damage prevention by Trolox under high-ethanol conditions (1.7 M), B) iron-mediated DNA damage prevention by Trolox and 1.7 M ethanol, C) copper-mediated DNA damage with Trolox and 10 mM ethanol, and D) iron-mediated DNA damage with Trolox and 10 mM ethanol.

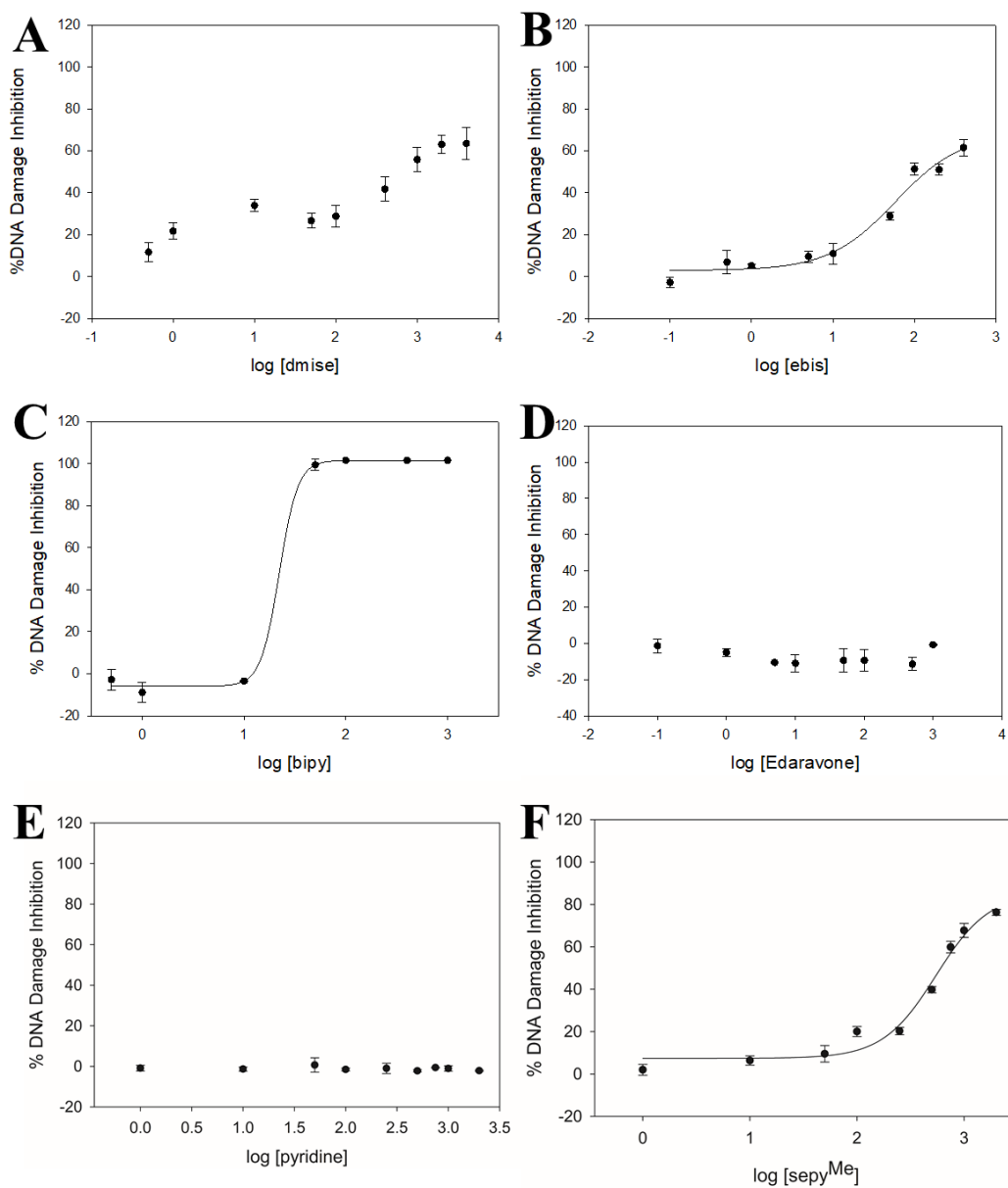


Figure 2.18. Dose-response curves for iron-mediated DNA damage prevention under ethanol (1.7 M) conditions for A) dmise, B) ebis, C) bipy, D) Edaravone, E) pyridine, and F) sepy^{Me}.

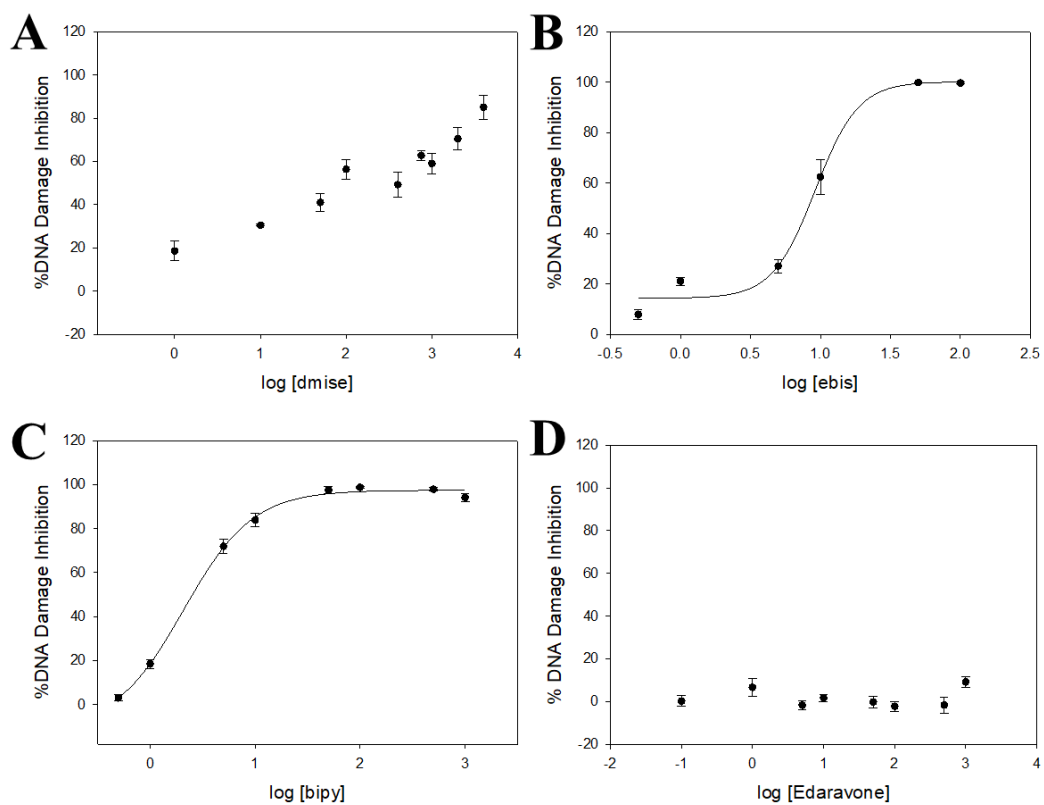


Figure 2.19. Dose-response curves for copper-mediated DNA damage prevention under ethanol (1.7 M) conditions for A) dmise, B) ebis, C) bipy, and D) Edaravone.

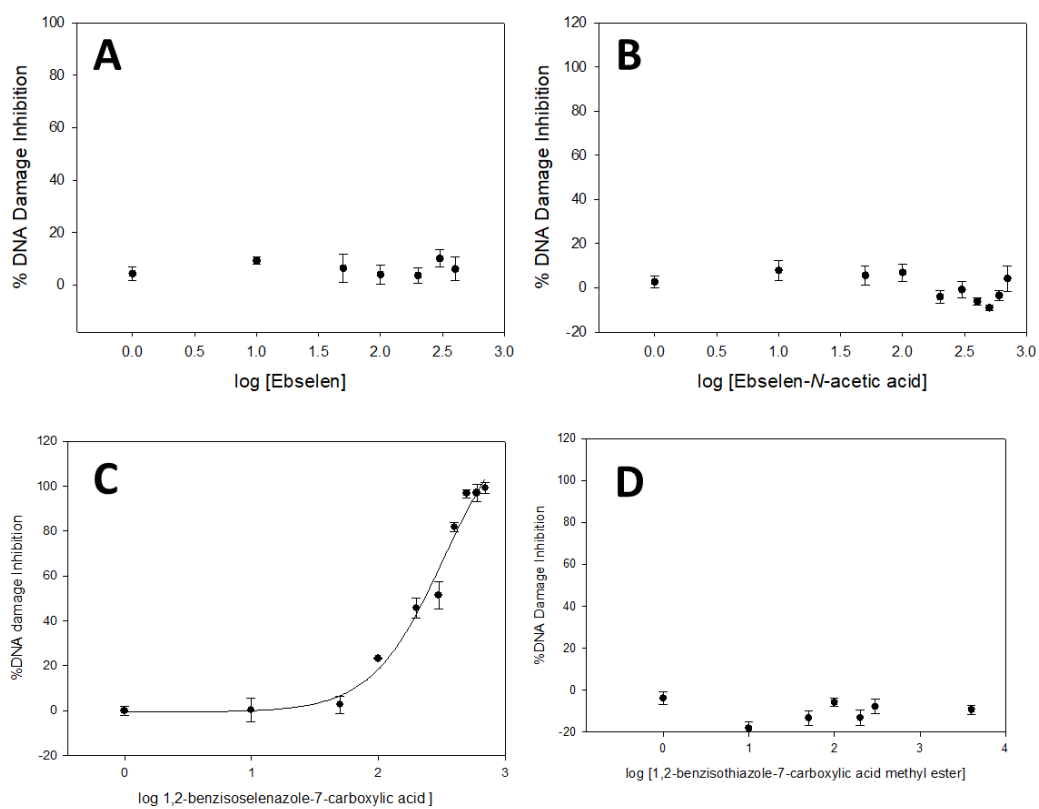


Figure 2.20. Dose-response curves for iron-mediated DNA damage prevention under high-ethanol (1.7 M) conditions for A) ebselen, B) ebselen-*N*-acetic acid, C) ebsulfur-7-carboxylic acid, and D) ebulfur-7-carboxylic acid methyl ester.

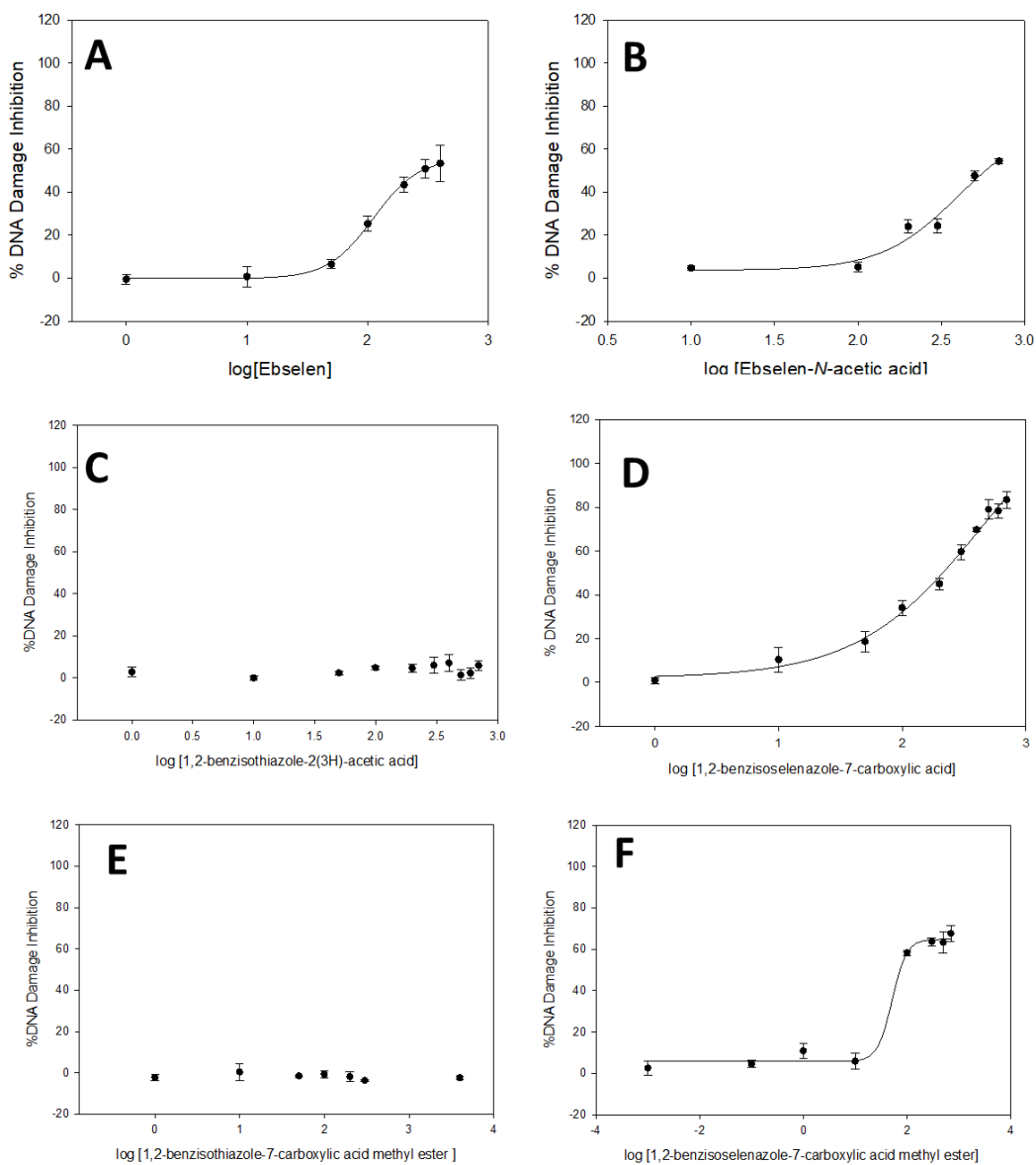


Figure 2.21. Dose-response curves for copper-mediated DNA damage prevention under high-ethanol conditions (1.7 M) for A) ebselen B) ebselen-*N*-acetic acid C) ebsulfur-*N*-acetic acid, D) ebsulfur-7-carboxylic acid, E) ebsulfur-7-carboxylic acid methyl ester, and F) ebselen-7-carboxylic acid methyl ester.

Table 2.3. Gel electrophoresis results for EC DNA damage assays with Fe²⁺, and 50 μM H₂O₂.^a

Gel lane	[EC], μM	% Supercoiled	% Nicked	% Damage	<i>p</i> Value
1: plasmid DNA (p)	-	99.99 ± 0.02	0.01	-	-
2: p + H ₂ O ₂ (50 μM)	-	99.99 ± 0.02	0.01	-	-
3: p + EC+ H ₂ O ₂ + ethanol (1.7 M)	2000	99.82 ± 0.31	0.18	-	-
4: p + Fe ²⁺ (2 μM) + H ₂ O ₂ + ethanol (10 mM)	-	20.01 ± 4.89	79.99	-	-
5: p + Fe ²⁺ (15 μM) + H ₂ O ₂ + ethanol (1.7 M)	-	4.19 ± 0.12	95.81	0	-
6: p + Fe ²⁺ (15 μM) + H ₂ O ₂ + EC + ethanol (1.7 M)	1	4.28 ± 1.44	95.72	0.09 ± 1.44	0.924
7:	10	2.83 ± 2.36	97.17	-1.41 ± 2.36	0.409
8:	50	1.05 ± 1.22	98.95	-3.28 ± 1.22	0.043
9:	100	1.12 ± 1.09	98.88	-3.21 ± 1.09	0.036
10:	250	4.09 ± 4.51	95.91	-0.10 ± 4.51	0.973
11:	500	22.20 ± 3.01	77.80	18.80 ± 3.01	0.008
12:	750	20.80 ± 5.99	79.20	17.34 ± 5.99	0.036
13:	1000	37.41 ± 2.82	62.59	34.67 ± 2.82	0.002
14:	2000	68.99 ± 1.20	31.01	67.63 ± 1.20	< 0.001

^aData are reported as the average of three trials with calculated standard deviations shown.**Table 2.4.** Gel electrophoresis results for GA DNA damage assays with Fe²⁺, and 50 μM H₂O₂.^a

Gel lane	[GA], μM	% Supercoiled	% Nicked	% Damage	<i>p</i> Value
1: plasmid DNA (p)	-	100 ±	0.00	-	-
2: p + H ₂ O ₂ (50 μM)	-	100 ±	0.00	-	-
3: p + GA+ H ₂ O ₂ + ethanol (1.7 M)	1000	100 ±	0.00	-	-
4: p + Fe ²⁺ (2 μM) + H ₂ O ₂ + ethanol (10 mM)	-	20.01 ± 4.89	79.99	-	-
5: p + Fe ²⁺ (15 μM) + H ₂ O ₂ + ethanol (1.7 M)	-	14.55 ± 2.04	85.45	0	-
6: p + Fe ²⁺ (15 μM) + H ₂ O ₂ + GA + ethanol (1.7 M)	1	10.99 ± 3.16	89.01	-4.01 ± 3.13	0.157
7:	10	11.11 ± 6.31	88.89	-3.90 ± 6.29	0.395
8:	50	36.36 ± 0.15	63.64	25.63 ± 0.15	< 0.001
9:	75	57.51 ± 2.41	42.49	50.33 ± 2.42	< 0.001
10:	100	66.59 ± 4.24	33.41	60.92 ± 4.25	< 0.001
11:	250	82.06 ± 4.43	17.94	79.04 ± 4.45	< 0.001
12:	500	93.36 ± 3.24	6.64	92.21 ± 3.24	< 0.001
13:	750	98.73 ± 1.96	1.27	98.52 ± 1.94	< 0.001
14:	1000	98.57 ± 0.36	1.43	98.29 ± 0.35	< 0.001

^aData are reported as the average of three trials with calculated standard deviations shown.

Table 2.5. Gel electrophoresis results for PCA DNA damage assays with Fe²⁺, and 50 μM H₂O₂.^a

Gel lane	[PCA], μM	% Supercoiled	% Nicked	% Damage	<i>p</i> Value
1: plasmid DNA (p)	-	100 ± 0	0.00	-	-
2: p + H ₂ O ₂ (50 μM)	-	100 ± 0	0.00	-	-
3: p + PCA+ H ₂ O ₂ + ethanol (1.7 M)	2000	100 ± 0	0.00	-	-
4: p + Fe ²⁺ (2 μM) + H ₂ O ₂ + ethanol (10 mM)	-	20.01 ± 4.89	79.99	-	-
5: p + Fe ²⁺ (15 μM) + H ₂ O ₂ + ethanol (1.7 M)	-	12.94 ± 2.12	87.06	0	-
6: p + Fe ²⁺ (15 μM) + H ₂ O ₂ + PCA + ethanol (1.7 M)	1	11.56 ± 3.68	88.44	-1.58 ± 3.68	0.535
7:	10	7.63 ± 4.56	92.37	-6.10 ± 4.56	0.146
8:	50	20.51 ± 2.37	79.49	8.70 ± 2.37	0.239
9:	100	42.17 ± 3.99	57.83	33.58 ± 3.99	0.005
10:	250	48.37 ± 2.01	51.63	40.70 ± 2.01	< 0.001
11:	500	68.40 ± 1.18	31.60	63.70 ± 1.18	< 0.001
12:	750	73.01 ± 5.30	26.99	69.00 ± 5.30	< 0.001
13:	1000	76.50 ± 3.01	23.50	73.01 ± 3.01	< 0.001
14:	2000	79.46 ± 4.95	20.54	76.40 ± 4.95	< 0.001

^aData are reported as the average of three trials with calculated standard deviations shown.**Table 2.6.** Gel electrophoresis results for TA DNA damage assays with Fe²⁺, and 50 μM H₂O₂.^a

Gel lane	[TA], μM	% Supercoiled	% Nicked	% Damage	<i>p</i> Value
1: plasmid DNA (p)		100 ± 0	0.00	-	-
2: p + H ₂ O ₂ (50 μM)		100 ± 0	0.00	-	-
3: p + TA+ H ₂ O ₂ + ethanol (1.7 M)	20	99.99 ± 0.02	0.01	-	-
4: p + Fe ²⁺ (2 μM) + H ₂ O ₂ + ethanol (10 mM)		10.61 ± 4.89	80.39	-	-
5: p + Fe ²⁺ (15 μM) + H ₂ O ₂ + ethanol (1.7 M)		13.53 ± 3.15	86.47	0	-
6: p + Fe ²⁺ (15 μM) + H ₂ O ₂ + TA + ethanol (1.7 M)	0.1	9.42 ± 1.69	90.58	-3.05 ± 1.69	0.089
7:	1	27.56 ± 3.84	72.44	17.60 ± 3.84	0.015
8:	2.5	57.11 ± 5.54	42.89	51.20 ± 5.54	0.004
9:	5	97.41 ± 1.50	2.59	97.06 ± 1.50	< 0.001
10:	7.5	99.76 ± 0.41	0.24	99.73 ± 0.41	< 0.001
11:	10	100 ± 0	0.00	100 ± 0	< 0.001
12:	20	100 ± 0	0.00	100 ± 0	< 0.001

^aData are reported as the average of three trials with calculated standard deviations shown.

Table 2.7. Gel electrophoresis results for EGC DNA damage assays with Fe²⁺, and 50 μM H₂O₂.^a

Gel lane	[EGC], μM	% Supercoiled	% Nicked	% Damage	<i>p</i> Value
1: plasmid DNA (p)		100.00 ± 0	0.00	-	-
2: p + H ₂ O ₂ (50 μM)		0.00 ± 0	0.00	-	-
3: p + EGC+ H ₂ O ₂ + ethanol (1.7 M)	2000	100.00 ± 0	0.00	-	-
4: p + Fe ²⁺ (2 μM) + H ₂ O ₂ + ethanol (10 mM)		20.94 ± 8.87	79.06	-	-
5: p + Fe ²⁺ (15 μM) + H ₂ O ₂ + ethanol (1.7 M)		5.44 ± 2.92	94.56	0	-
6: p + Fe ²⁺ (15 μM) + H ₂ O ₂ + EGC + ethanol (1.7 M)	1	4.43 ± 2.31	95.57	-0.69 ± 2.28	0.652
7:	10	0.33 ± 0.40	99.67	-5.40 ± 0.40	0.002
8:	50	2.02 ± 2.91	97.98	-3.61 ± 2.91	0.165
9:	100	6.20 ± 4.03	93.80	0.81 ± 4.03	0.761
10:	250	15.19 ± 5.65	84.81	10.31 ± 5.65	0.087
11:	500	37.53 ± 5.93	62.47	33.94 ± 5.93	0.010
12:	750	46.66 ± 1.78	53.34	43.59 ± 1.78	< 0.001
13:	1000	73.59 ± 3.25	26.41	72.08 ± 3.25	< 0.001
14:	2000	92.84 ± 1.66	7.16	92.43 ± 1.66	< 0.001

^aData are reported as the average of three trials with calculated standard deviations shown.**Table 2.8.** Gel electrophoresis results for EGCG DNA damage assays with Fe²⁺, and 50 μM H₂O₂.^a

Gel lane	[EGCG], μM	% Supercoiled	% Nicked	% Damage	<i>p</i> Value
1: plasmid DNA (p)		100.00 ± 0	0.00	-	-
2: p + H ₂ O ₂ (50 μM)		99.96 ± 0.06	0.04	-	-
3: p + EGCG+ H ₂ O ₂ + ethanol (1.7 M)	500	100.00 ± 0	0.00	-	-
4: p + Fe ²⁺ (2 μM) + H ₂ O ₂ + ethanol (10 mM)		12.86 ± 3.56	87.14	-	-
5: p + Fe ²⁺ (15 μM) + H ₂ O ₂ + ethanol (1.7 M)		13.25 ± 3.96	86.75	0	-
6: p + Fe ²⁺ (15 μM) + H ₂ O ₂ + EGCG + ethanol (1.7 M)	0.1	18.26 ± 4.61	81.74	5.83 ± 4.61	0.160
7:	1	11.57 ± 4.01	88.43	-1.89 ± 4.01	0.500
8:	5	3.15 ± 4.10	96.85	-11.59 ± 4.10	0.038
9:	10	43.98 ± 3.02	56.02	35.47 ± 3.02	0.002
10:	25	82.10 ± 5.48	17.90	79.41 ± 5.48	0.002
11:	50	84.80 ± 2.23	15.20	82.53 ± 2.23	< 0.001
12:	100	98.79 ± 0.91	1.21	98.65 ± 0.91	< 0.001
13:	250	99.98 ± 0.1	0.02	100.03 ± 0.01	< 0.001
14:	500	99.96 ± 0.7	0.04	100.00 ± 0.07	< 0.001

^aData are reported as the average of three trials with calculated standard deviations shown.

Table 2.9. Gel electrophoresis results for sepy^{Me} DNA damage assays with Fe²⁺, and 50 μM H₂O₂.^a

Gel lane	[sepy ^{Me}], μM	% Supercoiled	% Nicked	% Damage	<i>p</i> Value
1: plasmid DNA (p)		99.99 ± 0.02	0.01	-	-
2: p + H ₂ O ₂ (50 μM)		99.98 ± 0.04	0.02	-	-
3: p + sepy ^{Me} + H ₂ O ₂ + ethanol (1.7 M)	2000	100.00 ± 0	0.00	-	-
4: p + Fe ²⁺ (2 μM) + H ₂ O ₂ + ethanol (10 mM)		23.49 ± 3.90	76.51	-	-
5: p + Fe ²⁺ (15 μM) + H ₂ O ₂ + ethanol (1.7 M)		4.53 ± 2.26	95.47	0	-
6: p + Fe ²⁺ (15 μM) + H ₂ O ₂ + sepy ^{Me} + ethanol (1.7 M)	1	6.40 ± 2.57	93.60	1.97 ± 2.57	0.316
7:	10	10.56 ± 2.18	89.44	6.33 ± 2.19	0.038
8:	50	13.60 ± 3.90	86.40	9.51 ± 3.90	0.052
9:	100	23.63 ± 2.37	76.37	20.01 ± 2.37	0.005
10:	250	23.86 ± 1.75	76.14	20.25 ± 1.75	0.005
11:	500	42.51 ± 1.48	57.49	39.79 ± 1.48	< 0.001
12:	750	61.65 ± 2.75	38.35	59.84 ± 2.75	< 0.001
13:	1000	69.15 ± 3.33	30.85	67.70 ± 3.33	< 0.001
14:	2000	77.31 ± 1.42	22.69	76.24 ± 1.42	< 0.001

^aData are reported as the average of three trials with calculated standard deviations shown.**Table 2.10.** Gel electrophoresis results for pyridine DNA damage assays with Fe²⁺, and 50 μM H₂O₂.^a

Gel lane	[pyr], μM	% Supercoiled	% Nicked	% Damage	<i>p</i> Value
1: plasmid DNA (p)		100.00 ± 0	0.00	-	-
2: p + H ₂ O ₂ (50 μM)		100.00 ± 0	0.00	-	-
3: p + pyr+ H ₂ O ₂ + ethanol (1.7 M)	2000	100.00 ± 0	0.00	-	-
4: p + Fe ²⁺ (2 μM) + H ₂ O ₂ + ethanol (10 mM)		6.46 ± 5.17	93.54	-	-
5: p + Fe ²⁺ (15 μM) + H ₂ O ₂ + ethanol (1.7 M)		2.45 ± 1.63	97.55	0	-
6: p + Fe ²⁺ (15 μM) + H ₂ O ₂ + pyr + ethanol (1.7 M)	1	1.57 ± 1.39	98.43	-0.90 ± 1.39	0.379
7:	10	1.13 ± 1.05	98.87	-1.35 ± 1.05	0.156
8:	50	3.11 ± 3.53	96.89	0.68 ± 3.53	0.770
9:	100	0.94 ± 0.65	99.06	-1.55 ± 0.65	0.054
10:	250	1.46 ± 2.53	98.54	-1.02 ± 2.53	0.557
11:	500	0.30 ± 0.52	99.70	-2.21 ± 0.52	0.018
12:	750	1.84 ± 0.11	98.16	-0.63 ± 0.11	0.010
13:	1000	1.41 ± 1.33	98.59	-1.07 ± 1.33	0.298
14:	2000	0.34 ± 0.33	99.66	-2.16 ± 0.33	0.008

^aData are reported as the average of three trials with calculated standard deviations shown.

Table 2.11. Gel electrophoresis results for bipy DNA damage assays with Fe²⁺, and 50 μM H₂O₂.^a

Gel lane	[bipy], μM	% Supercoiled	% Nicked	% Damage	<i>p</i> Value
1: plasmid DNA (p)	0	100 ± 0	0	-	-
2: p + H ₂ O ₂ (50 μM)	0	99.37 ± 1.08	0.6	-	-
3: p + bipy+ H ₂ O ₂ + ethanol (1.7 M)	1000	100 ± 0	0	-	-
4: p + Fe ²⁺ (2 μM) + H ₂ O ₂ + ethanol (10 mM)	0	16.96 ± 5.20	83.04	-	-
5: p + Fe ²⁺ (15 μM) + H ₂ O ₂ + ethanol (1.7 M)	0	30.45 ± 6.49	69.55	0	-
6: p + Fe ²⁺ (15 μM) + H ₂ O ₂ + bipy + ethanol (1.7 M)	0.5	27.46 ± 4.92	72.54	-2.79 ± 4.92	0.427
7:	1	23.17 ± 4.82	76.83	-8.92 ± 4.89	0.085
8:	10	26.94 ± 0.15	73.06	-3.51 ± 0.15	0.001
9:	50	98.49 ± 2.62	1.51	99.40 ± 2.60	<0.001
10:	100	100 ± 0	0	101.55 ± 0	<0.001
11:	400	100 ± 0	0	101.55 ± 0	<0.001
12:	1000	100 ± 0	0	101.55 ± 0	<0.001

^aData are reported as the average of three trials with calculated standard deviations shown.**Table 2.12.** Gel electrophoresis results for bipy DNA damage assays with Cu⁺, and 50 μM H₂O₂.^a

Gel lane	[bipy], μM	% Supercoiled	% Nicked	% Damage	<i>p</i> Value
1: plasmid DNA (p)	0	100 ± 0	0.00	-	-
2: p + H ₂ O ₂ (50 μM)	0	100 ± 0	0.00	-	-
3: p + bipy+ H ₂ O ₂ + ethanol (1.7 M)	1000	100 ± 0	0.00	-	-
4: p + Cu ²⁺ (6 μM) + ascorbate (7.5 μM) H ₂ O ₂ + ethanol (10 mM)	0	12.30 ± 3.47	87.70	-	-
5: p + Cu ²⁺ (6 μM) + ascorbate (7.5 μM) + H ₂ O ₂ + ethanol (1.7 M)	0	21.20 ± 2.62	78.80	0	-
6: p + Cu ²⁺ (6 μM) + ascorbate (7.5 μM) + H ₂ O ₂ + bipy + ethanol (1.7 M)	0.5	23.57 ± 1.19	76.43	3.00 ± 1.44	0.069
7:	1	35.81 ± 1.70	64.19	18.53 ± 2.07	0.004
8:	5	77.89 ± 2.55	22.11	71.95 ± 3.12	< 0.001
9:	10	87.37 ± 2.37	12.63	83.97 ± 2.90	< 0.001
10:	50	98.08 ± 1.27	1.92	97.55 ± 1.55	< 0.001
11:	100	99.04 ± 0.44	0.96	98.77 ± 0.55	< 0.001
12:	500	98.25 ± 0.75	1.65	97.93 ± 0.91	< 0.001
13:	1000	95.41 ± 1.33	4.59	94.16 ± 1.66	< 0.001

^aData are reported as the average of three trials with calculated standard deviations shown.

Table 2.13. Gel electrophoresis results for dmise DNA damage assays with Fe²⁺, and 50 μM H₂O₂.^a

Gel lane	[dmise], μM	% Supercoiled	% Nicked	% Damage	<i>p</i> Value
1: plasmid DNA (p)	0	100.0 ± 0	0	-	-
2: p + H ₂ O ₂ (50 μM)	0	100.0 ± 0	0.0	-	-
3: p + dmise+ H ₂ O ₂ + ethanol (1.7 M)	4000	100.0 ± 0	0.0	-	-
4: p + Fe ²⁺ (2 μM) + H ₂ O ₂ + ethanol (10 mM)	0	13.7 ± 4.8	86.3	-	-
5: p + Fe ²⁺ (15 μM) + H ₂ O ₂ + ethanol (1.7 M)	0	36.9 ± 4.6	63.1	0	-
6: p + Fe ²⁺ (15 μM) + H ₂ O ₂ + dmise + ethanol (1.7 M)	0.5	44.3 ± 4.7	55.7	11.7 ± 4.7	0.050
7:	1	50.6 ± 3.8	49.4	21.7 ± 3.8	0.010
8:	10	58.3 ± 2.9	41.7	33.9 ± 2.9	0.002
9:	50	53.8 ± 3.4	46.2	26.7 ± 3.4	0.005
10:	100	55.1 ± 5.2	44.9	28.7 ± 5.2	0.011
11:	400	63.2 ± 5.8	36.8	41.6 ± 5.9	0.007
12:	1000	72.1 ± 5.8	27.9	55.8 ± 5.9	0.004
13:	2000	76.7 ± 4.4	23.3	63.1 ± 4.3	0.002
14:	4000	77.0 ± 7.6	23.0	63.5 ± 7.6	0.005

^aData are reported as the average of three trials with calculated standard deviations shown.**Table 2.14.** Gel electrophoresis results for dmise DNA damage assays with Cu⁺, and 50 μM H₂O₂.^a

Gel lane	[dmise], μM	% Supercoiled	% Nicked	% Damage	<i>p</i> Value
1: plasmid DNA (p)	0	99.98 ± 0.03	0.02	-	-
2: p + H ₂ O ₂ (50 μM)	0	99.97 ± 0.04	0.03	-	-
3: p + dmise+ H ₂ O ₂ + ethanol (1.7 M)	4000	99.94 ± 0.11	0.06	-	-
4: p + Cu ²⁺ (6 μM) + ascorbate (7.5 μM) H ₂ O ₂ + ethanol (10 mM)	0	15.97 ± 3.01	84.03	-	-
5: p + Cu ²⁺ (6 μM) + ascorbate (7.5 μM) + H ₂ O ₂ + ethanol (1.7 M)	0	20.65 ± 5.37	79.35	0	-
6: p + Cu ²⁺ (6 μM) + ascorbate (7.5 μM) + H ₂ O ₂ + dmise + ethanol (1.7 M)	1	32.39 ± 4.59	64.71	18.51 ± 4.59	0.020
7:	10	44.79 ± 0.42	55.21	30.44 ± 0.42	< 0.001
8:	50	53.10 ± 4.02	46.90	40.99 ± 4.02	0.003
9:	100	65.28 ± 4.57	34.72	56.32 ± 4.53	0.002
10:	400	59.66 ± 5.55	40.34	49.22 ± 5.60	0.004
11:	750	67.02 ± 3.43	32.98	62.71 ± 2.40	< 0.001
12:	1000	67.44 ± 4.72	32.56	59.01 ± 4.70	< 0.001
13:	2000	76.52 ± 5.18	23.48	70.48 ± 5.19	0.002
14:	4000	88.06 ± 5.55	11.94	85.01 ± 5.55	0.001

^aData are reported as the average of three trials with calculated standard deviations shown.

Table 2.15. Gel electrophoresis results for ebis DNA damage assays with Fe²⁺, and 50 μM H₂O₂.^a

Gel lane	[ebis], μM	% Supercoiled	% Nicked	% Damage	<i>p</i> Value
1: plasmid DNA (p)	0	100 ± 0	0.0	-	-
2: p + H ₂ O ₂ (50 μM)	0	100 ± 0	0.0	-	-
3: p + ebis+ H ₂ O ₂ + ethanol (1.7 M)	400	100 ± 0	0.0	-	-
4: p + Fe ²⁺ (2 μM) + H ₂ O ₂ + ethanol (10 mM)	0	9.6 ± 5.4	90.4	-	-
5: p + Fe ²⁺ (15 μM) + H ₂ O ₂ + ethanol (1.7 M)	0	31.0 ± 0.7	69.0	0	-
6: p + Fe ²⁺ (15 μM) + H ₂ O ₂ + ebis + ethanol (1.7 M)	0.1	29.1 ± 2.4	70.9	-2.8 ± 2.4	0.181
7:	0.5	35.8 ± 5.6	64.2	6.9 ± 5.6	0.166
8:	1	34.6 ± 0.8	65.4	5.2 ± 0.8	0.008
9:	5	37.6 ± 2.7	62.4	9.6 ± 2.7	0.025
10:	10	38.5 ± 5.0	61.5	11.0 ± 5.0	0.062
11:	50	50.9 ± 1.8	49.1	28.8 ± 1.8	0.001
12:	100	66.4 ± 2.8	33.6	51.4 ± 2.8	<0.001
13:	200	66.2 ± 2.6	33.8	51.0 ± 2.6	<0.001
14:	400	73.5 ± 3.9	26.5	61.6 ± 3.9	<0.001

^aData are reported as the average of three trials with calculated standard deviations shown.**Table 2.16.** Gel electrophoresis results for ebis DNA damage assays with Cu⁺, and 50 μM H₂O₂.^a

Gel lane	[ebis], μM	% Supercoiled	% Nicked	% Damage	<i>p</i> Value
1: plasmid DNA (p)	0	100 ± 0	0.00	-	-
2: p + H ₂ O ₂ (50 μM)	0	99.95 ± 0.04	0.05	-	-
3: p + ebis+ H ₂ O ₂ + ethanol (1.7 M)	100	100 ± 0.01	0.00	-	-
4: p + Cu ²⁺ (6 μM) + ascorbate (7.5 μM) H ₂ O ₂ + ethanol (10 mM)	0	26.51 ± 3.74	73.49	-	-
5: p + Cu ²⁺ (6 μM) + ascorbate (7.5 μM) + H ₂ O ₂ + ethanol (1.7 M)	0	14.54 ± 1.95	85.46	-	-
6: p + Cu ²⁺ (6 μM) + ascorbate (7.5 μM) + H ₂ O ₂ + ebis + ethanol (1.7 M)	0.5	23.77 ± 4.09	76.23	7.89 ± 1.99	0.021
7:	1	32.45 ± 1.63	67.55	21.04 ± 1.60	0.002
8:	5	37.61 ± 2.70	62.39	27.04 ± 2.69	0.003
9:	10	67.78 ± 6.82	32.22	62.34 ± 6.83	0.004
10:	50	99.81 ± 0.23	0.19	99.82 ± 0.26	< 0.001
11:	100	99.62 ± 0.41	0.38	99.63 ± 0.38	< 0.001

^aData are reported as the average of three trials with calculated standard deviations shown.

Table 2.17. Gel electrophoresis results for Trolox DNA damage assays with Fe²⁺, and 50 μM H₂O₂ and 1.7 M ethanol.^a

Gel lane	[Trolox], μM	% Supercoiled	% Nicked	% Damage	<i>p</i> Value
1: plasmid DNA (p)		100.00 ± 0	0.00	-	-
2: p + H ₂ O ₂ (50 μM)		99.69 ± 0.53	0.31	-	-
3: p + Trolox+ H ₂ O ₂ + ethanol (1.7 M)	1000	99.90 ± 0.10	0.10	-	-
4: p + Fe ²⁺ (2 μM) + H ₂ O ₂ + ethanol (10 mM)		9.55 ± 0.42	90.45	-	-
5: p + Fe ²⁺ (15 μM) + H ₂ O ₂ + ethanol (1.7 M)		22.74 ± 6.79	77.26	0	-
6: p + Fe ²⁺ (15 μM) + H ₂ O ₂ + Trolox + ethanol (1.7 M)	10	12.79 ± 4.11	87.21	3.51 ± 4.11	0.277
7:	50	0.96 ± 1.25	99.04	-9.61 ± 1.25	0.006
8:	100	0.13 ± 0.23	99.87	-10.52 ± 0.23	< 0.001
9:	500	0.00 ± 0.01	100.00	-10.67 ± 0.01	< 0.001
10:	1000	0.00 ± 0.01	100.00	-10.67 ± 0.01	< 0.001

^aData are reported as the average of three trials with calculated standard deviations shown.

Table 2.18. Gel electrophoresis results for Trolox DNA damage assays with Fe²⁺, and 50 μM H₂O₂ and 10 mM ethanol.^a

Gel lane	[Trolox], μM	% Supercoiled	% Nicked	% Damage	<i>p</i> Value
1: plasmid DNA (p)		100.00 ± 0	0.00	-	-
2: p + H ₂ O ₂ (50 μM)		100.00 ± 0	0.00	-	-
3: p + Trolox+ H ₂ O ₂ + ethanol (10 mM)	2000	100.00 ± 0	0.00	-	-
4: p + Fe ²⁺ (2 μM) + H ₂ O ₂ + ethanol (10 mM)		12.30 ± 3.47	87.70	0	-
5: p + Fe ²⁺ (15 μM) + H ₂ O ₂ + ethanol (10 mM)	0.1	21.20 ± 2.62	78.80	0.21 ± 4.51	0.943
6:	1	23.57 ± 1.19	76.43	-6.62 ± 4.87	0.143
7:	5	35.81 ± 1.70	64.19	-0.26 ± 0.69	0.581
8:	10	77.89 ± 2.55	22.11	3.74 ± 1.49	0.049
9:	50	87.37 ± 2.37	12.63	7.08 ± 5.82	0.170
10:	100	98.08 ± 1.27	1.92	23.47 ± 5.75	0.019
11:	500	99.04 ± 0.44	0.96	33.33 ± 5.16	0.008
12:	1000	98.35 ± 0.75	1.65	66.27 ± 7.88	0.005
13:	2000	95.41 ± 1.33	4.59	99.90 ± 0.12	< 0.001

^aData are reported as the average of three trials with calculated standard deviations shown.

Table 2.19. Gel electrophoresis results for Trolox DNA damage assays with Cu⁺, 1.7M ethanol and 50 μM H₂O₂.^a

Gel lane	[Trolox], μM	% Supercoiled	% Nicked	% Damage	<i>p</i> Value
1: plasmid DNA (p)		100.00 ± 0	0.00	-	-
2: p + H ₂ O ₂ (50 μM)		100.00 ± 0	0.00	-	-
3: p + Trolox+ H ₂ O ₂ + ethanol (1.7 M)	1000	99.07 ± 1.61	0.93	-	-
4: p + Cu ²⁺ (6 μM) + ascorbate (7.5 μM) + H ₂ O ₂ + ethanol (10 mM)		7.73 ± 4.47	92.27	-	-
5: p + Cu ²⁺ (6 μM) + ascorbate (7.5 μM) + H ₂ O ₂ + ethanol (1.7 M)		22.74 ± 6.79	77.26	0	-
6: p + Cu ²⁺ (6 μM) + ascorbate (7.5 μM) + H ₂ O ₂ + Trolox + ethanol (1.7 M)	0.1	15.62 ± 1.41	84.38	-4.87 ± 1.81	0.043
7:	1	6.15 ± 2.86	93.85	-17.09 ± 2.86	0.009
8:	5	0.18 ± 0.29	99.82	-24.26 ± 0.35	< 0.001
9:	10	0.00 ± 0.01	100.00	-24.76 ± 0.01	< 0.001
10:	50	0.01 ± 0.02	99.99	-24.74 ± 0.02	< 0.001
11:	100	2.65 ± 4.60	97.35	-21.45 ± 4.60	< 0.001
12:	500	0.38 ± 0.67	99.62	-24.28 ± 0.66	< 0.001
13:	1000	0.35 ± 0.61	99.65	-24.32 ± 0.61	< 0.001

^aData are reported as the average of three trials with calculated standard deviations shown.**Table 2.20.** Gel electrophoresis results for Trolox DNA damage assays with Cu⁺, and 50 μM H₂O₂ and 10 mM ethanol.^a

Gel lane	[Trolox], μM	% Supercoiled	% Nicked	% Damage	<i>p</i> Value
1: plasmid DNA (p)	0	100.00 ± 0	0.00	-	-
2: p + H ₂ O ₂ (50 μM)	0	99.99 ± 0.02	0.01	-	-
3: p + Trolox+ H ₂ O ₂ + ethanol (10 mM)	2000	99.98 ± 0.02	0.02	-	-
4: p + Cu ²⁺ (6 μM) + ascorbate (7.5 μM) + H ₂ O ₂ + ethanol (10 mM)	0	4.33 ± 0.73	95.67	0	-
5: p + Cu ²⁺ (6 μM) + ascorbate (7.5 μM) + H ₂ O ₂ + ethanol (10 mM)	0.1	5.69 ± 2.27	94.31	1.45 ± 2.27	0.384
6:	1	2.94 ± 2.00	97.06	-1.44 ± 2.00	0.339
7:	5	1.11 ± 0.92	98.89	-3.35 ± 0.92	0.024
8:	10	0.21 ± 0.36	99.79	-4.29 ± 0.36	0.002
9:	50	0.00 ± 0	100.00	-4.51 ± 0	< 0.001
10:	100	0.02 ± 0.03	99.98	-4.49 ± 0.03	< 0.001
11:	500	0.99 ± 1.72	99.01	-3.47 ± 1.72	0.073
12:	1000	0.26 ± 0.39	99.74	-4.23 ± 0.39	0.003
13:	2000	0.00 ± 0	100.00	-4.51 ± 0	< 0.001

^aData are reported as the average of three trials with calculated standard deviations shown.

Table 2.21. Gel electrophoresis results for Edaravone DNA damage assays with Fe²⁺, and 50 μM H₂O₂.^a

Gel lane	[Edaravone], μM	% Supercoiled	% Nicked	% Damage	<i>p</i> Value
1: plasmid DNA (p)		100.00 ± 0	0.00	-	-
2: p + H ₂ O ₂ (50 μM)		100.00 ± 0	0.00	-	-
3: p + Edaravone+ H ₂ O ₂ + ethanol (1.7 M)	1000	100.00 ± 0	0.00	-	-
4: p + Fe ²⁺ (2 μM) + H ₂ O ₂ + ethanol (10 mM)		15.35 ± 1.31	84.65	-	-
5: p + Fe ²⁺ (15 μM) + H ₂ O ₂ + ethanol (1.7 M)		10.00 ± 4.12	90.00	0	-
6: p + Fe ²⁺ (15 μM) + H ₂ O ₂ + Edaravone + ethanol (1.7 M)	0.1	14.26 ± 3.11	85.74	-1.29 ± 3.81	0.616
7:	1	11.13 ± 1.64	88.87	-4.99 ± 2.01	0.050
8:	5	6.43 ± 0.56	93.57	-10.54 ± 0.68	0.001
9:	10	6.04 ± 3.86	93.96	-11.00 ± 4.72	0.056
10:	50	7.43 ± 5.20	92.57	-9.36 ± 6.36	0.126
11:	100	7.42 ± 4.87	92.58	-9.37 ± 5.97	0.114
12:	500	5.71 ± 2.86	94.29	-11.39 ± 3.50	0.030
13:	1000	14.70 ± 0.30	85.30	-0.77 ± 0.37	0.069

^aData are reported as the average of three trials with calculated standard deviations shown.**Table 2.22.** Gel electrophoresis results for Edaravone DNA damage assays with Cu⁺, and 50 μM H₂O₂.^a

Gel lane	[Edaravone], μM	% Supercoiled	% Nicked	% Damage	<i>p</i> Value
1: plasmid DNA (p)		99.97 ± 0.05	0.03	-	-
2: p + H ₂ O ₂ (50 μM)		100.00 ± 0	0.00	-	-
3: p + Edaravone+ H ₂ O ₂ + ethanol (1.7 M)	1000	99.98 ± 0.03	0.02	-	-
4: p + Cu ²⁺ (6 μM) + ascorbate (7.5 μM) + H ₂ O ₂ + ethanol (10 mM)		2.75 ± 1.41	97.25	-	-
5: p + Cu ²⁺ (6 μM) + ascorbate (7.5 μM) + H ₂ O ₂ + ethanol (1.7 M)		6.01 ± 3.28	93.99	0	-
6: p + Cu ²⁺ (6 μM) + ascorbate (7.5 μM) + H ₂ O ₂ + Edaravone + ethanol (1.7 M)	0.1	5.25 ± 2.57	94.75	0.23 ± 2.57	0.891
7:	1	11.35 ± 4.06	88.65	6.66 ± 4.06	0.105
8:	5	3.37 ± 1.91	96.63	-1.74 ± 1.91	0.255
9:	10	6.68 ± 1.74	93.32	1.74 ± 1.74	0.225
10:	50	4.81 ± 2.77	95.19	-0.23 ± 2.77	0.899
11:	100	2.87 ± 2.33	97.13	-2.28 ± 2.33	0.232
12:	500	3.50 ± 3.68	96.50	-1.61 ± 3.68	0.528
13:	1000	14.18 ± 2.35	85.82	9.17 ± 2.64	0.894

^aData are reported as the average of three trials with calculated standard deviations shown.

Table 2.23. Gel electrophoresis results for Ebselen DNA damage assays with Fe²⁺, and 50 μM H₂O₂.^a

Gel lane	[Ebselen], μM	% Supercoiled	% Nicked	% Damage	<i>p</i> Value
1: plasmid DNA (p)	0	100.0 ± 0	0.0	-	-
2: p + H ₂ O ₂ (50 μM)	0	98.7 ± 2.2	1.3	-	-
3: p + Ebselen + H ₂ O ₂ + ethanol (1.7 M)	400	100.0 ± 0	0.0	-	-
4: p + Fe ²⁺ (2 μM) + H ₂ O ₂ + ethanol (10 mM)	0	7.6 ± 2.3	92.4	-	-
5: p + Fe ²⁺ (15 μM) + H ₂ O ₂ + ethanol (1.7 M)	0	25.1 ± 3.0	74.9	0	-
6: p + Fe ²⁺ (15 μM) + H ₂ O ₂ + Ebselen + ethanol (1.7 M)	1	27.0 ± 2.6	73.0	4.3 ± 2.7	0.110
7:	5	30.7 ± 1.2	69.3	9.2 ± 1.3	0.007
8:	10	28.6 ± 5.5	71.4	6.4 ± 5.5	0.181
9:	50	26.8 ± 3.5	73.2	3.9 ± 3.5	0.193
10:	100	26.4 ± 2.8	73.6	3.5 ± 2.9	0.172
11:	200	31.4 ± 3.2	68.6	10.0 ± 3.2	0.032
12:	400	28.4 ± 4.5	71.6	6.0 ± 4.5	0.147

^aData are reported as the average of three trials with calculated standard deviations shown.**Table 2.24.** Gel electrophoresis results for ebselen DNA damage assays with Cu⁺, and 50 μM H₂O₂.^a

Gel lane	[Ebselen], μM	% Supercoiled	% Nicked	% Damage	<i>p</i> Value
1: plasmid DNA (p)	0	99.8 ± 0.2	0.2	-	-
2: p + H ₂ O ₂ (50 μM)	0	98.9 ± 0.8	1.1	-	-
3: p + ebselen + H ₂ O ₂ + ethanol (1.7 M)	400	98.8 ± 1.6	1.2	-	-
4: p + Cu ²⁺ (2 μM) + ascorbate (7.5 μM) + H ₂ O ₂ + ethanol (10 mM)	0	14.9 ± 1.9	85.1	-	-
5: p + Cu ²⁺ (2 μM) + ascorbate (7.5 μM) + H ₂ O ₂ + ethanol (1.7 M)	0	13.7 ± 3.6	86.3	0	-
6: p Cu ²⁺ (2 μM) + ascorbate (7.5 μM) + ebselen + ethanol (1.7 M)	1	12.1 ± 2.4	87.9	-0.5 ± 2.4	0.753
7:	10	13.1 ± 4.8	86.9	0.7 ± 4.8	0.824
8:	50	18.1 ± 2.0	81.9	6.4 ± 2.0	0.310
9:	100	34.4 ± 3.4	65.6	25.3 ± 3.5	0.006
10:	200	50.0 ± 3.5	50.0	43.3 ± 3.5	0.002
11:	300	56.5 ± 4.4	43.5	50.9 ± 4.5	0.003
12:	400	58.6 ± 8.5	41.4	53.4 ± 8.5	0.008

^aData are reported as the average of three trials with calculated standard deviations shown.

Table 2.25. Gel electrophoresis results for ebselen-*N*-acetic acid DNA damage assays with Fe²⁺, and 50 μM H₂O₂.^a

Gel lane	[ebselen- <i>N</i> -acetic acid], μM	% Supercoiled	% Nicked	% Damage	<i>p</i> Value
1: plasmid DNA (p)	0	100.0 ± 0	0.0	-	-
2: p + H ₂ O ₂ (50 μM)	0	99.9 ± 0.1	0.1	-	-
3: p + ebselen- <i>N</i> -acetic acid + H ₂ O ₂ + ethanol (1.7 M)	700	100.0 ± 0	0.0	-	-
4: p + Fe ²⁺ (2 μM) + H ₂ O ₂ + ethanol (10 mM)	0	18.8 ± 3.1	81.2	-	-
5: p + Fe ²⁺ (15 μM) + H ₂ O ₂ + ethanol (1.7 M)	0	29.3 ± 2.9	70.7	0	-
6: p + Fe ²⁺ (15 μM) + H ₂ O ₂ + ebselen- <i>N</i> -acetic acid + ethanol (1.7 M)	1	31.1 ± 2.5	68.9	2.7 ± 2.5	0.202
7:	10	34.8 ± 4.5	65.2	7.9 ± 4.4	0.090
8:	50	32.8 ± 3.7	67.2	5.6 ± 4.2	0.147
9:	100	34.1 ± 3.8	65.9	6.9 ± 3.9	0.092
10:	200	26.4 ± 2.8	73.6	-4.0 ± 2.9	0.139
11:	300	28.7 ± 3.6	71.3	-0.8 ± 3.6	0.385
12:	400	24.9 ± 1.7	75.1	-6.1 ± 1.7	0.025
13:	500	22.8 ± 1.1	77.2	-9.0 ± 1.1	0.005
14:	600	26.8 ± 2.2	73.2	-3.4 ± 2.2	0.116
15:	700	32.2 ± 5.6	67.8	4.2 ± 5.6	0.324

^aData are reported as the average of three trials with calculated standard deviations shown.**Table 2.26.** Gel electrophoresis results for ebselen-*N*-acetic acid DNA damage assays with Cu⁺, and 50 μM H₂O₂.^a

Gel lane	[ebselen- <i>N</i> -acetic acid], μM	% Supercoiled	% Nicked	% Damage	<i>p</i> Value
1: plasmid DNA (p)	0	100 ± 0	0	-	-
2: p + H ₂ O ₂ (50 μM)	0	100 ± 0	0	-	-
3: p + ebselen- <i>N</i> -acetic acid + H ₂ O ₂ + ethanol (1.7 M)	700	100 ± 0	0	-	-
4: p + Cu ²⁺ (2 μM) + ascorbate (7.5 μM) + H ₂ O ₂ + ethanol (10 mM)	0	13.50 ± 1.11	86.50	-	-
5: p + Cu ²⁺ (2 μM) + ascorbate (7.5 μM) + H ₂ O ₂ + ethanol (1.7 M)	0	12.22 ± 4.94	87.78	0	-
6: p Cu ²⁺ (2 μM) + ascorbate (7.5 μM) + ebselen- <i>N</i> -acetic acid + ethanol (1.7 M)	10	16.36 ± 1.03	83.64	4.72 ± 1.07	0.017
7:	100	16.75 ± 2.11	83.25	5.14 ± 2.12	0.052
8:	200	33.29 ± 3.20	66.71	24.91 ± 3.18	0.005
9:	300	33.59 ± 3.44	66.41	24.36 ± 3.44	0.007
10:	500	54.05 ± 2.33	45.95	47.67 ± 2.30	0.002
11:	700	60.01 ± 1.12	39.99	54.43 ± 1.10	< 0.001

^aData are reported as the average of three trials with calculated standard deviations shown.

Table 2.27. Gel electrophoresis results for ebselen-7-carboxylic acid DNA damage assays with Fe²⁺, and 50 μM H₂O₂.^a

Gel lane	[ebselen-7-carboxylic acid], μM	% Supercoiled	% Nicked	% Damage	<i>p</i> Value
1: plasmid DNA (p)	0	99.96 ± 0.06	0.04	-	-
2: p + H ₂ O ₂ (50 μM)	0	98.01 ± 1.8	1.99	-	-
3: p + ebselen-7-carboxylic acid + H ₂ O ₂ + ethanol (1.7 M)	700	100 ± 0	0	-	-
4: p + Fe ²⁺ (2 μM) + H ₂ O ₂ + ethanol (10 mM)	700	100 ± 0	0	-	-
5: p + Fe ²⁺ (15 μM) + H ₂ O ₂ + ethanol (1.7 M)	0	15.85 ± 3.45	84.15	-	-
6: p + Fe ²⁺ (15 μM) + H ₂ O ₂ + ebselen-7-carboxylic acid + ethanol (1.7 M)	0	23.44 ± 4.05	76.56	0	-
7:	1	21.31 ± 1.70	78.69	-0.20 ± 2.10	0.884
8:	10	21.65 ± 4.28	78.35	0.28 ± 5.26	0.935
9:	50	23.44 ± 3.19	76.56	2.63 ± 3.91	0.364
10:	100	39.14 ± 0.25	60.86	23.14 ± 0.31	< 0.001
11:	200	56.42 ± 3.76	43.58	45.69 ± 4.62	0.003
12:	300	60.76 ± 5.03	39.24	51.53 ± 6.18	0.005
13:	400	84.10 ± 1.71	15.90	81.83 ± 2.08	< 0.001
14:	500	95.42 ± 1.47	4.58	96.63 ± 1.81	< 0.001
15:	600	95.71 ± 3.04	4.29	96.98 ± 3.74	< 0.001
16:	700	97.38 ± 2.00	2.62	99.20 ± 2.42	< 0.001

^aData are reported as the average of three trials with calculated standard deviations shown.

Table 2.28. Gel electrophoresis results for ebselen-7-carboxylic acid methyl ester DNA damage assays with Fe²⁺, and 50 μM H₂O₂.^a

Gel lane	[ebselen-7-carboxylic acid methyl ester], μM	% Supercoiled	% Nicked	% Damage	<i>p</i> Value
1: plasmid DNA (p)	0	100 ± 0	0.00	-	-
2: p + H ₂ O ₂ (50 μM)	0	100 ± 0	0.00	-	-
3: p + ebselen-7-carboxylic acid methyl ester + H ₂ O ₂ + ethanol (1.7 M)	400	99.76 ± 0.42	0.24	-	-
4: p + Fe ²⁺ (2 μM) + H ₂ O ₂ + ethanol (10 mM)	400	100 ± 0	0.00	-	-
5: p + Fe ²⁺ (15 μM) + H ₂ O ₂ + ethanol (1.7 M)	0	11.00 ± 1.70	89.00	-	-
6: p + Fe ²⁺ (15 μM) + H ₂ O ₂ + ebselen-7-carboxylic acid methyl ester + ethanol (1.7 M)	0	18.51 ± 5.45	81.49	0	-
7:	1	15.46 ± 2.96	84.54	-3.73 ± 2.99	0.163
8:	10	3.75 ± 2.88	96.25	-18.13 ± 2.90	0.008
9:	50	7.75 ± 3.47	92.25	-13.18 ± 3.50	0.023
10:	100	13.78 ± 1.95	86.22	-5.78 ± 1.93	0.035
11:	200	7.88 ± 3.82	92.12	-13.06 ± 3.84	0.028
12:	300	12.10 ± 3.46	87.90	-7.87 ± 3.48	0.059
13:	400	10.96 ± 2.10	89.04	-9.26 ± 2.12	0.017

^aData are reported as the average of three trials with calculated standard deviations shown.

Table 2.29. Gel electrophoresis results for ebsulfur-7-carboxylic acid DNA damage assays with Cu⁺, and 50 μM H₂O₂.^a

Gel lane	[ebsulfur-7-carboxylic acid], μM	% Supercoiled	% Nicked	% Damage	<i>p</i> Value
1: plasmid DNA (p)	0	100 ± 0	0.00	-	-
2: p + H ₂ O ₂ (50 μM)	0	100 ± 0	0.00	-	-
3: p + ebselen-7-carboxylic acid methyl ester + H ₂ O ₂ + ethanol (1.7 M)	700	99.77 ± 0.29	0.23	-	-
4: p + Cu ²⁺ (2 μM) + ascorbate (7.5 μM) + H ₂ O ₂ + ethanol (10 mM)	0	8.52 ± 5.60	91.48	-	-
5: p + Cu ²⁺ (2 μM) + ascorbate (7.5 μM) + H ₂ O ₂ + ethanol (1.7 M)	0	11.17 ± 3.58	88.83	0	-
6: p Cu ²⁺ (2 μM) + ascorbate (7.5 μM) + ebselen-7-carboxylic acid methyl ester + ethanol (1.7 M)	0.001	13.42 ± 3.25	86.58	2.54 ± 3.25	0.309
7:	0.1	15.19 ± 1.76	84.81	4.53 ± 1.73	0.045
8:	1	20.82 ± 3.63	79.18	10.84 ± 3.61	0.035
9:	10	16.31 ± 3.93	83.69	5.81 ± 3.91	0.124
10:	100	62.96 ± 1.27	37.04	58.31 ± 1.27	< 0.001
11:	300	67.58 ± 1.91	32.42	63.52 ± 1.93	0.001
12:	500	67.36 ± 5.03	32.64	63.22 ± 5.04	0.002
13:	700	71.20 ± 3.88	28.80	67.58 ± 3.84	0.001

^aData are reported as the average of three trials with calculated standard deviations shown.

Table 2.30. Gel electrophoresis results for ebsulfur-7-carboxylic acid DNA damage assays with Cu⁺, and 50 μM H₂O₂.^a

Gel lane	[ebsulfur-7-carboxylic acid], μM	% Supercoiled	% Nicked	% Damage	<i>p</i> Value
1: plasmid DNA (p)	0	100 ± 0	0 ± 0	-	-
2: p + H ₂ O ₂ (50 μM)	0	100 ± 0	0 ± 0	-	-
3: p + ebsulfur-7-carboxylic acid + H ₂ O ₂ + ethanol (1.7 M)	700	100 ± 0	0 ± 0	-	-
4: p + Cu ²⁺ (2 μM) + ascorbate (7.5 μM) + H ₂ O ₂ + ethanol (10 mM)	700	2.03 ± 1.40	97.97	-	-
5: p + Cu ²⁺ (2 μM) + ascorbate (7.5 μM) + H ₂ O ₂ + ethanol (1.7 M)	0	1.78 ± 1.80	98.22	0	-
6: p Cu ²⁺ (2 μM) + ascorbate (7.5 μM) + ebsulfur-7-carboxylic acid + ethanol (1.7 M)	1	4.43 ± 2.33	95.57	2.70 ± 2.37	0.187
7:	10	1.65 ± 0.96	98.35	-0.51 ± 0.97	0.459
8:	50	3.95 ± 0.90	96.05	2.23 ± 0.87	0.047
9:	100	6.42 ± 0.89	93.58	4.71 ± 0.85	0.011
10:	200	6.19 ± 1.74	93.81	4.50 ± 1.74	0.011
11:	300	7.56 ± 3.78	92.44	5.89 ± 3.81	0.116
12:	400	8.62 ± 3.94	91.38	6.98 ± 3.96	0.093
13:	500	3.06 ± 2.62	96.94	1.31 ± 2.64	0.481
14:	600	3.95 ± 2.37	96.05	2.20 ± 2.41	0.255
15:	700	7.45 ± 2.33	92.55	5.79 ± 2.31	0.049

^aData are reported as the average of three trials with calculated standard deviations shown.

Table 2.31. Gel electrophoresis results for ebsulfur-7-carboxylic acid methyl ester DNA damage assays with Cu⁺, and 50 μM H₂O₂.^a

Gel lane	[ebsulfur-7-carboxylic acid methyl ester], μM	% Supercoiled	% Nicked	% Damage	<i>p</i> Value
1: plasmid DNA (p)	0	99.99 ± 0.02	0.01	-	-
2: p + H ₂ O ₂ (50 μM)	0	99.98 ± 0.03	0.02	-	-
3: p + ebsulfur-7- carboxylic acid methyl ester + H ₂ O ₂ + ethanol (1.7 M)	400	99.96 ± 0.04	0.04	-	-
4: p + Cu ²⁺ (2 μM) + ascorbate (7.5 μM) + H ₂ O ₂ + ethanol (10 mM)	400	99.96 ± 0.07	0.04	-	-
5: p + Cu ²⁺ (2 μM) + ascorbate (7.5 μM) + H ₂ O ₂ + ethanol (1.7 M)	0	1.11 ± 1.09	97.78	-	-
6: p Cu ²⁺ (2 μM) + ascorbate (7.5 μM) + ebsulfur-7- carboxylic acid methyl ester + ethanol (1.7 M)	0	4.42 ± 1.97	95.58	0	-
7:	1	2.22 ± 1.63	97.78	-2.27 ± 1.63	0.137
8:	10	4.69 ± 3.98	95.31	0.31 ± 3.98	0.905
9:	50	2.88 ± 0.47	97.12	-1.60 ± 0.45	0.025
10:	100	3.67 ± 1.71	96.33	-0.77 ± 1.68	0.511
11:	200	2.51 ± 2.42	97.49	-1.95 ± 2.42	0.298
12:	300	0.78 ± 0.40	99.22	-3.80 ± 0.38	0.003
13:	400	2.01 ± 0.89	97.99	-2.51 ± 0.92	0.042

^aData are reported as the average of three trials with calculated standard deviations shown.

Table 2.32. DPPH scavenging assay results for EC.^a

[EC], μM	% Scavenged	<i>p</i> Value
DPPH	$0 \pm$	-
Trolox (50 μM)	100 ± 0	-
0.2	4.71 ± 1.23	0.022
2	9.81 ± 0.70	0.002
10	27.20 ± 1.04	< 0.001
20	40.03 ± 0.86	< 0.001
40	60.20 ± 0.12	< 0.001
100	76.67 ± 1.65	< 0.001
250	95.09 ± 0.06	< 0.001
500	98.70 ± 0.06	< 0.001

^aData are reported as the average of three trials with calculated standard deviations shown.

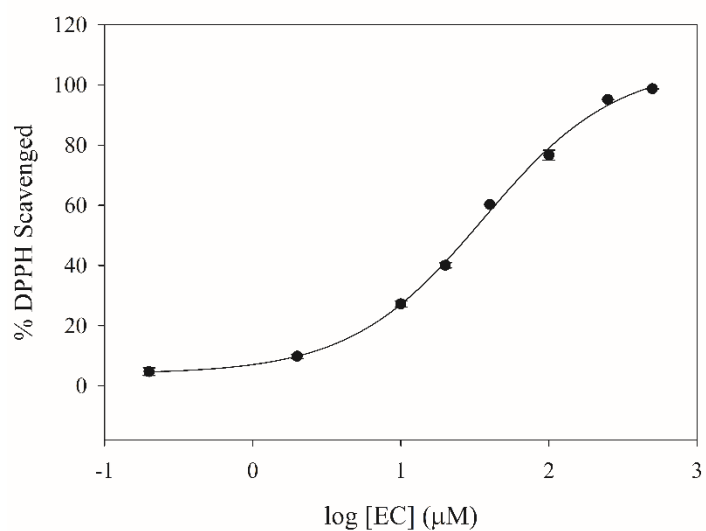


Figure 2.22. Dose-response plot for EC in the DPPH-scavenging assay. Error bars are smaller than the data point symbols.

Table 2.33. DPPH scavenging assay results for GA.^a

[GA], μM	% Scavenged	<i>p</i> Value
DPPH	$0 \pm$	-
Trolox (50 μM)	100 ± 0	-
0.01	-2.02 ± 5.30	0.577
0.1	2.31 ± 5.51	0.543
1	12.51 ± 0.76	0.001
5	38.02 ± 1.01	< 0.001
10	50.54 ± 1.71	< 0.001
20	63.68 ± 0.40	< 0.001
50	73.98 ± 0.23	< 0.001
100	82.31 ± 1.19	< 0.001
250	96.57 ± 0.38	< 0.001
500	98.84 ± 0.06	< 0.001

^aData are reported as the average of three trials with calculated standard deviations shown.

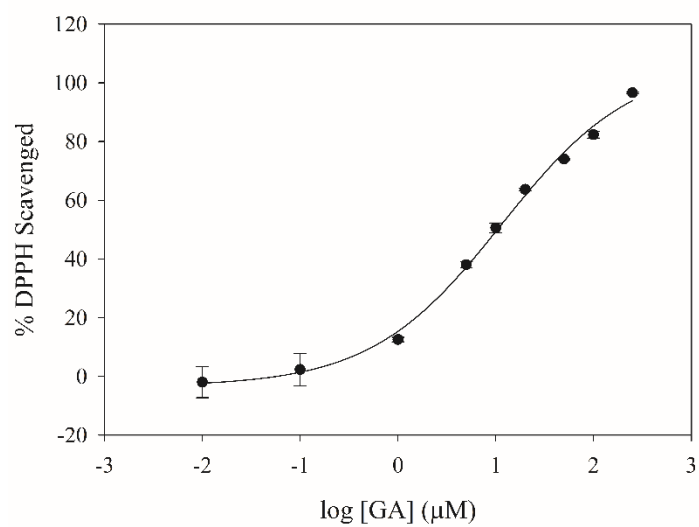
**Figure 2.23.** Dose-response plot for GA in the DPPH-scavenging assay.

Table 2.34. DPPH scavenging assay results for PCA.^a

[PCA], μM	% Scavenged	<i>p</i> Value
DPPH	$0 \pm$	-
Trolox (50 μM)	100 ± 0	-
0.1	4.86 ± 1.37	0.025
1	7.95 ± 1.83	0.017
5	14.75 ± 0.23	< 0.001
10	22.17 ± 0.89	< 0.001
15	27.35 ± 0.55	< 0.001
25	30.21 ± 0.56	< 0.001
1000	55.18 ± 1.05	< 0.001
2000	65.28 ± 0.05	< 0.001

^aData are reported as the average of three trials with calculated standard deviations shown.

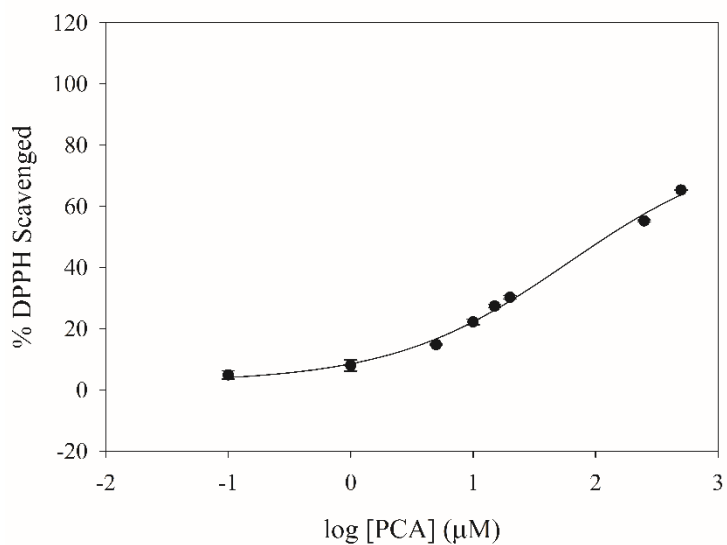


Figure 2.24. Dose-response plot for PCA in the DPPH-scavenging assay. Error bars are smaller than the data point symbols.

Table 2.35. DPPH scavenging assay results for TA.^a

[TA], μM	% Scavenged	<i>p</i> Value
DPPH	$0 \pm$	-
Trolox (50 μM)	100 ± 0	-
0.001	18.52 ± 0.06	< 0.001
0.01	51.39 ± 0.06	< 0.001
0.1	77.41 ± 0.80	< 0.001
1	91.76 ± 0.17	< 0.001
10	98.98 ± 0.15	< 0.001
25	99.54 ± 0.06	< 0.001
50	99.72 ± 0.06	< 0.001

^aData are reported as the average of three trials with calculated standard deviations shown.

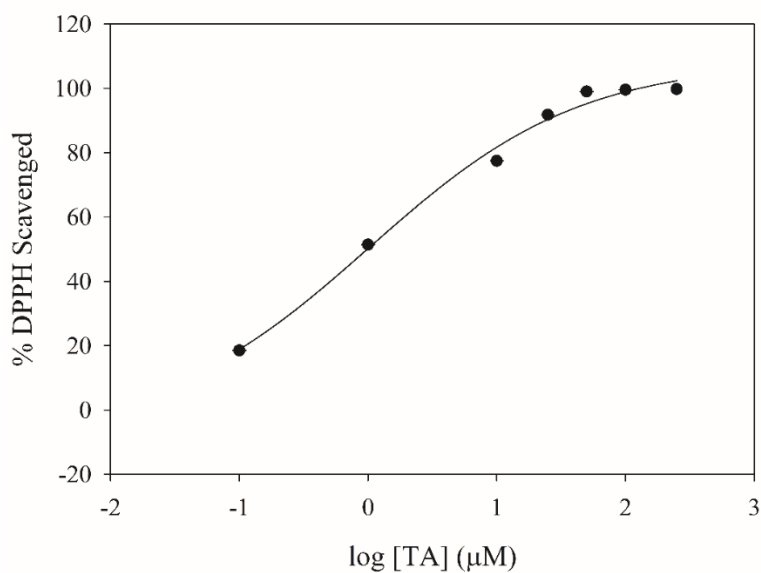


Figure 2.25. Dose-response plot for TA in the DPPH-scavenging assay. Error bars are smaller than the data point symbols.

Table 2.36. DPPH scavenging assay results for EGCG.^a

[EGCG], μM	% Scavenged	<i>p</i> Value
DPPH	$0 \pm$	-
Trolox (50 μM)	100 ± 0	-
0.01	4.09 ± 0.01	< 0.001
0.1	4.01 ± 0.05	< 0.001
1	61.28 ± 0.01	< 0.001
5	79.75 ± 0.01	< 0.001
20	98.89 ± 0.01	< 0.001

^aData are reported as the average of three trials with calculated standard deviations shown.

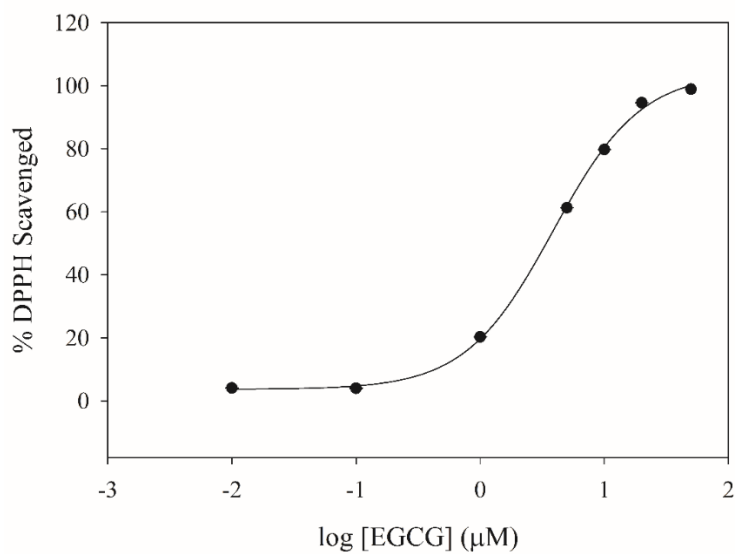


Figure 2.26. Dose-response plot for EGCG in the DPPH-scavenging assay. Error bars are smaller than the data point symbols.

Table 2.37. DPPH scavenging assay results for sepy^{Me}.^a

[sepy ^{Me}], μM	% Scavenged	<i>p</i> Value
DPPH	0 \pm	-
Trolox (50 μM)	100 \pm 0	-
0.01	9.25 \pm 0.40	< 0.001
1	10.53 \pm 0.26	< 0.001
10	33.99 \pm 0.32	< 0.001
25	43.70 \pm 0.75	< 0.001
50	49.02 \pm 0.20	< 0.001
100	53.70 \pm 0.36	< 0.001

^aData are reported as the average of three trials with calculated standard deviations shown.

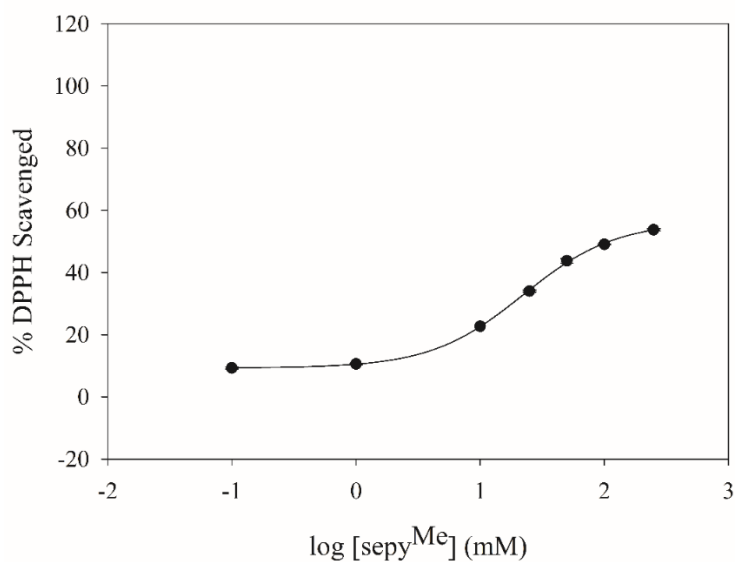


Figure 2.27. Dose-response plot for sepy^{Me} in the DPPH-scavenging assay. Error bars are smaller than the data point symbols.

Table 2.38. DPPH scavenging assay results for pyridine.^a

[pyridine], μM	% Scavenged	<i>p</i> Value
DPPH	$0 \pm$	-
Trolox (50 μM)	100 ± 0	-
0.1	4.57 ± 0.40	0.003
1	2.09 ± 2.28	0.253
10	0.53 ± 1.02	0.463
50	-1.67 ± 1.36	0.015
100	-0.75 ± 0.61	0.167
500	0.18 ± 0.40	0.517
1000	9.37 ± 0.06	< 0.001

^aData are reported as the average of three trials with calculated standard deviations shown.

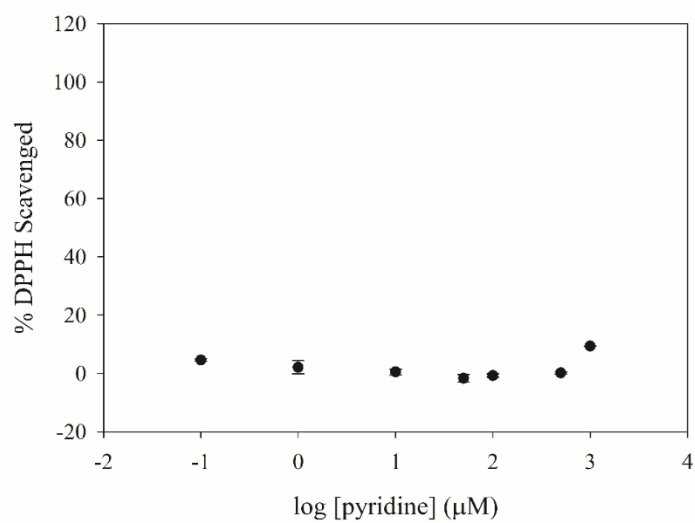


Figure 2.28. Dose-response plot for pyridine in the DPPH-scavenging assay. Error bars are smaller than the data point symbols.

Table 2.39. DPPH scavenging assay results for bipy.^a

[bipy], μM	% Scavenged	<i>p</i> Value
DPPH	$0 \pm$	-
Trolox (50 μM)	100 ± 0	-
0.1	1.65 ± 0.56	0.036
1	-3.41 ± 0.15	< 0.001
10	-0.55 ± 0.35	0.113
50	-1.54 ± 0.80	0.079
100	-3.74 ± 0.58	0.008
1000	3.30 ± 1.65	0.074

^aData are reported as the average of three trials with calculated standard deviations shown.

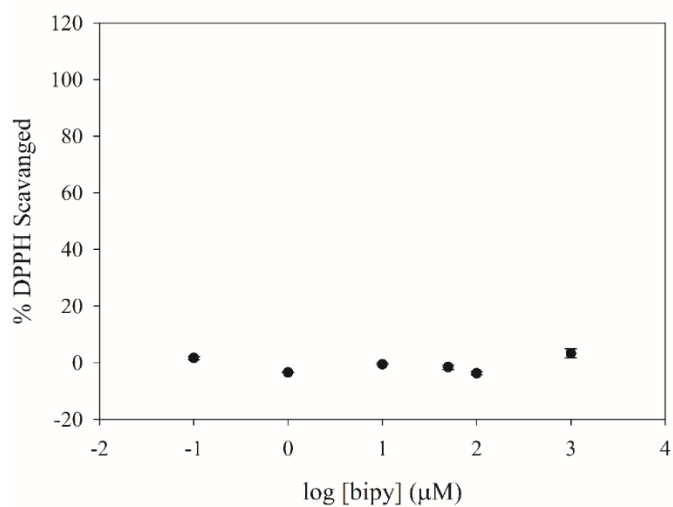


Figure 2.29. Dose-response plot for bipy in the DPPH-scavenging assay. Error bars are smaller than the data point symbols.

Table 2.40. DPPH scavenging assay results for dmise.^a

[dmise], μM	% Scavenged	<i>p</i> Value
DPPH	$0 \pm$	-
Trolox (50 μM)	100 ± 0	-
0.01	0.00 ± 0.10	0.878
0.1	0.99 ± 0.20	0.013
1	5.39 ± 0.12	< 0.001
10	17.38 ± 0.67	< 0.001
50	36.74 ± 0.21	< 0.001
100	49.62 ± 0.21	< 0.001
250	51.20 ± 0.15	< 0.001
500	59.35 ± 0.15	< 0.001
1000	75.15 ± 0.12	< 0.001
2000	94.51 ± 0.06	< 0.001

^aData are reported as the average of three trials with calculated standard deviations shown.

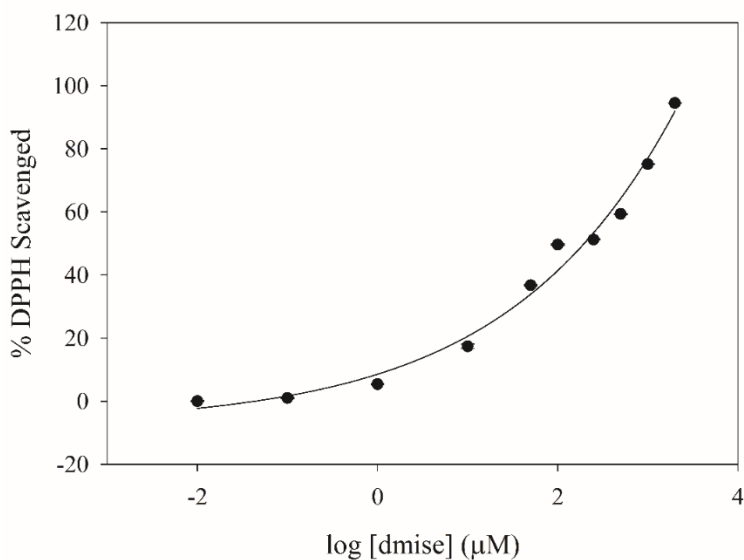


Figure 2.30. Dose-response plot for dmise in the DPPH-scavenging assay. Error bars are smaller than the data point symbols.

Table 2.41. DPPH scavenging assay results for ebis.^a

[ebis], μM	% Scavenged	<i>p</i> Value
DPPH	$0 \pm$	-
Trolox (50 μM)	100 ± 0	-
0.01	9.07 ± 0.15	< 0.001
0.1	45.74 ± 0.01	< 0.001
1	98.61 ± 0.25	< 0.001
10	100 ± 0.35	< 0.001
25	99.26 ± 0.01	< 0.001
50	100 ± 0.38	< 0.001
100	100 ± 0.01	< 0.001

^aData are reported as the average of three trials with calculated standard deviations shown.

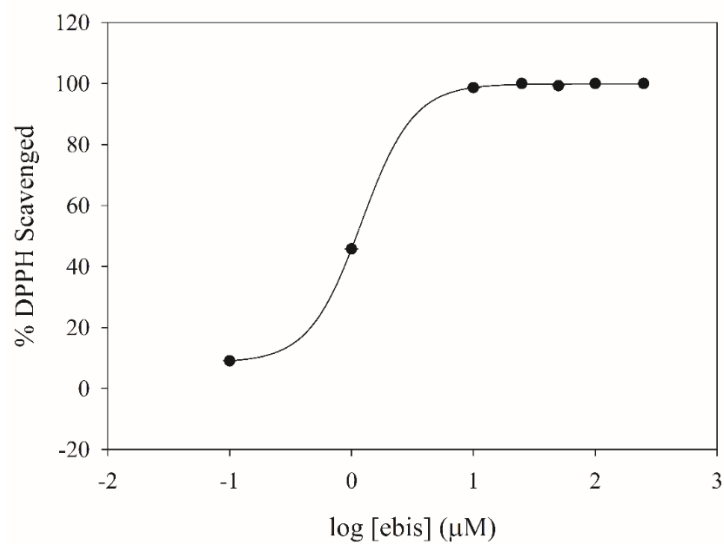


Figure 2.31. Dose-response plot for ebis in the DPPH-scavenging assay. Error bars are smaller than the data point symbols.

Table 2.42. DPPH scavenging assay results for Trolox.^a

[Trolox], μM	% Scavenged	<i>p</i> Value
DPPH	$0 \pm$	-
Trolox (50 μM)	100 ± 0	-
0.001	0.00 ± 0.17	0.928
0.1	0.44 ± 0.06	0.006
1	8.25 ± 0.17	< 0.001
5	31.24 ± 0.15	< 0.001
10	72.05 ± 0.15	< 0.001
50	100 ± 0.01	< 0.001
100	100 ± 0.01	< 0.001
150	100 ± 0.01	< 0.001

^aData are reported as the average of three trials with calculated standard deviations shown.

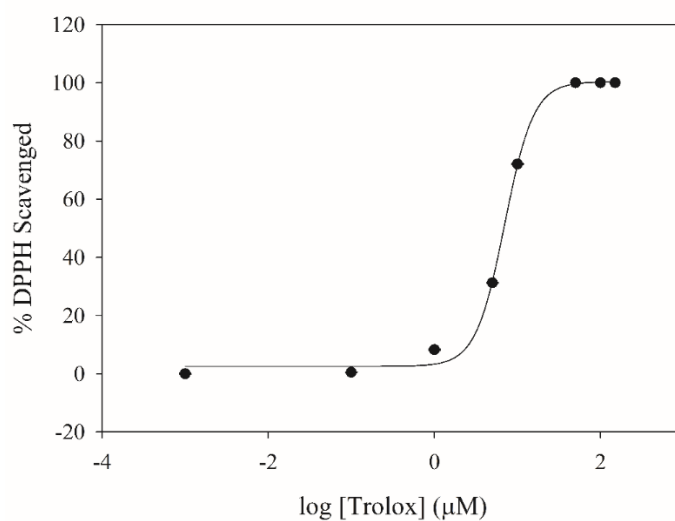


Figure 2.32. Dose-response plot for Trolox in the DPPH-scavenging assay. Error bars are smaller than the data point symbols.

Table 2.43. DPPH scavenging assay results for Edaravone.^a

[Edaravone], μM	% Scavenged	<i>p</i> Value
DPPH	$0 \pm$	-
Trolox (50 μM)	100 ± 0	-
0.001	-4.72 ± 0.1	< 0.001
0.1	13.19 ± 0.20	< 0.001
1	23.65 ± 0.15	< 0.001
5	60.51 ± 0.15	< 0.001
10	90.10 ± 0.20	< 0.001

^aData are reported as the average of three trials with calculated standard deviations shown.

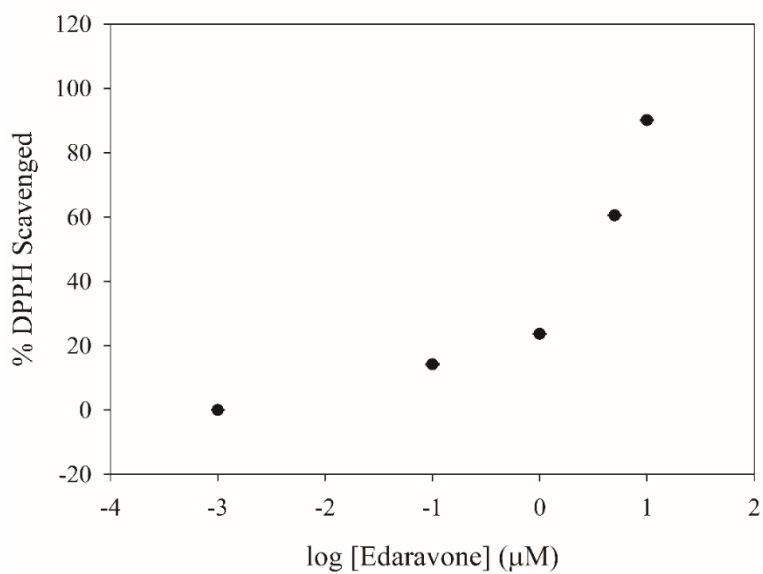


Figure 2.33. Dose-response plot for Edaravone in the DPPH-scavenging assay. Error bars are smaller than the data point symbols.

Table 2.44. DPPH scavenging assay results for ebselen.^a

[Ebselen], μM	% Scavenged	<i>p</i> Value
DPPH	$0 \pm$	-
Trolox (50 μM)	100 ± 0	-
0.1	11.66 ± 0.31	< 0.001
1	10.34 ± 0.15	< 0.001
10	5.28 ± 0.70	0.006
50	5.39 ± 0.45	0.002
100	3.74 ± 0.06	< 0.001
500	4.84 ± 0.25	< 0.001

^aData are reported as the average of three trials with calculated standard deviations shown.

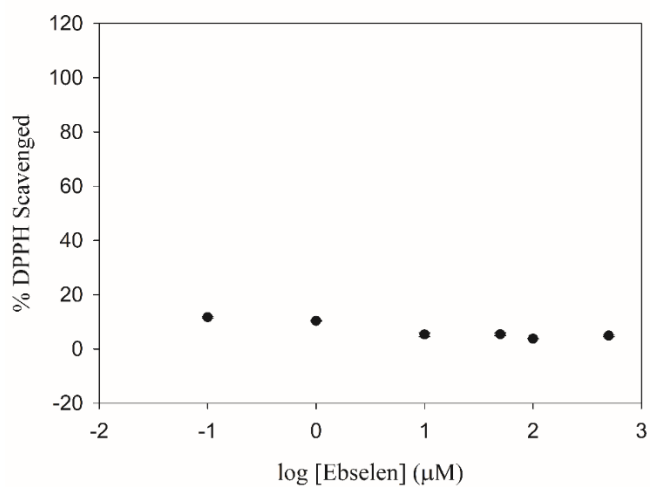


Figure 2.34. Dose-response plot for ebselen in the DPPH-scavenging assay. Error bars are smaller than the data point symbols.

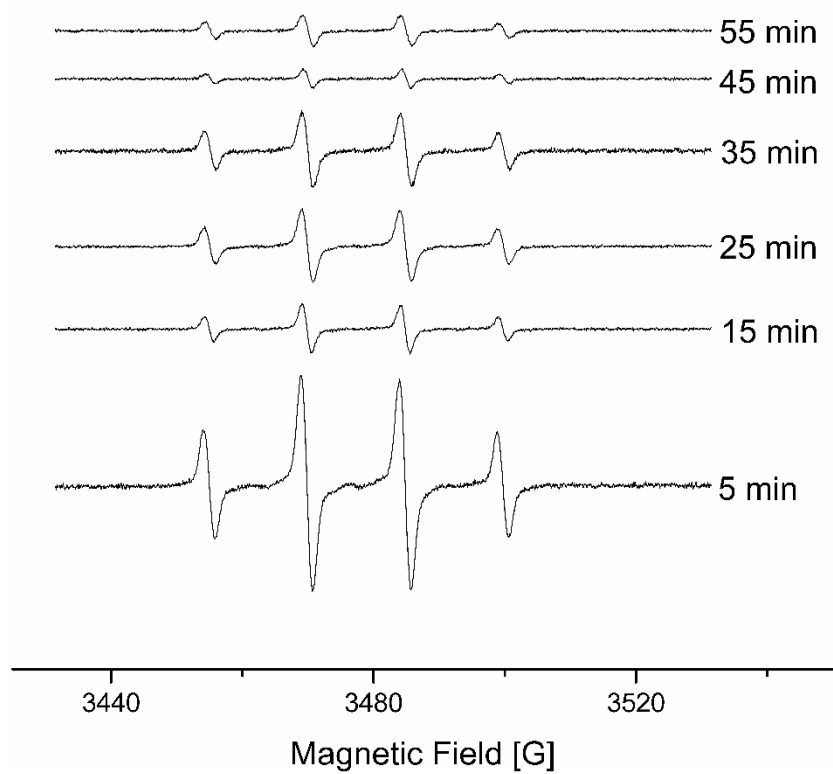


Figure 2.35. EPR spectra of Cu^{2+} (300 μM), ascorbic acid (375 μM), H_2O_2 (2.5 mM) and DMPO (30 mM) at the indicated time points.

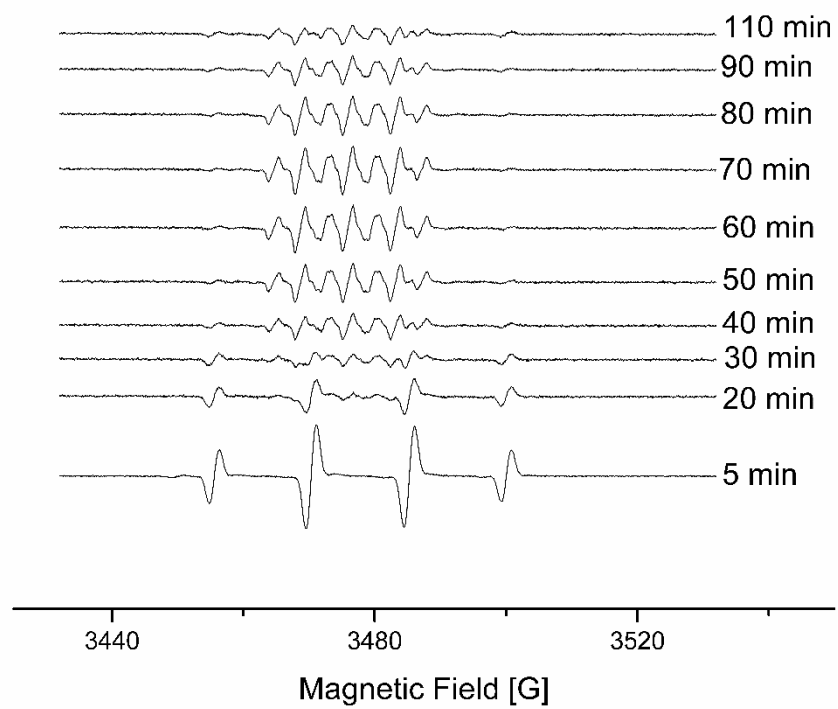


Figure 2.36. EPR spectra of Cu^{2+} (300 μM), ascorbic acid (375 μM), H_2O_2 (2.5 mM), DMPO (30 mM), and ethanol (1.7 M) at the indicated time points.

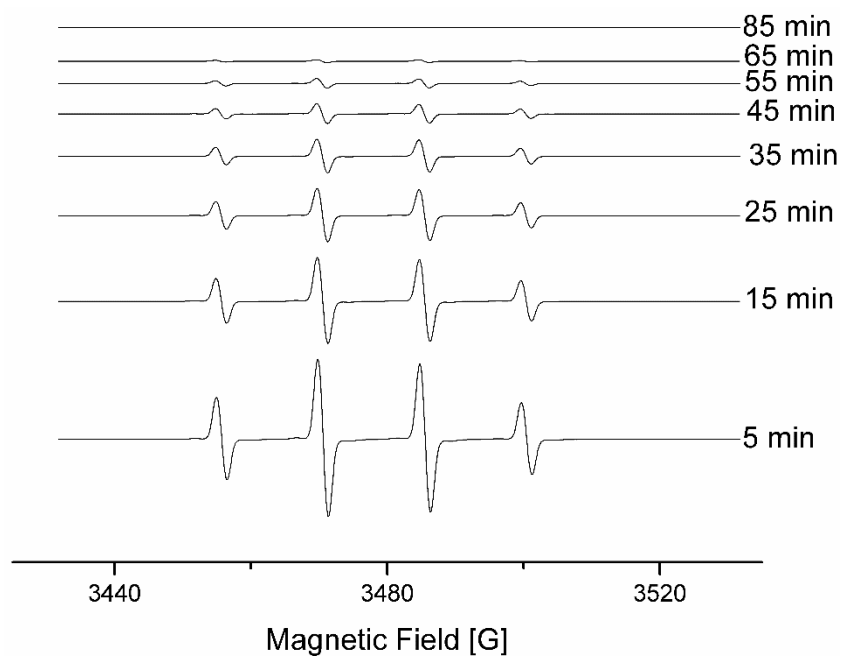


Figure 2.37. EPR spectra of Fe^{2+} (300 μM), H_2O_2 (2.5 mM), and DMPO (30 mM) at the indicated time points.

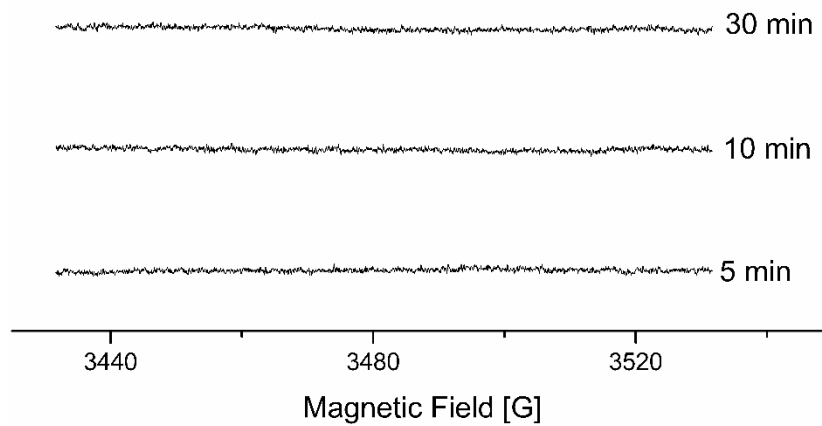


Figure 2.38. EPR spectra of Fe^{2+} (300 μM), H_2O_2 (2.5 mM), DMPO (30 mM), and ethanol (1.7 M) at the indicated time points.

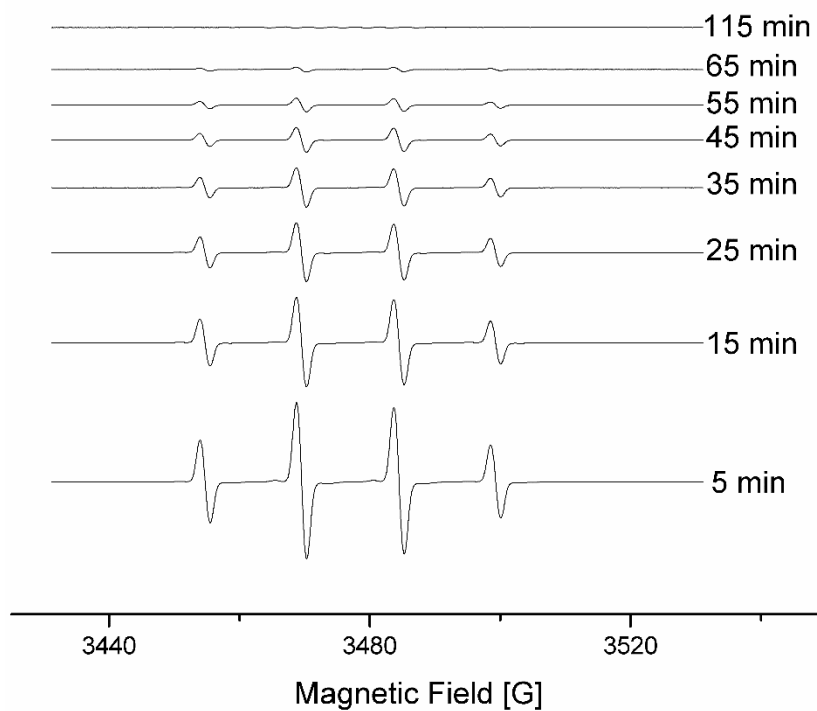


Figure 2.39. EPR spectra of Fe^{2+} (300 μM), H_2O_2 (2.5 mM), DMPO (30 mM), and ethanol (875 mM) at the indicated time points.

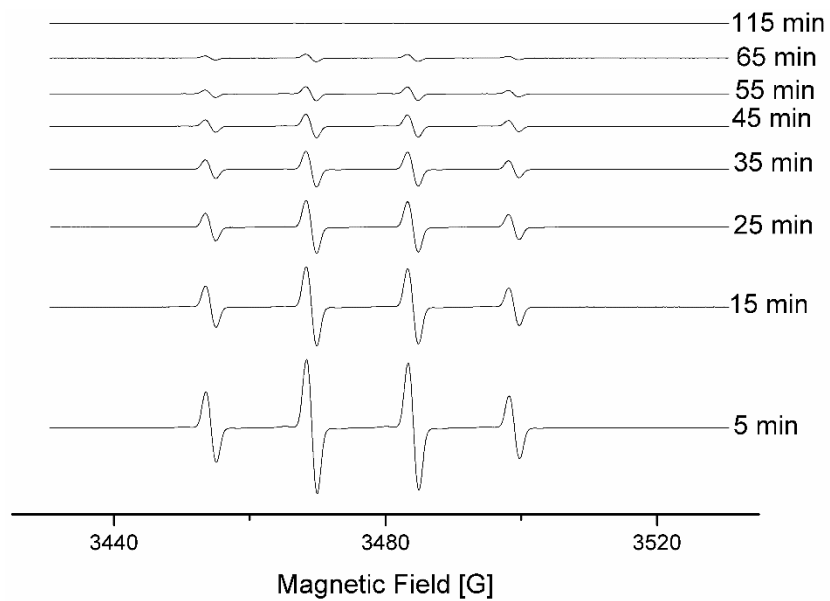


Figure 2.40. EPR spectra of Fe^{2+} (300 μM), H_2O_2 (2.5 mM), DMPO (30 mM), and ethanol (425 mM) at the indicated time points.

2.6 References

- (1) Azzi, A. *Biochem. Biophys. Res. Commun.* **2007**, *362*, 230–232.
- (2) Imlay, J. A.; Linn, S. *Science* **1988**, *240*, 1302–1309.
- (3) Battin, E. E.; Zimmerman, M. T.; Ramoutar, R. R.; Quarles, C. E.; Brumaghim, J. L. *Metallomics* **2011**, *3*, 503–512.
- (4) Garcia, C. R.; Angele-Martinez, C.; Wilkes, J. A.; Wang, H. C.; Battin, E. E.; Brumaghim, J. L. *Dalton Trans.* **2012**, *41*, 6458–6467.
- (5) Begonja, A. J.; Teichmann, L.; Geiger, J.; Gambaryan, S.; Walter, U. *Blood Cells Mol. Dis.* **2006**, *36*, 166–170.
- (6) Halliwell, B.; Gutteridge, J. M.C. *Mol. Aspects Med.* **1985**, *8*, 89–193.
- (7) Cross, C. E.; Halliwell, B.; Borish, E. T.; Pryor, W. A.; Ames, B. N.; Saul, R. L.; McCord, J. M.; Harman, D. *Ann. Intern. Med.* **1987**, *107*, 526–545.
- (8) Aust, S. D.; Morehouse, L. A.; Thomas, C. E. *J. Free Radic. Biol. Med.* **1985**, *1*, 3–25.
- (9) Oswald, M. C. W.; Garnham, N.; Sweeney, S. T.; Landgraf, M. *FEBS Lett.* **2018**, *592*, 679–691.
- (10) Akhtar, M. J.; Ahamed, M.; Alhadlaq, H. A.; Alshamsan, A. *Biochim. Biophys. Acta* **2017**, *1861*, 802–813.
- (11) Dixon, S. J.; Stockwell, B. R. *Nature Chem. Biol.* **2014**, *10*, 9–17.
- (12) Saeidnia, S.; Abdollahi, M. *Toxicol. Appl. Pharmacol.* **2013**, *273*, 442–455.
- (13) Heneka, M. T.; O'Banion, M. K. *J. Neuroimmunol.* **2007**, *184*, 69–91.

- (14) Fetoni, A. R.; Paciello, F.; Rolesi, R.; Paludetti, G.; Troiani, D. *Free Radic. Biol. Med.* **2019**, *135*, 46–59.
- (15) Moody, C. S.; Hassan, H. M. *Proc. Natl. Acad. Sci. USA* **1982**, *79*, 2855–2859.
- (16) Weitzman, S. A.; Weitberg, A. B.; Clark, E. P.; Stossel, T. P. *Science* **1985**, *227*, 1231–1233.
- (17) Brawn, M. K.; Fridovich, I. *J. Biol. Chem.* **1985**, *260*, 922–925.
- (18) Bhabak, K. P.; Mughesh, G. *Chem. Eur. J.* **2010**, *16*, 1175–1185.
- (19) Lee, S. H.; Blair, I. A. *Trends Cardiovasc. Med.* **2001**, *11*, 148–155.
- (20) Jeremy, J. Y.; Yim, A. P.; Wan, S.; Angelini, G. D. *J. Card. Surg.* **2002**, *17*, 324–327.
- (21) Hureau, C.; Faller, P. *Biochimie* **2009**, *91*, 1212–1217.
- (22) Puppo, A.; Halliwell, B. *Free Radic. Res. Commun.* **1988**, *4*, 415–422.
- (23) Halliwell, B.; Aruoma, O. I. *FEBS Lett.* **1991**, *281*, 9–19.
- (24) Aruoma, O. I.; Halliwell, B.; Gajewski, E.; Dizdaroglu, M. *Biochem. J.* **1991**, *273*, 601–604.
- (25) Halliwell, B. *Free Radic. Biol. Med.* **1989**, *7*, 645–651.
- (26) Nassi-Calò, L.; Mello-Filho, C.; Meneghini, R. *Carcinogenesis* **1989**, *10*, 1055–1057.
- (27) Aruoma, O. I.; Halliwell, B.; Hoey, B. M.; Butler, J. *Biochem. J.* **1988**, *256*, 251–255.
- (28) Gutteridge, J. M.C.; Halliwell, B. *Bail. Cl. Hae.* **1989**, *2*, 195–256.
- (29) Storz, G.; Imlay, J. A. *Curr. Opin. Microbiol.* **1999**, *2*, 188–194.

- (30) Park, S.; Imlay, J. A. *J. Bacteriol.* **2003**, *185*, 1942–1950.
- (31) Sorg, O. *C. R. Biol.* **2004**, *327*, 649–662.
- (32) Fridovich, I. *J. Biol. Chem.* **1989**, *264*, 7761–7764.
- (33) Duthie, G. G. *Proc. Nutr. Soc.* **1999**, *58*, 1015–1024.
- (34) Kedare, S. B.; Singh, R. P. *J. Food Sci. Technol.* **2011**, *48*, 412–422.
- (35) Mishra, K.; Ojha, H.; Chaudhury, N. K. *Food Chem.* **2012**, *130*, 1036–1043.
- (36) Schaich, K. M.; Tian, X.; Xie, J. *J. Funct. Foods* **2015**, *18*, 782–796.
- (37) Frankel, E. N.; Meyer, A. S. *J. Sci. Food Agric.* **2000**, *80*, 1925–1941.
- (38) Aruoma, O. I. *Mut. Res.* **2003**, *523-524*, 9–20.
- (39) Pérez-Jiménez, J.; Saura-Calixto, F. *Food Res. Int.* **2006**, *39*, 791–800.
- (40) Pinchuk, I.; Shoval, H.; Dotan, Y.; Lichtenberg, D. *Chem. Phys. Lipids* **2012**, *165*, 638–647.
- (41) Benzie, I. F.F.; Devaki, M. In *Measurement of antioxidant activity and capacity: Recent trends and applications*. Wiley: Hoboken, NJ, USA, 2018; pp 77–106.
- (42) Özyürek, M.; Güçlü, K.; Tütem, E.; Başkan, K. S.; Erçağ, E.; Esin Çelik, S.; Baki, S.; Yıldız, L.; Karaman, Ş.; Apak, R. *Anal. Methods* **2011**, *3*, 2439.
- (43) López-Alarcón, C.; Denicola, A. *Anal. Chim. Acta* **2013**, *763*, 1–10.
- (44) Martín, M. Á.; Fernández-Millán, E.; Ramos, S.; Bravo, L.; Goya, L. *Mol. Nutr. Food Res.* **2014**, *58*, 447–456.
- (45) Dajas, F.; Rivera, F.; Blasina, F.; Arredondo, F.; Echeverry, C.; Lafon, L.; Morquio, A.; Heinzen, H.; Heinzen, H. *Neurotox. Res.* **2003**, *5*, 425–432.
- (46) Singh, S.; Singh, R. P. *Food Rev. Int.* **2008**, *24*, 392–415.

- (47) Nascimento da Silva, L. C.; Bezerra Filho, C. M.; Paula, R. A. de; Silva E Silva, C. S.; Oliveira de Souza, L. I.; Silva, M. V. d.; Correia, M. T. D. S.; Figueiredo, R. C. B. Q. de. *Free Radic. Res.* **2016**, *50*, 801–812.
- (48) Carochio, M.; Ferreira, I. C. F. R. *Food Chem. Tox.* **2013**, *51*, 15–25.
- (49) Cao, G.; Alessio, H. M.; Cutler, R. G. *Free Radic. Biol. Med.* **1993**, *14*, 303–311.
- (50) Huang, D.; Ou, B.; Hampsch-Woodill, M.; Flanagan, J. A.; Deemer, E. K. *J. Agric. Food Chem.* **2002**, *50*, 1815–1821.
- (51) Huang, D.; Ou, B.; Prior, R. L. *J. Agric. Food Chem.* **2005**, *53*, 1841–1856.
- (52) Ou, B.; Hampsch-Woodill, M.; Prior, R. L. *J. Agric. Food Chem.* **2001**, *49*, 4619–4626.
- (53) Bank, G.; Schauss, A. *Nutraceuticals World* **2004**, 68–71.
- (54) Ou, B.; Hampsch-Woodill, M.; Flanagan, J.; Deemer, E. K.; Prior, R. L.; Huang, D. *J. Agric. Food Chem.* **2002**, *50*, 2772–2777.
- (55) Cao, G.; Verdon, C. P.; Wu, A. H.; Wang, H.; Prior, R. L. *Clin. Chem.* **1995**, *41*, 1738–1744.
- (56) Cunningham, E. *J. Acad. Nutr. Diet.* **2013**, *113*, 740.
- (57) Fraga, C. G.; Oteiza, P. I.; Galleano, M. *Biochim. Biophys. Acta* **2014**, *1840*, 931–934.
- (58) Chen, H.-Y. *ACS Omega* **2019**, *4*, 14105–14113.
- (59) Ryter, S. W.; Kim, H. P.; Hoetzel, A.; Park, J. W.; Nakahira, K.; Wang, X.; Choi, A. M. K. *Antiox. Redox Signal.* **2007**, *9*, 49–89.

- (60) Kroemer, G.; Dallaporta, B.; Resche-Rigon, M. *Annu. Rev. Physiol.* **1998**, *60*, 619–642.
- (61) Halliwell, B. *Am. J. Clin. Nutr.* **2000**, *72*, 1082–1087.
- (62) Arif, R.; Nayab, P. S.; Akrema; Abid, M.; Yadava, U.; Rahisuddin. *J. Anal. Sci. Technol.* **2019**, *10*, 1024.
- (63) Battin, E. E.; Perron, N. R.; Brumaghim, J. L. *Inorg. Chem.* **2006**, *45*, 499–501.
- (64) Soumya, K.; Haridas, K. R.; James, J.; Sameer Kumar, V. B.; Edatt, L.; Sudheesh, S. *J. Taibah Univ. Sci.* **2019**, *13*, 755–763.
- (65) Xu, J.-G.; Hu, Q.-P.; Liu, Y. *J. Agric. Food Chem.* **2012**, *60*, 11625–11630.
- (66) Hu, Q.-P.; Cao, X.-M.; Hao, D.-L.; Zhang, L.-L. *Sci. Rep.* **2017**, *7*, 45231.
- (67) Johnson, G. R. A.; Nazhat, N. B.; Saadalla-Nazhat, R. A. *J. Chem. Soc., Chem. Commun.* **1985**, 407.
- (68) Jung, Y.-J.; Surh, Y.-J. *Free Radic. Biol. Med.* **2001**, *30*, 1407–1417.
- (69) Roussyn, I.; Briviba, K.; Masumoto, H.; Sies, H. *Arch. Biochem. Biophys.* **1996**, *330*, 216–218.
- (70) Imlay, J. A.; Chin, S. M.; Linn, S. *Science* **1988**, *240*, 640–642.
- (71) Imlay, J. A.; Linn, S. *Science* **1988**, *240*, 1302–1309.
- (72) Mello-Filho, A. C.; Meneghini, R. *Mut. Res.* **1991**, *251*, 109–113.
- (73) Mello Filho, A. C.; Hoffmann, M. E.; Meneghini, R. *Biochem. J.* **1984**, *218*, 273–275.
- (74) Keyer, K.; Imlay, J. A. *Proc. Natl. Acad. Sci. USA* **1996**, *93*, 13635–13640.

- (75) Touati, D.; Jacques, M.; Tardat, B.; Bouchard, L.; Despied, S. *J. Bacteriol.* **1995**, *177*, 2305–2314.
- (76) Perron, N. R.; Brumaghim, J. L. *Cell Biochem. Biophys.* **2009**, *53*, 75–100.
- (77) Touati, D. Iron and oxidative stress in bacteria. *Arch. Biochem. Biophys.* **2000**, *373*, 1–6.
- (78) Blokhina, O.; Virolainen, E.; Fagerstedt, K. V. *Ann. Bot.* **2003**, *91*, 179–194.
- (79) Valko, M.; Morris, H.; Cronin, M. *Curr. Med. Chem.* **2005**, *12*, 1161–1208.
- (80) Tashiro, M.; Tursun, P.; Konishi, M. *Biophys. J.* **2005**, *89*, 3235–3247.
- (81) Stöckel, J.; Safar, J.; Wallace, A. C.; Cohen, F. E.; Prusiner, S. B. *Biochemistry* **1998**, *37*, 7185–7193.
- (82) Angelé-Martínez, C.; Goodman, C.; Brumaghim, J. *Metallomics* **2014**, *6*, 1358–1381.
- (83) Gaggelli, E.; Kozłowski, H.; Valensin, D.; Valensin, G. *Chem. Rev.* **2006**, *106*, 1995–2044.
- (84) Hopt, A.; Korte, S.; Fink, H.; Panne, U.; Niessner, R.; Jahn, R.; Kretzschmar, H.; Herms, J. *J. Neurosci. Meth.* **2003**, *128*, 159–172.
- (85) Liu, C. *J. Inorg. Biochem.* **1999**, *75*, 233–240.
- (86) Chikira, M.; Ng, C. H.; Palaniandavar, M. *Int. J. Mol. Sci.* **2015**, *16*, 22754–22780.
- (87) Galindo-Murillo, R.; García-Ramos, J. C.; Ruiz-Azuara, L.; Cheatham, T. E.; Cortés-Guzmán, F. *Nucleic Acids Res.* **2015**, *43*, 5364–5376.
- (88) Halliwell, B. *Free Radic. Biol. Med.* **2002**, *32*, 968–974.
- (89) Woodmansee, A. N.; Imlay, J. A. *Methods Enzymol.* **2002**, *349*, 3–9.

- (90) Linn, S. *J. Biol. Chem.* **2015**, *290*, 8748–8757.
- (91) Luo, Y.; Han, Z.; Chin, S. M.; Linn, S. *Proc. Natl. Acad. Sci. USA* **1994**, *91*, 12438–12442.
- (92) Henle, E. S.; Han, Z.; Tang, N.; Rai, P.; Luo, Y.; Linn, S. *J. Biol. Chem.* **1999**, *274*, 962–971.
- (93) Henle, E. S.; Linn, S. *J. Biol. Chem.* **1997**, *272*, 19095–19098.
- (94) Ogusucu, R.; Rettori, D.; Netto, L. E. S.; Augusto, O. *J. Biol. Chem.* **2009**, *284*, 5546–5556.
- (95) Augusto, O. *Free Radic. Biol. Med.* **1993**, *15*, 329–336.
- (96) Nakao, L. S.; Augusto, O. *Chem. Res. Toxicol.* **1998**, *11*, 888–894.
- (97) Nakao, L. S.; Fonseca, E.; Augusto, O. *Chem. Res. Toxicol.* **2002**, *15*, 1248–1253.
- (98) Perron, N. R.; Wang, H. C.; Deguire, S. N.; Jenkins, M.; Lawson, M.; Brumaghim, J. L. *Dalton Trans.* **2010**, *39*, 9982–9987.
- (99) Battin, E. E.; Zimmerman, M. T.; Ramoutar, R. R.; Quarles, C. E.; Brumaghim, J. L. *Metallomics* **2011**, *3*, 503–512.
- (100) Abbas, M.; Gaertner, A. A. E.; McMillen, C. D.; Brumaghim, J. L. *Dalton trans.* *In preparation.*
- (101) Briviba, K.; Roussyn, I.; Sharov, V. S.; Sies, H. *Biochem. J.* **1996**, *319*, 13–15.
- (102) Morgan, B.; Lahav, O. *Chemosphere* **2007**, *68*, 2080–2084.
- (103) Floyd, R. A.; Lewis, C. A. *Biochemistry* **1983**, *22*, 2645–2649.
- (104) Halliwell, B.; Gutteridge, J. M.C. *FEBS Lett.* **1992**, *307*, 108–112.
- (105) Steiner, M. G.; Babbs, C. F. *Arch. Biochem. Biophys.* **1990**, *278*, 478–481.

- (106) Burkitt, M. J.; Mason, R. P. *Proc. Natl. Acad. Sci. USA* **1991**, *88*, 8440–8444.
- (107) Kadiiska, M. B.; Burkitt, M. J.; Xiang, Q. H.; Mason, R. P. *J. Clin. Invest.* **1995**, *96*, 1653–1657.
- (108) Schraufstatter, I.; Hyslop, P. A.; Jackson, J. H.; Cochrane, C. G. *J. Clin. Invest.* **1988**, *82*, 1040–1050.
- (109) Olsen, M. J. *J. Tox. Environ. Health* **1988**, *23*, 407–423.
- (110) Jonas, S. K.; Riley, P. A.; Willson, R. L. *Biochem. J.* **1989**, *264*, 651–655.
- (111) Sagripanti, J. L.; Kraemer, K. H. *J. Biol. Chem.* **1989**, *264*, 1729–1734.
- (112) Fujimoto, S.; Adachi, Y.; Ishimitsu, S.; Ohara, A. *Chem. Pharm. Bull.* **1986**, *34*, 4848–4851.
- (113) Rowley, D. A.; Halliwell, B. *Arch. Biochem. Biophys.* **1983**, *225*, 279–284.
- (114) Reed, C. J.; Douglas, K. T. *Biochem. Biophys. Res. Commun.* **1989**, *162*, 1111–1117.
- (115) Masarwa, M.; Cohen, H.; Meyerstein, D.; Hickman, D. L.; Bakac, A.; Espenson, J. H. *J. Am. Chem. Soc.* **1988**, *110*, 4293–4297.
- (116) Goldstein, S.; Meyerstein, D. *Acc. Chem. Res.* **1999**, *32*, 547–550.
- (117) Ingraham, L. L. *Arch. Biochem. Biophys.* **1959**, *81*, 309–318.
- (118) Yamamoto, K.; Kawanishi, S. *J. Biol. Chem.* **1989**, *264*, 15435–15440.
- (119) Sutton, H. C.; Winterbourn, C. C. *Free Radic. Biol. Med.* **1989**, *6*, 53–60.
- (120) Johnson, G. R. A.; Nazhat, N. B.; Saadalla-Nazhat, R. A. *J. Chem. Soc., Faraday Trans. 1* **1988**, *84*, 501.
- (121) Sigman, D. S. *Acc. Chem. Res.* **1986**, *19*, 180–186.

- (122) Rodriguez, H.; Drouin, R.; Holmquist, G. P.; O'Connor, T. R.; Boiteux, S.; Laval, J.; Doroshov, J. H.; Akman, S. A. *J. Biol. Chem.* **1995**, *270*, 17633–17640.
- (123) Dizdaroglu, M.; Rao, G.; Halliwell, B.; Gajewski, E. *Arch. Biochem. Biophys.* **1991**, *285*, 317–324.
- (124) Stoewe, R.; Prütz, W. A. *Free Radic. Biol. Med.* **1987**, *3*, 97–105.
- (125) Taniguchi, H.; Madden, K. P. *Radiat. Res.* **2000**, *153*, 447–453.
- (126) Haire, D. L.; Kotake, Y.; Janzen, E. G. *Can. J. Chem.* **1988**, *66*, 1901–1911.
- (127) Kotake, Y.; Kuwata, K.; Janzen, E. G. Electron spin resonance spectra of diastereomeric nitroxyls produced by spin trapping hydroxylalkyl radicals. *J. Phys. Chem.* **1979**, *83*, 3024–3029.
- (128) Kirino, Y.; Ohkuma, T.; Kwan, T. *Spin Chem. Pharm. Bull.* **1981**, *29*, 29–34.
- (129) Hedrick, W. R.; Webb, M. D.; Zimbrick, J. D. *Int. J. Rad. Biol. Rel. Stud. Phys. Chem. Med.* **1982**, *41*, 435–442.
- (130) Wei, J.; Liang, Y.; Hu, Y.; Kong, B.; Zhang, J.; Gu, Q.; Tong, Y.; Wang, X.; Jiang, S. P.; Wang, H. *Angew. Chem. Int. Ed.* **2016**, *55*, 12470–12474.
- (131) Rice-Evans, C. A.; Miller, N. J.; Paganga, G. *Free Radic. Biol. Med.* **1996**, *20*, 933–956.
- (132) El Gharras, H. *Int. J. Food Sci. Technol.* **2009**, *44*, 2512–2518.
- (133) Sánchez-Moreno, C.; Larrauri, J. A.; Saura-Calixto, F. *J. Sci. Food Agric.* **1998**, *76*, 270–276.
- (134) Sanchez-Moreno, C. *Food Sci Technol. Int.* **2002**, *8*, 121–137.

- (135) Perron, N. R. Effects of Polyphenol Compounds on Iron- and Copper-mediated DNA damage: Mechanism and Predictive Models. Dissertation, Clemson University, Clemson, 2008.
- (136) Imlay, J. A.; Linn, S. *J. Bact.* **1987**, *169*, 2967–2976.
- (137) Duthie, G. G. *Pr. Nutr. Soc.* **1999**, *58*, 1015–1024.
- (138) Stadelman, B. S.; Kimani, M. M.; Bayse, C. A.; McMillen, C. D.; Brumaghim, J. L. *Dalton Trans.* **2016**, *45*, 4697–4711.
- (139) Kimani, M. M.; Watts, D.; Graham, L. A.; Rabinovich, D.; Yap, G. P. A.; Brumaghim, J. L. *Dalton Trans.* **2015**, *44*, 16313–16324.
- (140) Kimani, M. M.; Bayse, C. A.; Stadelman, B. S.; Brumaghim, J. L. *Inorg. Chem.* **2013**, *52*, 11685–11687.
- (141) Fábíán, I. *Inorg. Chem.* **1989**, *28*, 3805–3807.
- (142) Inskeep, R. G. *J. Inorg. Nucl. Chem.* **1962**, *24*, 763–776.
- (143) Zimmerman, M. T. Determining DNA damage prevention mechanisms for multifunctional selenium and sulfur antioxidants and the DNA-damaging capabilities of clotrimazole and pseudophedrine-derived metal complexes. Dissertation, Clemson, 2014.
- (144) Cabani, S.; Moretti, G.; Scrocco, E. *J. Chem. Soc.* **1962**, *0*, 88–93.
- (145) Sun, M. S.; Brewer, D. G. *Can. J. Chem.* **1967**, *45*, 2729–2743.
- (146) Abraham, A.; Nefussy, B.; Fainmesser, Y.; Ebrahimi, Y.; Karni, A.; Drory, V. E. *Amyotroph. Lat. Sci. & Fr. Deg.* **2019**, *20*, 260–263.
- (147) Yoshino, H. *Expert Rev. Neurother.s* **2019**, *19*, 185–193.

- (148) Homma, T.; Kobayashi, S.; Sato, H.; Fujii, J. *Exp. Cell Res.* **2019**, *384*, 111592-111611.
- (149) Watanabe, K.; Tanaka, M.; Yuki, S.; Hirai, M.; Yamamoto, Y. *J. Clin. Biochem. Nutr.* **2018**, *62*, 20–38.
- (150) Cruz, M. P. *Pharm. Ther.* **2018**, *43*, 25–28.
- (151) Oberley, L. W.; Buettner, G. R. *Cancer Res.* **1979**, *39*, 1141–1149.
- (152) Mruk, D. D.; Silvestrini, B.; Mo, M.-y.; Cheng, C.Y. *Contraception* **2002**, *65*, 305–311.
- (153) Tokuda, E.; Furukawa, Y. *Int. J. Mol. Sci.* **2016**, *17*, 636-650.
- (154) Oliveira, R.; Geraldo, D.; Bento, F. *Talanta* **2014**, *129*, 320–327.
- (155) Alberto, M. E.; Russo, N.; Grand, A.; Galano, A. *Phys. Chem. Chem. Phys.* **2013**, *15*, 4642–4650.
- (156) Mitarai, A.; Ouchi, A.; Mukai, K.; Tokunaga, A.; Mukai, K.; Abe, K. *J. Agric. Food Chem.* **2008**, *56*, 84–91.
- (157) Friaa, O.; Brault, D. *Org. Biomol. Chem.* **2006**, *4*, 2417–2423.
- (158) Wang, L.-F.; Zhang, H.-Y. *Bioorg. Med. Chem. Lett.* **2003**, *13*, 3789–3792.
- (159) Tokumaru, O.; Shuto, Y.; Ogata, K.; Kamibayashi, M.; Bacal, K.; Takei, H.; Yokoi, I.; Kitano, T. *J. Surg. Res.* **2018**, *228*, 147–153.
- (160) Minnelli, C.; Laudadio, E.; Galeazzi, R.; Rusciano, D.; Armeni, T.; Stipa, P.; Cantarini, M.; Mobbili, G. *Antioxidants* **2019**, *8*, 258-262.
- (161) Pardridge, W. M. *Drug Discov. Today* **2007**, *12*, 54–61.
- (162) Jamieson, J. J.; Searson, P. C.; Gerecht, S. *J. Biol. Eng.* **2017**, *11*, 37.

- (163) Piętka-Ottlik, M.; Wójtowicz-Młochowska, H.; Kołodziejczyk, K.; Piasecki, E.; Młochowski, J. *Chem. Pharm. Bull.* **2008**, *56*, 1423–1427.
- (164) Santi, C.; Tidei, C.; Scalera, C.; Piroddi, M.; Galli, F. *Curr. Chem. Biol.* **2013**, *7*, 25–36.
- (165) Zade, S. S.; Panda, S.; Tripathi, S. K.; Singh, H. B.; Wolmershäuser, G. *Eur. J. Org. Chem.* **2004**, *2004*, 3857–3864.
- (166) Azad, G. K.; Tomar, R. S. *Mol. Biol. Rep.* **2014**, *41*, 4865–4879.
- (167) Álvarez-Pérez, M.; Ali, W.; Marć, M. A.; Handzlik, J.; Domínguez-Álvarez, E. *Molecules* **2018**, *23*, 628–647.
- (168) Steinbrenner, H.; Brigelius-Floh, R. *Aktue.l Ernährungsmed.* **2015**, *40*, 368–378.
- (169) Yamaguchi, T.; Sano, K.; Takakura, K.; Saito, I.; Shinohara, Y.; Asano, T.; Yasuhara, H. *Stroke* **1998**, *29*, 12–17.
- (170) Kil, J.; Lobarinas, E.; Spankovich, C.; Griffiths, S. K.; Antonelli, P. J.; Lynch, E. D.; Le Prell, C. G. *Lancet* **2017**, *390*, 969–979.
- (171) Parnham, M. J. *Adv. Exp. Med. Biol.* **1990**, *264*, 193–197.
- (172) Sies, H.; Masumoto, H. In *Advances in Pharmacology*. Elsevier, 1996. pp 229–246.
- (173) Maiorino, M.; Roveri, A.; Coassin, M.; Ursini, F. *Biochem. Pharmacol.* **1988**, *37*, 2267–2271.
- (174) Masumoto, H.; Sies, H. *Chem. Res. Toxicol.* **1996**, *9*, 262–267.
- (175) Fujisawa, S.; Kadoma, Y. *Anticancer Res.* **2005**, *25*, 3989–3994.

- (176) Adams, G. E.; Boag, J. W.; Michael, B. D. *Trans. Faraday Soc.* **1965**, *61*, 1417–1424.
- (177) Woodmansee, A. N.; Imlay, J. A. In *Superoxide dismutase*. Academic Press: San Diego, London, 2002. pp 3–9.
- (178) Gordhan, H. M.; Patrick, S. L.; Swasy, M. I.; Hackler, A. L.; Anayee, M.; Golden, J. E.; Morris, J. C.; Whitehead, D. C. *Bioorg. Med. Lett.* **2016**, *27*, 537–541.
- (179) Cannan, R. K.; Kibrick, A. *J. Am. Chem. Soc.* **1938**, *60*, 2314–2320.
- (180) Bala, T.; Prasad, B. L. V.; Sastry, M.; Kahaly, M. U.; Waghmare, U. V. *J. Phys. Chem. A* **2007**, *111*, 6183–6190.
- (181) Battin, E. E.; Brumaghim, J. L. *J. Inorg. Biochem.* **2008**, *102*, 2036–2042.
- (182) Perkowski, D. A.; Perkowski, M. *Data and probability connection*. Pearson Education Ltd: Upper Saddle River, N.J., 2007, pp 647-648.

CHAPTER THREE

FLUCONAZOLE PRODUCES REACTIVE OXYGEN SPECIES IN THE PRESENCE OF COPPER AND IRON TO CAUSE DNA DAMAGE

3.1 Introduction

Cryptococcus neoformans is a basidiomycetous yeast that causes pneumonia and meningitis primarily in immunocompromised patients, and is responsible for approximately 620,000 deaths per year.¹⁻³ Global prevalence of cryptococcal disease is 5–10% in the Americas and Europe and exceeds 15% in South East Asia and Sub-Saharan Africa.^{4,5} Azoles are a class of five-membered heterocyclic compounds containing at least one nitrogen atom and drugs containing azoles are commonly used to treat various fungal infections. Complexes of three FDA-approved antifungal drugs were tested in the Brumaghim group^{6,7} for their ability to facilitate DNA damage in combination with transition metals. In this study, fluconazole (FLC; Figure 3.1), a triazole-containing drug that accumulates in the cerebrospinal fluid that has been used as an antifungal agent since 1990,^{8,9} is evaluated for its ability to cause DNA damage with copper and iron. FLC and clotrimazole (CTZ)⁷ are being used to treat ectopic as well as systemic fungal infections, whereas tinidazole (TNZ) is only approved for topical treatments.^{6,10}

FLC is used as an antifungal drug due to its metabolic stability, relatively high water-solubility, and good tolerability when used to treat cryptococcosis,^{11-14,14,15} however, due to the fungistatic rather than fungicidal effects of FLC, emergence of FLC resistance to the drug complicates treatments.^{7,16,17} Thus, there is a need to understand mechanisms

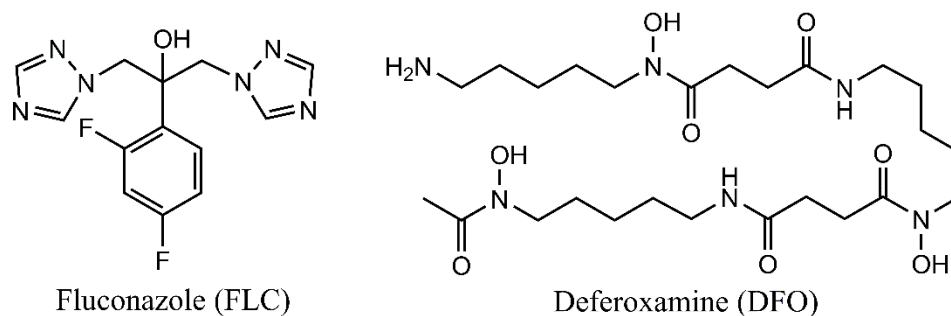


Figure 3.1. Structures of fluconazole (FLC) and deferoxamine (DFO)

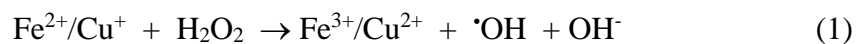
for FLC drug resistance to develop more effective therapies for cryptococcal meningitis.

The mechanisms that attribute to the increasing *C. neoformans* azole drug resistance include lanosterol 14 α demethylase (ERG11) gene mutation,¹⁸ gene duplication,¹⁹ and drug efflux pump Afr1 upregulation.^{20,21} In addition, a number of kinases involved in TOR signaling (Ypk1, Ipk1, Gsk3), related to vacuole transport (Vps15) and involved in the pathogenicity-related kinase cell cycle (Cdc7), are associated with FLC resistance.²² FLC inhibits (ERG11), a conserved enzyme that catalyzes the conversion of lanosterol to ergosterol.²³ Fungal growth arrest upon exposure to FLC is attributed to the reduction of ergosterol in the plasma membrane combined with an accumulation of potentially toxic sterols.²⁴

In addition, depletion of ergosterol has been associated with the disruption of V-ATPase function.²⁵ Only a single copy of the ERG11 gene was mapped to *C. neoformans* chromosome #1 (Chr1).²³ However, in FLC resistant strains, Chr1 was found to possess disomic duplication.¹⁹ Integrity of the endoplasmic reticulum is a major factor in the emergence of disomy of Chr1 and Chr4, leading to FLC resistance by overcoming the drug stress.^{26,27} Chr1 contains two genes that are important involved with drug resistance, AFR1,

the drug transporter, and ERG11, the target of FLC. Recent findings suggest that decoupling of cellular growth and nuclear division during FLC treatment leads to increased DNA content, which may be a conserved way to acquire azole resistance in fungal pathogens;^{28,29} however, the exact mechanisms underlying chromosomal changes in cells treated with FLC remain unknown.

Chromosomal instability is associated with chronic oxidative stress mediated by elevated reactive oxygen species (ROS), and it is well established that ROS can damage DNA. For example, human-hamster hybrid GM10115 cells acquire 22% chromosomal instability after exposure to H₂O₂.³⁰ In the model organism *Saccharomyces cerevisiae*, mutant strains with impaired DNA repair and reduced ROS scavenging enzymes show increased frequency of chromosomal rearrangement upon H₂O₂ challenge.³¹ One ROS, hydroxyl radical, is generated by the oxidation of metal ions *in vivo* and *in vitro* (Reaction 1).³²



Metallothioneins (MTs) are cysteine-rich, metal-chelating proteins that help to maintain physiological ROS concentrations.^{33,34} Two copper-detoxifying MTs were identified in the *C. neoformans* proteome: CMT1 (13.4 kDa) and CMT2 (20.1 kDa), both of which are upregulated in the presence of copper.³⁵ Metal-chelating domains in *C. neoformans* MTs provide high capacity MT-Cu⁺ binding, which is critical for counteracting the first line of copper-based immunity of the host.^{36,37} Impaired MT proteins result in ROS accumulation and cell cycle arrest in mice embryonic fibroblast cells.³⁸ Thus, accumulated evidence suggests that FLC leads to an increase of ROS in *C. neoformans*,

and such a response may lead to chromosomal instability. However, no direct study has addressed this possibility.

Peng *et al.*³⁹ have determined that FLC induces accumulation of intracellular ROS, which correlates with plasma membrane damage in *C. neoformans*, and caused transcription changes of oxidative-stress-related genes encoding superoxide dismutase (SOD1), catalase (CAT3), and thioredoxin reductase (TRR1). FLC also increases DNA damage *in vitro*, suggesting that FLC treatment leads to increase of ROS concurrently with plasma membrane damage. FLC also triggers adverse transcription of genes encoding primary antioxidant defense genes: copper/zinc superoxide dismutase (SOD1)⁴⁰ and catalase (CAT3).³⁹ Consistent with FLC affecting DNA integrity, FLC treatment of *C. neoformans* leads to transcription changes of genes associated with DNA repair and chromosome segregation (RAD54 and SCC1).³⁹ These findings suggest that FLC treatment results in increase of ROS in *C. neoformans* and this effect may lead to chromosomal instability.⁴¹ To evaluate the importance of metal coordination of FLC to iron, deferoxamine (DFO), a hexadentate iron chelator produced by soil bacteria to obtain iron from their environment,^{42,43} was tested for its ability to cause or prevent DNA damage cause by FLC and iron. Iron chelators have been shown to be effective in killing fungi^{44,44} but it has not been fully determined whether iron depletion or another mechanism causes the observed fungal killing.

This work was carried out in collaboration with Prof. Lukasz Kozubowski, Department of Genetics and Biochemistry at Clemson University, but this Chapter highlights only the *in vitro* DNA damage assay results performed by the author and does

not include the work performed by the collaborators. The majority of this work was published in *PLOS One* (doi: 10.1371/journal.pone.0208471)³⁹ reproduced with permission of the publisher (Appendix A), but this Chapter also includes additional studies of the effects of ascorbic acid treatment as well as an investigation into the effect of DFO addition on FLC's ability to damage DNA.

3.2 Results and Discussion

Metal Coordination of FLC and Change to Metal Redox Potential. Since results reported by Peng *et al.*³⁹ suggest an increase of ROS in FLC-treated cells, we hypothesized that treatment with FLC leads to chromosomal instability through the mechanism that involves ROS. Previous studies by Betanzos-Lara *et al.*⁷ and Castro-Ramirez *et al.*⁶ have indicated that antimicrobial drugs bind metals to potentiate DNA damage. Our hypothesis is that most azole containing antifungal drugs coordinate to redox-active transition metals, iron and /or copper to change the redox potential resulting in enhanced DNA damage abilities and potentially reduced development of drug resistance.

Most crystal structures of FLC with transition metals have been obtained using hydrothermal growth conditions and therefore may not be biologically relevant. Coordination of FLC to copper and iron in aqueous solution was confirmed using MALDI-TOF mass spectrometry (Table 3.3 and Figure 3.6) and is consistent with the findings of Ali *et al.*⁴⁵ who synthesized FLC complexes with Cu^{2+} , Fe^{2+} , Cd^{2+} , Co^{2+} , Ni^{2+} , and Mn^{2+} verified the structures of these complexes by further characterization with infrared spectroscopy, elemental analysis, UV-vis and NMR spectroscopy. In our mass

spectrometry studies, two equivalents of FLC bound per metal ion (Fe^{2+} and Cu^{2+}). Even when metal:FLC ratios were increased to 1:4 or 1:6, only complexes with a 1:2 ratio of metal to FLC were observed (Table 3.2 and Figure 3.5). Although Nagaj et al.⁴⁶ observed pH/pD-dependent metal-FLC complexes with a variety of metal:FLC ratios using NMR spectroscopy, we chose a ratio of 1:2 metal:FLC for our subsequent electrochemical and DNA damage studies since this was the only complex ratio we observed.

Cyclic voltammetry (CV) experiments were performed on FLC in the presence of metal ions to evaluate how FLC binding alters the redox activity of copper and iron. All experiments were performed in aqueous solutions at physiologically relevant pH with potassium nitrate as supporting electrolyte. FLC alone does not exhibit electrochemical activity. Upon addition of FLC to copper, the Cu^{+0} and $\text{Cu}^{2+/+}$ redox potentials shift to more positive potentials relative to aqueous CuSO_4 ($E_{1/2}$ values of 250 vs. 11 mV, respectively), indicating that FLC binding stabilizes hydroxyl-radical-generating Cu^+ over Cu^{2+} . Similar stabilization of Fe^{2+} over Fe^{3+} is observed upon iron-FLC binding ($\text{Fe}^{3+/2+}$ $E_{1/2}$ values shift from 65 mV for aqueous FeSO_4 to 98 mV for FeSO_4 with FLC). In both cases, the redox potentials of the FLC-metal complexes are well within the potential window for biological hydroxyl radical generation (-320 to 460 mV).⁴⁷

FLC Coordination to Metals Causes DNA Damage in Vitro. The ability of FLC to promote DNA damage in the presence of iron and copper was investigated using gel electrophoresis studies under physiologically relevant conditions. DNA damage caused by increasing concentrations of FLC and iron (in a 2:1 ratio) is shown in Figure 3.2; complete data tables for these studies are provided in Tables 3.4 - 3.19. DNA damage is defined as

percentage of shift between the fluorescent band corresponding to intact (circular) DNA and the band corresponding to the nicked (damaged) DNA.

Lane 2 in Figures 3.2A and B shows that hydrogen peroxide alone does not cause DNA damage. Similarly, FLC in the presence or absence of hydrogen peroxide does not cause DNA damage (Figure 3.2A, lanes 3 and 4). Quantification of the band intensities in lane 5 (Figure 3.2A) shows that Fe^{2+} (FeSO_4 , 2 μM) and hydrogen peroxide cause ~90% DNA damage. Increasing concentrations of FLC and Fe^{2+} in the presence of hydrogen peroxide cause DNA damage in a dose-dependent manner (Figure 3.2A, lanes 6–13; Table 3.1). Addition of FLC (2 μM) and Fe^{2+} (1 μM) with hydrogen peroxide causes ~90% DNA damage but it takes 2 μM Fe^{2+} and hydrogen peroxide to cause the same damage without FLC.

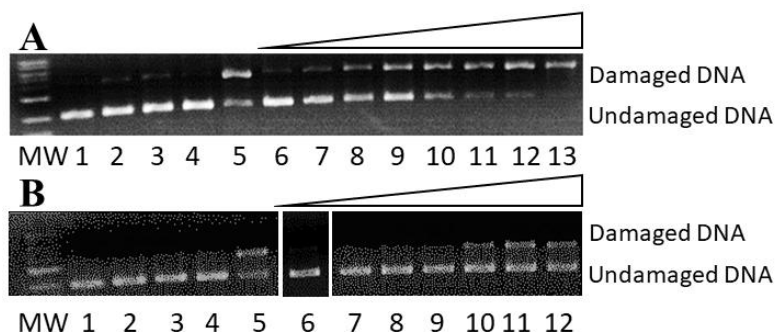


Figure 3.2. Gel electrophoresis images showing FLC-metal-mediated DNA damage for MW: 1 kb molecular weight marker; lane 1: plasmid DNA (p); lane 2: p + H₂O₂ and A) lane 3: p + FLC (50 μM) + H₂O₂; lane 4: p + FLC (50 μM); lane 5: p + FeSO₄ (2 μM) + H₂O₂; lanes 6-13: p + H₂O₂ + FLC (0.01, 0.1, 0.5, 1, 2, 4, 10, 50 μM , respectively) and FeSO₄ (0.005, 0.05, 0.25, 0.5, 1, 2, 5, and 25 μM , respectively) or B) lane 3: p + H₂O₂ + FLC (25 μM); lane 4: p + FLC (25 μM); lane 5: p + H₂O₂ + CuSO₄ (6 μM) + ascorbate (7.5 μM); lane 6: p + H₂O₂ + CuSO₄ (12.5 μM); lanes 7-12: p + H₂O₂ + FLC (0.1, 1, 5, 10, 18, 25 μM , respectively) + CuSO₄ (0.05, 0.5, 2.5, 5, 9, and 12.5 μM , respectively).

Similar DNA damage assays were conducted to evaluate the effects of FLC with Cu^{2+} on DNA damage.

The plasmid DNA band intensities from these studies were quantified to obtain EC_{50} plots (Figure 3.3), showing the Fe^{2+} or Cu^{+} concentrations needed to cause 50% DNA damage in the presence of FLC and hydrogen peroxide. An EC_{50} value of $0.46 \pm 0.01 \mu\text{M}$ ($p < 0.001$) was determined for Fe^{2+} and FLC with H_2O_2 . The EC_{50} plots in Figure 3.3A illustrate that addition of FLC shifts the iron-mediated DNA damage curve so that lower concentrations of iron in combination with FLC cause the same damage. Statistical analyses indicate that this enhancement of iron-mediated DNA damage in the presence of FLC is significant (Figure 3.3A, Table 3.19).

In similar studies with Cu^{2+} and FLC, DNA damage is observed in the presence of hydrogen peroxide upon increasing concentrations of FLC and Cu^{2+} concentrations ranging from 5 to 12.5 μM (Figure 3.2, lanes 7–12 and Fig 3.11B), suggesting that the observed DNA damage results from copper-FLC binding. A maximum of 40% DNA damage is

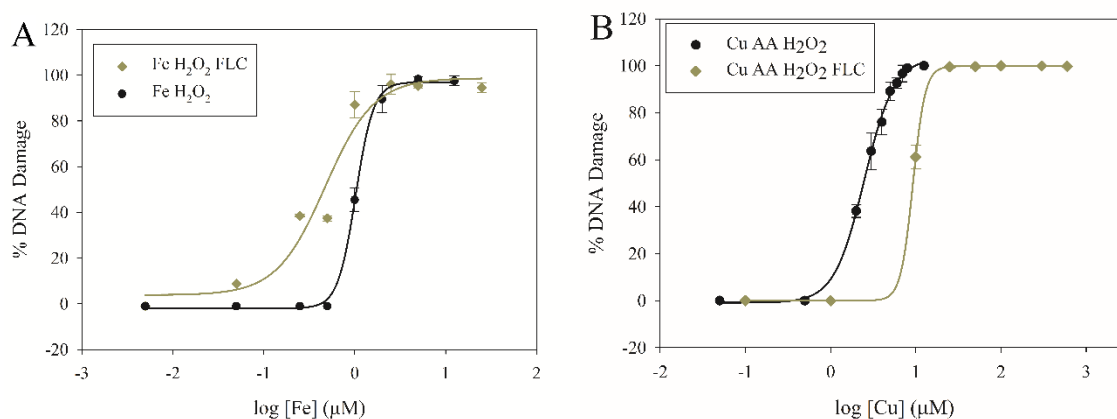


Figure 3.3. Dose-response curves of DNA damage by A) Fe^{2+} , H_2O_2 with and without FLC and B) Cu^{2+} , H_2O_2 , and ascorbate (AA) with and without FLC (1.25 equiv ascorbate was added to reduce Cu^{2+} to Cu^{+})

Table 3.1. EC₅₀ table of iron or copper with and without FLC and the effect of ascorbate (AA).

DNA Assay Conditions	EC ₅₀ FLC [$\mu\text{M Cu}$]	EC ₅₀ [$\mu\text{M Cu}$]
Cu ²⁺	No damage (0.05-300 μM)	No damage (0.05-300 μM)
Cu ²⁺ + H ₂ O ₂	40% DNA damage @12.5 μM	No damage (0.05-12.5 μM)
Cu ²⁺ + AA	17.74 \pm 0.03	25.61 \pm 0.05
Cu ²⁺ + AA + H ₂ O ₂	4.62 \pm 0.01	2.45 \pm 0.01
	EC ₅₀ FLC [$\mu\text{M Fe}$]	EC ₅₀ [$\mu\text{M Fe}$]
Fe ²⁺	No damage (0.05-300 μM)	No damage (0.05-300 μM)
Fe ²⁺ + H ₂ O ₂	0.46 \pm 0.01	1.04 \pm 0.01
Fe ²⁺ + AA	180.8 \pm 0.3	187.7 \pm 0.4
Fe ²⁺ + AA + H ₂ O ₂	0.68 \pm 0.01	0.76 \pm 0.01

observed with 25 μM FLC and 12.5 μM Cu²⁺ (Figure 4.2B, lane 12), whereas Cu²⁺ at the same concentration without FLC addition does not cause any DNA damage. Since FLC alone does not damage DNA, these results highlight the importance of metal binding for FLC-mediated DNA damage. These plasmid damage assay results indicate that FLC binding to iron or copper significantly increases the metal's ability to generate ROS generation and DNA damage (Table 3.1).

To evaluate whether addition of ascorbic acid changes the effectiveness of FLC in causing DNA damage in the presence of Cu²⁺ or Fe²⁺, 1.25 equiv. of ascorbic acid was added per metal ion. In the Fe²⁺ system, added ascorbate with and without FLC addition results in EC₅₀ values of 187.8 \pm 0.4 μM and 180.8 \pm 0.3 μM , respectively. When Cu²⁺ is reduced to DNA-damaging Cu⁺ by ascorbate addition prior to hydrogen peroxide, DNA damage is observed (Figure 4.2B, lane 5), and the EC₅₀ value under these conditions is 2.45 \pm 0.01 μM .

In general, FLC increases copper and iron's ability to cause DNA damage. The most significant effect is observed when the copper and ascorbate or iron and H₂O₂ are combined

with FLC. FLC halves the EC₅₀ for iron-mediated DNA damage and, in the case of copper, changes the stabilizes the more reactive Cu⁺ resulting in DNA damage.

FLC-Iron-mediated DNA Damage with DFO Treatment. To evaluate whether FLC has similar DNA damaging effects if iron is chelated, one equivalent of the hexadentate chelator deferoxamine (DFO), a siderophore produced by soil bacteria and FDA-approved drug to treat iron overload,^{48,49} was added to the Fe²⁺ solution (prepared with FeSO₄) prior to addition of DNA. DFO has a low dissociation constant with iron ($K_d = 10^{-31}$ M),⁵⁰ so it will completely coordinates Fe²⁺ under the gel conditions. Upon DFO addition, an EC₅₀ of 7.84 μM ± 0.03 is measured for iron-mediated DNA damage in the presence of hydrogen peroxide (Figure 4.13F). For similar DNA damage studies with DFO, constant concentrations of 9 μM each for Fe²⁺ and DFO were chosen because this concentration range close to the EC₅₀ for iron-coordinated DFO in the presence of hydrogen peroxide, allowing both increased and decreased DNA damage to be readily quantified. FLC in various concentrations was added with Fe²⁺/DFO under these conditions at 1/3:1, 1:1, 3:1 and 9:1 ratios of FLC to Fe²⁺/DFO. No change in DNA damage upon addition of FLC relative to the Fe:DFO control lanes is observed (Figure 3.4), indicating that direct FLC-iron coordination is responsible for its enhancement of iron-mediated DNA damage. In addition, these results strengthen the observation that FLC-metal coordination is essential for DNA damage promotion.

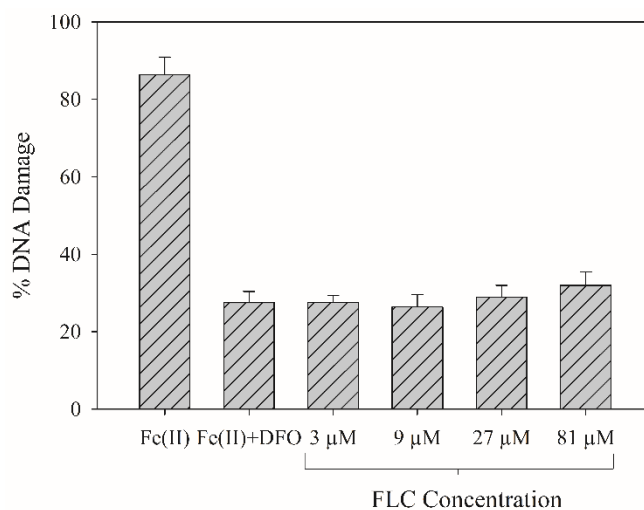


Figure 3.4. Percent DNA damage caused by Fe^{2+} (2 μM) + H_2O_2 and Fe^{2+} (9 μM) + DFO (9 μM) + H_2O_2 with and without FLC addition (3 μM , 9 μM , 27 μM , and 81 μM , respectively).

3.3 Conclusion

Electrochemical studies demonstrate that FLC-metal binding favors Cu^+ and Fe^{2+} over Cu^{2+} and Fe^{3+} , respectively, and mass spectrometry studies indicate FLC-metal coordination ratios of only 2:1. Plasmid DNA damage studies show that FLC causes no DNA damage by itself or in combination with H_2O_2 or ascorbate. However, FLC enhances the ability of copper and iron to cause DNA damage, halving the EC_{50} for iron-mediated DNA damage. These experiments highlight the impact of metals for FLC mediated DNA damage. Research to date has primarily focused on the impact FLC has on the cell membrane of *C. neoformans*, but these studies show that FLC mechanism of action is more complex and could be modulated through the addition of different drugs resulting in drug synergism. Since the FLC resistance of *C. neoformans* is increasing, the use of FLC-metal complexes would be worth exploring to enhance DNA damage to the pathogen and reduce the development of resistant strains.

3.4 Experimental and Methods

Materials. Water was deionized (diH₂O) using a Nano Pure DIAMOND Ultrapure H₂O system (Barnstead International). CuSO₄ and H₂O₂ were purchased from Fisher. 3-(*N*-morpholino)propanesulfonic acid (MOPS), were attained from Sigma Aldrich. 2-(*N*-morpholino)ethanesulfonic acid (MES) was obtained from BDH. FeSO₄ was purchased from Acros. Ascorbic acid, 99% fluconazole, and NaCl were obtained from Alfa Aesar.

Mass spectrometry. Matrix assisted laser desorption/ionization time of flight (MALDI-TOF) mass spectrometry experiments were performed using a Bruker Microflex mass spectrometer with trans-2-[3-(4-*tert*-butylphenyl)-2-methyl-2-propenyldiene (250.34 *m/z*) as the matrix. Samples with 1:1 and 1:4 Cu²⁺: FLC ratios were prepared by combining aqueous solutions of CuSO₄ (100 μL; 300 μM) and fluconazole (100 μL; 300 or 1200 μM, respectively). Samples with 1:1 and 1:6 Fe²⁺: FLC ratios were made by combining aqueous solutions of FeSO₄ (100 μL; 300 μM) and fluconazole (100 μL; 300 or 1800 μM, respectively).

Electrochemical studies of FLC and FLC-metal complexes. Cyclic voltammetry (CV) was conducted with a CH Electrochemical Analyzer (CH Instruments, Inc.) at a sweep rate of 100 mV/s using a glassy carbon working electrode, a Pt counter electrode, and a Ag/AgCl (+0.197 V vs. NHE).⁵¹ All experiments were externally referenced to potassium ferricyanide (0.361 V vs. NHE).⁵¹ Studies were conducted in degassed MOPS buffer (10 mM, pH 7.0) for FLC and copper studies or MES buffer (10 mM, pH 6.0) for iron studies, with KNO₃ (100 mM) as a supporting electrolyte. For iron binding studies, a solution of 1:2 iron-FLC ratio was made by adding aqueous solutions of FeSO₄ (3 mL; 900

μM) and FLC (3 mL; 1800 μM), then diluting with the MES buffer (3 mL; 30 mM). For the copper study, a 1:2 solution was made by adding CuSO_4 (3 mL; 300 μM) to FLC (3 mL; 900 μM), then diluting with the MOPS buffer (3 mL; 30 mM). All samples were deaerated for 10 minutes with N_2 before each experiment. Samples were cycled between -0.6 and 1.0 V for copper and -1.0 and 1.0 V for iron complexes.

Plasmid DNA transfection, amplification, and purification. Plasmid DNA (pBSSK) was purified from DH1 *E. coli* competent cells using a Zyppy™ Plasmid Miniprep Kit (400 count, Zymo Research). Tris-EDTA buffer (pH 8.01) was used to elude the plasmid from the spin columns. Plasmid was dialyzed against 130 mM NaCl for 24 hours at 4°C to ensure all Tris-EDTA buffer and metal contaminants were removed, and plasmid concentration was determined by UV-vis spectroscopy at a wavelength of 260 nm. Absorbance ratios of $A_{250}/A_{260} \geq 0.95$ and $A_{260}/A_{280} \geq 1.8$ were determined for DNA used in all experiments. Plasmid purity was determined through digestion of plasmid (0.1 pmol) with Sac I and KpnI in a mixture of NEB buffer and BSA (bovine serum albumin) at 37°C for 90 minutes. Digested plasmids were compared to an undigested plasmid sample and a 1 kb molecular weight marker using gel electrophoresis.

DNA damage gel electrophoresis experiments. Deionized water, MOPS buffer (10 mM, pH 7.0), NaCl (130 mM), ethanol (100% metal free, 10 mM), as well as the indicated concentrations of $\text{CuSO}_4 \cdot 5\text{H}_2\text{O}$, AA (7.5 μM , to reduce Cu^{2+} to Cu^+), and FLC were combined in an acid-washed (1 M HCl for ~ 1 h) microcentrifuge tube and allowed to stand for 5 min at room temperature. Plasmid (pBSSK, 0.1 pmol in 130 mmol NaCl) was then added to the reaction mixture and allowed to stand for 5 min at room temperature. H_2O_2

(50 μM) was added and allowed to react at room temperature for 30 min. EDTA (50 μM) was added after 30 min to quench the reaction. For the Fe^{2+} DNA damage experiments, the indicated $\text{FeSO}_4 \cdot 7\text{H}_2\text{O}$ concentrations and MES (10 mM, pH 6.0) were used. All concentrations are final concentrations in a 10 μM volume. Samples were loaded into a 1% agarose gel in a TAE running buffer (50 \times); damaged and undamaged plasmid was separated by electrophoresis (140 V for 60 min). Gels were stained using ethidium bromide and imaged using UV light. The amounts of nicked (damaged) and circular (undamaged) were analyzed using UViProMW (Jencons Scientific Inc., 2007). Intensity of circular plasmid was multiplied by 1.24, due to the lower binding affinity of ethidium bromide to supercoiled plasmid.^{52,53} Intensities of the nicked and supercoiled bands were normalized for each lane so that % nicked + % supercoiled = 100%. All percentages were corrected for residual nicked DNA prior to calculation. Results were obtained in triplicate for all experiments, and standard deviations are represented as error bars. The plots of percent DNA damage versus log concentration of copper or iron were fit to a variable-slope sigmoidal dose-response curve using SigmaPlot (v. 11.0, Systat Software, Inc.).

EC₅₀ Determination. Plots of percent DNA damage versus log concentration of FLC or the respective metal were fit to a variable slope sigmoidal dose-response curve using SigmaPlot, version 11 (Systat Software, Inc.). EC_{50} value errors were calculated from error propagation of the gel electrophoresis measurements. Statistical significance was determined by calculating p values at 95% confidence ($p < 0.05$ indicates significance) as described by Perkowski *et al.*,⁵⁴ calculated values can be found in Tables 3.4-3.19.

3.5. Supporting Information

Table 3.2. MALDI mass spectrometry data for FLC with Fe²⁺ and Cu²⁺ prepared in H₂O.

Metal	<i>m/z</i> (Da)	Metal:Ligand Ratio
Copper	693.1	1:2
Iron	666.7	1:2

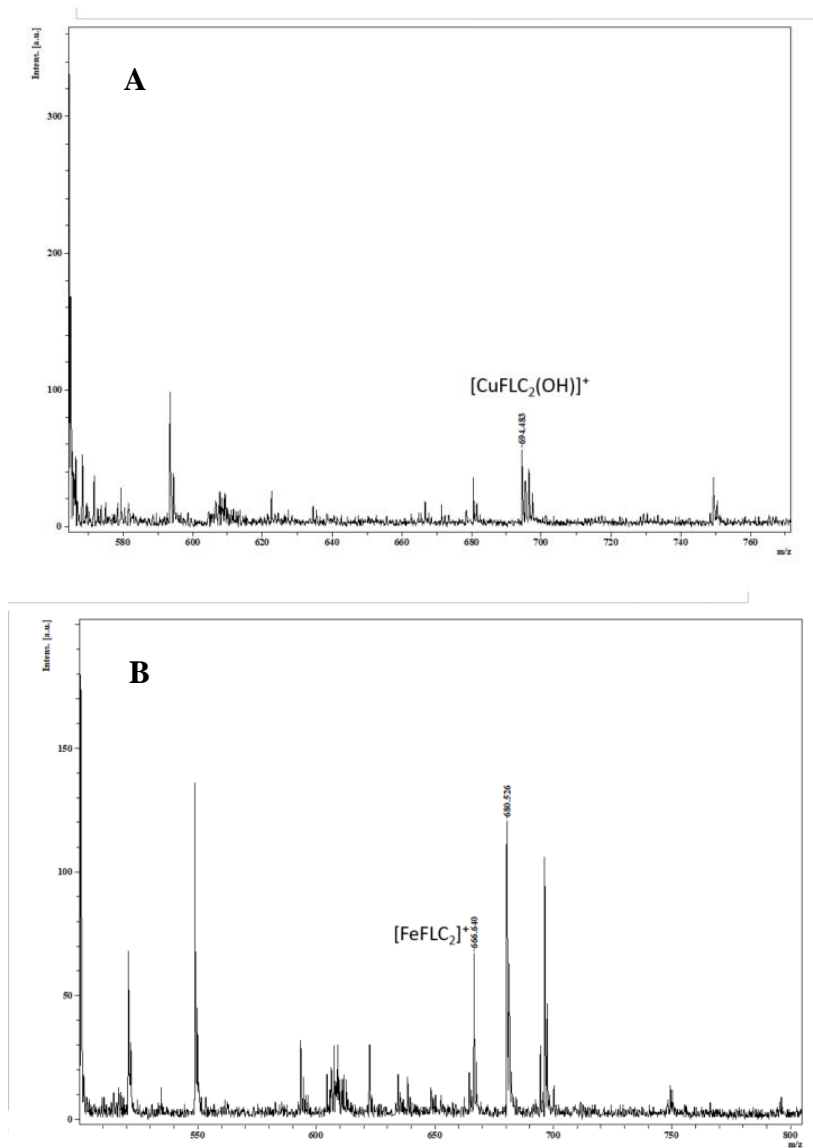
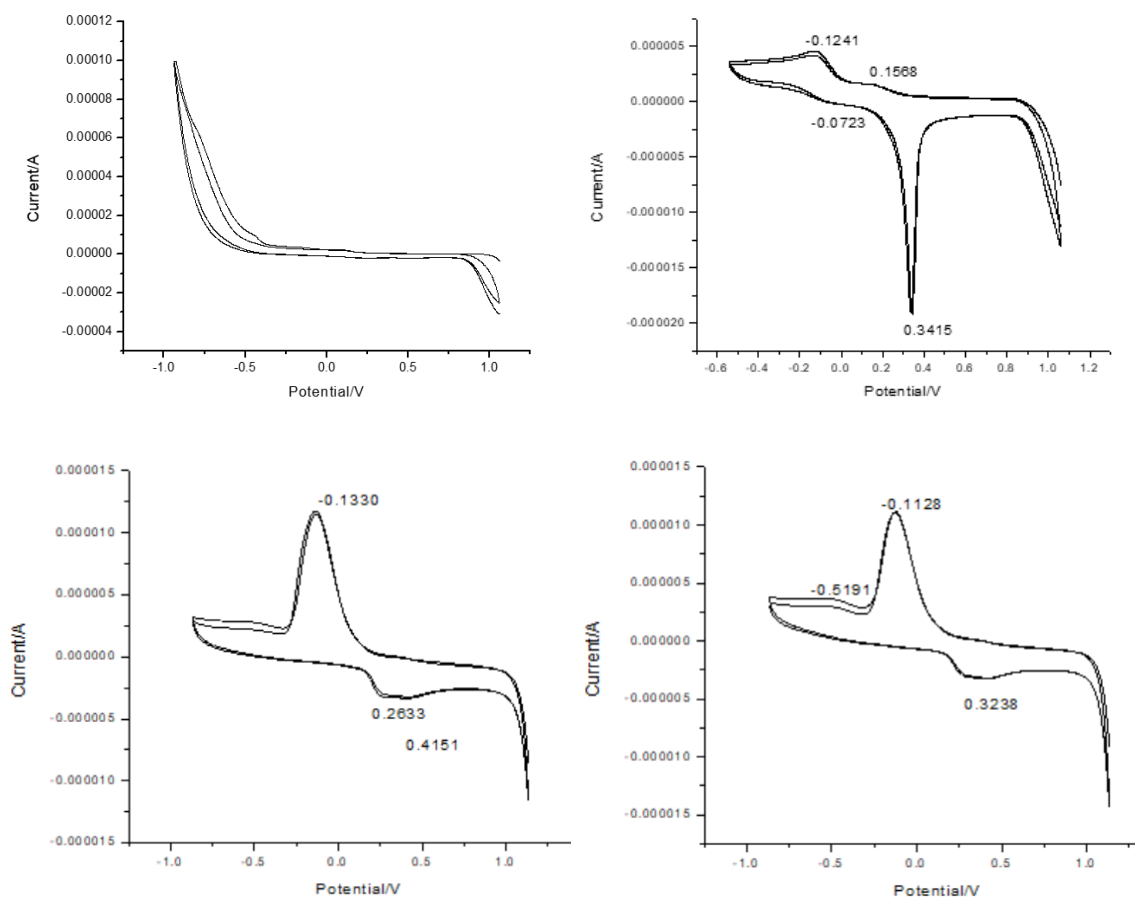


Figure 3.5. MALDI-TOF spectra of the identified A) [Cu(FLC)₂(OH)]⁺ and B) [Fe(FLC)₂]⁺ complexes.

Table 3.3. CV data for FLC with Fe²⁺ and Cu²⁺.

Metal	E_{p_a} (mV)	E_{p_c} (mV)	ΔE (mV)	$E_{1/2}$ (mV)
FLC	-	-	-	-
Copper	-83 ^a , 121 ^b	-796 ^a , -100 ^b	713 ^a , 212 ^b	-440 ^a , 11 ^b
Copper: FLC (1:2)	-73 ^a , 342 ^b	-124 ^a , 157 ^b	51 ^a , 499 ^b	-99 ^a , 250 ^b
Iron	263	-133	396	65
Iron: FLC (1:2)	324	-128	452	98

^a Cu⁺⁰ potential. ^b Cu^{2+/+} potential.**Figure 3.6.** Cyclic voltammograms for A) CuSO₄ (100 μM), B) 1:2 Cu²⁺:FLC (100 μM:200 μM) in MOPS buffer (10 mM, pH 7.0), C) FeSO₄ (300 μM), and D) 1:2 Fe²⁺:FLC (300 μM:600 μM) in MES buffer (10 mM, pH 6.0). All contain KNO₃ (10 mM) as a supporting electrolyte. All samples were cycled at a scan rate of 100 mV/s.

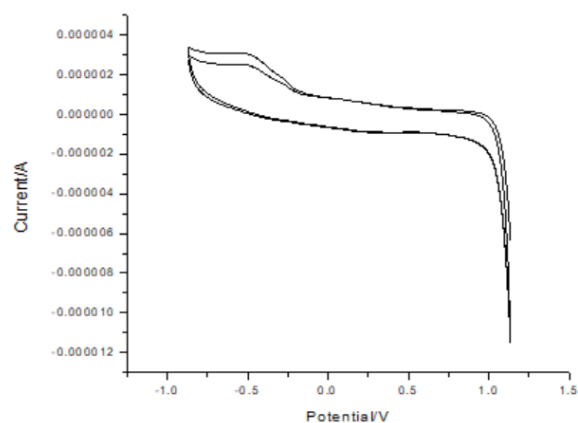


Figure 3.7: Cyclic voltammograms for FLC (300 μM) in MES buffer (10 mM, pH 6.0) with KNO_3 (10 mM) as a supporting electrolyte. The solution was cycled at a scan rate of 100 mV/s.

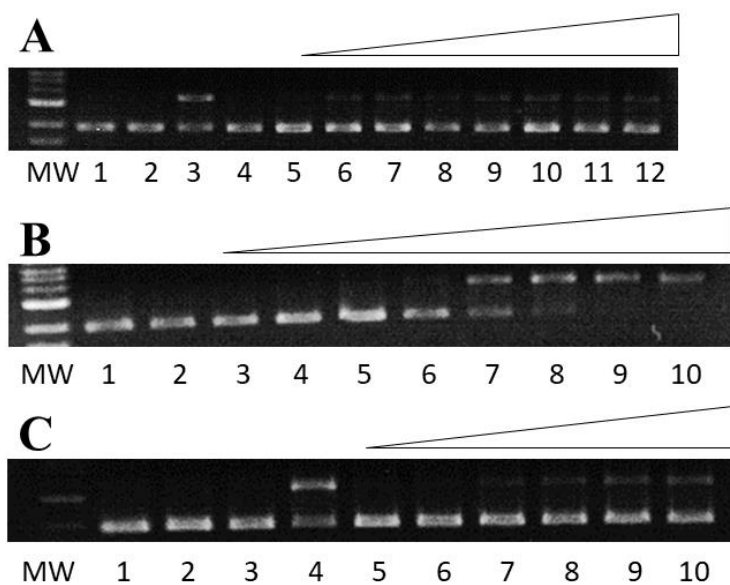


Figure 3.8. Gel image of DNA damage by iron with and without H_2O_2 and FLC. For all gel images, MW: 1 kb molecular weight marker; lane 1: plasmid DNA (p); lane 2: p + H_2O_2 . (50 μM); A) lane 3: p + FeSO_4 (2 μM) + H_2O_2 ; lanes 4-12: p + FeSO_4 (0.05, 0.5, 5, 25, 37.5, 50, 75, 100, and 150 μM , respectively); B) lanes 3-10: p + H_2O_2 + FeSO_4 , (0.005, 0.5, 0.25, 0.5, 1, 2, 5, and 12.5 μM , respectively); C) lane 3: p + FLC (200 μM); lane 4: p + FeSO_4 (2 μM) + H_2O_2 ; lanes 5-10: p + FLC (0.1, 1, 10, 50, 100, and 200 μM , respectively) + FeSO_4 (0.05, 0.5, 5, 25, 50, and 100 μM , respectively).

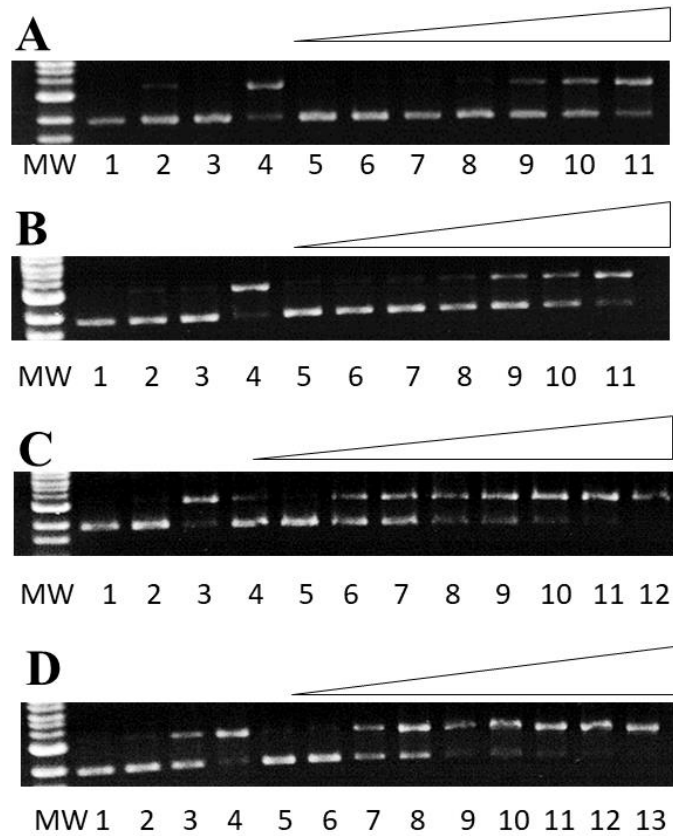


Figure 3.9. Gel image of DNA damage by iron with and without H_2O_2 and FLC and ascorbate. For all gel images, MW: 1 kb molecular weight marker; lane 1: plasmid DNA (p); lane 2: p + H_2O_2 . (50 μM); A) lane 3: p + ascorbate (375 μM); lane 4: p + FeSO_4 (2 μM) + H_2O_2 ; lane 5-11: p + FeSO_4 (2, 10, 25, 50, 100, 150, 500 μM , respectively) + ascorbate (2.5, 12.5, 31.25, 62.5, 125, 187.5, and 375 μM , respectively); B) lane 3: p + FLC (600 μM); lane 4: p + H_2O_2 + FeSO_4 (2 μM); lanes 5-11: p + FeSO_4 (2, 10, 25, 50, 100, 150, and 300 μM , respectively) + ascorbate (3.5, 12.5, 31.25, 62.5, 125, 187.5, and 375 μM , respectively) + FLC (4, 20, 50, 100, 200, 300, and 600 μM , respectively); C) lane 3: p + H_2O_2 + FeSO_4 (2 μM); lanes 4-12: p + FeSO_4 (0.005, 0.5, 0.25, 0.5, 0.75, 1, 1.5, 2 and 5 μM , respectively) + ascorbate (0.00625, 0.0625, 0.3125, 0.625, 0.9375, 1.25, 1.875, 2.5 and 6.25 μM , respectively); D) lane 3: p + H_2O_2 + FLC (20 μM) + ascorbate (12.5 μM); lane 4: p + H_2O_2 + FeSO_4 (2 μM); lanes 5-13: p + H_2O_2 + FeSO_4 (0.005, 0.5, 0.25, 0.5, 0.75, 1, 1.5, 2 and 5 μM , respectively) + FLC (0.01, 0.1, 0.5, 1, 1.5, 2, 3, 4, and 10 μM , respectively) + ascorbate (0.00625, 0.0625, 0.3125, 0.625, 0.9375, 1.25, 1.875, 2.5 and 6.25 μM , respectively).

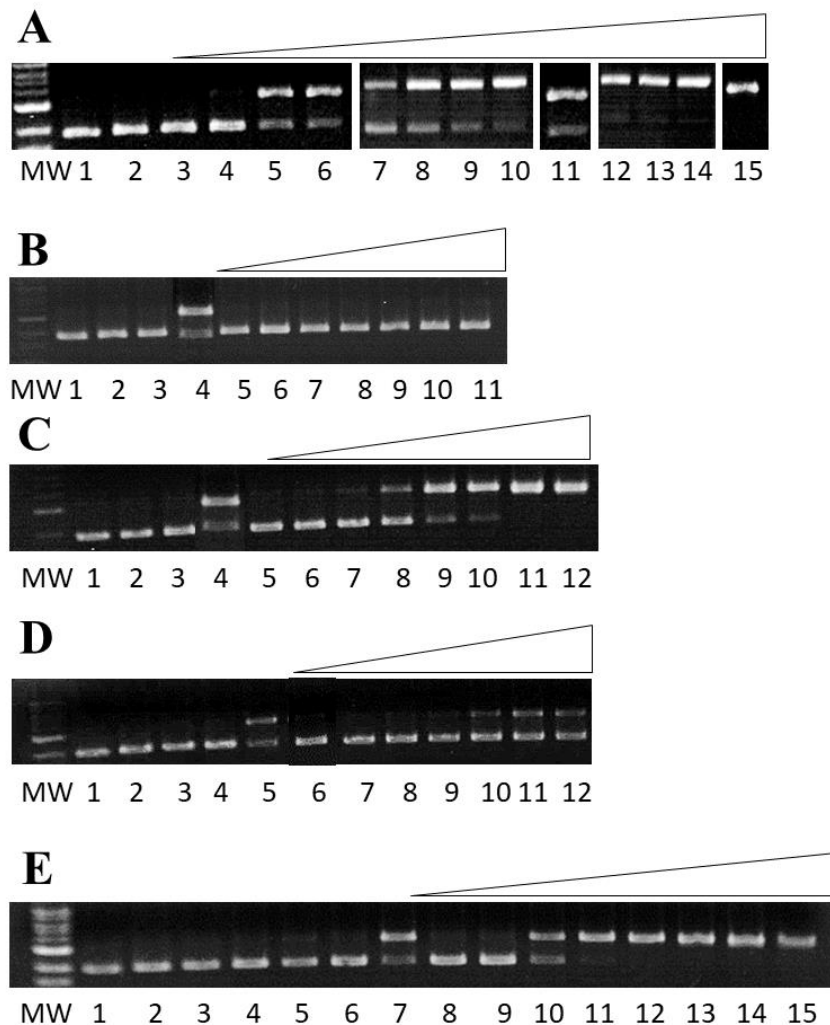


Figure 3.10. Gel image of DNA damage by copper FLC, H₂O₂ and, where indicated, ascorbate. For all gel images, MW: 1 kb molecular weight marker; lane 1: plasmid DNA (p); lane 2: p + H₂O₂ (50 μM); A) lanes 3-15: p + H₂O₂ + CuSO₄ (0.05, 0.5, 2, 3, 4, 5, 6, 7, 8 and 12.5 μM, respectively) + ascorbate (0.0625, 0.625, 2.5, 3.75, 5, 6.25, 7.5, 8.75, 10 and 15.625 μM, respectively); B) lane 3: p + FLC (600 μM); lane 4: p + H₂O₂ + CuSO₄ (6 μM) + ascorbate (7.5 μM); lane 5: p + CuSO₄ (300 μM); lanes 6-11: p + FLC (0.1, 1, 10, 100, 300, and 600 μM, respectively) + CuSO₄ (0.05, 0.5, 5, 50, 150, and 300 μM, respectively); C) lane 3: p + FLC (600 μM); lane 4: p + H₂O₂ + CuSO₄ (6 μM) + ascorbate (7.5 μM); lanes 5-12: p + CuSO₄ (0.05, 0.5, 5, 12.5, 25, 50, 150, and 300 μM, respectively) + ascorbate (0.0625, 0.625, 6.25, 15.625, 31.25, 62.5, 187.5, and 375 μM, respectively) + FLC (0.1, 1, 10, 25, 50, 100, 300, and 600 μM, respectively); D) lane 3: p + H₂O₂ + FLC (25 μM); lane 4: p + FLC (25 μM); lane 5: p + H₂O₂ + CuSO₄ (6 μM) + ascorbate (7.5 μM); lane 6: p + H₂O₂ + CuSO₄ (12.5 μM); lanes 7-12: p + H₂O₂ + FLC (0.1, 1, 5, 10, 18, and 25 μM, respectively) + CuSO₄ (0.05, 0.5, 2.5, 5, 9, and 12.5 μM, respectively); E) lane 3: p + H₂O₂ + FLC (600 μM); lane 4: p + FLC (600 μM); lane 5: p + H₂O₂ + FLC (600 μM) + ascorbate (375 μM); lane 6: p + FLC (600 μM) + ascorbate (375 μM); lane 7: p + H₂O₂ + CuSO₄ (6 μM) + ascorbate (7.5 μM); lanes 8-15: p + H₂O₂ + CuSO₄ (0.05, 0.5, 5, 12.5, 25, 50, 150, and 300 μM, respectively) + ascorbate (0.0625, 0.625, 6.25, 15.625, 31.25, 62.5, 87.5, and 375 μM, respectively) + FLC (0.1, 1, 10, 25, 50, 100, 300, and 600 μM, respectively).

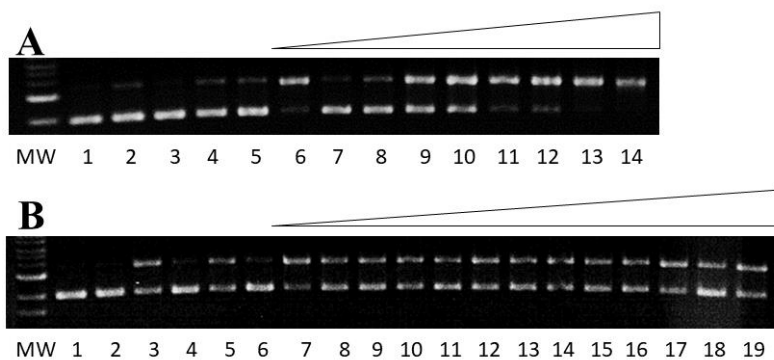


Figure 3.11. Gel image of DNA damage by copper or iron FLC, H₂O₂, and DFO. For all gel images, MW: 1 kb molecular weight marker; lane 1: plasmid DNA (p); lane 2: p + H₂O₂. (50 μM); A) lane 3: p + H₂O₂ + DFO (50 μM); lane 4: p + DFO (50 μM); lane 5: p + FeSO₄ (50 μM) + DFO (50 μM); lane 6: p + H₂O₂ + FeSO₄ (2 μM); lanes 7-8: p + H₂O₂ + FeSO₄ (0.1, 1, 2, 5, 7.5, 10, 25, and 50 μM, respectively) + DFO (0.1, 1, 2, 5, 7.5, 10, 25, and 50 μM, respectively, respectively); B) lane 3: p + FeSO₄ (9 μM); lane 4: p + H₂O₂ + FLC (9 μM); lane 5: p + H₂O₂ + FeSO₄ (9 μM) + DFO (9 μM); lane 6: p + FeSO₄ (9 μM) + DFO (9 μM); lane 7: p + H₂O₂ + FeSO₄ (2 μM); lanes 8-10: p + H₂O₂ + FeSO₄ (9 μM) + DFO (9 μM) + FLC (3 μM); lanes 11-13: p + H₂O₂ + FeSO₄ (9 μM) + DFO (9 μM) + FLC (9 μM); lanes 14-16: p + H₂O₂ + FeSO₄ (9 μM) + DFO (9 μM) + FLC (27 μM); lanes 17-19: p + H₂O₂ + FeSO₄ (9 μM), + DFO (9 μM) + FLC (81 μM).

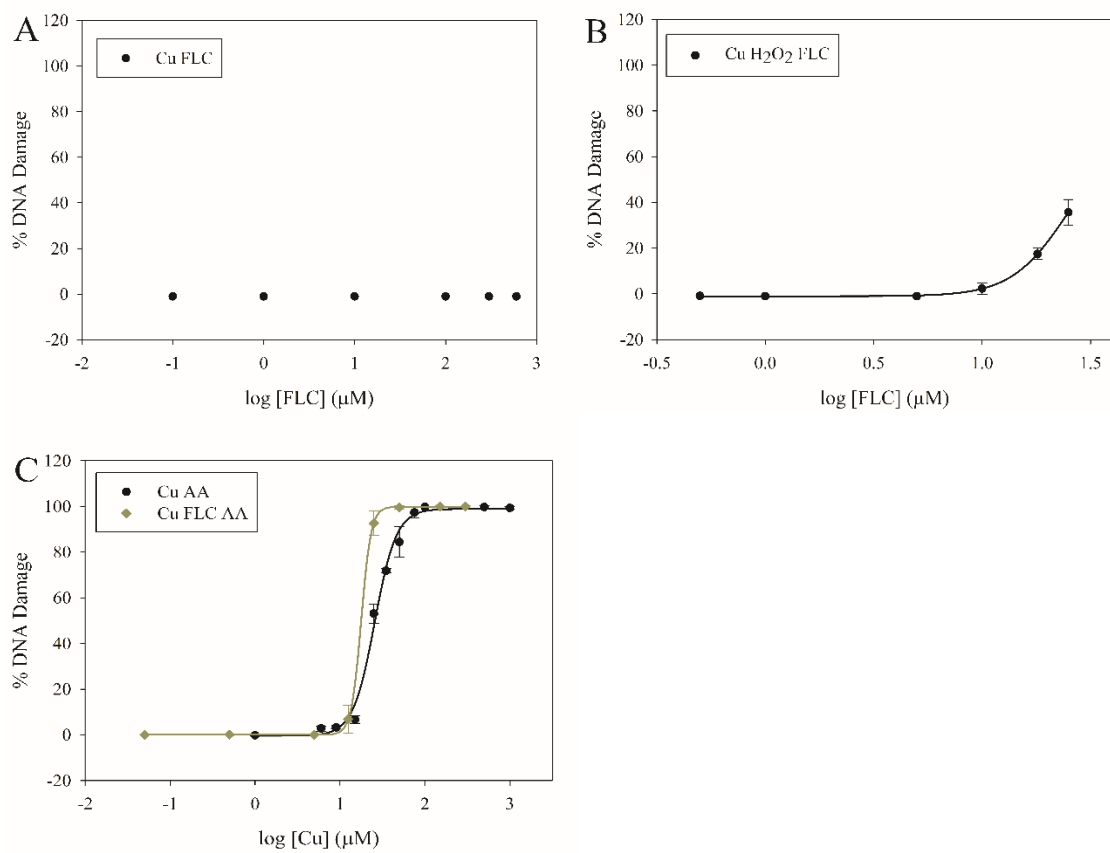


Figure 3.12. Dose-response curves for DNA damage by A) Cu²⁺ and FLC, B) Cu²⁺, FLC, and H₂O₂, and C) Cu²⁺ and ascorbate with and without FLC.

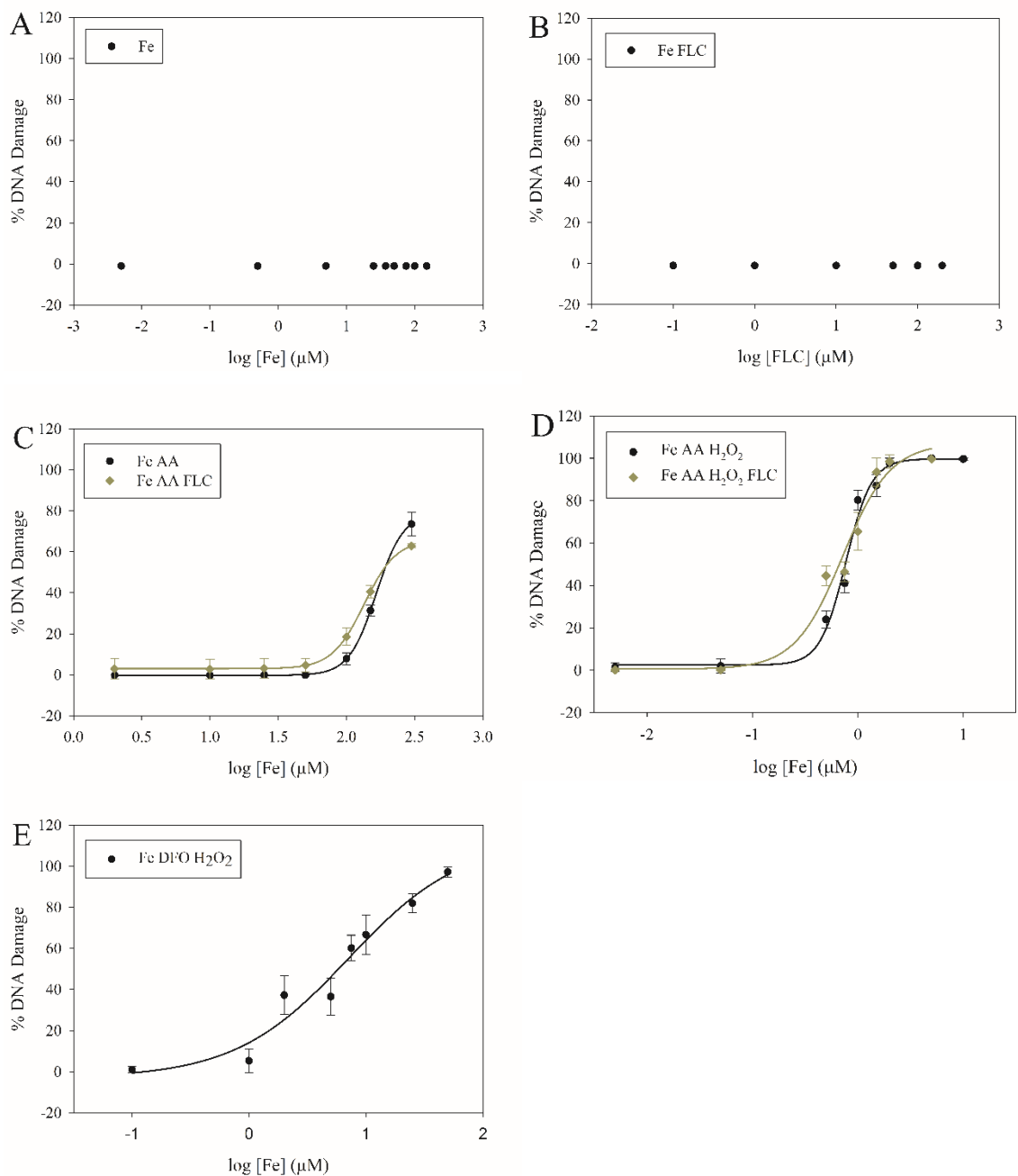


Figure 3.13. Dose-response curves for DNA damage by A) Fe^{2+} ; B) Fe^{2+} and FLC; C) Fe^{2+} and ascorbate (AA) with and without FLC; D) Fe^{2+} , ascorbate, and H_2O_2 with and without FLC; and E) Fe^{2+} , DFO, and H_2O_2 .

Table 3.4. Gel electrophoresis results for FLC DNA damage assays with Cu²⁺ and H₂O₂.^a

Gel lane	[FLC], μM	% Supercoiled	% Nicked	% Damage	<i>p</i> Value
1: plasmid DNA (p)	0	99.87 ± 0.19	0.13	-	-
2: p + H ₂ O ₂ (50 μM)	0	100 ± 0	0	-	-
3: p + FLC + H ₂ O ₂	25	100 ± 0	0	-	-
4: p + FLC	25	100 ± 0	0	-	-
5: p + Cu ²⁺ (6 μM) + AA (7.5 μM) + H ₂ O ₂	0	4.42 ± 0.05	95.58	-	-
6: p + Cu ²⁺ (12.5 μM) + H ₂ O ₂	0	100 ± 0	0	-1 ± 0	< 0.001
7: p + Cu ²⁺ (0.05 μM) + FLC + H ₂ O ₂	0.5	99.91 ± 0.12	0.09	-0.91 ± 0	< 0.001
8: p + Cu ²⁺ (0.5 μM) + FLC + H ₂ O ₂	1	100 ± 0	0	-1 ± 0	< 0.001
9: p + Cu ²⁺ (2.5 μM) + FLC + H ₂ O ₂	5	100 ± 0	0	-1 ± 0	< 0.001
10: p + Cu ²⁺ (5 μM) + FLC + H ₂ O ₂	10	96.68 ± 2.54	3.32	2.32 ± 2.54	0.254
11: p + Cu ²⁺ (9 μM) + FLC + H ₂ O ₂	18	81.57 ± 2.49	18.43	17.43 ± 2.49	0.007
12: p + Cu ²⁺ (12.5 μM) + FLC + H ₂ O ₂	25	63.33 ± 5.6	36.67	35.67 ± 5.6	0.008

^aData are reported as the average of three trials with calculated standard deviations shown.

Table 3.5. Gel electrophoresis results for FLC DNA damage assays with Cu²⁺, ascorbate (AA) and H₂O₂.^a

Gel lane	[FLC], μM	% Supercoiled	% Nicked	% Damage	<i>p</i> Value
1: plasmid DNA (p)	0	100 ± 0	0	-	-
2: p + H ₂ O ₂ (50 μM)	0	100 ± 0	0	-	-
3: p + FLC + H ₂ O ₂	600	100 ± 0	0	-	-
4: p + FLC	600	100 ± 0	0	-	-
5: p + Cu ²⁺ (6 μM) + AA (7.5 μM) + H ₂ O ₂	0	18.40 ± 3.29	81.60	-	-
6: p + Cu ²⁺ (0.05 μM) + AA (0.0625 μM) + FLC + H ₂ O ₂	0.1	99.97 ± 0.03	0.03	-0.97 ± 0.03	< 0.001
7: p + Cu ²⁺ (0.5 μM) + AA (0.625 μM) + FLC + H ₂ O ₂	1	100 ± 0	0	-1 ± 0	< 0.001
8: p + Cu ²⁺ (5 μM) + AA (6.25 μM) + FLC + H ₂ O ₂	10	71.44 ± 3.11	28.56	27.56 ± 3.11	0.004
9: p + Cu ²⁺ (12.5 μM) + AA (15.625 μM) + FLC + H ₂ O ₂	25	0.12 ± 0.17	99.88	98.88 ± 0.17	< 0.001
10: p + Cu ²⁺ (25 μM) + AA (31.25 μM) + FLC + H ₂ O ₂	50	0 ± 0	100	99.00 ± 0	< 0.001
11: p + Cu ²⁺ (50 μM) + AA (62.5 μM) + FLC + H ₂ O ₂	100	0.24 ± 0.34	99.76	98.76 ± 0.34	< 0.001
12: p + Cu ²⁺ (150 μM) + AA (187.5 μM) + FLC + H ₂ O ₂	300	0.65 ± 0.92	99.35	98.35 ± 0.92	< 0.001
13: p + Cu ²⁺ (300 μM) + AA (375 μM) + FLC + H ₂ O ₂	600	0 ± 0	100.00	99.00 ± 0	< 0.001

^aData are reported as the average of three trials with calculated standard deviations shown.

Table 3.6. Gel electrophoresis results for FLC DNA damage assays with Cu²⁺ and ascorbate (AA).^a

Gel lane	[FLC], μM	% Supercoiled	% Nicked	% Damage	<i>p</i> Value
1: plasmid DNA (p)	0	100 ± 0	0.00	-	-
2: p + H ₂ O ₂ (50 μM)	0	100 ± 0	0.00	-	-
3: p + FLC + H ₂ O ₂	600	99.97 ± 0.03	0.03	-	-
4: p + Cu ²⁺ (6 μM) + AA (7.5 μM)	0	18.40 ± 3.29	81.60	-	-
5: p + Cu ²⁺ (0.05 μM) + AA (0.0625 μM) + FLC	0.1	100 ± 0	0.00	-1 ± 0	< 0.001
6: p + Cu ²⁺ (0.5 μM) + AA (0.625 μM) + FLC	1	99.93 ± 0.13	0.07	-0.97 ± 0.13	0.006
7: p + Cu ²⁺ (5 μM) + AA (6.25 μM) + FLC	10	100 ± 0	0.00	-1 ± 0	< 0.001
8: p + Cu ²⁺ (12.5 μM) + AA (15.625 μM) + FLC	25	93.10 ± 5.99	6.90	5.90 ± 5.99	0.230
9: p + Cu ²⁺ (25 μM) + AA (31.25 μM) + FLC	50	7.36 ± 5.29	92.64	91.64 ± 5.29	0.001
10: p + Cu ²⁺ (75 μM) + AA (91.75 μM) + FLC	150	0.40 ± 0.70	99.60	98.60 ± 0.70	< 0.001
11: p + Cu ²⁺ (150 μM) + AA (187.5 μM) + FLC	300	0 ± 0	100.00	99.00 ± 0	< 0.001
12: p + Cu ²⁺ (300 μM) + AA (375 μM) + FLC	600	0 ± 0	100.00	99.00 ± 0	< 0.001

^aData are reported as the average of three trials with calculated standard deviations shown.

Table 3.7. Gel electrophoresis results for FLC DNA damage assays with Cu²⁺.^a

Gel lane	[FLC] μM	% Supercoiled	% Nicked	% Damage	<i>p</i> Value
1: plasmid DNA (p)	0	100 ± 0	0	-	-
2: p + H ₂ O ₂ (50 μM)	0	100 ± 0	0	-	-
3: p + FLC	600	100 ± 0	0	-	-
4: p + Cu ²⁺ (6 μM) + AA (7.5 μM) + H ₂ O ₂	0	18.40 ± 3.29	81.60	-	-
5: p + Cu ²⁺ (300 μM)	0	100 ± 0	0	-1 ± 0	< 0.001
6: p + Cu ²⁺ (0.05 μM) + FLC	0.1	100 ± 0	0	-1 ± 0	< 0.001
7: p + Cu ²⁺ (0.5 μM) + FLC	1	100 ± 0	0	-1 ± 0	< 0.001
8: p + Cu ²⁺ (5 μM) + FLC	10	100 ± 0	0	-1 ± 0	< 0.001
9: p + Cu ²⁺ (50 μM) + FLC	100	100 ± 0	0	-1 ± 0	< 0.001
10: p + Cu ²⁺ (150 μM) + FLC	300	100 ± 0	0	-1 ± 0	< 0.001
11: p + Cu ²⁺ (300 μM) + FLC	600	100 ± 0	0	-1 ± 0	< 0.001

^aData are reported as the average of three trials with calculated standard deviations shown.

Table 3.8. Gel electrophoresis results for CuSO₄ DNA damage assays with ascorbate (AA).^a

Gel lane	[Cu ²⁺], μM	% Supercoiled	% Nicked	% Damage	p Value
1: plasmid DNA (p)	0	99.94 ± 0.09	0.06	–	–
2: p + H ₂ O ₂	0	99.85 ± 0.27	0.15	–	–
3: p + Cu ²⁺ + AA (7.5 μM) + H ₂ O ₂	6	12.44 ± 3.47	87.56	-	–
4: p + Cu ²⁺ + AA (1.25 μM)	1	100 ± 0	0	-1.15 ± 0.27	< 0.001
5: p + Cu ²⁺ + AA (7.5 μM)	6	97.03 ± 1.18	2.97	1.82 ± 1.09	0.102
6: p + Cu ²⁺ + AA (11.25 μM)	9	96.57 ± 0.57	3.43	2.28 ± 0.70	0.030
7: p + Cu ²⁺ + AA (18.75 μM)	15	93.10 ± 1.45	6.90	5.74 ± 1.63	0.026
8: p + Cu ²⁺ + AA (31.25 μM)	25	46.72 ± 3.87	53.28	52.13 ± 4.14	0.002
9: p + Cu ²⁺ + AA (43.75 μM)	35	28.03 ± 0.62	71.97	70.82 ± 0.86	< 0.001
10: p + Cu ²⁺ + AA (62.5 μM)	50	15.39 ± 7.00	84.61	83.45 ± 6.82	0.002
11: p + Cu ²⁺ + AA (93.75 μM)	75	2.50 ± 2.71	97.50	96.34 ± 2.50	< 0.001
12: p + Cu ²⁺ + AA (125 μM)	100	0.00 ± 0	100.00	98.85 ± 0.27	< 0.001
13: p + Cu ²⁺ + AA (625 μM)	500	0.14 ± 0.24	99.86	98.71 ± 0.51	< 0.001
14: p + Cu ²⁺ + AA (1250 μM)	1000	0.49 ± 0.69	99.51	98.36 ± 0.64	< 0.001

^aData are reported as the average of three trials with calculated standard deviations shown.**Table 3.9.** Gel electrophoresis results for DNA damage assays with Cu²⁺, ascorbate (AA) and H₂O₂.^a

Gel lane	[Cu ²⁺], μM	% Supercoiled	% Nicked	% Damage	p Value
1: plasmid DNA (p)	0	100 ± 0	0	-	-
2: p + H ₂ O ₂ (50 μM)	0	100 ± 0	0	-	-
3: p + Cu ²⁺ + AA (0.0625 μM) + H ₂ O ₂	0.05	100 ± 0	0 ± 0	0 ± 0	
4: p + Cu ²⁺ + AA (0.625 μM) + H ₂ O ₂	0.5	100 ± 0	0 ± 0	0 ± 0	
5: p + Cu ²⁺ + AA (2.5 μM) + H ₂ O ₂	2	60.86 ± 2.73	39.14	38.14 ± 2.73	0.002
6: p + Cu ²⁺ + AA (3.75 μM) + H ₂ O ₂	3	35.39 ± 7.79	64.61	63.61 ± 7.79	0.005
7: p + Cu ²⁺ + AA (5 μM) + H ₂ O ₂	4	22.99 ± 5.44	77.01	76.01 ± 5.44	0.002
8: p + Cu ²⁺ + AA (6.25 μM) + H ₂ O ₂	5	9.86 ± 3.96	90.14	89.14 ± 3.96	< 0.001
9: p + Cu ²⁺ + AA (7.5 μM) + H ₂ O ₂	6	7.42 ± 2.17	92.58	92.58 ± 2.17	< 0.001
10: p + Cu ²⁺ + AA (8.75 μM) + H ₂ O ₂	7	2.28 ± 3.52	97.72	96.72 ± 3.52	< 0.001
11: p + Cu ²⁺ + AA (10 μM) + H ₂ O ₂	8	0.00 ± 0	100.00	99.0 ± 0	< 0.001
12: p + Cu ²⁺ + AA (15.625 μM) + H ₂ O ₂	12.5	0.00 ± 0	100.00	100 ± 0	< 0.001

^aData are reported as the average of three trials with calculated standard deviations shown.

Table 3.10. Gel electrophoresis results for FLC DNA damage assays with Fe²⁺, and H₂O₂.^a

Gel lane	[FLC], μM	% Supercoiled	% Nicked	% Damage	<i>p</i> Value
1: plasmid DNA (p)	0	100 ± 0	0	-	-
2: p + H ₂ O ₂ (50 μM)	0	100 ± 0	0	-	-
3: p + FLC + H ₂ O ₂	50	100 ± 0	0	-	-
4: p + FLC	50	100 ± 0	0	-	-
5: p + Fe ²⁺ (2 μM) + H ₂ O ₂	0	6.35 ± 5.53	93.65	-	-
6: p + Fe ²⁺ (0.005 μM) + FLC + H ₂ O ₂	0.01	100 ± 0	0	-1 ± 0	< 0.001
7: p + Fe ²⁺ (0.05 μM) + FLC + H ₂ O ₂	0.1	90.20 ± 0.10	9.8	8.8 ± 0.01	< 0.001
8: p + Fe ²⁺ (0.25 μM) + FLC + H ₂ O ₂	0.5	60.46 ± 0.58	39.54	38.54 ± 0.58	< 0.001
9: p + Fe ²⁺ (0.5 μM) + FLC + H ₂ O ₂	1	61.65 ± 1.22	38.35	37.35 ± 1.22	< 0.001
10: p + Fe ²⁺ (1 μM) + FLC + H ₂ O ₂	2	11.95 ± 5.69	88.05	87.05 ± 5.69	0.001
11: p + Fe ²⁺ (2.5 μM) + FLC + H ₂ O ₂	5	3.03 ± 4.28	96.97	95.97 ± 4.28	< 0.001
12: p + Fe ²⁺ (5 μM) + FLC + H ₂ O ₂	10	3.79 ± 0.76	96.21	95.21 ± 0.76	< 0.001
13: p + Fe ²⁺ (25 μM) + FLC + H ₂ O ₂	50	4.43 ± 2.02	95.57	94.57 ± 2.02	< 0.001

^aData are reported as the average of three trials with calculated standard deviations shown.**Table 3.11.** Gel electrophoresis results for Fe²⁺ DNA damage assays with H₂O₂.^a

Gel lane	[Fe ²⁺], μM	% Supercoiled	% Nicked	% Damage	<i>p</i> Value
1: plasmid DNA (p)	0	100 ± 0	0	-	-
2: p + H ₂ O ₂ (50 μM)	0	100 ± 0	0	-	-
3: p + Fe ²⁺ + H ₂ O ₂	0.005	100 ± 0	0	-1 ± 0	< 0.001
4: p + Fe ²⁺ + H ₂ O ₂	0.05	100 ± 0	0	-1 ± 0	< 0.001
5: p + Fe ²⁺ + H ₂ O ₂	0.25	100 ± 0	0	-1 ± 0	< 0.001
6: p + Fe ²⁺ + H ₂ O ₂	0.5	100 ± 0	0	-1 ± 0	< 0.001
7: p + Fe ²⁺ + H ₂ O ₂	1	53.49 ± 5.0	46.51	45.51 ± 5.0	0.004
8: p + Fe ²⁺ + H ₂ O ₂	2	9.51 ± 5.88	90.49	89.49 ± 5.88	0.001
9: p + Fe ²⁺ + H ₂ O ₂	5	0.73 ± 1.03	99.27	98.27 ± 1.03	< 0.001
10: p + Fe ²⁺ + H ₂ O ₂	12.5	1.51 ± 2.14	98.49	97.49 ± 2.14	< 0.001

^aData are reported as the average of three trials with calculated standard deviations shown.

Table 3.12. Gel electrophoresis results for FLC DNA damage assays with Fe²⁺.^a

Gel lane	[FLC], μM	% Supercoiled	% Nicked	% Damage	<i>p</i> Value
1: plasmid DNA (p)	0	100 ± 0	0	-	-
2: p + H ₂ O ₂ (50 μM)	0	100 ± 0	0	-	-
3: p + FLC + H ₂ O ₂	200	100 ± 0	0	-	-
4: p + Fe ²⁺ (2 μM) + H ₂ O ₂	0	16.35 ± 5.53	83.65	-	-
5: p + Fe ²⁺ (0.05 μM) + FLC	0.1	100 ± 0	0	-1 ± 0	< 0.001
6: p + Fe ²⁺ (0.5 μM) + FLC	1	100 ± 0	0	-1 ± 0	< 0.001
7: p + Fe ²⁺ (5 μM) + FLC	10	100 ± 0	0	-1 ± 0	< 0.001
8: p + Fe ²⁺ (25 μM) + FLC	50	100 ± 0	0	-1 ± 0	< 0.001
9: p + Fe ²⁺ (50 μM) + FLC	100	100 ± 0	0	-1 ± 0	< 0.001
10: p + Fe ²⁺ (100 μM) + FLC	200	100 ± 0	0	-1 ± 0	< 0.001

^aData are reported as the average of three trials with calculated standard deviations shown.

Table 3.13. Gel electrophoresis results for Fe²⁺ DNA damage assays.^a

Gel lane	[Fe ²⁺], μM	% Supercoiled	% Nicked	% Damage	<i>p</i> Value
1: plasmid DNA (p)	0	100 ± 0	0	-	-
2: p + H ₂ O ₂ (50 μM)	0	100 ± 0	0	-	-
3: p + Fe ²⁺ + H ₂ O ₂	0	6.35 ± 5.53	93.65	-	-
4: p + Fe ²⁺	0.005	100 ± 0	0	-1 ± 0	< 0.001
5: p + Fe ²⁺	0.5	100 ± 0	0	-1 ± 0	< 0.001
6: p + Fe ²⁺	5	100 ± 0	0	-1 ± 0	< 0.001
7: p + Fe ²⁺	25	100 ± 0	0	-1 ± 0	< 0.001
8: p + Fe ²⁺	37.5	100 ± 0	0	-1 ± 0	< 0.001
9: p + Fe ²⁺	50	100 ± 0	0	-1 ± 0	< 0.001
10: p + Fe ²⁺	75	100 ± 0	0	-1 ± 0	< 0.001
11: p + Fe ²⁺	100	100 ± 0	0	-1 ± 0	< 0.001
12: p + Fe ²⁺	150	100 ± 0	0	-1 ± 0	< 0.001

^aData are reported as the average of three trials with calculated standard deviations shown.

Table 3.14. Gel electrophoresis results for Fe²⁺ DNA damage assays with ascorbate (AA).^a

Gel lane	[Fe ²⁺], μM	% Supercoiled	% Nicked	% Damage	<i>P</i> Value
1: plasmid DNA (p)	0	100.00 ± 0	0.00	-	-
2: p + H ₂ O ₂ (50 μM)	0	99.77 ± 0.21	0.23	-	-
3: p + AA (375 μM)		97.36 ± 4.57	2.64	-	-
4: p + Fe ²⁺ + H ₂ O ₂	2	13.62 ± 4.56	86.38	-	-
5: p + Fe ²⁺ + AA (2.5 μM)	2	100.00 ± 0	0.00	-0.23 ± 0	< 0.001
6: p + Fe ²⁺ + AA (12.5 μM)	10	99.97 ± 0.06	0.03	-0.20 ± 0.06	0.029
7: p + Fe ²⁺ + AA (31.25 μM)	25	99.93 ± 0.13	0.07	-0.16 ± 0.13	0.167
8: p + Fe ²⁺ + AA (62.5 μM)	50	99.95 ± 0.08	0.05	-0.18 ± 0.08	0.060
9: p + Fe ²⁺ + AA (125 μM)	100	91.94 ± 2.96	8.06	7.83 ± 2.96	0.045
10: p + Fe ²⁺ + AA (187.5 μM)	150	68.66 ± 2.77	31.34	31.11 ± 2.77	0.003
11: p + Fe ²⁺ + AA (375 μM)	300	26.24 ± 5.73	73.76	73.53 ± 5.73	0.002

^aData are reported as the average of three trials with calculated standard deviations shown.**Table 3.15.** Gel electrophoresis results for Fe²⁺ DNA damage assays with ascorbate (AA), FLC, and H₂O₂.^a

Gel lane	[FLC], μM	% Supercoiled	% Nicked	% Damage	<i>P</i> Value
1: plasmid DNA (p)	0	100.00 ± 0	0.00	-	-
2: p + H ₂ O ₂ (50 μM)	0	98.49 ± 2.07	1.51	-	-
3: p + FLC + AA (12.5 μM) + H ₂ O ₂	20	98.46 ± 2.66	1.54	-	-
4: p + Fe ²⁺ (μM) + H ₂ O ₂	0	10.17 ± 8.90	89.83	-	-
5: p + FLC + Fe ²⁺ (0.005 μM) + AA (0.00625 μM) + H ₂ O ₂	0.01	99.89 ± 0.26	0.11	-1.40 ± 0.26	0.011
6: p + FLC + Fe ²⁺ (0.05 μM) + AA (0.0625 μM) + H ₂ O ₂	0.1	99.89 ± 0.23	0.11	0.11 ± 0.23	0.495
7: p + FLC + Fe ²⁺ (0.25 μM) + AA (0.3125 μM) + H ₂ O ₂	0.5	55.41 ± 4.75	44.59	43.08 ± 4.75	0.004
8: p + FLC + Fe ²⁺ (0.5 μM) + AA (0.625 μM) + H ₂ O ₂	1	53.56 ± 4.75	46.44	44.93 ± 4.75	0.004
9: p + FLC + Fe ²⁺ (0.75 μM) + AA (0.9375 μM) + H ₂ O ₂	1.5	34.53 ± 8.93	65.47	63.96 ± 8.93	0.006
10: p + FLC + Fe ²⁺ (1 μM) + AA (1.25 μM) + H ₂ O ₂	2	6.46 ± 6.69	93.54	92.03 ± 6.69	0.002
11: p + FLC + Fe ²⁺ (1.5 μM) + AA (1.875 μM) + H ₂ O ₂	3	1.53 ± 3.27	98.47	96.96 ± 3.27	< 0.001
12: p + FLC + Fe ²⁺ (2 μM) + AA (2.5 μM) + H ₂ O ₂	4	0.29 ± 0.51	99.71	98.20 ± 0.51	< 0.001
13: p + FLC + Fe ²⁺ (5 μM) + AA (6.25 μM) + H ₂ O ₂	10	0.01 ± 0.01	99.99	98.48 ± 0.01	< 0.001

^aData are reported as the average of three trials with calculated standard deviations shown.

Table 3.16. Gel electrophoresis results for Fe²⁺ DNA damage assays with ascorbate (AA) and FLC.^a

Gel lane	[FLC], μM	% Supercoiled	% Nicked	% Damage	<i>p</i> Value
1: plasmid DNA (p)	0	100.00 ± 0	0.00	-	-
2: p + H ₂ O ₂ (50 μM)	0	99.95 ± 0.09	0.05	-	-
3: p + FLC	600	100.00 ± 0	0.00	-	-
4: p + Fe ²⁺ (2 μM)	0	6.72 ± 3.60	93.28	-	-
5: p + Fe ²⁺ (2 μM) + AA (1.5 μM) + FLC	4	97.05 ± 4.96	2.95	2.90 ± 4.96	0.418
6: p + Fe ²⁺ (10 μM) + AA (12.5 μM) + FLC	20	97.15 ± 4.76	2.85	2.80 ± 4.76	0.415
7: p + Fe ²⁺ (25 μM) + AA (31.25 μM) + FLC	50	96.80 ± 4.93	3.20	3.15 ± 4.93	0.384
8: p + Fe ²⁺ (50 μM) + AA (62.5 μM) + FLC	100	95.27 ± 3.27	4.73	4.68 ± 3.27	0.131
9: p + Fe ²⁺ (100 μM) + AA (125 μM) + FLC	200	81.35 ± 4.15	18.65	18.60 ± 4.15	0.016
10: p + Fe ²⁺ (150 μM) + AA (187.5 μM) + FLC	300	59.31 ± 3.03	40.69	40.64 ± 3.03	0.002
11: p + Fe ²⁺ (300 μM) + AA (375 μM) + FLC	600	37.11 ± 1.00	62.89	62.84 ± 1.00	< 0.001

^aData are reported as the average of three trials with calculated standard deviations shown.

Table 3.17. Gel electrophoresis results for Fe²⁺ DNA damage assays with ascorbate (AA) and H₂O₂.^a

Gel lane	[Fe ²⁺], μM	% Supercoiled	% Nicked	% Damage	<i>p</i> Value
1: plasmid DNA (p)	0	100.00 ± 0	0.00	-	-
2: p + H ₂ O ₂ (50 μM)	0	99.39 ± 1.05	0.61	-	-
3: p + Fe ²⁺ + H ₂ O ₂	2	4.59 ± 2.49	95.41	-	-
3: p + Fe ²⁺ + AA (0.00625 μM) + H ₂ O ₂	0.005	98.58 ± 1.92	1.42	0.81 ± 1.92	0.541
3: p + Fe ²⁺ + AA (0.0625 μM) + H ₂ O ₂	0.05	98.01 ± 3.44	1.99	1.38 ± 3.44	0.559
3: p + Fe ²⁺ + AA (0.625 μM) + H ₂ O ₂	0.5	76.07 ± 4.20	23.93	23.33 ± 4.20	0.011
3: p + Fe ²⁺ + AA (0.9375 μM) + H ₂ O ₂	0.75	58.97 ± 4.46	41.03	40.42 ± 4.46	0.004
3: p + Fe ²⁺ + AA (1.25 μM) + H ₂ O ₂	1	19.71 ± 4.64	80.29	79.69 ± 4.64	0.001
3: p + Fe ²⁺ + AA (1.875 μM) + H ₂ O ₂	1.5	12.92 ± 5.21	87.08	86.47 ± 5.21	0.001
3: p + Fe ²⁺ + AA (2.5 μM) + H ₂ O ₂	2	2.34 ± 2.34	97.66	97.05 ± 2.34	< 0.001
3: p + Fe ²⁺ + AA (5 μM) + H ₂ O ₂	5	0.03 ± 0.06	99.97	99.36 ± 0.06	< 0.001
3: p + Fe ²⁺ + AA (10 μM) + H ₂ O ₂	10	0.33 ± 0.57	99.67	99.07 ± 0.57	< 0.001

^aData are reported as the average of three trials with calculated standard deviations shown.

Table 3.18. Gel electrophoresis results for Fe²⁺ DNA damage assays with H₂O₂ and DFO.^a

Gel lane	[DFO], μM	% Supercoiled	% Nicked	% Damage	<i>p</i> Value
1: plasmid DNA (p)	0	99.95 ± 0.08	0.08	-	-
2: p + H ₂ O ₂ (50 μM)	0	98.55 ± 1.25	01.45	-	-
3: p + DFO + H ₂ O ₂	50	98.87 ± 1.34	1.13	-	-
4: p + DFO	50	93.62 ± 2.65	6.38	-	-
5: p + Fe ²⁺ (50 μM) + DFO	50	92.34 ± 2.23	7.66	-	-
6: p + Fe ²⁺ (2 μM) + H ₂ O ₂	0	12.43 ± 6.92	87.57	-	-
7: p + Fe ²⁺ (0.1 μM) + H ₂ O ₂ + DFO	0.1	97.54 ± 1.62	2.46	1.01 ± 1.62	0.393
8: p + Fe ²⁺ (1 μM) + H ₂ O ₂ + DFO	1	93.23 ± 5.81	6.77	5.32 ± 5.81	0.254
9: p + Fe ²⁺ (2 μM) + H ₂ O ₂ + DFO	2	61.33 ± 8.42	38.67	37.22 ± 8.42	0.166
10: p + Fe ²⁺ (5 μM) + H ₂ O ₂ + DFO	5	62.31 ± 9.05	37.69	36.52 ± 9.05	0.199
11: p + Fe ²⁺ (7.5 μM) + H ₂ O ₂ + DFO	7.5	38.41 ± 6.28	61.59	60.15 ± 6.28	0.004
12: p + Fe ²⁺ (10 μM) + H ₂ O ₂ + DFO	10	31.94 ± 9.72	68.06	66.61 ± 9.72	0.007
13: p + Fe ²⁺ (25 μM) + H ₂ O ₂ + DFO	25	16.65 ± 4.69	83.35	81.90 ± 4.69	0.001
14: p + Fe ²⁺ (50 μM) + H ₂ O ₂ + DFO	50	1.40 ± 2.43	98.60	97.15 ± 2.43	<0.001

^aData are reported as the average of three trials with calculated standard deviations shown.

Table 3.19. Statistical analysis of Fe²⁺ and Fe²⁺ FLC DNA damage through one-tailed t-test analysis.

[Fe ²⁺], μM	% DNA Damage Fe ²⁺	% DNA Damage Fe ²⁺ + FLC	<i>p</i> Value
0.005	-1 ± 0	-1 ± 0	< 0.001
0.05	-1 ± 0	8.8 ± 0.01	< 0.001
0.25	-1 ± 0	38.54 ± 0.58	< 0.001
0.5	-1 ± 0	37.35 ± 1.22	< 0.001
1	45.51 ± 5.00	87.05 ± 5.69	0.006
2	89.49 ± 1.03	95.97 ± 4.28	0.120
5	98.27 ± 2.14	95.21 ± 0.76	0.002

3.6. References

- (1) Brown, G. D.; Denning, D. W.; Levitz, S. M. *Science* **2012**, *336*, 647-648.
- (2) Idnurm, A.; Bahn, Y.-S.; Nielsen, K.; Lin, X.; Fraser, J. A.; Heitman, J. *Nat. Rev. Microbiol.* **2005**, *3*, 753–764.
- (3) Park, B. J.; Wannemuehler, K. A.; Marston, B. J.; Govender, N.; Pappas, P. G.; Chiller, T. M. *AIDS* **2009**, *23*, 525–530.
- (4) Dzoyem, J. P.; Kechia, F. A.; Ngaba, G. P.; Lunga, P. K.; Lohoue, P. J. *Afr. Health Sci.* **2012**, *12*, 129–133.
- (5) May, R. C.; Stone, N. R. H.; Wiesner, D. L.; Bicanic, T.; Nielsen, K. *Nat. Rev. Microbiol.* **2016**, *14*, 106–117.
- (6) Castro-Ramírez, R.; Ortiz-Pastrana, N.; Caballero, A. B.; Zimmerman, M. T.; Stadelman, B. S.; Gaertner, A. A. E.; Brumaghim, J. L.; Korrodi-Gregório, L.; Pérez-Tomás, R.; Gamez, P. Barba-Behrens, N. *Dalton Trans.* **2018**, *47*, 7551–7560.
- (7) Betanzos-Lara, S.; Chmel, N. P.; Zimmerman, M. T.; Barrón-Sosa, L. R.; Garino, C.; Salassa, L.; Rodger, A.; Brumaghim, J. L.; Gracia-Mora, I.; Barba-Behrens, N. *Dalton Trans.* **2015**, *44*, 3673–3685.
- (8) Pasko, M. T.; Piscitelli, S. C.; van Slooten, A. D. *Ann. Pharmacother.* **1990**, *24*, 860–867.
- (9) Goa, K. L.; Barradell, L. B. *Drugs* **1995**, *50*, 658–690.
- (10) Rodriguez F.G.; Cancino B.L.; Lopez-Nigro, M.; Palermo, A.; Mudry, M.; González E.P.; Carballo, M.A. *Toxicol. Lett.* **2002**, *132*, 109–115.
- (11) Shiba, K.; Saito, A.; Miyahara, T. *Clin. Ther.* **1990**, *12*, 206–215.

- (12) Rogers, T. R. *Int. J. Antimicrob. Agents* **2006**, *27*, 7–11.
- (13) Mahl, C. D.; Behling, C. S.; Hackenhaar, F. S.; Carvalho e Silva, M. N. de; Putti, J.; Salomon, T. B.; Alves, S. H.; Fuentefria, A.; Benfato, M. S. *Diagn. Microbiol. Infect. Dis.* **2015**, *82*, 203–208.
- (14) Liu, S.; Hou, Y.; Chen, X.; Gao, Y.; Li, H.; Sun, S. *Int. J. Antimicrob. Agents* **2014**, *43*, 395–402.
- (15) Allen, D.; Wilson, D.; Drew, R.; Perfect, J. *J. Expert Rev. Anti. Infect. Ther.* **2015**, *13*, 787–798.
- (16) Chen, Y.-C.; Chang, T.-Y.; Liu, J.-W.; Chen, F.-J.; Chien, C.-C.; Lee, C.-H.; Lu, C.-H. *BMC Infect. Dis.* **2015**, *15*, 277.
- (17) Smith, K. D.; Achan, B.; Hullsiek, K. H.; McDonald, T. R.; Okagaki, L. H.; Alhadab, A. A.; Akampurira, A.; Rhein, J. R.; Meya, D. B.; Boulware, D. R. Nielsen, K. *Antimicrob. Agents Chemother.* **2015**, *59*, 7197–7204.
- (18) Gast, C. E.; Basso, L. R.; Bruzual, I.; Wong, B. *Antimicrob. Agents Chemother.* **2013**, *57*, 5478–5485.
- (19) Sionov, E.; Lee, H.; Chang, Y. C.; Kwon-Chung, K. J. *PLoS Pathog.* **2010**, *6*, e1000848-1000861.
- (20) Posteraro, B.; Sanguinetti, M.; Sanglard, D.; La Sorda, M.; Boccia, S.; Romano, L.; Morace, G.; Fadda, G. *Mol. Microbiol.* **2003**, *47*, 357–371.
- (21) Cowen, L. E.; Sanglard, D.; Howard, S. J.; Rogers, P. D.; Perlin, D. S. *Cold Spring Harb. Perspect. Med.* **2014**, *5*, a019752-a019775.

- (22) Lee, K.-T.; So, Y.-S.; Yang, D.-H.; Jung, K.-W.; Choi, J.; Lee, D.-G.; Kwon, H.; Jang, J.; Wang, L. L.; Cha, S. Gena Lee Meyers, G.; Jeong, E.;J in, J.H.; Lee, Y.; Hong, J.; Bang, S.; Ji, J.H.; Park, G.; Byun, H.J.; Park, S. W.; Park, Y.-M.; Adedoyin, G.; Kim, T.; Averette, A.F.; Choi, J-S.; Heitman, J.; Cheong, E.; Lee, Y.-H.; Bahn, Y.-S. *Nature Commun.* **2016**, *7*, 12766-12782.
- (23) Revankar, S. G.; Fu, J.; Rinaldi, M. G.; Kelly, S. L.; Kelly, D. E.; Lamb, D. C.; Keller, S. M.; Wickes, B. L. *Biochem. Biophys. Res. Commun.* **2004**, *324*, 719–728.
- (24) Vanden Bossche, H. *Curr. Top. Med. Mycol.* **1985**, *1*, 313–351.
- (25) Zhang, Y.-Q.; Gamarra, S.; Garcia-Effron, G.; Park, S.; Perlin, D. S.; Rao, R. *PLoS Pathog.* **2010**, *6*, e1000939-e1000954.
- (26) Ngamskulrunroj, P.; Chang, Y.; Hansen, B.; Bugge, C.; Fischer, E.; Kwon-Chung, K. J. *PloS one* **2012**, *7*, e33022-e33031.
- (27) Ngamskulrunroj, P.; Chang, Y.; Hansen, B.; Bugge, C.; Fischer, E.; Kwon-Chung, K. J. *FEMS Yeast Res.* **2012**, *12*, 748–754.
- (28) Altamirano, S.; Fang, D.; Simmons, C.; Sridhar, S.; Wu, P.; Sanyal, K.; Kozubowski, L. *mSphere* **2017**, *2*, e00205-e00217.
- (29) Harrison, B. D.; Hashemi, J.; Bibi, M.; Pulver, R.; Bavli, D.; Nahmias, Y.; Wellington, M.; Sapiro, G.; Berman, J. *PLoS Biol.* **2014**, *12*, e1001815-e1001833.
- (30) Limoli, C. L.; Giedzinski, E. *Neoplasia* **2003**, *5*, 339–346.
- (31) Degtyareva, N. P.; Chen, L.; Mieczkowski, P.; Petes, T. D.; Doetsch, P. W. *Mol. Cell. Biol.* **2008**, *28*, 5432–5445.

- (32) Angelé-Martínez, C.; Goodman, C.; Brumaghim, J. *Metallomics* **2014**, *6*, 1358–1381.
- (33) Vasák, M. *J. Trace Elem. Med. Biol.* **2005**, *19*, 13–17.
- (34) Ruttkay-Nedecky, B.; Nejdil, L.; Gumulec, J.; Zitka, O.; Masarik, M.; Eckschlager, T.; Stiborova, M.; Adam, V.; Kizek, R. *Int. J. Mol. Sci.* **2013**, *14*, 6044–6066.
- (35) Ding, C.; Yin, J.; Tovar, E. M. M.; Fitzpatrick, D. A.; Higgins, D. G.; Thiele, D. J. *Mol. Microbiol.* **2011**, *81*, 1560–1576.
- (36) Espart, A.; Gil-Moreno, S.; Palacios, Ò.; Capdevila, M.; Atrian, S. *Mol. Microbiol.* **2015**, *98*, 977–992.
- (37) Ding, C.; Festa, R. A.; Chen, Y.-L.; Espart, A.; Palacios, Ò.; Espín, J.; Capdevila, M.; Atrian, S.; Heitman, J.; Thiele, D. J. *Cell Host Microbe* **2013**, *13*, 265–276.
- (38) Yukihiisa, T.; Yasumitsu, O.; Kenji, I.; Kazuo T., S. *J. Health Sci.* **2004**, *50*, 154–158.
- (39) Peng, C.; Gaertner, A.; Henriquez, S.; Fang, D.; Brumaghim, J.; Kozubowski, L. *PloS One* **2018**, *13*, e0208471.
- (40) Chaturvedi, S.; Hamilton, A. J.; Hobby, P.; Zhu, G.; Lowry, C. V.; Chaturvedi, V. *Gene* **2001**, *268*, 41–51.
- (41) Peng, C. A.; Gaertner, A. A. E.; Henriquez, S. A.; Fang, D.; Colon-Reyes, R. J.; Brumaghim, J. L.; Kozubowski, L. *PloS One* **2018**, *13*, e0208471.
- (42) Tam, T.; Leung-Toung, R.; Li, W.; Wang, Y.; Karimian, K.; Spino, M. *Curr. Med. Chem.* **2003**, *10*, 983–995.
- (43) Bernhardt, P. V. *Dalton Trans.* **2007**, *30*, 3214–3220.

- (44) Lai, Y.-W.; Campbell, L. T.; Wilkins, M. R.; Pang, C. N. I.; Chen, S.; Carter, D. A. *Int. J. Antimicrob. Agents* **2016**, *48*, 388–394.
- (45) Ali, M.; Ahmed, M.; Ahmed, S.; Ali, S. I.; Perveen, S.; Mumtaz, M.; Haider, S. M.; Nazim, U. F *Pak. J. Pharm. Sci.* **2017**, *30*, 187–194.
- (46) Nagaj, J.; Starosta, R.; Szczepanik, W.; Barys, M.; Młynarz, P.; Jeżowska-Bojczuk, M. *J. Inorg. Biochem.* **2012**, *106*, 23–31.
- (47) Pierre, J. L.; Fontecave, M. *BioMetals* **1999**, *12*, 195–199.
- (48) Hatcher, H. C.; Singh, R. N.; Torti, F. M.; Torti, S. V. *Future Med. Chem.* **2009**, *1*, 1643–1670.
- (49) Howland, M. A. *J. Toxicol. Clin. Toxicol.* **1996**, *34*, 491–497.
- (50) Denicola, A.; Souza, J.; Gatti, R. M.; Augusto, O.; Radi, R. *Free Radic. Biol. Med.* **1995**, *19*, 11–19.
- (51) Bard, A. J.; Faulkner, L. R. *Electrochemical methods: Fundamentals and applications*; John Wiley: New York, Chichester, 2001, pp 286-293.
- (52) Battin, E. E.; Perron, N. R.; Brumaghim, J. L. *Inorg. Chem.* **2006**, *45*, 499–501.
- (53) Battin, E. E.; Brumaghim, J. L. *J. Inorg. Biochem.* **2008**, *102*, 2036–2042.
- (54) Perkowski, D. A.; Perkowski, M. *Data and probability connections*; Connections in mathematics courses for teachers; Pearson Education Ltd: Upper Saddle River, N.J., 2007., p318-337

CHAPTER FOUR

INVESTIGATION OF PROCYANIDIN-RICH CONDENSED TANNINS FOR PREVENTION OF COPPER- AND IRON-MEDIATED DNA DAMAGE

4.1 Introduction

Condensed tannins occur in a variety of common fruits and vegetables¹ and are noted for a variety of effects on human health,²⁻⁴ often attributed to their antioxidant activity.⁵⁻⁸ Cranberry (*Vaccinium macrocarpon*) consumption is associated with many health benefits,⁹ including prevention of urinary tract infections.^{10,11} *V. macrocarpon* extract has been reported to have anti-virulence,¹² anti-bacterial,¹³ and anti-microbial^{8,14} activities as well as antioxidant and anticancer activities *in vitro* and *in vivo*.^{11,15-18} Cranberry extract consumption may also protect against diet-induced obesity,^{19,20} and cranberry juice exhibits cardioprotective effects due to its antioxidant abilities; however, the cause of these effects must be further investigated to exploit these applications.²¹

Many of the health benefits of cranberry consumption are attributed to polyphenol compounds in *V. macrocarpon*. These polyphenols protect liver cells from oxidative stress through observed modulation of glutathione concentration, prevention of reactive oxygen species generation and lipid peroxidation, antioxidant enzyme activity, and cell signaling pathways.²² Condensed tannins (CTs), also known as proanthocyanidins (PCs), are a group of plant secondary metabolite polyphenols that are comprised of oligomers and polymers of flavan-3-ol subunits.²³⁻²⁶ In *V. macrocarpon*, these tannins are comprised of a group of heterogeneous structures, with the polyphenol (-)-epicatechin being the predominant

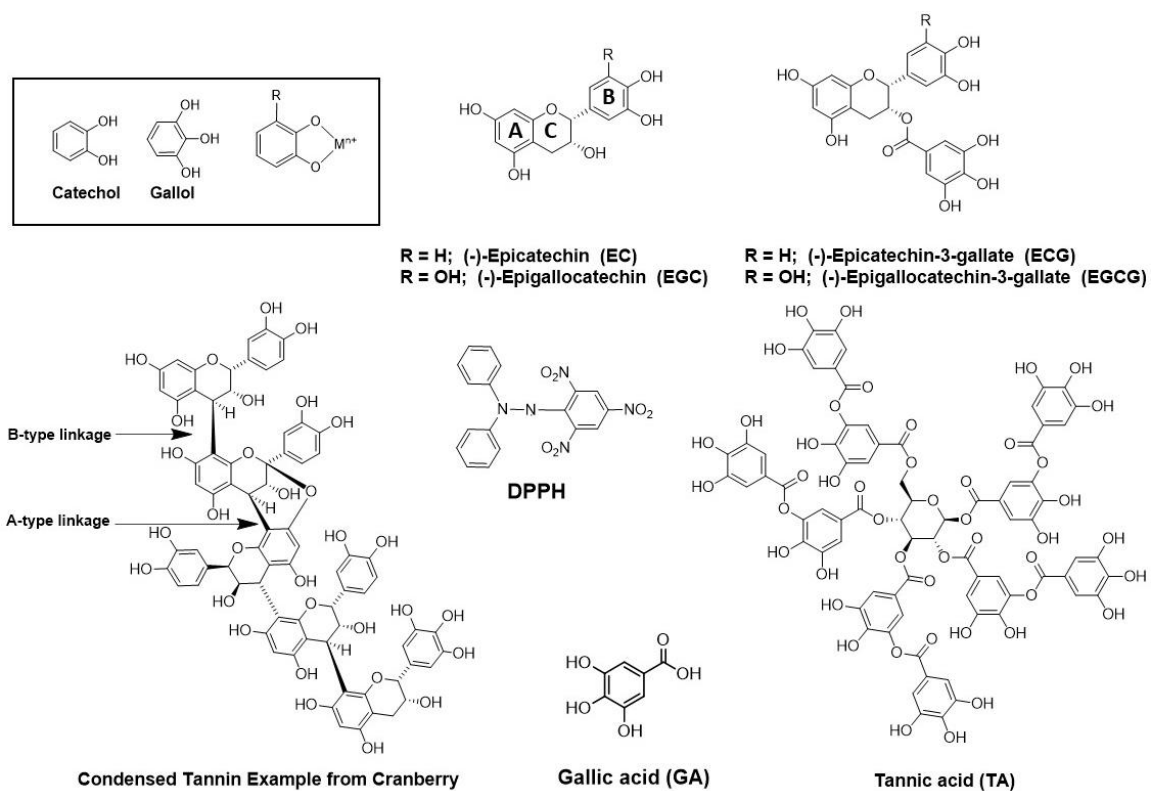


Figure 4.1. In box: Structures of catechol and gallol groups and their metal coordination modes. Outside box: an example condensed tannin structure showing A-type and B-type linkages, selected polyphenol structures, and the structure of 2,2-diphenyl-1-picrylhydrazyl (DPPH).

constitutive unit with trace amounts of (+)-catechin and (epi)gallocatechin (EGCG).^{21,25,26}

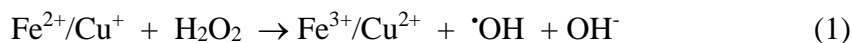
Proanthocyanin concentrations in cranberries are observed from 13.6 to 419 mg/100 g depending on fruit size, ripeness, variety and other factors, making it a potentially significant dietary source of proanthocyanins.^{27,27}

Polyphenol concentrations of 80 $\mu\text{g/mL}$ in human blood plasma after consumption of 1800 mL cranberry juice are reported,^{22,27,28} but the number of studies evaluating the bioavailability of proanthocyanins is limited, since the interest in their health benefits is recent and purification of sufficient amounts for testing has been a significant challenge.⁸

The distribution of the subunits catechin, EC, EGC, and EGCG (Figure 5.1) in CTs can vary depending on the source of the CTs. Additionally, these subunits can be connected

via a number of interflavan-3-ol linkages but the most commonly isolated CTs contain three types of bond connectivity. Two of these types have single bonds from either the C-4 carbon to the C-8 carbon (4,8-B-type interflavan-3-ol linkage; Figure 5.1) or the C-4 carbon to the C-6 carbon (4,6-B-type interflavan-3-ol linkage; Figure 5.1) of adjacent flavan-3-ol subunits. One additional common type of interflavan-3-ol linkage involves formation of two single bonds between adjacent flavan-3-ol subunits, involving both C-C and C-O bonds and is referred to as an A-type interflavan-3-ol linkage (Figure 4.1).

Condensed tannins possess catechol or gallol substituents (Figure 4.1; inside box) on the B-ring of the constituent flavan-3-ol subunits. These phenolic moieties have been shown to prevent oxidative DNA damage caused by the Fenton reaction (Reaction 1).^{29,30} Overproduction of hydroxyl radical can result in oxidative damage and other biomolecules and is an underlying cause of neurodegenerative diseases, cancer, and many other conditions.³¹ *In vitro* and in cells, polyphenols can prevent iron-mediated DNA damage from hydroxyl radical by coordinating Fe²⁺.^{29,30,32-34} Polyphenol binding to Fe²⁺ promotes autooxidation to non-hydroxyl-generating Fe³⁺ in the presence of O₂.³⁰



In this study, we investigated the antioxidant capabilities of a series of procyanidin-rich CTs with different structural features for their ability to inhibit copper and iron-mediated DNA damage, including purified CTs from *V. macrocarpon* (cranberry), *Humulus lupulus* (hops), *Vitis vinifera* (grapeseed) and *Tilia inflorosa* (lime tree) flowers. The activity of these CTs was also compared to the activity of six commercially available polyphenolic compounds (Figure 4.1): epigallocatechin (EGC),

(-)-epigallocatechin-3-gallate (EGCG), gallic acid (GA), epicatechin (EC), epicatechin gallate (ECG), and tannic acid (TA). No study has investigated the effect of the different CT linkages and degree of galloylation and the resulting 3-dimensional structural changes, but Brumaghim *et al.*^{29,30,35,36} highlighted the importance of metal interaction for the antioxidant activity of proanthocyanidins. This is the first study to investigate CTs with structural differences and their ability to prevent metal-mediated DNA damage.

CTs from cranberry (*V. macrocarpon*), hops (*H. lupulus*), grapeseed (*V. vinifera* seed), and lime tree (*T. inflorosa* flowers) were extracted and purified by Dr. Wayne Zeller, Research Chemist at the United States Department of Agriculture, U.S. Dairy Forage Research Center in Madison, Wisconsin. This research was supported by National Science Foundation grants CHE 1213912 and 1807709.

4.2 Results and Discussion

Compositional Analysis of Purified Condensed Tannins. The aim of this project is to overcome the difficulty of purifying CTs with specific structural characteristics, therefore enabling the investigation in their ability to prevent metal-mediated DNA damage *in vitro* in comparison to their subunits. Zeller *et al.*^{37,38} have previously shown that volume integration ratios of appropriate cross-peak signals in ¹H-¹³C HSQC NMR spectra provide a strong correlation with thiolysis data in determination of procyanidin/prodelphinidin (PC/PD) and *cis/trans* ratios, mean degree of polymerization (mDP), percent galloylation, and A-type interflavan linkages (Table 4.1). The mDP for the purified CTs were similar as were the PC/PD and *cis/trans* ratios. *V. vinifera* seed CTs were included in this study to

Table 4.1. Classification of condensed tannin flavan-3-ol subunits and interflavan-3-ol linkages (ND = not detected).

CT Source	mDP NMR/thio	PC/PD NMR/thio	cis/trans NMR/thio	%galloyl NMR/thio	%A- type	Method
<i>V. macrocarpon</i> (cranberry)	7.4	95/5	90/10	ND	28	NMR
<i>H. lupulus</i> (hops)	6.4	92/8	72/28	ND	2.6	NMR
<i>V. vinifera</i> (grapeseed)	4.2 (NMR) 5.6 (thio)	>99/1 (NMR) 100/0 (thio)	73/27 (NMR) 81/19 (thio)	16.5 (NMR) 18 (thio)	2.5	NMR/ thiolysis
<i>T. inflorescentia</i> (lime tree)	5.4 (NMR) 9.4 (thio)	>99/1 (NMR) 99/1 (thio)	91/9	ND	ND	NMR/ thiolysis

examine the effect of C-3 galloylation. A-type linkages were prevalent in the *V. macrocarpon* CTs but were also present, to a small degree (~3%), in the CTs purified from *H. lupulus*.

CTs from cranberry (*V. macrocarpon*), hops (*H. lupulus*), grapeseed (*V. vinifera* seed), and lime tree (*T. inflorescentia* flowers) were chosen for their similar mean degree of polymerization and similar average molecular weights, on average 4.2-6.5 flavan-3-ol subunits on average (Table 4.1). The mean degree of polymerization can affect antioxidant activity as highlighted by Gaulejac *et al.*,³⁹ who reported an up to 2-fold increase in antioxidant activity as measured by scavenging of superoxide anion radical by proanthocyanidins from grape extracts with mDP of 1 to 4.

Jerez *et al.*⁴⁰ also observed an increase in the ability to scavenge 2,2-diphenyl-1-picrylhydrazyl (DPPH) radicals (Figure 4.1) up to by proanthocyanidins with mDP of 6-7 from barks. *V. macrocarpon* condensed CTs contain mostly A-type linkages (C2-C7 and O7-C2; Figure 4.1),²¹ whereas *T. inflorescentia* has primarily B-type linkages (C4-C8 or

C4-C6; Figure 4.1).⁴¹ In addition, *H. lupulus* CTs have a relatively high number of *trans* flavan-3-ol subunits containing a higher catechin concentration than epicatechin. *V. vinifera* seed CTs has a high percentage of galloylation at C3 subunits such as EGCG (Figure 4.1).

Metal-mediated DNA Damage Prevention by CTs. Plasmid DNA gel electrophoresis assays were conducted to determine the ability of predominantly proanthocyanidin (PC) CTs from *V. macrocarpon*, *H. lupulus*, *V. vinifera* and *T. inflorescentia*, varying in distinct structural features, to prevent copper- or iron-mediated DNA damage. Both Fe^{2+} and Cu^+ can produce DNA-damaging hydroxyl radical (Reaction 1),^{29,42-44} and the polyphenol substituents in CTs are known to bind both iron and copper.^{29,34,45-47} This DNA assay evaluates the ability of antioxidants to prevent metal-mediated DNA damage under biological relevant conditions. The naturally supercoiled (undamaged) and damaged (nicked) plasmid DNA can be separated using gel electrophoresis, therefore allowing a quantitative analysis of antioxidant activity.

In the DNA assay gel images (Figure 4.2A and 4.2B), lane 3 shows that *V. macrocarpon* CTs do not cause DNA damage in the presence of H_2O_2 , but Cu^+ and H_2O_2 cause over 90% damage (Figure 4.2A, lane 4). The same amount of DNA damage occurs with Fe^{2+} and H_2O_2 (Figure 4.2B, lane 4). Increasing *V. macrocarpon* CT concentrations up to 5 or 200 mg/mL (Figures 4.2A and 4.2B, lanes 5-12) prevent this iron- or copper-mediated DNA damage, respectively. Similar plasmid DNA damage assays were

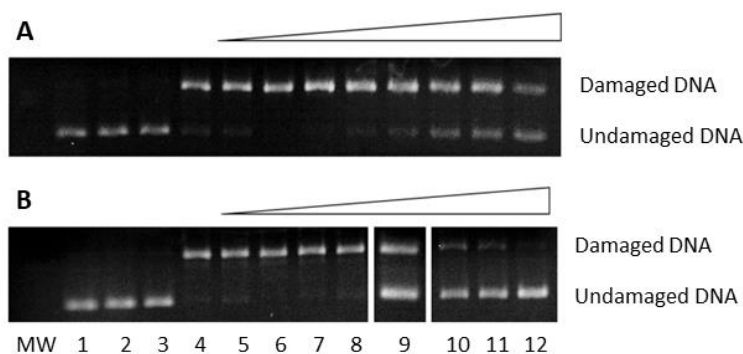


Figure 4.2. Agarose gel electrophoresis images of DNA treated with various concentrations of *V. macrocarpon* CTs with A) Cu^{2+} ($6 \mu\text{M}$) and ascorbate ($7.5 \mu\text{M}$) or B) Fe^{2+} ($2 \mu\text{M}$) and H_2O_2 . Damaged (nicked) plasmid DNA (p) is the top band and undamaged (supercoiled) DNA is in the bottom band. Lanes are MW: 1 kb DNA ladder; 1: p; 2: p + H_2O_2 ($50 \mu\text{M}$); A) 3: p + H_2O_2 + *V. macrocarpon* CTs (200 mg/L); 4: p + H_2O_2 + Cu^{2+} ($6 \mu\text{M}$) + ascorbate ($7.5 \mu\text{M}$); 5-14: p + H_2O_2 + Cu^{2+} ($6 \mu\text{M}$) + ascorbate + *V. macrocarpon* CTs ($0.1, 1, 5, 15, 25, 50, 100,$ and 200 mg/L respectively). B) 3: p + H_2O_2 + *V. macrocarpon* CTs (5 mg/L); 4: p + H_2O_2 + Fe^{2+} ($2 \mu\text{M}$); 5-13: p + H_2O_2 + Fe^{2+} ($2 \mu\text{M}$) + *V. macrocarpon* CTs ($0.001, 0.01, 0.1, 0.5, 1, 2.5,$ and 5 mg/L respectively).

performed for CTs from *V. vinifera* seed, *H. lupulus*, and *T. inflorescentia* (data provided in Figures 4.4 and 4.5 and Tables 4.4 to 4.9).

From analysis of the intensities of the gel bands, best-fit dose-response curves for copper- and iron-mediated DNA damage prevention were obtained for *V. macrocarpon*, *V. vinifera* seed, *H. lupulus*, and *T. inflorescentia* CTs (Figure 4.3). From these plots, the concentrations of each of the CTs required to inhibit 50% of DNA damage (IC_{50} values) were quantified (Table 4.2). *V. macrocarpon* CTs has IC_{50} values of 162.6 ± 0.3 and $0.75 \pm 0.01 \text{ mg/L}$ for copper- and iron- mediated DNA damage prevention, respectively.

Compared to *V. macrocarpon* CTs, *V. vinifera* seed and *H. lupulus* CTs exhibit much less inhibition of copper-mediated DNA damage, with 27 and 28% inhibition at 200 mg/L , respectively (Table 4.2), insufficient DNA damage prevention to determine an IC_{50} value. *T. inflorescentia* CTs prevent no copper-mediated DNA damage at the highest

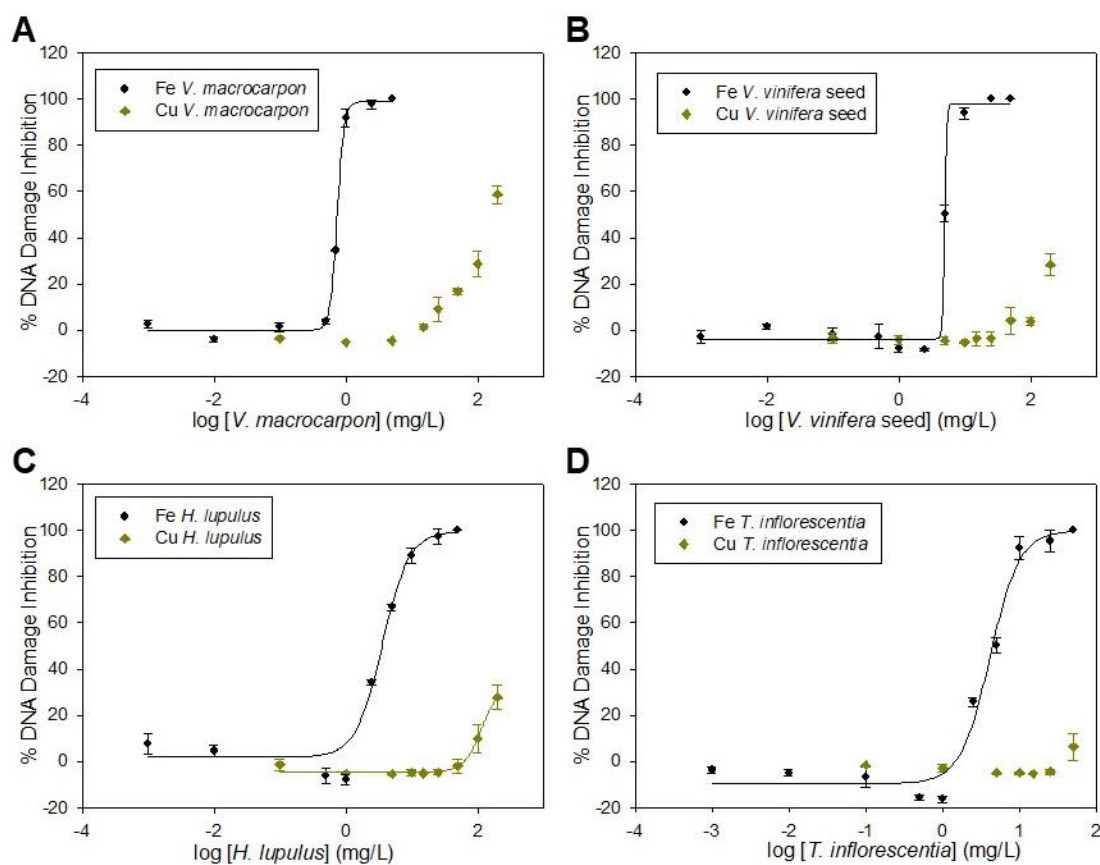


Figure 4.3. Dose-response curves for copper- and iron-mediated DNA damage prevention by A) *V. macrocarpon* CTs, B) *V. vinifera* seed CTs, C) *H. lupulus* CTs (the data point at 0.01 mg/L was excluded from the iron-mediated DNA damage fit due to its negative value), and D) *T. inflorescentia* CTs (the data points at 0.1 and 0.5 mg/L were excluded from the iron-mediated DNA damage due to their negative values).

tested concentration of 50 mg/L. At concentrations greater than 50 mg/L, *T. inflorescentia* CTs alone and with copper interacted with the DNA so that the DNA no longer moved out of the wells of the agarose gel (Figure 4.4C).

Condensed tannins are polymers of the polyphenol subunits EGCG, EC, gallic acid (GA) and epigallocatechin (EGC; Figure 4.1). EGCG is a catechin formed from condensation of gallic acid with an epigallocatechin ester. It is the most abundant green tea flavan-3-ol and is found in many dietary supplements due to its potential beneficial

Table 4.2. IC₅₀ values for metal-mediated DNA damage prevention by CTs of the indicated foods.

Compound	IC ₅₀ Cu ⁺ [mg/L]	IC ₅₀ Fe ²⁺ [mg/L]	IC ₅₀ Fe ²⁺ [μM] ^{a)}	Ref.
<i>V. macrocarpon</i> CTs	IC ₅₀ 162.5 ± 0.3	IC ₅₀ 0.75 ± 0.01	0.40	
<i>H. lupulus</i>	27% Damage inhibition at 200 mg/L	Prooxidant 0.001-1 mg/L Antioxidant 1-50 mg/L IC ₅₀ 3.60 ± 0.01	2.3	
<i>V. vinifera</i> seed CTs	28% Damage inhibition at 200 mg/L	IC ₅₀ 4.96 ± 0.01	3.4	
<i>T. inflorescentia</i> CTs	No DNA damage inhibition 0.1-50 mg/L	Prooxidant 0.001-1 mg/L Antioxidant 1-50 mg/L IC ₅₀ 4.41 ± 0.01	2.8	
Tannic acid (TA)	IC ₅₀ 9 ± 1	IC ₅₀ 0.51 ± 0.01	0.30	[48]
Epigallocatechin (EGC)	Prooxidant 0.12–306 mg/L	IC ₅₀ 3.00 ± 0.31	9.8	[36]
Gallic acid (GA)	Prooxidant 0.68–1.70 mg/L Antioxidant 16 % at 85.06 mg/L	IC ₅₀ 2.38 ± 0.17	14	[36,35]
Epicatechin (EC)	Prooxidant 0.06–145 mg/L	IC ₅₀ 17.16 ± 0.29	59	[36,35]
Epicatechin gallate (EGCG)	Prooxidant 0.04–1.77 mg/L Antioxidant 4.42–442 mg/L IC ₅₀ 23.5 ± 0.9	IC ₅₀ 1.02 ± 0.44	1.1	[36,35]

^{a)} IC_{50s} were calculated based upon average molecular weight.

effects on human health.⁴⁹ EC is an antioxidant flavonoid, occurring especially in woody plants as both (+)-catechin and (-)-epicatechin. In human plasma, EGCG, and EC are found at concentrations of 5-150 ng/mL.^{50,51}

Tannic acid (TA; Figure 4.1) is a commercially available tannin with multiple phenolic groups.⁵² It is used as an aroma compound in soft drinks and juices and as a clarifying agent, color stabilizer, and taste enhancer in the wine industry.⁴⁹ TA concentrations in red wine have been shown to increase from 250.5 to 524.4 mg/mL upon aging, correlating with increased DPPH radical scavenging activity.⁵³ TA is a representative of the hydrolysable tannins group of polyphenols, consisting of sets of gallic acid esters protruding from a glucose core molecule, and inhibits growth of many fungi, yeast, bacteria, and viruses.^{30,52} TA is also an antioxidant, and its antioxidant behavior may be linked to its anti-carcinogenic and anti-mutagenic properties.^{30,52,54}

Under copper-mediated DNA damage conditions, GA, EGC, and EC show prooxidant activity. ECG prevention of copper-mediated DNA damage shows prooxidant activity at low concentrations but shows antioxidant activity at concentrations greater than 4.42 mg/L with an IC₅₀ of 23.5 mg/L. Interestingly, the CTs of *V. vinifera* seed and *T. inflorescentia* show no prooxidant activity in the tested concentration range with copper even though its constituent monomers do.

Under iron-mediated DNA damage conditions, *V. vinifera* seed CTs showed only antioxidant activity at all concentrations examined. Its IC₅₀ value is higher than the IC₅₀ of its monomers EGC, GA, and EGCG but lower than EC. The IC₅₀ value for *T. inflorescentia* CT prevention of iron-mediated DNA damage is 4.41 mg/L. Similar to *H. lupulus* CTs, *T.*

inflorescentia CTs exhibit prooxidant activity with iron at low concentrations (0.1 and 1 mg/L). Such concentration-dependent prooxidant/antioxidant activity has not been previously observed for polyphenol inhibition of iron-mediated DNA damage, except when chelated iron is used as the iron source.^{35,36}

V. vinifera seed, *H. lupulus*, and *T. inflorescentia* prevented iron-mediated DNA damage with IC₅₀ values of 4.96, 3.60, and 4.41 mg/L, respectively. Although these IC₅₀ values are substantially lower than their corresponding IC₅₀ values for prevention of copper-mediated damage (Table 4.2), they are 5-6 fold higher than that of *V. macrocarpon* CTs. The IC₅₀ values for DNA damage inhibition by *H. lupulus* CTs falls between those of its constituent monomers: 3-fold higher than EGCG, but 5-fold lower than EC. Under these conditions, we observed slight prooxidant activity at 0.1 mg/L concentration ($p = 0.017$), similar to the prooxidant results observed for EC and ECGC.

V. macrocarpon and *T. inflorescentia* CTs have different interflavan linkages (Table 4.1); *V. macrocarpon* CTs have a more rigid structure due to the two interflavan A-type linkages⁵⁵ compared to *T. inflorescentia*'s B-type linkages. The significantly lower IC₅₀ values for *V. macrocarpon* may suggest that CTs with A-type linkages are more effective antioxidants than those with more B-type linkages, although more extensive testing of a variety of CT samples are needed to fully explore this relationship. It is likely that these different linkage patterns affect CT structure and metal coordination, leading to observed antioxidant behaviors.

Mackenzie *et al.*⁵⁶ showed through Monte Carlo simulation that in a dimer of EC subunits connected by B-linkages, subunits are stacked through formation of internal

hydrogen bonds. Based on this work, Verstraeten *et al.*⁵⁷ argued that a dimer with EC or catechin monomers connected by A-type linkages should not be able to fold over themselves due to the two covalent bonds and may not be able to stack, and should therefore exhibit a more elongated structure than condensed polyphenols with B-type linkages. This could result in A-type linkages having a greater number of accessible metal coordination sites. The presence of these accessible binding sites, may, in turn, result in greater antioxidant efficacy, since polyphenol-iron binding typically results in antioxidant rather than prooxidant effects.^{29,58,59} Thus, the greater percentage of A-type linkages found in *V. macrocarpon* CTs may correlate with greater efficacy in preventing both iron- and copper-mediated DNA damage, although additional studies are needed to elucidate the structures of condensed polyphenols as well as their metal binding properties to confirm this result.

Dong *et al.*⁴¹ tested A- and B-type dimers of either EC, EGC, or EGCG for their ability to scavenge DPPH (Figure 5.1) and observed the opposite trend as discussed in this Chapter of A-type linkages being better antioxidants than B-type linkages. DPPH is a long-lived, sterically-hindered, nitrogen-based radical with significantly different properties^{60,61} compared to the short-lived, more reactive hydroxyl and superoxide radicals.⁶² In addition, the steric bulk of the phenyl rings in DPPH may hinder reactivity at the radical site but still allow H-atom donors to donate their H-atom to form DPPH-H.⁶¹ Additionally, Gaulejac *et al.*³⁹ reported that B-type linked dimers of either two (+)-catechin or one (+)-catechin and one (-)-epicatechin are more effective at scavenging superoxide radical anion, a variance from the results presented here could be due to the different origin and reactivity these radical species. Although superoxide radical can react with iron, resulting in hydroxyl

radical formation,⁶³ metal coordination could play a more significant role in the antioxidant activity in our assay since the CTs could affect the redox potential of the metals as seen by some CTs having prooxidant activity at low concentrations (Table 5.1). It is likely that chemical differences between the radicals, such as size, stability, and charge, also alter the antioxidant abilities of CTs in addition to the type of linkages present between the polyphenol subunits.

V. macrocarpon CTs have a higher EC fraction than *H. lupulus* CTs (Table 4.1); *H. lupulus* CTs have more catechin subunits. Catechin and EC are isomers since that they differ in the stereochemical position of the phenolic OH group on the C-ring (Figure 4.1), resulting in EC and catechin having *R*- and *S*-confirmations at this site, respectively. From the DNA damage studies, CTs with a higher epicatechin content are 2- and 7-fold more effective in preventing copper- and iron-mediated DNA damage compared to catechin CTs, respectively (Table 4.2). This difference in activity between EC and catechin was also observed by Gaulejac *et al.*³⁹ who reported that EC as monomer was almost 2-fold more effective at scavenging the superoxide anion radical, and Vivas *et al.*⁶⁴ who reported that epicatechin monomers are more quickly oxidized during potentiometric titrations.^{39,64}

V. macrocarpon CTs are 7-fold more effective at preventing iron- and 2-fold more effective for copper-mediated DNA damage than CTs from *V. Vinifera* seed. This difference may result from *V. vinifera* seed CTs having a higher percentage of galloylation compared to *V. macrocarpon* CTs. Gaulejac *et al.*³⁹ report that galloyl groups in CTs have increased intramolecular π - π or σ - π interactions compared to CTs without galloylation, potentially increasing CT astringency and constraining proanthocyanidin conformations

within these compounds. These intramolecular interactions result in a very compact molecule, with some of the molecule being protected from external influences,³⁹ potentially shielding the inner functional groups from metal interactions.

Interestingly, all monomer polyphenols in Table 4.2 show prooxidant activity at low concentrations only for copper-mediated DNA damage but not for iron-mediated DNA damage; however, the condensed CTs exhibit the opposite trend. Prooxidant activity is observed for CTs with more B-type linkages or higher catechin content. Polyphenol prooxidant activity can arise from polyphenol compounds that can be readily oxidized after coordinating Cu^{2+} or Fe^{3+} , and reducing these ions to hydroxyl-radical-generating Cu^+ or Fe^{2+} .^{29,59}

Although metal coordination ability has not been well studied with regard to differences in CT structures, a study of grapeseed proanthocyanins showed that they strongly sequester metals with stoichiometric ratios of 2:1 and 4:1 for Fe^{2+} - and Cu^{2+} -proanthocyanin complexes, respectively.⁶⁵ Yoneda et al.⁶⁶ tested the relative stability of an aluminum-proanthocyanin complex, concluding that the catechol functionality of the B-ring is important for metal coordination. They also determined that at CT concentrations above 400 μM , increasing degree of polymerization generally increases the relative stability of the aluminum complex, but at lower concentrations, no significant difference in complex stability is observed. Powell et al.⁵¹ and Yoneda et al.⁵² describe the importance of the three-dimensional structure of CTs for metal binding, due to the potential new coordination sites that can arise from spatially adjacent functional groups, but little work has investigated the impact of various conformations on the number, availability, and

location of metal coordination sites. These scattered results highlight the need to independently understand the effects of different CT linkages, galloylation percentages, monomer compositions, and polymer lengths on metal coordination to better predict antioxidant activity of CTs from various sources.

5.3 Conclusions

V. macrocarpon CTs are the most effective at inhibiting both copper- and iron-mediated DNA damage compared to *H. lupulus*, *V. vinifera* seed, and *T. inflorescentia* CTs. Although *H. lupulus*, *V. vinifera* seed, and *T. inflorescentia* CTs prevent little-to-no copper-mediated DNA damage, they prevent significantly more iron-mediated DNA damage at low micromolar concentrations. Only *H. lupulus* and *T. inflorescentia* CTs promote iron-mediated DNA damage at very low (0.1 and 1 mg/L) concentrations in addition to antioxidant activity at higher concentrations, the first report of this dual activity with iron.

This is the first study to investigate the ability of CTs with several different structural characteristics for prevention metal-mediated DNA damage. CTs with A-type linkages, such as in *V. macrocarpon* may more effectively inhibit copper- and iron-mediated DNA damage than CTs with B-type linkages. In addition, higher percentages of catechin compared to epicatechin subunits and higher percentages of galloylation may also reduce CT antioxidant activity. Although these results require further study to establish trends among a variety of CTs, these results demonstrate the significant effects of CT structural features on antioxidant efficacy.

4.4 Experimental Methods

Materials. Water was deionized (diH₂O) using a Nano Pure DIAMOND Ultrapure H₂O system (Barnstead International). CuSO₄ and H₂O₂ were purchased from Fisher. 3-(*N*-morpholino)propanesulfonic acid (MOPS), was purchased from Sigma Aldrich, 2-(*N*-morpholino)ethanesulfonic acid (MES) was purchased from BDH, FeSO₄ was purchased from Acros and ascorbic acid and NaCl were purchased from Alfa Aesar. The condensed CTs were provided by Dr. Wayne Zeller at the USDA (Madison, WI).

Isolation and Purification of Condensed Tannins. Condensed tannins were purified from *H. lupulus* (hops), *V. vinifera* (grapeseed) and *T. inflorescentia* flowers using methods previously described.³³ *V. macrocarpon* (cranberry) CTs were obtained through purification of commercially available fresh frozen cranberries obtained from a local grocer. Thawed cranberries were placed in a blender, diluted and homogenized. The homogenate was vacuum filtered with a Buchner funnel equipped with a filter paper. The resulting press cake was lyophilized and ground in a cyclone mill (UDY Corporation, For Collins, CO) to ≤ 1 mm. Portions of the ground cranberry press cake were extracted with acetone/water (7:3, 5 ml/g of cake), and the combined extracts were concentrated under reduced pressure and lyophilized. The lyophilized cranberry CT extract was subjected to the batch method of purification using Sephadex LH-20 as previously described using the methanol/water (1:1) washes followed by consecutive elution of the CT-laden Sephadex LH-20 gel with acetone/water mixtures of (3:7), (1:1) and (7:3) v/v. Fractions eluting with 7:3 acetone/water portion were combined and lyophilized. Lyophilized powders were examined by ¹H-¹³C HSQC NMR spectroscopy. The fractions containing high CT content

were pooled and the lipid impurities present in these fractions were removed by centrifugation of their aqueous suspensions. dissolved in water (at 4 mg/mL), centrifugation at 10,000 X g for 20 min. The supernatant was decanted and lyophilized to provide the target *V. macrocarpon* CT preparation. Structural composition (PC/PD and cis/trans ratios, determination of mean degrees of polymerization, mDP) of CTs isolated were determined through a combination of thiolytic degradation and analysis of their respective ^1H - ^{13}C HSQC NMR spectra.^{37,38} The percent A-type linkage present in the cranberry CT was estimated through relative integration of the H/C-4 cross-peak arising from A-type linked subunit to sum of the normal internal and terminal B-type linked subunits cross-peaks.

NMR Analysis. ^1H , ^{13}C and ^1H - ^{13}C HSQC NMR spectra were recorded at 27 °C on a BrukerBiospin DMX-500 (^1H 500.13 MHz, ^{13}C 125.76 MHz) instrument equipped with TopSpin 3.5 software and a cryogenically cooled 5-mm TXI $^1\text{H}/^{13}\text{C}/^{15}\text{N}$ gradient probe in inverse geometry. Spectra were recorded in DMSO-*d*6 and were referenced to the residual signals of DMSO-*d*6 (2.49 ppm for ^1H and 39.5 ppm for ^{13}C spectra). ^{13}C NMR spectra were obtained using 1K scans (acquisition time 56 min). For ^1H - ^{13}C HSQC experiments, spectra were obtained using between 200 and 620 scans (depending on sample size and instrument availability) obtained using the standard Bruker pulse program (hsqcetgpsisp.2) with the following parameters: Acquisition: TD 1024 (F2), 256 (F1); SW 16.0 ppm (F2), 165 ppm (F1); O1 2350.61 Hz; O2 9431.83 Hz; D1 = 1.50 s; CNST2 = 145. Acquisition time: F2 channel, 64 ms, F1 channel 6.17 ms. Processing: SI =1024 (F2, F1), WDW = QSINE, LB = 1.00 Hz (F2), 0.30 Hz (F1); PH_mod = pk; baseline

correction ABSG =5 (F2, F1), BCFW = 1.00 ppm, BC mod = quad (F2), no (F1); linear prediction = no (F2), LPfr (F1). Sample sizes used for these spectra ranged from 5-10 mg providing NMR sample solutions with concentrations of 10-20 mg/mL.

Plasmid Transfection, Amplification, and Purification: 2.5-3 μL (1 pmol) of plasmid DNA (pBSSK) was purified from DH1 *E. coli* competent cells using Zyppy™ Plasmid Miniprep Kit (400 count, Zymo Research). Tris-EDTA buffer (pH 8.01) was used to elude the plasmid from the spin columns. Plasmid was dialyzed against 130 mM NaCl for 24 hours at 4°C to ensure all Tris-EDTA buffer and metal contaminants were removed. Plasmid concentration was determined by UV-vis spectroscopy at a wavelength of 260 nm. Organic and protein contents were also determined using UV-vis spectroscopy from ratios of $A_{250}/A_{260} \leq 0.95$ and $A_{260}/A_{280} \geq 1.8$ respectively. Plasmid purity was determined through digestion of plasmid with Sac I and KpnI in a mixture of NEB buffer and BSA (bovine serum albumin) was conducted at 37°C for 90 min. Comparison to an undigested plasmid sample and a 1 kb molecular-weight marker was conducted by gel electrophoresis.

Plasmid DNA damage inhibition assays. Gel electrophoresis samples were prepared in deionized H₂O, MOPS buffer (10 mM, pH 7) for copper or MES buffer (10 mM, pH 6) for iron, NaCl (130 mM), 100% ethanol (10 mM), ascorbate (7.25 μM) and CuSO₄ (6 μM) or FeSO₄ (2 μM) and indicated concentrations of the CTs were combined in a microcentrifuge tube and allowed to stand for 5 min at room temperature. Since Cu⁺ is unstable in aqueous solution, ascorbic acid was added to reduce Cu²⁺ to Cu⁺ before the addition of H₂O₂ in these studies. Plasmid (pBSSK; 0.1 pmol in 130 mmol NaCl solution) was then added to the reaction mixture and allowed to stand for 5 min at room temperature.

Hydrogen peroxide (50 μM) was added to the indicated lanes and allowed to react at room temperature for 30 min, then EDTA (50 μM) was added to quench the reaction and loading dye (2 μL) was added. All given concentrations are final concentrations in a 12 μL volume. Samples were loaded into a 1% agarose gel in TAE running buffer; and damaged and undamaged plasmid DNA was separated by electrophoresis (140 V for 30 min). Gels were then stained using ethidium bromide and washed with dH_2O before being imaged under UV light. The amounts of nicked (damaged) and circular (undamaged) DNA were quantified using UViProMW (Jencons Scientific Inc.). The intensity of the circular plasmid band was multiplied by 1.24, due to the different binding abilities of ethidium bromide to supercoiled and nicked plasmid DNA.^{67,68} Intensities of the nicked and supercoiled bands were normalized for each lane so that % nicked + % supercoiled = 100%. All percentages were corrected for residual nicked DNA prior to calculation. Results were obtained in triplicate for all experiments, and standard deviations are represented as error bars.

Calculation of percent DNA damage inhibition. The formula $1 - [\%N - \%B] * 100$ was used to calculate percent DNA damage inhibition; %N = percent of nicked DNA in lanes 4, and %B = the percent of nicked DNA in the $\text{Cu}^{2+}/\text{H}_2\text{O}_2$ or $\text{Fe}^{2+}/\text{H}_2\text{O}_2$ control lanes. Percentages were corrected for residual nicked DNA (lane 2) prior to calculations. Results were obtained from an average of three trials, with indicated standard deviations.

IC₅₀ Determination. Plots of percent inhibition of DNA damage versus log concentration of CTs were fit to a variable slope sigmoidal dose-response curve using SigmaPlot, version 11 (Systat Software, Inc.). DNA damage inhibition were omitted (concentrations 0.1 mg/L for *H. lupulus* CTs and 0.5 and 1 mg/L for *T. inflorescentia* CTs).

IC₅₀ value errors were calculated from error propagation of the gel electrophoresis measurements. Statistical significance was determined by calculating p values at 95% confidence ($p < 0.05$ indicates significance) as described by Perkowski et al.⁶⁹ Data from DNA damage assays are provided in Tables 4.5-4.10.

4.5. Supporting Information

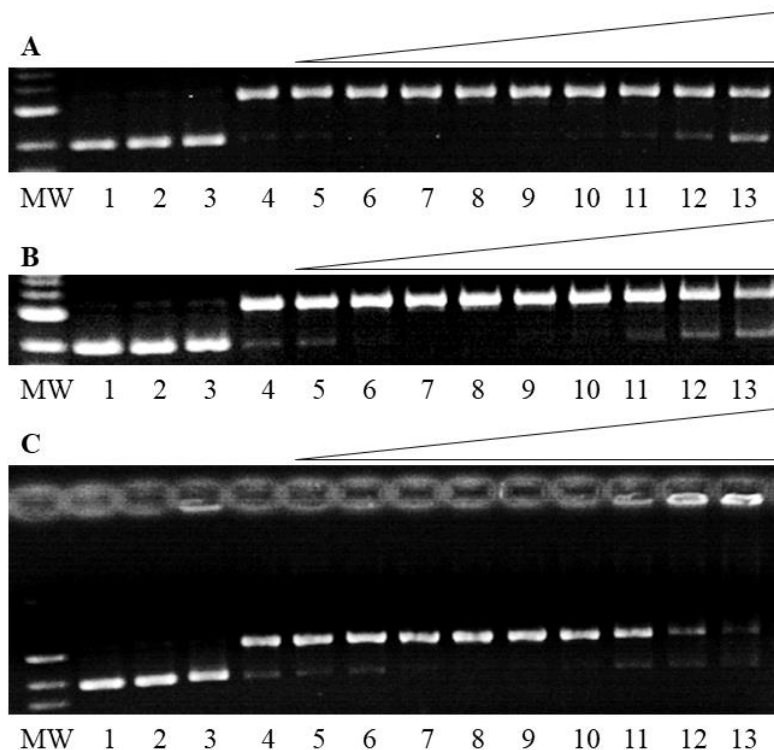


Figure 4.4. Agarose gel electrophoresis images of copper-mediated DNA damage prevention with *Vitis vinifera* seed, *Humulus lupulus*, or *Tilia inflourescentia* condensed tannins. Lanes are: MW: 1 kb molecular weight marker; lane 1: plasmid DNA (p); lane 2: p + H₂O₂ (50 μM); A) lane 3: p + 200 mg/L *V. vinifera* seed + H₂O₂, lane 4: p + Cu²⁺ (6 μM) + ascorbate (7.5 μM) + H₂O₂; lanes 5-13: p + Cu²⁺ + ascorbate + H₂O₂ + 0.1, 1, 5, 10, 15, 25, 50, 100, and 200 mg/L *V. vinifera* seed, respectively; B) lane 3: p + 200 mg/L *H. lupulus* + H₂O₂, lane 4: p + Cu²⁺ (6 μM) + ascorbate (7.5 μM) + H₂O₂; lanes 5-13: p + Cu²⁺ + ascorbate + H₂O₂ + 0.1, 1, 5, 10, 15, 25, 50, 100, and 200 mg/L *H. lupulus*, respectively; C) lane 3: p + 200 mg/L *T. inflourescentia* + H₂O₂, lane 4: p + Cu²⁺ (6 μM) + ascorbate (7.5 μM) + H₂O₂; lanes 5-13: p + Cu²⁺ + ascorbate + H₂O₂ + 0.1, 1, 5, 10, 15, 25, 50, 100, and 200 mg/L *T. inflourescentia*, respectively.

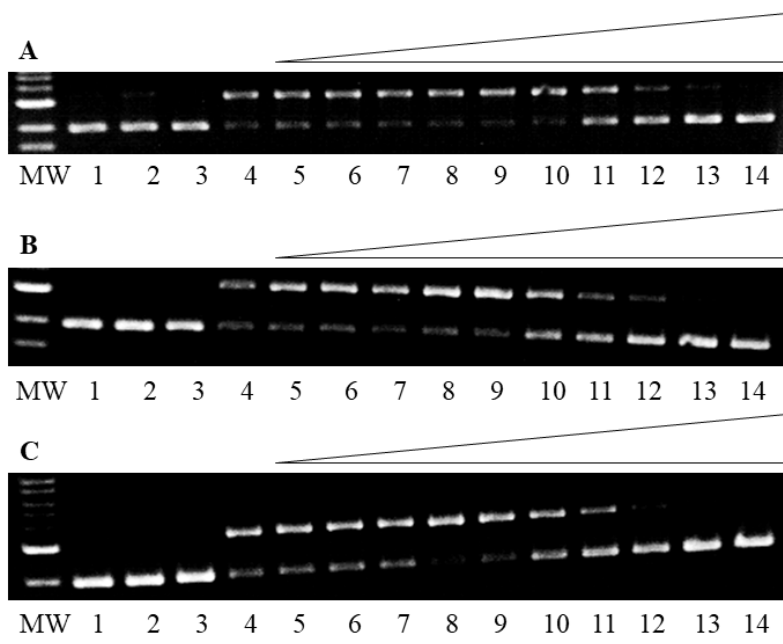


Figure 4.5. Agarose gel electrophoresis images of iron-mediated DNA damage prevention with *Vitis vinifera* seed, *Humulus lupulus*, or *Tilia inflorrescentia* condensed tannins. Lanes are: MW: 1kb molecular weight marker; lane 1: plasmid DNA (p); lane 2: p + H₂O₂ (50 μM); A) lane 3: p + 200 mg/L *V. vinifera* seed + H₂O₂, lane 4: p + Fe²⁺ (2 μM) + H₂O₂; lane 5-14: p + Fe²⁺ + H₂O₂ + 0.001, 0.01, 0.1, 0.5, 1, 2.5, 5, 10, 25, and 50 mg/L *V. vinifera* seed, respectively); B) lane 3: p + 200 mg/L *H. lupulus* + H₂O₂, lane 4: p + Fe²⁺ (2 μM) + H₂O₂; lane 5-14: p + Fe²⁺ + H₂O₂ + 0.001, 0.01, 0.1, 0.5, 1, 2.5, 5, 10, 25, and 50 mg/L *H. lupulus*, respectively; C) lane 3: p + 200 mg/L *T. inflorrescentia* + H₂O₂, lane 4: p + Fe²⁺ (2 μM) + H₂O₂; lane 5-14: p + Fe²⁺ + H₂O₂ + 0.001, 0.01, 0.1, 0.5, 1, 2.5, 5, 10, 25, and 50 mg/L *T. inflorrescentia*, respectively.

Table 4.3. Gel electrophoresis results for Cu⁺ DNA damage prevention assays with *Vaccinium macrocarpon* condensed tannins.^a

Gel lane	[<i>V. macrocarpon</i>] mg/L	% Supercoiled	% Nicked	% Damage Inhibition	<i>p</i> Value
1: plasmid DNA (p)	0	100 ± 0	0	–	–
2: p + H ₂ O ₂ (50 µM)	0	99.96 ± 0.07	0.04	–	–
3: p + <i>V. macrocarpon</i> + H ₂ O ₂	0.1	99.99 ± 0.01	0.01	–	–
4: p + Cu ²⁺ (6 µM) + ascorbate (7.5 µM) + H ₂ O ₂	0	5.13 ± 0.59	94.87	0	–
5: p + Cu ²⁺ + ascorbate + H ₂ O ₂ + <i>V. macrocarpon</i>	0.1	1.63 ± 0.15	98.37	-3.64 ± 0.15	< 0.001
6:	1	0.13 ± 0.12	99.87	-5.26 ± 0.10	< 0.001
7:	5	0.79 ± 0.24	99.21	-4.52 ± 0.26	0.001
8:	15	6.31 ± 1.12	93.69	1.31 ± 1.12	0.180
9:	25	13.71 ± 5.51	86.29	9.08 ± 5.48	0.103
10:	50	20.99 ± 1.62	79.01	16.77 ± 1.59	0.003
11:	100	32.31 ± 5.30	67.69	28.68 ± 5.31	0.011
12:	200	60.73 ± 3.92	39.27	58.72 ± 3.82	0.001

^aData are reported as the average of three trials with calculated standard deviations shown.

Table 4.4. Gel electrophoresis results for Fe²⁺ DNA damage prevention assays with *Vaccinium macrocarpon* condensed tannins.^a

Gel lane	[<i>V. macrocarpon</i>] mg/L	% Supercoiled	% Nicked	% Damage Inhibition	<i>p</i> Value
1: plasmid DNA (p)	0	100 ± 0	0	–	–
2: p + H ₂ O ₂ (50 µM)	0	100 ± 0	0	–	–
3: p + <i>V. macrocarpon</i> + H ₂ O ₂	0.001	99.96 ± 0.07	0.04	–	–
4: p + Fe ²⁺ (2 µM) + H ₂ O ₂	0	5.69 ± 3.81	94.31	0	–
5: p + Fe ²⁺ + H ₂ O ₂ + <i>V. macrocarpon</i>	0.001	8.27 ± 1.54	91.73	2.73 ± 1.56	0.938
6:	0.01	1.95 ± 1.16	98.05	-3.95 ± 1.17	0.280
7:	0.1	7.01 ± 2.01	92.99	1.42 ± 2.02	0.348
8:	0.5	9.25 ± 1.31	90.75	3.76 ± 1.30	0.376
9:	0.7	38.20 ± 0.70	61.80	34.47 ± 0.50	< 0.001
10:	1	92.02 ± 3.88	7.98	91.55 ± 3.90	< 0.001
11:	2.5	97.90 ± 1.99	2.10	97.77 ± 1.99	< 0.001
12:	5	99.99 ± 0.01	0.01	100 ± 0	< 0.001

^aData are reported as the average of three trials with calculated standard deviations shown.

Table 4.5. Gel electrophoresis results for Cu⁺ DNA damage prevention assays with *Vitis vinifera* seed condensed tannins.^a

Gel lane	[<i>V. vinifera</i> seed]mg/L	% Supercoiled	% Nicked	% Damage Inhibition	<i>p</i> Value
1: plasmid DNA (p)	0	100.00 ± 0	0.00	-	-
2: p + H ₂ O ₂ (50 μM)	0	99.94 ± 0.05	0.06	-	-
3: p + <i>V. vinifera</i> seed + H ₂ O ₂	200	100.00 ± 0	0.00	-	-
4: p + Cu ²⁺ (6 μM) + ascorbate (7.5 μM) + H ₂ O ₂	0	5.26 ± 3.94	94.74	-	-
5: p + Cu ²⁺ + ascorbate + H ₂ O ₂ + <i>V. Vinifera</i> seed	0.1	1.95 ± 2.21	98.05	-3.45 ± 2.23	0.116
6:	1	1.18 ± 1.86	98.82	-4.26 ± 1.85	0.057
7:	5	1.04 ± 1.81	98.96	-4.40 ± 1.79	0.051
8:	10	0.27 ± 0.33	99.73	-5.21 ± 0.31	0.001
9:	15	1.74 ± 2.95	98.26	-3.63 ± 2.97	0.168
10:	25	1.75 ± 2.90	98.25	-3.63 ± 2.89	0.162
11:	50	9.06 ± 5.95	90.94	4.08 ± 5.99	0.359
12:	100	8.75 ± 1.48	91.25	3.73 1.53	0.052
13:	200	32.00 ± 4.51	68.00	28.28 ± 4.55	0.009

^aData are reported as the average of three trials with calculated standard deviations shown.

Table 4.6. Gel electrophoresis results for Fe²⁺ DNA damage prevention assays with *Vitis vinifera* seed condensed tannins.^a

Gel lane	[<i>V. vinifera</i> seed] mg/L	% Supercoiled	% Nicked	% Damage Inhibition	<i>p</i> Value
1: plasmid DNA (p)	0	100.00 ± 0	0.00	-	-
2: p + H ₂ O ₂ (50 μM)	0	99.99 ± 0.02	0.01	-	-
3: p + <i>V. vinifera</i> seed + H ₂ O ₂	50	100.00 ± 0	0.00	-	-
4: p + Fe ²⁺ (2 μM) + H ₂ O ₂	0	8.58 ± 4.81	91.42	-	-
5: p + Fe ²⁺ + H ₂ O ₂ + <i>V. vinifera</i> seed	0.001	5.91 ± 2.96	94.09	-2.87 ± 2.94	0.233
6:	0.01	10.00 ± 1.30	90.00	1.58 ± 1.30	0.170
7:	0.1	6.75 ± 2.71	93.25	-2.00 ± 2.75	0.335
8:	0.5	6.07 ± 5.18	93.93	-2.73 ± 5.18	0.458
9:	1	1.39 ± 1.54	98.61	-7.87 ± 1.53	0.124
10:	2.5	0.80 ± 0.45	99.20	-8.49 ± 0.44	>0.001
11:	5	54.73 ± 3.63	45.27	50.47 ± 3.64	0.002
12:	10	94.37 ± 2.49	5.63	93.86 ± 2.48	>0.001
13:	25	100.00 ± 0	0.00	100.02 ± 0	>0.001
14:	50	99.95 ± 0.09	0.05	99.95 ± 0.12	>0.001

^aData are reported as the average of three trials with calculated standard deviations shown.

Table 4.7. Gel electrophoresis results for Cu⁺ DNA damage prevention assays with *Humulus lupulus* condensed tannins.^a

Gel lane	[<i>H. lupulus</i>], mg/L	% Supercoiled	% Nicked	% Damage Inhibition	<i>p</i> Value
1: plasmid DNA (p)	0	100.00 ± 0	0.00	-	-
2: p + H ₂ O ₂ (50 μM)	0	98.71 ± 2.23	1.29	-	-
3: p + <i>H. lupulus</i> + H ₂ O ₂	200	100.00 ± 0	0.00	-	-
4: p + Cu ²⁺ (6 μM) + ascorbate (7.5 μM) + H ₂ O ₂	0	3.20 ± 3.22	96.80	-	-
5: p + Cu ²⁺ + ascorbate + H ₂ O ₂ + <i>H. lupulus</i>	0.1	3.75 ± 2.33	96.25	-1.52 ± 2.33	0.376
6:	1	0.13 ± 0.17	99.87	-5.35 ± 0.15	>0.001
7:	5	0.07 ± 0.12	99.93	-5.42 ± 0.12	>0.001
8:	10	0.72 ± 1.25	99.28	-4.72 ± 1.27	0.023
9:	15	0.36 ± 0.52	99.64	-5.10 ± 0.55	0.004
10:	25	0.74 ± 1.15	99.26	-4.68 ± 1.16	0.020
11:	50	3.43 ± 3.06	96.57	-1.87 ± 3.03	0.397
12:	100	14.68 ± 6.11	85.32	10.02 ± 6.09	0.104
13:	200	31.45 ± 5.26	68.55	27.69 ± 5.27	0.012

^aData are reported as the average of three trials with calculated standard deviations shown.

Table 4.8. Gel electrophoresis results for Fe²⁺ DNA damage prevention assays with *Humulus lupulus* condensed tannins.^a

Gel lane	[<i>H. lupulus</i>], mg/L	% Supercoiled	% Nicked	% Damage Inhibition	<i>p</i> Value
1: plasmid DNA (p)	0	99.83 ± 0.29	0.17	-	-
2: p + H ₂ O ₂ (50 μM)	0	99.95 ± 0.09	0.05	-	-
3: p + <i>H. lupulus</i> + H ₂ O ₂	50	99.99 ± 0.02	0.01	-	-
4: p + Fe ²⁺ (2 μM) + H ₂ O ₂	0	25.20 ± 3.99	74.80	-	-
5: p + Fe ²⁺ + H ₂ O ₂ + <i>H. lupulus</i>	0.001	30.88 ± 4.53	69.12	7.74 ± 4.52	0.097
6:	0.01	28.49 ± 2.41	71.51	4.53 ± 2.39	0.082
7:	0.1	14.53 ± 3.29	85.47	-14.18 ± 3.27	0.017
8:	0.5	20.49 ± 3.20	79.51	-6.16 ± 3.21	0.939
9:	1	19.24 ± 2.04	80.76	-7.86 ± 2.06	0.022
10:	2.5	50.65 ± 1.13	49.35	34.17 ± 1.11	>0.001
11:	5	75.09 ± 1.37	24.91	66.79 ± 1.34	>0.001
12:	10	91.71 ± 3.33	8.29	89.02 ± 3.38	>0.001
13:	25	97.94 ± 3.43	2.06	97.40 ± 3.44	>0.001
14:	50	99.89 ± 0.19	0.11	99.99 ± 0.17	>0.001

^aData are reported as the average of three trials with calculated standard deviations shown.

Table 4.9. Gel electrophoresis results for Cu⁺ DNA damage prevention assays with *Tilia inflourescentia* condensed tannins.^a

Gel lane	[<i>T. inflourescentia</i>], mg/L	% Supercoiled	% Nicked	% Damage Inhibition	<i>p</i> Value
1: plasmid DNA (p)	0	100.00 ± 0	0.00	-	-
2: p + H ₂ O ₂ (50 μM)	0	100.00 ± 0	0.00	-	-
3: p + <i>T. inflourescentia</i> + H ₂ O ₂	200	99.99 ± 0.02	0.01	-	-
4: p + Cu ²⁺ (6 μM) + ascorbate (7.5 μM) + H ₂ O ₂	0	3.68 ± 2.47	96.32	-	-
5: p + Cu ²⁺ + ascorbate + H ₂ O ₂ + <i>T. inflourescentia</i>	0.1	3.62 ± 0.10	96.38	-1.66 ± 0.06	>0.001
6:	1	2.34 ± 1.72	97.66	-3.03 ± 1.71	0.092
7:	5	0.50 ± 0.09	99.50	-4.96 ± 0.10	>0.001
8:	10	0.46 ± 0.44	99.54	-5.00 ± 0.45	0.003
9:	15	0.25 ± 0.19	99.75	-5.25 ± 0.21	>0.001
10:	25	1.01 ± 1.07	98.99	-4.40 ± 1.07	0.019
11:	50	11.16 ± 5.66	88.84	6.26 ± 5.66	0.195

^aData are reported as the average of three trials with calculated standard deviations shown.

Table 4.10. Gel electrophoresis results for Fe²⁺ DNA damage prevention assays with *Tilia inflourescentia* condensed tannins.^a

Gel lane	[<i>T. inflourescentia</i>], mg/L	% Supercoiled	% Nicked	% Damage Inhibition	<i>p</i> Value
1: plasmid DNA (p)	0	100.00 ± 0	0.00	-	-
2: p + H ₂ O ₂ (50 μM)	0	99.96 ± 0.06	0.04	-	-
3: p + <i>T. inflourescentia</i> + H ₂ O ₂	50	100.00 ± 0	0.00	-	-
4: p + Fe ²⁺ (2 μM) + H ₂ O ₂	0	26.22 ± 1.84	73.78	-	-
5: p + Fe ²⁺ + H ₂ O ₂ + <i>T. inflourescentia</i>	0.001	23.40 ± 1.21	76.60	-3.77 ± 1.22	0.033
6:	0.01	22.47 ± 1.26	77.53	-5.03 ± 1.31	0.022
7:	0.1	21.30 ± 4.38	78.70	-6.61 ± 4.36	0.120
8:	0.5	14.56 ± 0.95	85.44	-15.74 ± 0.95	0.001
9:	1	14.12 ± 1.31	85.88	-16.33 ± 1.32	0.002
10:	2.5	45.10 ± 1.99	54.90	25.64 ± 1.95	0.002
11:	5	63.36 ± 3.28	36.64	50.40 ± 3.31	0.001
12:	10	93.85 ± 4.53	6.15	92.15 ± 4.95	>0.001
13:	25	96.52 ± 4.83	3.48	95.36 ± 4.84	>0.001
14:	50	100 ± 0	0	100.05 ± 0	>0.001

^aData are reported as the average of three trials with calculated standard deviations shown.

4.6. References

- (1) Gu, L.; Kelm, M. A.; Hammerstone, J. F.; Beecher, G.; Holden, J.; Haytowitz, D.; Prior, R. L. *J. Agric. Food Chem.* **2003**, *51*, 7513–7521.
- (2) Scalbert, A.; Déprez, S.; Mila, I.; Albrecht, A.-M.; Huneau, J.-F.; Rabot, S. *BioFactors* **2000**, *13*, 115–120.
- (3) Beecher, G. R. *Arch. Physiol. Biochem.* **2004**, *42*, 2–20.
- (4) Serrano, J.; Puupponen-Pimiä, R.; Dauer, A.; Aura, A.-M.; Saura-Calixto, F. *Mol. Nutr. Food Res.* **2009**, *53*, 310–329.
- (5) Es-Safi, N.-E.; Guyot, S.; Ducrot, P. *J. Agric. Food Chem.* **2006**, *54*, 6969–6977.
- (6) Tian, Y.; Zou, B.; Li, C.-M.; Yang, J.; Xu, S.-f.; Hagerman, A. E. *Food Res. Int.* **2012**, *45*, 26–30.
- (7) Hagerman, A. E.; Riedl, K. M.; Jones, G. A.; Sovik, K. N.; Ritchard, N. T.; Hartzfeld, P. W.; Riechel, T. L. *J. Agric. Food Chem.* **1998**, *46*, 1887–1892.
- (8) Cos, P.; Bruyne, T.; Hermans, N.; Apers, S.; Berghe, D.; Vlietinck, A. *Curr. Med. Chem.* **2004**, *11*, 1345–1359.
- (9) Glisan, S. L.; Ryan, C.; Neilson, A. P.; Lambert, J. D. *J. Nutr. Biochem.* **2016**, *37*, 60–66.
- (10) Bártíková, H.; Boušová, I.; Jedličková, P.; Lněničková, K.; Skálová, L.; Szotáková, B. *Molecules* **2014**, *19*, 14948–14960.
- (11) Wojnicz, D.; Sycz, Z.; Walkowski, S.; Gabrielska, J.; Aleksandra, W.; Alicja, K.; Anna, S.-Ł.; Hendrich, A. B. *Phytomedicine* **2012**, *19*, 506–514.

- (12) Maisuria, V. B.; Los Santos, Y. L.-d.; Tufenkji, N.; Déziel, E. *C Sci. Rep.* **2016**, *6*, 30169-30181.
- (13) Ramirez-Hernandez, A.; Rupnow, J.; Hutkins, R. W. *J. Food Prot.* **2015**, *78*, 1496–1505.
- (14) Morán, A.; Gutiérrez, S.; Martínez-Blanco, H.; Ferrero, M. A.; Monteagudo-Mera, A.; Rodríguez-Aparicio, L. B. *Biofouling* **2014**, *30*, 1175–1182.
- (15) Lee, J. H.; Ji, Y. J. *Korean Soc. Food Sci. Nutr.* **2015**, *44*, 1100–1103.
- (16) Begcevic, I.; Simundic, A.-M.; Nikolac, N.; Dobrijevic, S.; Rajkovic, M. G.; Tesija-Kuna, A. *Clin. Lab.* **2013**, *59*, 1053-1060.
- (17) Houlton, S. *Chem. Ind.* **2006**, *16*, 17–19.
- (18) Prasain, J. K.; Rajbhandari, R.; Keeton, A. B.; Piazza, G. A.; Barnes, S. *Food Funct.* **2016**, *7*, 4012–4019.
- (19) Anhe, F. F.; Roy, D.; Pilon, G.; Dudonne, S.; Matamoros, S.; Varin, T. V.; Garofalo, C.; Moine, Q.; Desjardins, Y.; Levy, E. Murette, A. *Gut* **2015**, *64*, 872–883.
- (20) Bousova, I.; Bartikova, H.; Matouskova, P.; Lnenickova, K.; Zappe, L.; Valentova, K.; Szotakova, B.; Martin, J.; Skalova, L. *Nutr. Res.* **2015**, *35*, 901–909.
- (21) Blumberg, J. B.; Camesano, T. A.; Cassidy, A.; Kris-Etherton, P.; Howell, A.; Manach, C.; Ostertag, L. M.; Sies, H.; Skulas-Ray, A.; Vita, J. A. *Adv. Nutr.* **2013**, *4*, 618–632.
- (22) Martín, M. A.; Ramos, S.; Mateos, R.; Marais, J. P.J.; Bravo-Clemente, L.; Khoo, C.; Goya, L. *Food Res. Int.* **2015**, *71*, 68–82.

- (23) Haslam, E. *Practical polyphenolics: From structure to molecular recognition and physiological action*: Cambridge University Press: Cambridge, 2005.
- (24) Schofield, P.; Mbugua, D.M.; Pell, A.N. *Anim. Feed Sci. Tech.* **2001**, *91*, 21–40.
- (25) Hümmer, W.; Schreier, P. *Mol. Nutr. Food Res.* **2008**, *52*, 1381–1398.
- (26) Quideau, S.; Deffieux, D.; Douat-Casassus, C.; Pouységu, L. *Angew. Chem.* **2011**, *50*, 586–621.
- (27) Pappas, E.; Schaich, K. M. *Crit. Rev. Food Sci. Nutr.* **2009**, *49*, 741–781.
- (28) Zhang, K.; Zuo, Y. *J. Agric. Food Chem.* **2004**, *52*, 222–227
- (29) Perron, N. R.; Brumaghim, J. L. *Cell Biochem. Biophys.* **2009**, *53*, 75–100.
- (30) Perron, N. R.; Wang, H. C.; Deguire, S. N.; Jenkins, M.; Lawson, M.; Brumaghim, J. L. *Dalton Trans.* **2010**, *39*, 9982–9987.
- (31) Zimmerman, M. T.; Bayse, C. A.; Ramoutar, R. R.; Brumaghim, J. L. *J. Inorg. Biochem.* **2015**, *145*, 30–40.
- (32) Avdeef, A.; Sofen, S. R.; Bregante, T. L.; Raymond, K. N. *J. Am. Chem. Soc.* **1978**, *100*, 5362–5370.
- (33) Kipton, H.; Powell, J.; Rate, A. W. *Aust. J. Chem.* **1987**, *40*, 2015–2022.
- (34) Chvátalová, K.; Slaninová, I.; Březinová, L.; Slanina, J. *Food Chem.* **2008**, *106*, 650–660.
- (35) Perron, N. R.; García, C. R.; Pinzón, J. R.; Chaur, M. N.; Brumaghim, J. L. *J. Inorg. Biochem.* **2011**, *105*, 745–753.
- (36) Perron, N. R.; Hodges, J. N.; Jenkins, M.; Brumaghim, J. L. *Inorg. Chem.* **2008**, *47*, 6153–6161.

- (37) Naumann, H.; Sepela, R.; Rezaire, A.; Masih, S. E.; Zeller, W. E.; Reinhardt, L. A.; Robe, J. T.; Sullivan, M. L.; Hagerman, A. E. *Molecules* **2018**, *23*, 2123-2139.
- (38) Zeller, W. E.; Ramsay, A.; Ropiak, H. M.; Fryganas, C.; Mueller-Harvey, I.; Brown, R. H.; Drake, C.; Grabber, J. H. *J. Agric. Food Chem.* **2015**, *63*, 1967–1973.
- (39) Gaulejac, N. S.-C. de; Vivas, N.; Freitas, V. de; Bourgeois, G. *J. Sci. Food Agric.* **1999**, *79*, 1081–1090.
- (40) Jerez, M.; Touriño, S.; Sineiro, J.; Torres, J. L.; Núñez, M. J. *Food Chem.* **2007**, *104*, 518–527.
- (41) Dong, X.-Q.; Zou, B.; Zhang, Y.; Ge, Z.-Z.; Du, J.; Li, C.-M. *Fitoterapia* **2013**, *91*, 128–139.
- (42) Touati, D. *Arch. Biochem. Biophys.* **2000**, *373*, 1–6.
- (43) Blokhina, O.; Virolainen, E.; Fagerstedt, K. V. *Ann. Bot.* **2003**, *91*, 179–194.
- (44) Valko, M.; Morris, H.; Cronin, M. *Curr. Med. Chem.* **2005**, *12*, 1161–1208.
- (45) Çakar, S.; Güy, N.; Özacar, M.; Fındık, F. *Electrochim. Acta* **2016**, *209*, 407–422.
- (46) Zeng, X.; Du, Z.; Sheng, Z.; Jiang, W. *Food Res. Int.* **2019**, *123*, 518–528.
- (47) Zeng, X.; Du, Z.; Xu, Y.; Sheng, Z.; Jiang, W. *LWT- Food Sci. Technol.* **2019**, *114*, 108384-108393.
- (48) Perron, N. R. Effects of polyphenol compounds on iron-and copper-mediated DNA damage: mechanisms and predictive models. Dissertation, Clemson Univeristy, Clemson, 2008.
- (49) Oscar, S.-V.; Fernando, O.-C. L.; Del Pilar, C.-M. M. *Food Chem.* **2017**, *221*, 1062–1068.

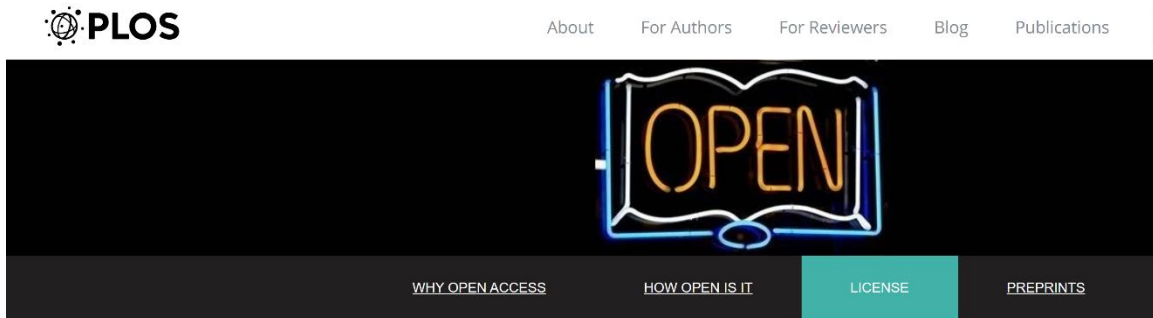
- (50) Yashin, A.; Nemzer, B.; Yashin, Y. *J. Food Res.* **2012**, *1*, 281-290.
- (51) Kleemann, R.; Verschuren, L.; Morrison, M.; Zadelaar, S.; van Erk, M. J.; Wielinga, P. Y.; Kooistra, T. *Atherosclerosis* **2011**, *218*, 44–52.
- (52) Chung, K. T.; Wong, T. Y.; Wei, C. I.; Huang, Y. W.; Lin, Y. *Crit. Rev. Food Sci. Nutr.* **1998**, *38*, 421–464
- (53) Larrauri, J. A.; Sánchez-Moreno, C.; Rupérez, P.; Saura-Calixto, F. *J. Agric. Food Chem.* **1999**, *47*, 1603–1606.
- (54) Perron, N. R. Effects of polyphenol compounds on iron-and copper-mediated DNA damage: mechanisms and predictive models. Dissertation, Clemson Univeristy, Clemson, 2008.
- (55) Watson, R. R.; Preedy, V. R.; Zibadi, S. *Polyphenols in human health and disease.*; Elsevier/Academic Press: Amsterdam, Boston, 2014; pp 339-351.
- (56) Mackenzie, G. G.; Carrasquedo, F.; Delfino, J. M.; Keen, C. L.; Fraga, C. G.; Oteiza, P. I. *FASEB J.* **2004**, *18*, 167–169.
- (57) Verstraeten, S. V.; Hammerstone, J. F.; Keen, C. L.; Fraga, C. G.; Oteiza, P. I. *J. Agric. Food Chem.* **2005**, *53*, 5041–5048.
- (58) Moran, J. F.; Klucas, R. V.; Grayer, R. J.; Abian, J.; Becana, M. *Free Radic. Biol. Med.* **1997**, *22*, 861–870.
- (59) Schweigert, N.; Zehnder, A. J. B.; Eggen, R. I. L. *Environ. Microbiol.* **2001**, *3*, 81–91.
- (60) Schaich, K. M.; Tian, X.; Xie, J. *J. Funct. Foods* **2015**, *18*, 782–796.
- (61) Foti, M. C. *J. Agric. Food Chem.* **2015**, *63*, 8765–8776.

- (62) Kehrer, J. P.; Robertson, J. D.; Smith, C. V. *Comprehensive Toxicology*; Elsevier, 2010; pp 277–307.
- (63) Battelli, M. G.; Polito, L.; Bortolotti, M.; Bolognesi, A. *Oxid. Med. Cell. Longev.* **2016**, 2016, 3527579- 3527587.
- (64) Vivas, N.; Glories, Y.; Lagune, Laure; Saucier, C.; Augustin, Monique *J. Int. Sci. Vigne Vin.* **1994**, 28, 319-336.
- (65) Facinó, R.; Carini, M.; Aldini, G.; Berti, F.; Rossoni, G.; Bombardelli, E.; Morazzoni, P. *Planta Med.* **1996**, 62, 495–502.
- (66) Yoneda, S.; Nakatsubo, F. *J. Wood Chem. Tech.* **1998**, 18, 193–205.
- (67) Hertzberg, R. P.; Dervan, P. B. *J. Am. Chem. Soc.* **1982**, 104, 313–315.
- (68) Lloyd, R. S.; Haidle, C. W.; Robberson, D. L. *Biochem.* **1978**, 17, 1890–1896.
- (69) Perkowski, D. A.; Perkowski, M. *Data and probability connections*; Connections in mathematics courses for teachers; Pearson Prentice Hall; London : Pearson Education Ltd: Upper Saddle River, N.J., 2007; pp 318-337.

APPENDIX A


COPYRIGHT PERMISSION FOR WORK PRESENTED IN CHAPTER 3

Chapter 3



License

PLOS applies the [Creative Commons Attribution \(CC BY\)](#) license to works we publish. Under this license, authors retain ownership of the copyright for their content, but they allow anyone to download, reuse, reprint, modify, distribute and/or copy the content as long as the original authors and source are cited.

Appropriate attribution can be provided by simply citing the original article (e.g., *Huntingtin Interacting Proteins Are Genetic Modifiers of Neurodegeneration*. Kaltenbach LS et al. *PLOS Genetics*. 2007. 3(5) doi:10.1371/journal.pgen.0030082) .

If you have a question about the license, please [email us](#).
